BYSTANDER CELL DEATH FOLLOWING LOW-LET IRRADIATION

EXAMINATION OF BYSTANDER CELL DEATH FOLLOWING LOW-LET IRRADIATION

By
MICHAEL DOUGLAS GOW, B.Sc.

A Thesis

Submitted to the School of Graduate Studies

in Partial Fulfillment of the Requirements

for the Degree

Doctor of Philosophy

McMaster University

Doctor of Philosophy (2011) McMaster University
(Medical Physics) Hamilton, Ontario

TITLE: Examination of Bystander Cell Death following Low-LET Irradiation

AUTHOR: Michael Douglas Gow, B.Sc.
(McMaster University)

SUPERVISOR: Dr. Carmel E. Mothersill

NUMBER OF PAGES: xiv, 275

Abstract

This thesis describes an analysis of the influence of dose and dose rate from low LET radiation on the induction of a cytotoxic bystander effect. The general direction was as follows:

- Utilize a well – established reporter cell line with two types of low – LET radiation across varying dose and dose rates in order to assess the possibility of a dose rate effect. These results identified the recovery of bystander cell survival to control levels after high dose treatment. Additionally, dose rate effects were seen at high dose treatments following electron irradiation as well as between similar low – LET sources.

- Apply aggressive radiation treatment for toxic medium production in order to elicit a bystander cell death response in a cell line with no previous observed effect. Results indicated a similar response to a reporter line including an increase in cell survival at high doses. Transforming growth factor β1 (TGF-β1) was identified as necessary to the observed effect.

- Develop a dosimetry model for *in vitro* bystander studies following toxic medium production with a β-emitting radiopharmaceutical. Furthermore, use this model to re-examine survival fraction data in comparison with traditional external beam treatment. A code-base and application were developed. Comparison between treatments indicated a similar survival curve shape with differences in the magnitude of the response. This is possibly the result of cell response to low – dose rates from radiopharmaceutical treatment.

The overall conclusion points to the importance dose rate in observed bystander cell death as well as the differentiating response at high doses. Additionally, the similarity in survival curve behaviour across differing cell type's further points to common underlying critical mechanisms. However, it is believed that further data acquisition and aggregation is required in order to build a robust model for the influence of these factors.

Acknowledgements

I would like to say a word of thanks to the following individuals. First, to Dr. Carmel Mothersill, Dr. Colin Seymour and Dr. Fiona McNeill, thank you for your encouragement and enthusiasm for my work over what is likely one of the most unusual paths in graduate school. Your confidence in me as a scientist has pushed me to be better at all things analytical. Specially, to Dr. Mothersill, your persistence and belief in my work has brought me here and I thank you for that. Secondly, thank you to all individuals I have worked with in the lab. Specifically, thanks to Lorna Ryan whose commitment and helping hand were inspiring. Thirdly, thank you to my mother and father, Debra and Robert, whose pride in my work and shoulder to lean on during tough decisions have been a definitive guiding light. Lastly, I would like to thank my wonderful wife Michelle. Your support through hard times and decisions has made all this possible. I could never write enough words to describe my love and appreciation for you.

Table of Contents

List of Figures and Tables

Introduction

Part A

Part B

Part C

List of Abbreviations

ALARA	As Low As Reasonably Acheivable
ANOVA	Analysis of Variance
Bq	Becquerel
CDKI	Cyclin Dependent Kinase Assay
CHO	Chinese Hamster Ovary
CSDA	Continuous Slowing-Down Approximation
DNA	Deoxyribonucleic Acid
DSB	Double – Strand Break
DT	Doubling Time
ELISA	Enzyme-Linked Immuno-Staining Assay
eV	Electonvolt
Gy	Grey
HPV	Human Papillomavirus
HRS	Low-Dose Hypersensitivity
ICCM	Irradiated Cell Conditioned Medium
IORT	Intraoperative Radiation Therapy
IRR	Increased Radiation Radioresistance
LAP	Latency Assoicated Peptide
LDR	Low – Dose Rate
LET	Linear Energy Transfer
LINAC	Linear Accelerator
LNT	Linear No Threshold
LQ	Linear Quadratic
mAb	Monoclonal Antibody
MABG	meta - astatobenzylguanidine
mcc	MATLAB C - Compiler
MIBG	meta - iodobenzylguanidine
NAT	Noradreniline Transporter
NO	Nitric oxide
PAI	Plasminogen Activator Inhibitor
PBS	Phosphate Buffer Solution
RIBBE	Radiation Induced Biological Bystander Effects
RNA	Ribonucleic Acid
ROS	Reactive Oxygen Species
SCE	Sister Chromativ Exchange
SF	Surviving Fraction
SSB	Single Strand Break
TGF	Transforming Growth Factor
tPA	Tissue Plasminogen Activator
VW	Vynckier - Wambersie

Author Contribution

Part A:

The experiments of this paper were designed and performed by the author of this thesis under ther supervision of Dr. Mothersill, with helpful discussion from Dr. Seymour. All analysis and writing was performed by the thesis author with editing by the thesis author in conjunction with Dr. Mothersill, Dr. Seymour, and Dr. Byun.

Part B:

The experiments of this paper were designed and performed by the author of this thesis under ther supervision of Dr. Mothersill, with helpful discussion from Dr. Seymour. All analysis and writing was performed by the thesis author with editing by the thesis author in conjunction with Dr. Mothersill, Dr. Seymour, and Lorna Ryan.

Part C:

The modelling, programming, application development, analysis and writing were performed by the thesis author under the supervision of Dr. Mothersill. Editing was performed by the thesis author in conjunction with Dr. Mothersill and Dr. Seymour. Additionally, the writer notes useful discussion with Dr. William Prestwich (modelling) and Dr. Robert Mairs (cellular treatment).

INTRODUCTION

Historical Context

On December 28th, 1895, Wilhelm Conrad Röntgen presented a paper to the president of the Physical Medical Society of Würzburg on the discovery of a "new kind of ray" he had identified merely weeks earlier (Röntgen, 1895). This discovery of a novel radiation type, coined X-rays, is what most scholars mark as the start of the modern physics era and the genesis of what has evolved into the field of radiobiology. A cross section of biology, physics, and chemistry, the field of radiobiology seeks to understand the action of ionizing radiation on biological tissues and living organisms. Röntgen's original paper contained what can be interpreted as the original biological study of these new radiations, namely a radiographic image of Frau Röntgen's hand as well as the now unsettling observation that, "[t]he retina of the eye is quite insensitive to these rays: the eyes placed close to the apparatus sees nothing" (Rockwell, 1998). As scientists world-wide eagerly worked to confirm Röntgen's results and study these mysterious X-rays, severe, adverse effects began to manifest themselves (Miller, 1995). By using unshielded and relatively inexpensive Crookes tubes, operators and scientists were regularly exposed to high doses of X-rays, often on purpose as researchers aimed to assess the effects of this radiation or to study its use in imaging. Within months, injuries to the eye, hair loss, erythema, and chronic dermatitis were reported (although not well publicized until 1936) (Doll, 1995; Miller, 1995; Rockwell, 1998). It was evident from these anecdotal observations that radiation in fact had a very pronounced and damaging effect on

biological tissue but may be able to be exploited for use in cancer treatments. Thus, starting in 1896, the first patients were treated with X-rays (del Regato, 1996; Ewing, 1934; Kaplan, 1970) for which marked improvements in superficial lesions were noted even though the relatively primitive nature of the technology precluded its use as a curative therapy (Rockwell, 1998).

During this feverish pace of research into X-rays, a near parallel stream of research and discovery was taking place for naturally occurring radioactivity. Becquerel was the first to discover this in 1896 with his observations of radiation emissions from uranium compounds (Hall, 2000). Rutherford expanded on this research, observing two distinct types of radiations he named α- and β-rays (later found to be composed of helium nuclei and electrons respectively). Additionally, Marie and Pierre Curie discovered radium and polonium in 1898 and together with skin injuries received by both Becquerel as well as the Curie's, it was clear that naturally occurring radioactive elements also produced damaging effects to biological tissues (Rockwell, 1998). As with X-rays, radioactive elements (particularly widely available radium) began their use in cancer treatments producing both palliative effects as well as occasional cures (del Regato, 1996; Ewing, 1934; Kaplan, 1970).

With continued maturation of physics and technology, studies and applications of ionizing radiation's use as a therapeutic mechanism for cancer patients also grew. The development of the first ^{60}Co radiotherapy machine in London, Ontario, Canada in 1951 (Hall, 2000) and the use of a linear accelerator (LINAC) at Hammersmith Hospital in the United Kingdom (Hall, 2000) laid the foundation for today's external beam therapy.

Furthermore, the use of ionizing radiation and radioactivity as an internal therapeutic agent (e.g. brachytherapy) as well as a diagnostic aid would continue to evolve starting in the early 20th century. But during all this time, the real essence of radiobiology as it applies to the scientific community's ability to describe the mechanism(s) of action on biological tissues lagged behind. Several factors can be attributed to this all essentially falling under the scope of the large evolutionary gap in biology relative to other fundamental disciplines such as physics and chemistry. Having said this, although the exact nature of radiation damage was unknown, it was believed that this damage reflected both direct action of critical biological components and / or indirect mechanisms by way of ion and radical products of water interacting with these components. This turned out to be quite prophetic as radiobiological research would indeed adapt such a model for explaining radiation damage which continues to be the centre of our understanding today.

Preliminary attempts to explain radiation-induced biological damage were initiated in the 1940's when Timofeff-Ressovsky and Lea in parallel wrote books centred on this subject (Lea, 1946; Timofeeff-Ressovsky and Zimmer, 1947). Without a true understanding of underlying cellular or molecular biology, their theories were derived almost exclusively from chemistry-based experiments involving ionizing radiation. The primary premise revolved around the concept of water-based intermediaries being activated and further propagating reactions in solutions; the so-called 'indirect action' which Lea proposed was always proportional to dose (Lea, 1946). Thus, biological damage induced by ionizing radiation was thought to be the result of chemical changes. With this however, was the acknowledgement that this chemistry-based theory was

unable to explain substantial biological effects that occurred at low doses where little chemical change was observed. Furthermore, the spread of ionization in biological material also required explanation. As discussed by Mothersill and Seymour, two separate solutions were postulated (2006a). First, it was believed that perhaps the direct action of radiation damage was inversely proportional to a cell's molecular weight which could be related to the localization of radiation damage and subsequently explain low dose biological damage. This concept led Timofeeff-Ressovsky and Zimmer to propose the initial target theory for radiation damage whereby a calculation of the size of the target molecule was developed based on the proportion of effected organisms at a given dose (Mothersill and Seymour, 2006a; Timofeeff-Ressovsky and Zimmer, 1947). Second, to explain the propagation of ionization and radiation damage throughout a biological system, it was thought that perhaps the ionizing radiation was a source of heat (Mothersill and Seymour, 2006a) or, as Louis Gray favoured, ionizing radiation yielded the production of hydroxyl and hydrogen radicals (Gray, 1954). These ideas coupled with the discovery of DNA's pivotal role in cellular function laid the foundation for the development of classic radiation target theory which has been central dogma in radiation biology for the better part of fifty years.

Cellular Damage

Ionizing radiation, either electromagnetic (e.g. X-rays and γ-rays) or particulate (α or β particles), invoke damage to the cell's critical target, DNA, via either **direct** or **indirect** action. For direct damage, the radiation's energy is absorbed by the cell's critical targets leading to ionization / excitation of these atoms and initiating a chain of reactions leading to damage. Such direct radiation damage is dominated by radiation types with high linear energy transfer (high-LET) whereby LET describes the rate of energy lost (absorbed by cell) along the track of an ionizing particle (primarily expressed as keV μm^{-1}) (Hall, 2000). Typically damage is reflected as single-strand DNA breaks (SSB), double-strand DNA breaks (DSB), or base alteration. On the other hand, indirect damage is mitigated via the production of free radicals that are able to diffuse relatively large distances within the cell and damage critical targets. Irradiation with photons (e.g. γ-rays) or particles (e.g. electrons) can ionize water molecules which are highly reactive and subsequently interact with neighbouring water molecules to form the hydroxyl radical (OH•), hydrogen radical (H•), and an aqueous electron (e^-_{aq}). These products are then subsequently capable of invoking DNA damage (Figure 1-1).

Generally speaking, radiation exposure typically leaves a large number of lesions in the DNA with most of them being repairable. Base alterations and DNA SSB's dominate the damage seen but are relatively easily corrected as the opposite strand of the DNA double-helix can be used as a template for repair. As such, cell killing does not correlate well with SSB's (Hall, 2000). It is noted however that if this damage is improperly repaired, carcinogenesis may result as defects are passed on to a cell's

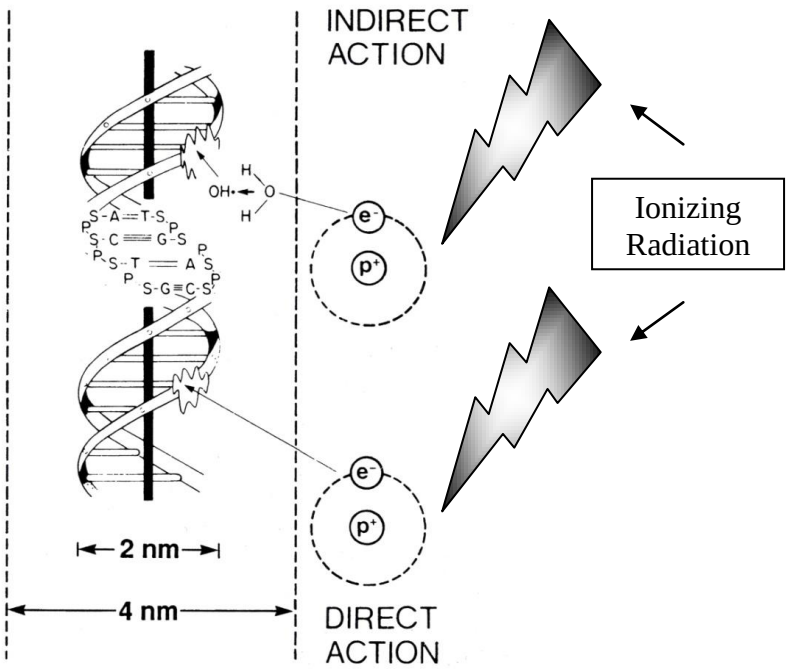

Figure 1-1: Illustration of biological damage to DNA by direct and indirect action of ionizing radiation. Adapted from (Hall, 2000).

progeny. On the other hand, DSB's, caused by breaks in opposite DNA strands in close proximity, have a much stronger correlation with subsequent cell death primarily due to their ability to induce various chromosome aberrations.

There are various forms of cell death induced by radiation, including:

Mitotic Death / Mitotic Catastrophe:

References a cell's premature entry into mitosis with unrepaired DNA damage and chromosome aberrations ultimately resulting in cell death (Galluzzi *et al.*, 2007). Chromosome aberrations (specifically, asymmetric aberrations) have been shown to be directly correlated with this form of radiation-induced cell death (Cornforth and Bedford, 1987; Hall, 2000). In addition to cell death during mitosis, aberrant mitosis may also

occur leading to subsequent giant cells with incorrect nuclear morphology (Eriksson *et al.*, 2007; Eriksson *et al.*, 2008a), as well as multiple or micronuclei (Erenpreisa *et al.*, 2005a; Erenpreisa *et al.*, 2005b; Roninson *et al.*, 2001). These abnormal cells may survive for a few divisions but eventually die via delayed necrosis or apoptosis.

Apoptosis:

A process whereby a cell initiates a series of events leading to programmed cell death. Along with mitotic death, apoptosis is a primary mechanism for radiation-induced cell death (Dewey *et al.*, 1995; Hall, 2000). A regulated process to ensure the safety of the surrounding cells, there are various characteristics of the process including a maintenance of membrane integrity, chromatin condensation, reduction and fragmentation of the nucleus, as well as shrinkage and ruffling of the plasma membrane (Kroemer *et al.*, 1995; Kroemer *et al.*, 1998; Thompson, 1995). This is followed by a subsequent division of the cell into apoptotic bodies which are generally broken-down and destroyed by neighbouring cells (Eriksson *et al.*, 2008b). The dominance of mitotic or apoptotic cell death is dependent on cell type with many types undergoing a combination of both. However, there is a general correlation between apoptosis and radiosensitivity with those cells that are radiosensitive having apoptosis as the dominant mechanism (Hall, 2000). The expression of p53 phospho-protein (encoded in the TP53 gene) is a dominant pathway for the initiation of apoptosis and it plays an important role in tumour suppression and cellular response to radiation (Cuddihy and Bristow, 2004; Eriksson and

Stigbrand, 2010; Fei and El Deiry, 2003; Helton and Chen, 2007; Vousden and Lu, 2002).

Senescence:

Cellular senescence is a mechanism by which cell growth is limited and cells lose their ability to divide while maintaining regular function. There are specific morphological changes that define this particular cell growth arrest including a flattened and enlarged morphology, chromatin condensation, changes to various gene expressions and increased granularity (Eriksson *et al.*, 2008b).

Autophagy:

A form of cell death characterized by cytoplasmic autophagic vacuoles called autophagosomes as well as an intact nucleus (Baehrecke E.H., 2002; Reggiori and Klionsky, 2010). Essentially this process involves the digestion of sub-cellular membranes and sequestered cytoplasm by lysosomal hydrolases within the lysosomes (Eriksson *et al.*, 2008b). If this degradation is too extensive, cell death can be induced. The exact purpose of the process is unknown and may be an attempt to increase cell viability or clean up cell remnants already destined for death (Levine and Yuan, 2005). It is also thought that autophagy may be up-regulated when apoptosis is not induced (Eriksson *et al.*, 2008b). This process has been shown to take place via radiation exposure (Ito *et al.*, 2005; Kim *et al.*, 2006; Paglin *et al.*, 2001; Paglin and Yahalom, 2006).

Dose, Dose Rate, and Cell Survival

Development of sufficient end points and reproducible models were essential to the quantification radiation damage on biological systems. Although original cell culturing techniques began as early as the 19th century, limited success was seen even through the early 1950's where most cell culture systems were limited to small, high density cultures (Rockwell, 1998). However, in 1955, Puck and Marcus reported that the utilization of a "feeder layer" of radiation sterilized cells could overcome low density seeding limitations and support the growth of a small monolayer of viable cells (Puck and Marcus, 1955). With this technique, cells could be plated at low densities in order to determine their colony-forming ability as descendents multiply to form localized, macroscopic colonies. As a result of this, Puck and Marcus developed the now widely used clonogenic assay which is a quantifiable measure of cell viability following an applied stress such as ionizing radiation. Their ground breaking paper demonstrating HeLa cell survival as a function of dose was the first radiation cell survival curve produced and directly illustrated cellular dose-response (Puck and Marcus, 1956). This response indicated a slow decrease in cell survival for low doses (a so-called "shoulder") followed by an apparent exponential decrease as dose increased. Following these *in vitro* techniques, *in vivo* assays were developed (Hewitt and Wilson, 1959) and comparison of tumour cells cell viability in these experiments yielded results similar to Puck and Marcus. Together, these findings moved radiobiology from the tissue level to the cellular level (Rockwell, 1998).

A typical survival curve is illustrated in Figure 1-2. Qualitatively, the curve is quite simple to describe. For low-LET radiation, the curve starts out with a finite initial slope at low dose indicating a cellular surviving fraction is an exponential function of dose (straight-line in a log – liner plot as in Figure 1-2). As dose increases, the curve begins to bend until very high doses are reached where it tends to straighten and hence return to an exponential function. For high-LET radiation, the curve remains straight across all doses and thus always represents exponential behaviour.

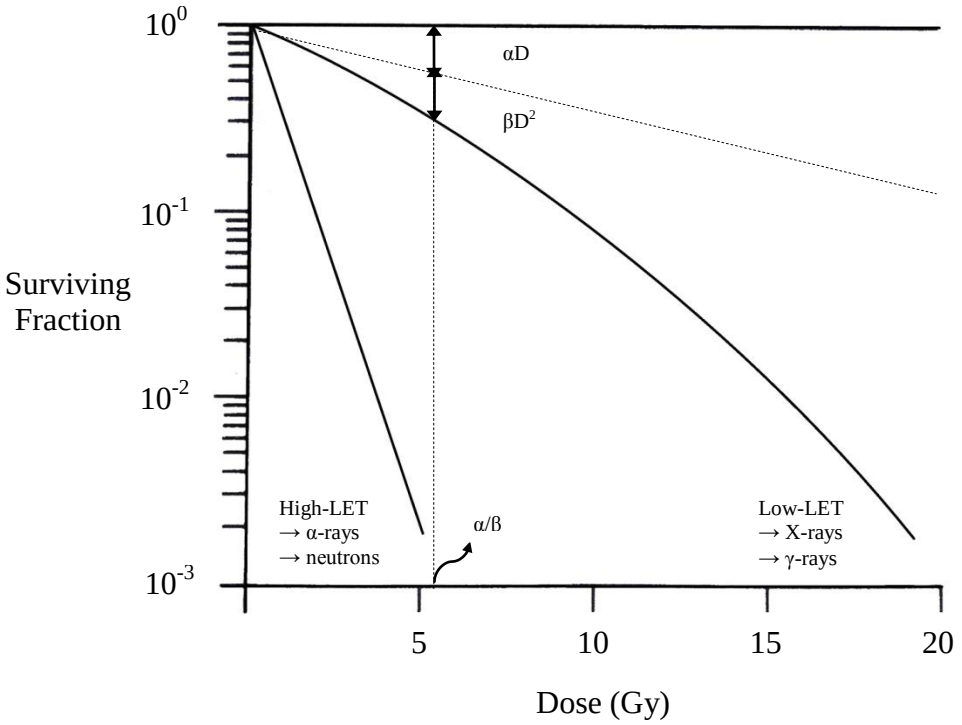

Figure 1-2: Illustration of a typical log-linear survival curve plot. Low-LET radiation tends to consist of a portion with an initial slope followed by a large curved section which tends to straighten at very high doses. Conversely, high-LET radiation remains far straighter throughout the entire dose range. Also indicated above are the parameters for describing the low-LET curve via the linear-quadratic model. Here we have two components involved in cell killing; one proportional to dose (αD) and one proportional to the square of the dose (βD^2). The ratio α/β is the dose at which the linear and quadratic components are equal. It is noted that the linear-quadratic curve has no finite slope (i.e. bends continuously) but tends to provide a sufficient fit for cell survival data. Adapted from (Hall, 2000).

Several mathematical models over the years of varying complexity have been developed to define the shape of cell survival curves, all essentially based on the nature by which radiation deposits energy in the cell (Nias, 1998). Today, the linear-quadratic (LQ) formalism is the typical model of choice as it provides good-fit and time-dose dependencies as well as providing an underlying mechanistic explanation for the observed cell death of both normal and tumour tissue (Brenner *et al.*, 1998; Douglas and Fowler, 1976; Sachs and Brenner, 1998). The rationale of the LQ model stems from the curvilinear behaviour of the survival fraction curve in a log-linear plot (see Figure 1-2) and this cell killing is explained as follows:

1) A single track of radiation can give rise to a lethal mutation by such mechanisms as the deletion or mutation of a vital gene or the induction of apoptosis (Sachs *et al.*, 1997). These lesions are linearly related to dose, αD.
2) DNA double-strand breaks (DSB) are produced in proportion to radiation dose and any given DSB can be repaired based on first order kinetics with a particular repair half-life (i.e. $\ln 2 / T_{1/2}$) (Brenner *et al.*, 1998). DSBs that are not repaired and are produced from different tracks can produce lethal lesions via creation of chromosome aberrations (e.g. dicentric aberration). The yield of these lesions is proportional to the square of the dose, βD^2. Note however that these lesions do not have to occur at the same time, thus allowing repair of the first DSB prior to any misrepair with a second DSB.

The total lethal lesion yield is the sum of the linear and quadratic components, and with lethal lesions following a Poisson distribution from cell-to-cell we obtain the surviving fraction (SF) for a single, non-fractionated dose is given by:

$$SF = e^{-\alpha D - \beta D^2}$$

By this expression the linear and quadratic portions of cell killing are equal if $\alpha D = \beta D^2$ which occurs at a dose $D = \alpha/\beta$. For densely ionizing radiation such as those with high-LET, single track events are the primary lethal lesion and hence the linear contribution to surviving fraction dominates. This is why the curve is more linear in Figure 1-2 for high-LET sources. Conversely, sparsely ionizing, low-LET radiation effects surviving fraction to a greater extent via the quadratic portion of the above expression, leading to a large shoulder and curvature on the log-linear plot seen in Figure 1-2.

In addition to the effect of dose on overall cell survival and modelling the underlying mechanisms of this effect, the rate at which we apply the dose can also alter cell survival. Among the first to notice this effect were Elkind and Sutton who observed that by dividing one large single dose into two equal fractions increased cellular survival (Elkind and Sutton, 1960). Cell survival curves indicated that at the time of the second irradiation, an increase in cell survival was reflected in a return of the "shoulder" of the cell survival curve (Figure 1-3). This is indicative of a cell's ability to accumulate sublethal damage and subsequently repair this damage during the time between irradiation treatments. More specifically, if sufficient time is allowed between irradiations, damage via double-strand breaks can be given time to repair themselves and decrease the likelihood of interaction to form lethal lesions (e.g. dicentric chromosome

aberrations). While fractionation is irrelevant for damage from single-strand breaks, double-strand breaks benefit from the fractionation window by in effect having less DSBs available per unit time to interact and subsequently result in lethal lesions. Later experiments would demonstrate that this effect of dose-splitting yielded marked increases in cell survival of low-LET radiations (e.g. X-rays and γ-rays) which primarily produced lesions via multi-track, indirect damage as opposed to high-LET radiations (e.g. neutrons and α-particles) which generate damage predominantly via a singular track.

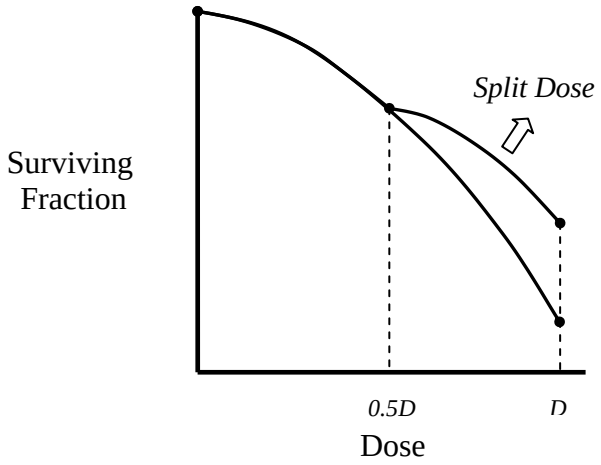

Figure 1-3: An illustrative example of the effect of fractionating a dose as opposed to a single dose on cell survival.

For low-LET radiations, dose rate is a significant factor in the biological response of a particular absorbed dose. Generally speaking, as dose rate decreases, a given biological effect also decreases due to the ability and opportunity to repair the sublethal damage (one can image a continuous low-dose rate as approximating an infinite number of infinitely small fractions). This results in a levelling out of the shoulder (or "shallowing") on a cell survival curve and a continued decrease in dose rate can lead to

effectively a linear decline in cell survival (representing non-repairable damage). This is in contrast to an acute, high dose exposure which typically results in an initial shoulder followed by a sharp decline in surviving fraction. The magnitude of the dose rate effect is dependent on the type of cell being examined and its ability to accumulate and repair sub-lethal damage (Hall, 2000). In addition, there are instances in certain cell types whereby a decrease in dose rate can decrease cell survival; the so - called inverse dose rate effect as, for example, seen in cervix carcinoma cells (e.g. HeLa) (Furre *et al.*, 1999). In this instance, the dose rate is low enough to allow passage of cells through portions of their cycle that are less sensitive to radiation but is not low enough to pass through a sensitive phase (i.e. G_2). This result's in a cell population blocked in a sensitive phase and an apparent increase in cell death. Upon further lowering of the dose rate, cells can pass through their sensitive phase and survival increases as would expected.

The LNT model and Mechanisms of Change

Through studies across various populations and established via various global and national bureaucratic entities, the central dogmatic model that underlies the relationship between dose and biological effects is the Linear No Threshold (LNT) model. Derived primarily from extrapolated data of the atomic bomb survivors in Japan exposed to acute, high dose irradiations, the LNT model's main premise is the belief that ionizing radiation has purely a negative impact on cellular function and that any amount of dose, however low, can increase the probability of cancer production with DNA being the critical target. In the classic model of radiation-induced carcinogenesis, radiation can induce rare mutagenic events that ultimately lead to stimulation of cell proliferation or a decrease in cell differentiation (Brooks, 2005). Furthermore, the model supports the belief that a single radiation event in a single cell can lead to a single mutagenic effect and ultimately introduce some finite risk of carcinogenesis. Thus, a linear increase in dose ultimately leads to a linear increase in risk of cancer and hence a LNT model (Charles, 2006). This is the foundation upon which the "as low as reasonably achievable" (ALARA) principle is founded and mandated within the health physics and radiation protection community in industry, research, and the public at large.

Although still essential to estimating radiation exposure risk and protection guidelines, evidence has accumulated, particularly over the last two decades, which challenges the fundamental assumptions of the LNT model and are altering our perception as to how radiation exposure elicits biological effects. This evidence has demonstrated several biological effects from radiation exposure which result from

mechanisms besides direct DNA damage and point the radiation research community in the direction of modifying the LNT model. These effects include:

Adaptive response:

Originally described in 1984 (Olivieri *et al.*, 1984), this effect involves the increased resistance of cells to high radiation exposure following an initial low dose irradiation coined the priming dose (Rigaud and Moustacchi, 1996). The effect has been seen across a range of cell types, priming doses and dose rates (Day *et al.*, 2007a; Day *et al.*, 2007b; de Toledo and Azzam, 2006; Mitchel, 2010; Olivieri *et al.*, 1984; Pinto *et al.*, 2010; Sawant *et al.*, 2001b; Zhou *et al.*, 2004). Furthermore, there is also evidence suggesting the presence of this effect in increasing radioresistance and decreasing cancer rates in both animals (Mitchel *et al.*, 1999; Mitchel *et al.*, 2003; Mitchel *et al.*, 2004; Plews *et al.*, 2010) as well as *in vivo* in humans (Ghiassi-Nejad *et al.*, 2002; Monsieurs *et al.*, 2000).

Low-Dose Hypersensitivity (HRS) / Increased Radiation Radioresistance (IRR):

HRS is in reference to the sub – LQ clonal survival values seen in some cell lines at low doses while IRR refers to the abrupt increase in clonal survival values back to those predicted by the LQ model (see Figure 1-4).

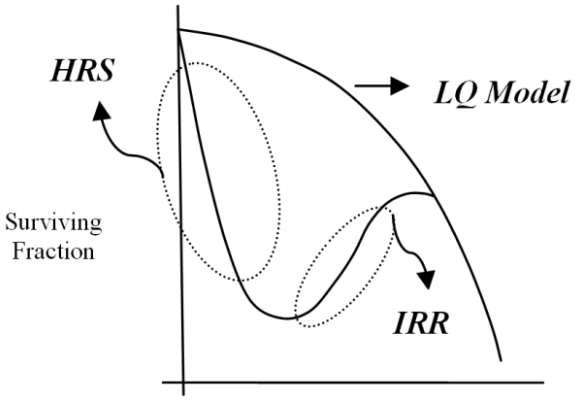

Figure 1-4: An illustration example indicating HRS and IRR effects compared to standard LQ model at very low doses.

Originally defined in mammalian cell lines (Lambin *et al.*, 1993; Marples and Joiner, 1993), HRS / IRR has been seen across a variety of cell lines (Dey *et al.*, 2003; Krueger *et al.*, 2007; Wouters *et al.*, 1996) using different radiation qualities and biological endpoints (for reviews, see Joiner *et al.*, 2001; Marples *et al.*, 2004). It has been suggested that this dose response could be explained by a two – population model, whereby low doses would eliminate cells in sensitive cell cycle phases and high doses required to eliminate those in a resistant cycle (Joiner *et al.*, 1999). Furthermore, recent evidence has confirmed that HRS is linked to the early G_2/M checkpoint through the damage response of G_2-phase cells (Krueger *et al.*, 2010).

Non – Targeted Effects:

In a very general sense, non-targeted effects refers to biological events occurring in the unirradiated neighbours of irradiated cells and / or in the progeny of irradiated cells (also labelled as delayed effects) (Morgan and Sowa, 2009). These phenomena are referred to as ***bystander effects*** and ***genomic instability*** respectively (as bystander effects are the

primary driver for the research presented here, there is a dedicated discussion in the next section). With respect to genomic instability, this effect is defined as the increased risk of genetic mutation / alterations in the progeny of cells exposed to radiation (Morgan *et al.*, 1996) and is examined via clonal growth and genetic sampling of cells surviving a given radiation insult. Various biological end points can exist and be perpetuated through several generations including chromosomal aberrations, micronuclei formation as well gene mutation / alteration (for reviews see (Kadhim *et al.*, 2006; Little, 2003; Lorimore and Wright, 2003; Morgan *et al.*, 1996)) and this effect has been measured for various irradiation procedures and cell types (Kadhim *et al.*, 2006; Moore *et al.*, 2005; Mothersill *et al.*, 2000; Natarajan *et al.*, 2007). As illustrated in Figure 1-5, these instability events have been hypothesized to occur either via progeny of surviving irradiated cells (A) or possibly through soluble factor transmission (B).

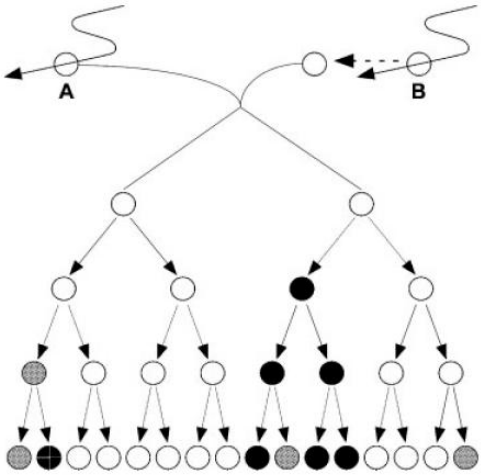

Figure 1-5: A schematic representation of radiation-induced genomic instability. Pathways **A** represents a cell surviving irradiation and genetic instability develops in progeny during clonal expansion. Pathway **B** represents an irradiated cell producing a soluble factor that affects other non-irradiated cells. The progeny of this cell then develop genomic instability during clonal expansion. Cells with varying degrees of instability are represented by grey and dark circles that can subsequently yield instable subpopulations (Sowa Resat and Morgan, 2004).

Bystander Effects

In the context of radiation biology, the "bystander effect" refers to the detection of biological effects in unirradiated cells which they themselves could not have been traversed by ionizing radiation. Often coined "Radiation – Induced Biological Bystander Effects" (RIBBE), these phenomena have become well established across a range of cell types and experimental methodologies. With no intention of being a comprehensive review of RIBBE subject matter, what follows is aimed at providing a backdrop and context to the scope of research presented here.

Although examination RIBBE has occurred over the last two decades, research dating back to the 1950's had shown indirect effects of low – LET radiation and the resultant production in a plasma – borne factor leading to chromosome breakage and cytogenetic abnormalities (Faguet *et al.*, 1984; Hollowell and Littlefield, 1967; Hollowell and Littlefield, 1968; Mothersill and Seymour, 2001; Parsons *et al.*, 1954; Scott, 1969). The genesis of modern radiation – induced bystander research is largely attributed to pioneering work by H. Nagasawa and J. B. Little in 1992. In their experiment, the authors exposed Chinese hamster ovary (CHO) cells to low fluencies of α – particles in order to yield a nuclei traversal rate of 1% (Nagasawa and Little, 1992). Through utilization of sister chromatid exchanges (SCE) as an end point, the authors showed that 30% of cells suffered such damage, far greater than anticipated given the low fluency provided. As such, it was suggested that some mechanism was conveying radiation – damage responses to unirradiated cells.

In addition to this, pioneering work by Mothersill and Seymour in 1997 and 1998 indicated that cytotoxic factors were secreted into growth medium and cells need not be in close proximity in order to be effected (Mothersill and Seymour, 1997; Mothersill and Seymour, 1998). By using various epithelial cell lines, Mothersill and Seymour demonstrated that irradiation of "donor" cells with low – LET γ – rays yielded a growth medium that can induce cell death in "recipient" cells when filtered and transferred post-irradiation. A typical medium transfer experiment is illustrated in Figure 1-5. This "irradiated cell conditioned medium" (ICCM) was maximal when 300,000 donor cells were plated and appeared to be toxic as early as 30 minutes following irradiation (Mothersill and Seymour, 1997). These experiments also appeared to indicate no contrast in ICCM effect with medium transfers occurring one hour or more after irradiation and doses up to 5 Gy (Mothersill and Seymour, 1997). This apparent saturation in bystander cell death occurring at ~0.5 Gy ICCM as well as donor cell levels needed to produce the ICCM suggested that the factor(s) where likely signal transducers involved in controlling cellular death or survival as opposed to being directly cytotoxic (Mothersill and Seymour, 1998). Overall, these findings suggested that cell – to – cell contact was not required for these bystander effects (Mothersill and Seymour, 1998).

With these ground breaking papers as springboards, this arena of research has become filled with ample evidence confirming various bystander radiation effects using low fluency irradiations and medium transfer protocols across a wide array of end points for both high - and low - LET radiation types. Various bystander end points include:

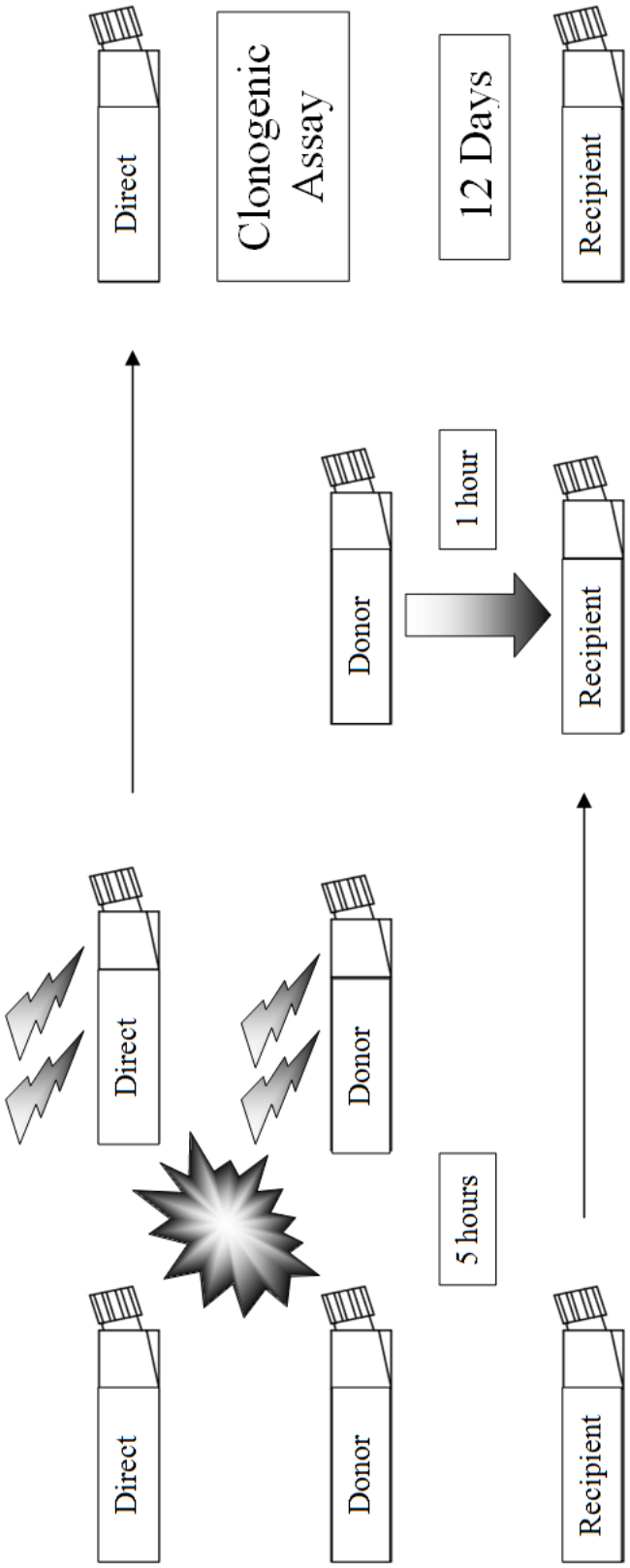

Figure 1-6: Schematic representation of medium transfer methodology when examining bystander cell death. Donors are plated with 300,000 cells and recipients with 750 cells. Five hours following cell plating, direct and donor cells are irradiated at desired end points and returned to incubator. Following ~1 hour, irradiated cell conditioned medium (ICCM; i.e. donor medium) is passed through 0.22 µm filter and applied to recipient cells. Recipient and direct cells are incubated for 12 days and then stained with carbol fushin for clonogenic assay.

i) Cell death / decrease in clonogenic survival / apoptosis
e.g.(Eriksson and Stigbrand, 2010; Liu *et al.*, 2007; Lyng *et al.*, 2006a; Mothersill *et al.*, 2004; Sawant *et al.*, 2002)

ii) Micronucleus formation
e.g.(Konopacka and Rzeszowska-Wolny, 2006; Shao *et al.*, 2005)

iii) Gene mutation
e.g.(Nagasawa and Little, 1999; Zhou *et al.*, 2002)

iv) Chromosome instability
e.g.(Burr *et al.*, 2010; Lorimore *et al.*, 2003; Watson *et al.*, 2000)

v) Sister chromatid exchange / chromosome aberrations
e.g.(Nagasawa *et al.*, 2005; Nagasawa and Little, 1992; Suzuki *et al.*, 2004)

vi) Transformation
e.g.(Lorimore *et al.*, 2008; Sawant *et al.*, 2001a)

vii) Cell proliferation
e.g.(Baskar *et al.*, 2007; Iyer *et al.*, 2000; Shao *et al.*, 2003)

viii) γH2AX foci induction (indicative of DSB's)
e.g.(Burdak-Rothkamm *et al.*, 2007; Sokolov *et al.*, 2007)

[For reviews, see (Baskar, 2010; Matsumoto *et al.*, 2009; Morgan and Sowa, 2007; Mothersill and Seymour, 2001; Prise *et al.*, 2003; Snyder, 2004)]

The cell's ability to induce or respond to bystander signalling is clearly affected by way of genetic factors (Mothersill and Seymour, 2001) but recent advances in microbeam technology have specifically demonstrated that DNA targeting is not essential for the production of bystander responses (Zhou *et al.*, 2009). For example, research by Shao *et al* has demonstrated that targeted cytoplasmic irradiation can in fact induce micronuclei formation in radioresistant glioma cells (Shao *et al.*, 2004). Furthermore, cytoplasmic irradiation has demonstrated a potential role for mitochondria – dependent signalling pathway for some cell types (Chen *et al.*, 2008; Tartier *et al.*, 2007).

But even with this plethora of evidence across varied cell types and experimental conditions, the underlying mechanism(s) involved remain fuzzy and undefined. A vast array of experiments has indicated that bystander signalling can be mediated via both gap junction communications (for closely seeded populations) as well as secreted factors. Additionally, a number of factors have been implicated as being essential to eliciting various bystander responses including Ca^{2+} (Lyng *et al.*, 2006b; Shao *et al.*, 2006), nitric oxide (NO) (Han *et al.*, 2010; Shao *et al.*, 2008), reactive oxygen species (ROS) (Chen *et al.*, 2009; Lyng *et al.*, 2002; Shao *et al.*, 2005), and cytokines such as transforming growth factor beta-1 (TGF-β1) (Burdak-Rothkamm *et al.*, 2007; Iyer *et al.*, 2000; Shao *et al.*, 2008) to name but a few. But with such a wide array of experimental opportunities available in this area of research and the expansive amount of unanswered questions, some specific, fundamental parameters have been inadequately studied or ignored. The research presented here aims to shine some light on just such parameters; broadly, how dose rate and high doses affect bystander response.

Scope of Thesis

As indicated earlier in Section 1.3, dose rate has a pronounced effect on cellular survival following irradiation. While this is well established in a traditional radiobiological research context, this is not the case with bystander radiation research. Examination of dose rate and bystander response has been largely ignored in the field and the originating aim of this research was to examine if bystander cell death is affected in any way by changes in dose rate during ICCM production. A human keratinocyte cell line (HPV-G) was utilized which has shown stable bystander effects (including cell death) using a medium transfer protocol. Additionally, while most bystander experimentation caps irradiation dose at 5 Gy (presumably based on the well observed apparent saturation seen in early experiments (Mothersill and Seymour, 1997; Mothersill and Seymour, 1998)), dose was increased for ICCM production to 10 Gy in the hopes of potentially gaining insight into the behaviour of the underlying bystander cell death mechanism. This work is described in Part A, "Effect of dose rate on the radiation-induced bystander response" which was accepted in the academic journal *Physics in Medicine and Biology* (Gow *et al.*, 2008).

Using this as a foundation, experiments were undertaken to determine the effect of high dose, high dose rate irradiation in ICCM production of a radiorestitant, human glioma cell line (T98G) which has previously shown no bystander cell death response in medium transfer experiments. By using doses of up to 20 Gy and a dose rate of 10 Gy min^{-1}, it was hypothesized that by providing a large enough radiation stress to donor cells, one could produce an ICCM toxic to recipients, especially considering the utilized cell

line has previously shown bystander effects such as micronuclei formation (Shao *et al.*, 2008) and γH2AX foci induction (Burdak-Rothkamm *et al.*, 2007). Supplementing this work is an examination of the potential roles of transforming growth factors α and β1 (TGF-α and TGF-β1) in the observed bystander cell death response (or lack thereof). This work is described in Part B, "Induction of bystander response in human glioma cell line using high energy electrons: A role for TGF – β1" and was accepted in the academic journal *Radiation Research* (Gow *et al.*, 2010).

Lastly, an examination was undertaken as to the effect of dose and dose rate on bystander cell death from ICCM produced by donor cell irradiation through uptake of a targeted radiopharmaceutical, ^{131}I – *meta*iodobenzylguanidine ([^{131}I] MIBG), a low – LET β – particle emitter. Based on work from (Boyd *et al.*, 2006), a dosimetric model was developed for the given experimental setup in order to provide efficient means of determining dose rate at various experimental phase and ultimately provide a measure of absorbed dose to donor cells used in ICCM production. These values were calculated across the various activity concentrations utilized and allowed for comparison of cell survival levels with traditional medium transfer results using ^{60}Co γ – rays. Furthermore, this model was compiled into a standalone application in order to facilitate and enhance continued bystander research with similar β-emitting radiopharmaceuticals. This work is described in Part C, "Dose Calculations for Targeted Radiopharmaceutical [^{131}I] *meta*iodobenzylguanidine *in vitro* for Examination of Radiation- Induced Biological Bystander Effects" and has been prepared for submission to the *Journal of Nuclear Medicine* for publication.

Part A

Effect of dose rate on the radiation-induced bystander response

M D Gow[1,2], C B Seymour [1,2], Soo-Hyun Byun[1], and C E Mothersill [1,2]

[1] Medical Physics and Applied Radiation Sciences Department, McMaster University, Hamilton, Ontario, Canada L8S 4K1
[2] Juravinski Cancer Centre, 699 Concession St., Hamilton, Ontario, Canada L8V 5C2

Address for correspondence:
Medical Physics and Applied Radiation Sciences Department
McMaster University
1280 Main Street West, Hamilton, Ontario, Canada
L8S 4K1

OBJECTIVE

To determine the effect of clinical dose rates on observed bystander cell survival following use of a medium transfer protocol. Additionally, compare any potential distinctive behaviour between similar, low - LET radiation γ-rays and electrons. Overall, these experiments seek to determine the relevancy of dose rate in ICCM production, subsequent impact on the observation and interpretation of bystander surviving fraction data, and gain possible insight into underlying mechanisms.

This work has been published in the academic journal *Physics in Medicine and Biology*:

Gow M D, Seymour C B, Byun S H, and Mothersill C E 2008 Effect of dose rate on the radiation-induced bystander response *Phys. Med. Bio.* 53 119-132.

Differences from the published version include minor modification to figure numbering and formatting to coincide with the structure of the thesis.

Abstract

Radiation-induced biological bystander effects have become a well-established phenomenon associated with the interaction of radiation with cells. These so-called bystander effects have been seen across a variety of end points for both high and low linear energy transfer (LET) radiations, utilizing a variety of dose rates and radiation sources. In this study, the effect of dose rate and different low LET sources on the bystander cell survival fraction (SF) was examined. The cell line investigated was the human keratinocyte HPV-G. The bystander response was measured via clonogenic assay after medium transfer protocol. Cells were irradiated using ^{60}Co γ -rays and 20 MeV electrons at doses of 0.5, 5 and 10 Gy with varying dose rates. Both γ and electron irradiation decreased recipient SF at 0.5 Gy and 5 Gy, respectively. Subsequent recovery of the SF to control levels for 10 Gy was observed. There was no dose rate dependence for ^{60}Co irradiation. A significant difference in the survival fraction was observed for electron irradiation at 10 Gy and a high dose rate. Furthermore, survival fractions were compared between ^{60}Co and 20 MeV electron irradiations. This showed a significant increase in the survival fraction 'recovery' at 10 Gy for a ^{60}Co dose rate of 1.1 Gy min^{-1} compared to 20 MeV electrons at 1.0 Gy min^{-1}. No such difference was observed when comparing at higher dose rates. Lastly, increases in survival fraction at 10 Gy were abolished and the SF decreased by the plating of increased numbers of recipient cells. Such evidence may help gain insight into the nature and mechanism(s) surrounding

bystander signal production, how these phenomena are tested and their eventual application in a clinical setting.

Introduction

External radiation therapy with low-LET radiation has been used in cancer treatment for well over fifty years. Since the advent of the first clinical ^{60}Co unit and clinical linear accelerator in the 1950's, γ radiation and high energy electrons have been a staple in the regression therapy of solid tumours. With research during the 1970's leading to DNA as the sensitive target for radiation damage (Prise *et al* 2003), it was believed that these therapies worked exclusively by inducing DNA damage in the targeted cells, leading to cell death and ultimately a reduction in tumour size. However, Nagasawa and Little showed in the early 1990's using low-fluences of α-particles that traversed only 1% of cells *in vitro* can lead to an increase in sister chromatid exchange in 30% of the cells in culture (Nagasawa and Little 1992). These observed 'bystander' effects were similarly shown to be true using low-LET radiation (Mothersill and Seymour 1997).

Since this time, these Radiation-Induced Biological Bystander Effects (RIBBE) have become a well established phenomena associated with radiation interaction with biological material. The effect can be defined as the response detected in unirradiated cells that are influenced by irradiated cells (see reviews, e.g., (Hall 2003, Little 2006, Mothersill and Seymour 2001, 2005, Prise *et al* 2003)). Both high and low LET radiation have shown bystander effects using a variety of end points including micronucleus formation (Belyakov *et al* 2005, Prise *et al* 1998, Shao *et al* 2001), gene mutation (Nagasawa and Little 1999, Zhou *et al* 2000), chromosomal instability (Lorimore *et al* 2003), sister chromatid exchange (Nagasawa and Little 1992), transformation (Sawant *et*

al 2001), decreased clonogenic survival (Liu *et al* 2006, Mothersill *et al* 2004, Mothersill and Seymour 1997, 1998, Sawant *et al* 2002), and apoptosis (Lyng *et al* 2006a). In addition, there has also been evidence showing more positive or protective response including increases in cell proliferation (Iyer *et al* 2000, Shao *et al* 2003a) as well as adaptive radioresistance (Iyer and Lehnert 2002a, 2002b, Mitchell *et al* 2004).

While it is clear that a cell's ability to induce or respond to bystander signals is affected through genetic factors (McIlrath *et al* 2003, Mothersill *et al* 2001) the use of a 'DNA-sensitive target' model is continually incapable of explaining the ever increasing amount of bystander observations. This is clear through targeted microbeam irradiation of cell cytoplasm (Shao *et al* 2004) as well as through experiments where medium is transferred from irradiated cells to non-irradiated cells (Liu *et al* 2006, Mothersill *et al* 2002, Mothersill and Seymour 1997, 1998, Poon *et al* 2007). Although the nature of the bystander signal still remains in question, recent research using targeted-microbeam and medium transfer experiments have shown that communication between irradiated and non-irradiated cells can take place via gap junction (Bishayee *et al* 2001, Shao *et al* 2003b) and / or secreted factors (Burdak-Rothkamm *et al* 2007, Hei 2006, Iyer *et al* 2000, Mothersill and Seymour 1998), leading to the extension of the radiation/stress response beyond targeted cells. In addition to this, reactive oxygen species (ROS) (Azzam *et al* 2002, Lyng *et al* 2000, 2002, Shao *et al* 2005), nitric oxide (NO) (Matsumoto *et al* 2001, Shao *et al* 2004, 2005) and Ca^{2+} (Lyng *et al* 2002, 2006b) have also been seen to affect bystander signal transmission.

The aim of this study is to investigate whether differences in dose rate have any effect on radiation bystander effect. Two different radiotherapy sources of similar LET are used consisting of a ^{60}Co γ-radiation and high energy electrons. The immortalized keratinocyte cell line HPV-G is a well established reporter of bystander effects (Lyng *et al* 2002, Maguire *et al* 2005) and is therefore used in this study. Cells were irradiated to doses of 0.5, 5, and 10 Gy over a range of dose rates. The end point measured is standard clonogenic cell death, and the survival fraction is assessed by means of clonogenic assay. Finally, implications of results in radiation therapy and insights into possible mechanisms are discussed.

Methods

Cell culture

The clonogenic cell line used were HPV-G cells which are adherent epithelial cells derived originally from a human foreskin primary culture and immortalized by the HPV virus (Pirisi *et al* 1988). They were obtained as a gift from Prof. J. DiPaolo and have been used in our laboratory as a reporter system for bystander signal production in a wide range of experiments (Mothersill *et al* 2001, 2005).

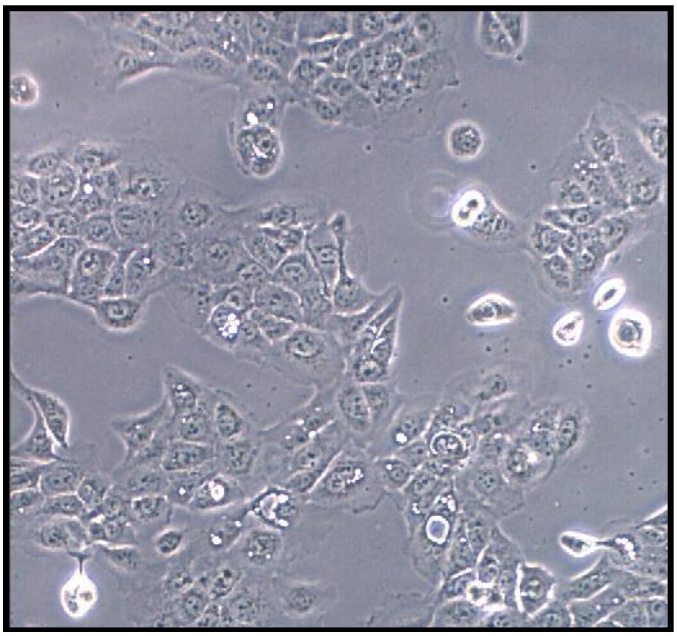

Figure A-1: Morphology of HPV-G cells.

The cell line was grown in DMEM:F12 (1:1) obtained from Gibco Biocult, Irvine, Scotland. This was supplemented with 10% fetal bovine serum, 1 mg ml^{-1} hydrocortisone (Sigma, Poole Dorset, UK), 5 ml penicillin:streptomycin solution and 5

ml L-glutamine solution. Hepes buffer (12.5ml of IM solution) was added to help maintain pH. Except where indicated, all reagents were obtained from Gibco Biocult. The line was maintained in T75 flasks (NUNC Inc, Uden, The Netherlands) and subcultured into T25 flasks (40 ml volume) for experiments. The cells are non-tumourigenic, have about 30% wild-type p53 expression (Cooper *et al* 2003) and have a normal epithelial pattern of cobblestone-density-inhibited cell growth. They are used because when exposed to a medium harvested from irradiated cells, they have been shown to give a stable bystander effect (for example, see Seymour and Mothersill (2000)).

Bystander Medium Transfer Protocol and Clonogenic Assay

Flasks which were 85–90% confluent and that had received a medium change the previous day were chosen. The cells were removed from the flask using 0.25% w/v trypsin/1mM EDTA solution (1:1). When the cells had detached, they were resuspended in medium, and an aliquot was counted using a Coulter counter model D_N set at a threshold calibrated for each cell line using a haemocytometer. Appropriate cell numbers were plated for survival using the clonogenic assay technique of Puck and Marcus (1956). Flasks destined to donate medium (i.e. donor flasks) were plated with cell numbers in the region of 3×10^5 per 5ml medium (60,000 cells ml^{-1}) in T25 40 ml volume flasks (Nucleon, Denmark). Recipient flasks, destined to receive irradiated cell conditioned medium (ICCM), were set up with a plating of approximately 750 cells at the same time that donors were plated. When changes in recipient number were examined,

recipient flasks were plated with 1000 cells for 0.5 Gy ICCM, 2000 cells for 5 Gy ICCM, and 3000 cells for 10 Gy ICCM. The medium was harvested 1-h post-irradiation, which took place 5 h after plating. Controls for medium only and actual irradiation effects (i.e. direct flasks) were included in each experiment. Controls for transfer of unirradiated medium from densely seeded cultures to cultures seeded at cloning densities were also always included. Cultures were incubated in 5 ml of culture medium in 25 cm^2, 40 ml flasks (Nunclon, Denmark), in a humidified 37 ºC incubator in an atmosphere of 5% CO_2 in air.

The technique used has been described in detail in Mothersill and Seymour (1997). Briefly, medium was poured off donor flasks (HPV-G cells) and as shown in previous results, contact times after irradiation from 30 min to 4 h showed no significant difference in effect on recipient plating efficiency (Mothersill and Seymour 1997). The donor medium was filtered through a 0.22 μm filter used to sterilizing solutions to ensure that no cells could still be present in the transferred medium. The culture medium was then removed from the flasks designated to receive an irradiated conditioned medium and the filtrate was immediately added to these recipient flasks. A medium change of unirradiated but similarly filtered medium from unirradiated donor flasks containing cells seeded at the donor density of 3×10^5 cells/flask was given to controls at the same time. Standard plating efficiency controls were also set up and there was never a significant difference between these two controls. No effect of changing the medium alone was found.

After medium transfer, cultures were left undisturbed in the incubator for ~12 days to allow for macroscopic colonies to develop. These were then stained with carbol fuchsin.

Irradiation Procedures

Where indicated, cultures were irradiated at room temperature with γ-radiation produced by a Theratron 780-C ^{60}Co teletherapy unit or 20 MeV electrons produced by a Varian 21C/D linear accelerator (LINAC).

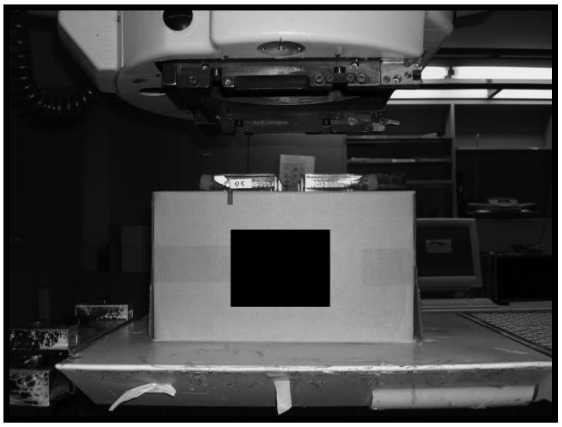
A

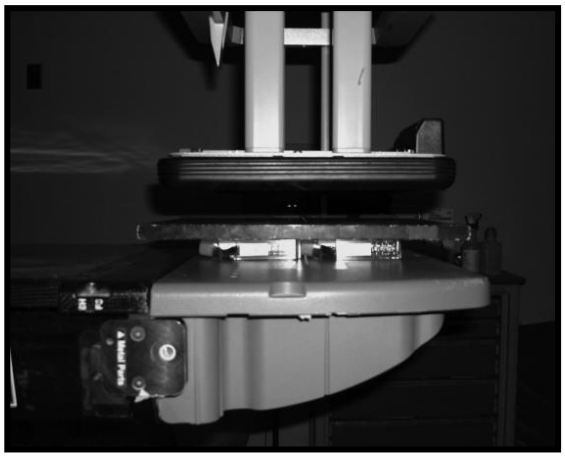
B

Figure A-2: Images of irradiation setup for ^{60}Co irradiations **(A)** and 20 Mev electron irradiations **(B)**.

The doses used were 0.5, 5, and 10 Gy. Both forms of radiation have low linear energy transfer (0.2 keV μm^{-1} for 20 MeV electrons and 0.2-2 keV μm^{-1} for ^{60}Co γ) (Johns and Cunningham 1983, p 672) and the same radiation quality factor of 1.

For ^{60}Co irradiations, dose rate was changed by increasing or decreasing the source-to-surface distance (SSD). The dose rate was measured to be 1.7 Gy min^{-1} at the standard SSD of 80 cm. The SSD was then changed to 100 cm, 60 cm and 48 cm (the closest distance possible due to physical impedance by the unit's collimator). The dose rate was calculated at these distances using

$$\dot{D}_{SSD} = \dot{D}_{80cm}\left(\frac{80cm}{SSD}\right)^2 \qquad (1)$$

Thus, dose rates of 1.1, 1.7, 3, and 4.7 Gy min^{-1} were achieved at an SSD of 100, 80, 60, and 48 cm, respectively. The dose rates given are the average dose rate obtained during experiments due to radioactive decay of the ^{60}Co source. Fluctuations in dose rate were less than 5% at all SSDs over the course of the experiments. No build-up material was used as ^{60}Co γ-radiation has a depth dose maximum of ~0.5 cm in water, the approximate depth of 5 ml of medium in T25 cm^2 flasks.

For 20 MeV electron irradiations, dose rates of 1.0, 3.0, 5.0 and 10.0 Gy min^{-1} were used. Since 20 MeV electrons have an approximate depth-dose maximum of 1.8 cm in water, 1.3 cm of polystyrene was used as build-up material in addition to a medium depth of 0.5 cm.

Controls and recipient flasks were sham-irradiated by placing them on the radiotherapy couch without exposing them to the beam. This controlled for the effects of temperature, movement or light.

Statistical analysis

Data are presented as mean ± standard error for three independent experiments with three replicate flasks per experiment in accordance with previous literature (Mothersill *et al* 2005, Mothersill and Seymour 1997, 1998). Recipient cell data were analyzed using two-way ANOVA (dose and dose rate as variables) followed by one-way ANOVA (dose rate as variable) at each dose point. When significance was found, student t-tests were performed comparing dose rates at a confidence level (p) of p 0.05. Where indicated, Bonferroni corrections were applied to the calculated p values to limit type 1 error and ensure confidence levels remain at 0.05. Potential outliers were determined using a Grubb's Test for outliers.

Results and discussion

Results

The first set of experiments focused on the effect of dose rate variation with ^{60}Co γ radiation and its effect on bystander clonogenic survival fraction. As mentioned in the Methods section, this was achieved by varying source-to-surface distance. Figure A-3 shows the survival fraction of directly irradiated cells while Figure A-4 shows the survival fraction of bystander recipient cells after treatment with ICCM.

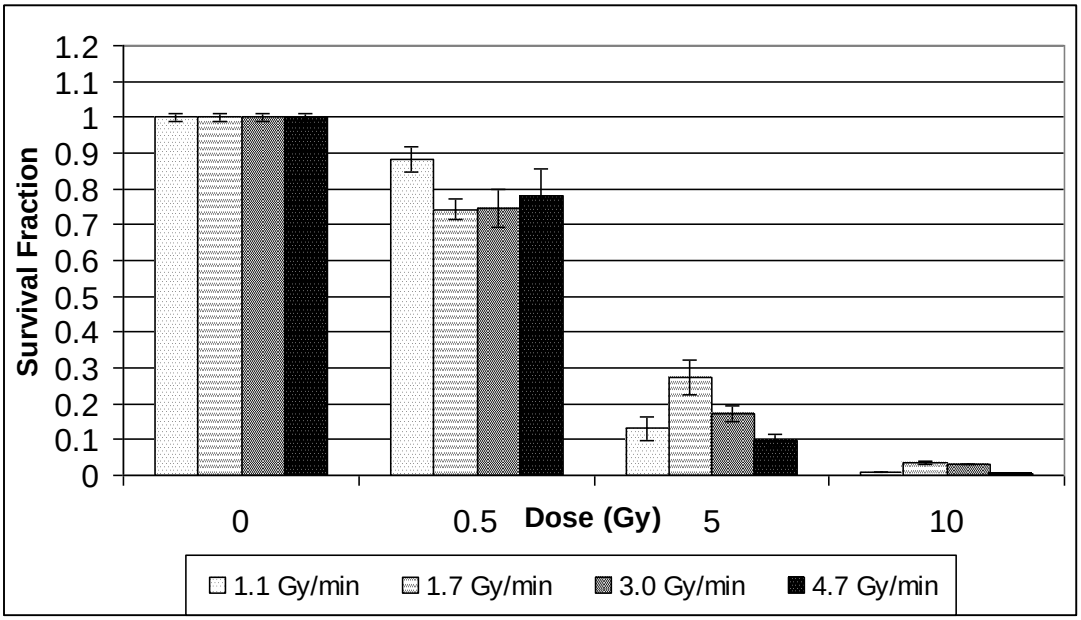

Figure A-3: Variation in the clonogenic survival fraction (% of control plating efficiency (PE)) of directly irradiated cells using the ^{60}Co source. The number of flasks used per dose and dose rate is n = 9.

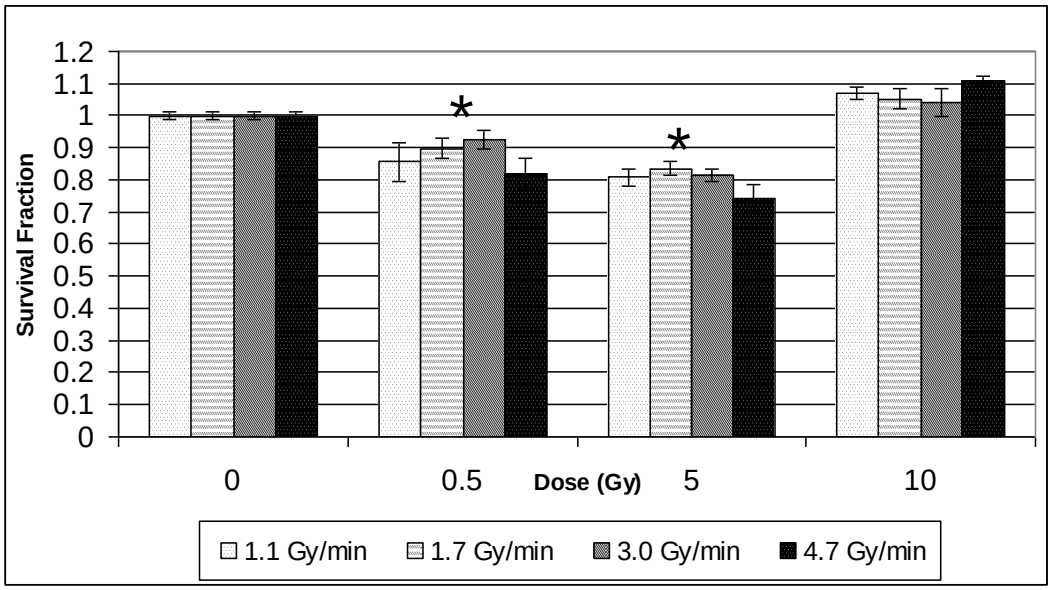

Figure A-4: Variation in the clonogenic survival fraction (% of control plating efficiency (PE)) of bystander cells using the ^{60}Co source. The number of flasks used per dose and dose rate is n = 9. * $p < 0.03$ relative to control SF for all dose rates.

Figure A-4 shows a clear decrease in the survival fraction of bystander cells at doses of 0.5 and 5 Gy. These average survival fractions (SF) ranged from 92% to 82% for 0.5 Gy and 83% to 74% for 5 Gy. The decrease in survival fraction from controls was statistically significant (* $p < 0.03$) across all dose rates for both 0.5 and 5 Gy but no significant differences in the SF were seen between dose rates at these doses.

In order to examine if possible dose rate effects could be seen at higher doses, irradiation at 10 Gy was performed. This dose has largely been unexamined with HPV-G due to the previous literature showing a decrease in the survival fraction at low doses that subsequently 'saturates' as dose increases upwards to 5 Gy (Seymour and Mothersill 2000). As clearly seen in Figure A-4, survival fraction at 10 Gy increased significantly across all dose rates relative to both 0.5 Gy and 5 Gy reaching levels either at or above

control levels. There was no statistically significant difference in survival fraction between dose rates at 10 Gy.

Next, cells were irradiated over a range of dose rates using 20 MeV electrons obtained via LINAC. Figure A-5 illustrates the survival fraction data for direct cell irradiation while Figure A-6 shows data for bystander recipients.

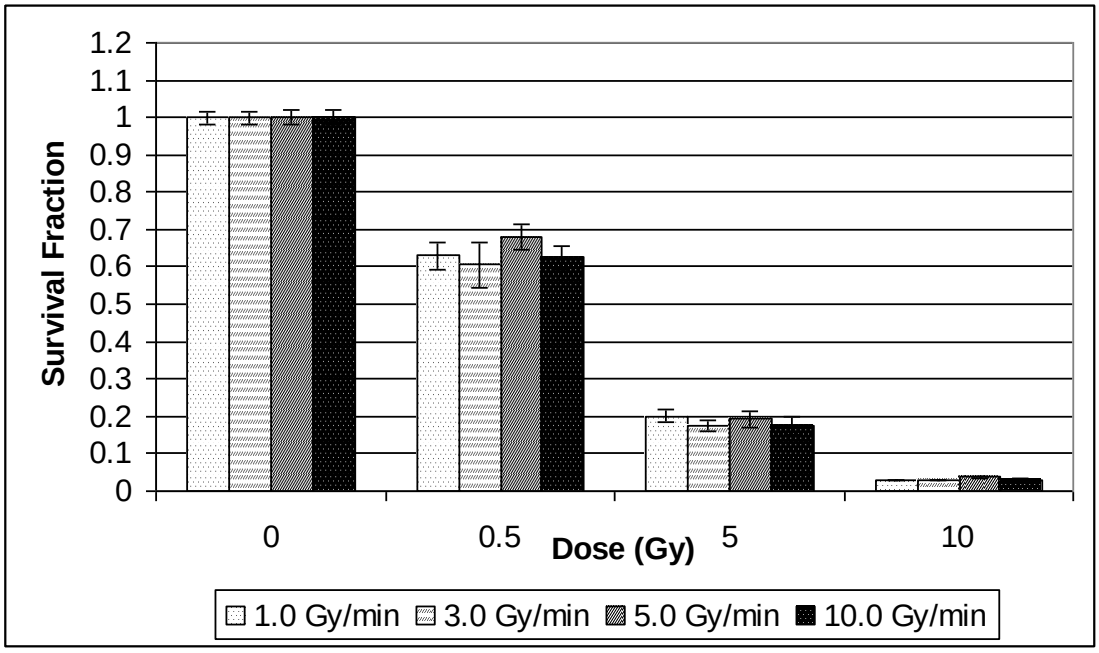

Figure A-5: Variation in clonogenic survival fraction (% of control plating efficiency (PE)) of directly irradiated cells using 20 MeV electrons. The number of flasks used per dose and dose rate is n = 9.

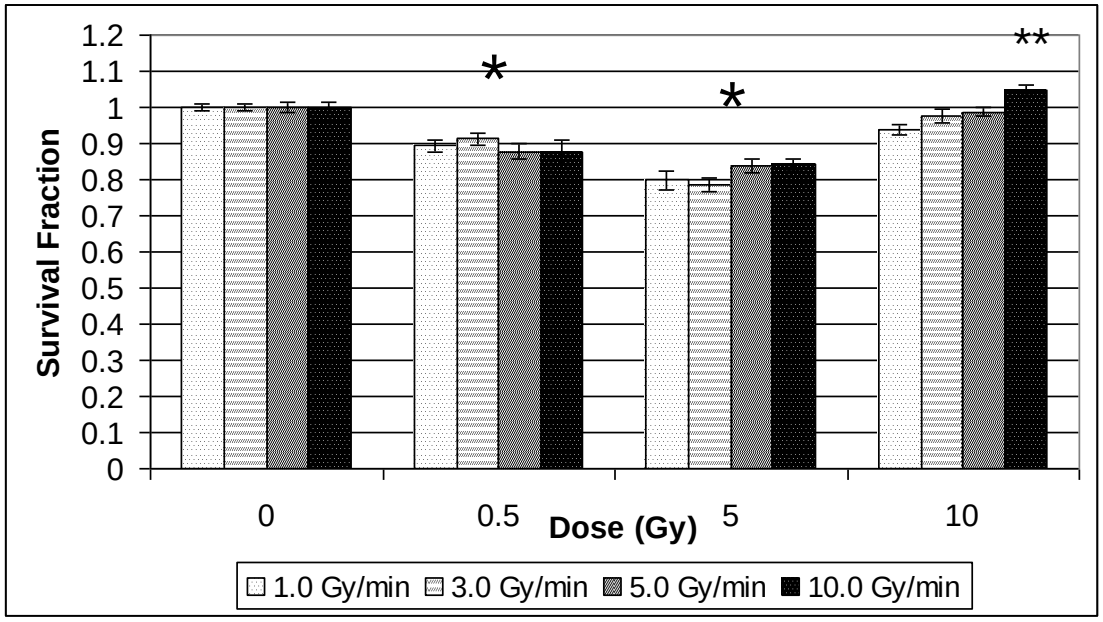

Figure A-6: Variation in clonogenic survival fraction (% of control plating efficiency (PE)) of bystander cells using 20 MeV electrons. The number of flasks used per dose and dose rate is n = 9 except for 1.0 Gy min^{-1} and 3.0 Gy min^{-1} at 10 Gy where n = 6. * $p <$ 0.0004 relative to control for all dose rates. ** Statistically significant for 10.0 Gy min^{-1} SF relative to 1 Gy min^{-1} SF at 10 Gy. See Table A-1 for p values.

As was the case with ^{60}Co source, a decrease in survival fraction was seen across all dose rates at doses of 0.5 and 5 Gy. The average SF ranged from 91% - 87% for 0.5 Gy and 84% - 79% for 5 Gy. This decrease in SF was statistically significant (* $p < 0.0004$) across all dose rates for 0.5 and 5 Gy, but no differences were seen between dose rates at these doses. Similar to the ^{60}Co irradiation at 10 Gy, there was an increase in SF for electron irradiation at 10 Gy relative to either 0.5 Gy or 5 Gy. This SF ranged from slightly below and above control levels (94% - 105% as dose rate increased) with $p <$ 0.02 for all dose rates (without Bonferroni correction relative to 5 Gy).

Of particular interest is that the increase in SF at 10 Gy appears to be stronger as dose rate increases, a phenomenon not seen with ^{60}Co. Upon further analysis, it is clear that a significant difference in SF can be seen when comparing 10.0 Gy min^{-1} SF with 1

Gy min^{-1} SF but not with 5 Gy min-1 or 3 Gy min-1 SF (with Bonferroni correction; see Table A-1).

Table A-1: A comparison of dose rate survival fractions at 10 Gy using 20 MeV electrons[a].

Dose rate 1 vs. Dose rate 2	Dose rate 1 SF	Dose rate 2 SF	*p* value	Bonferroni Corrected *p* value
10 Gy min^{-1} vs. 5 Gy min^{-1}	1.05 (± 0.02)	0.99 (± 0.02)	0.0077	0.069
10 Gy min^{-1} vs. 3 Gy min^{-1}	1.05 (± 0.02)	0.98 (± 0.02)	0.0191	0.1146
10 Gy min^{-1} vs. 1 Gy min^{-1}	1.05 (± 0.02)	0.94 (± 0.02)	0.0008	0.0048

[a] The number of flasks used is n = 9 for all SF except 1.0 Gy min^{-1} and 3.0 Gy min^{-1} where n = 6. Data are presented as mean ± (standard error). *p* values obtained using the student t-test.

It is noteworthy that the dependence on dose rate occurred with a dose rate (10.0 Gy min^{-1}), which was unattainable with the ^{60}Co unit (due to a minimum SSD of 48 cm because of the collimator on the unit). Next, we examined clinically relevant dose rates between ^{60}Co and LINAC radiotherapy machines. Since the dose rates examined were not all identical, closely matched dose rates were compared to minimize any changes in survival fraction due to dose rate and thus we strictly look at difference created via the radiation of similar LET. Therefore, these doses were 1.1 and 3.0 Gy min^{-1} for the ^{60}Co unit and 1.0 and 3.0 Gy min^{-1} with 20 MeV electrons. Figure A-7 compares 1.1 Gy min^{-1} (^{60}Co) and 1.0 Gy min^{-1} (electrons) while Figure A-8 compares 3.0 Gy min^{-1} (^{60}Co) and 3.0 Gy min^{-1} (electrons).

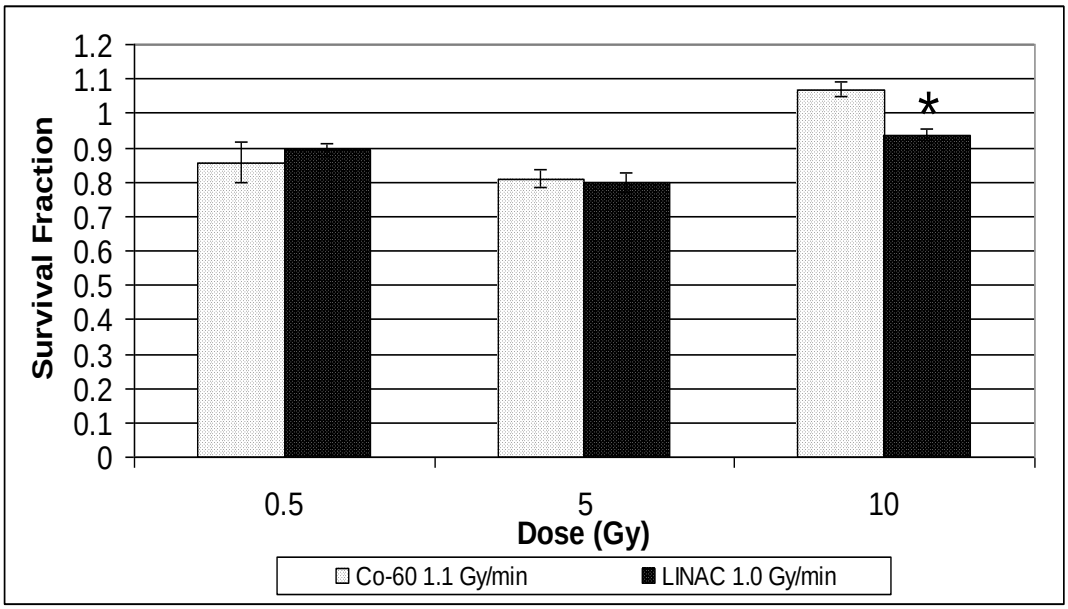

Figure A-7: Variation in clonogenic survival fraction (% of control plating efficiency (PE)) of bystander cells using ^{60}Co source and 20 MeV electrons at 1.1 Gy min^{-1} and 1.0 Gy min^{-1} respectively. The number of flasks used per dose and dose rate is n = 9 for ^{60}Co and n = 6 for electrons. *p = 0.009 for SF difference at 10 Gy.

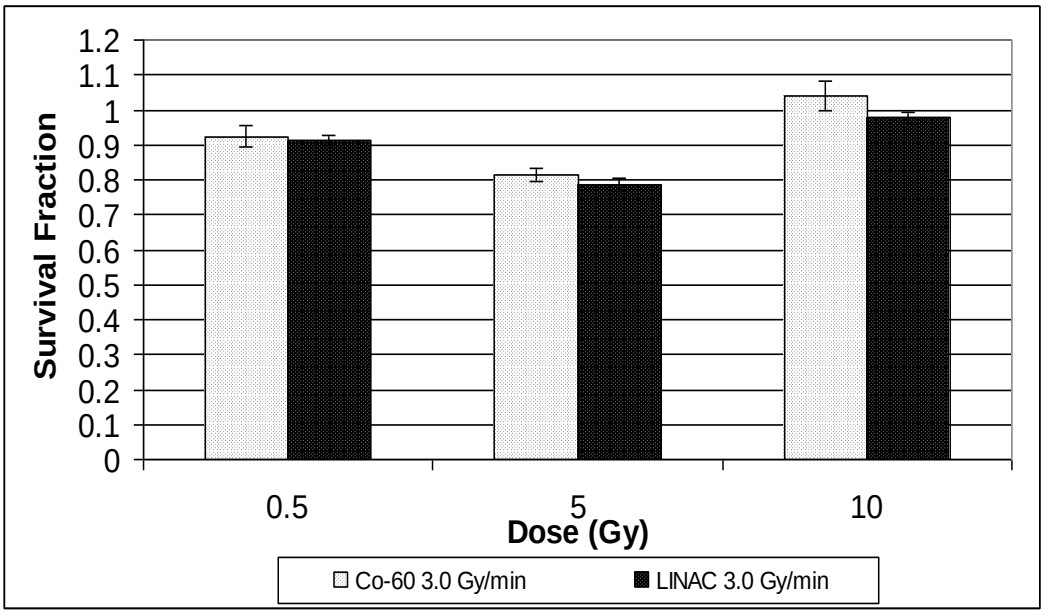

Figure A-8: Variation in clonogenic survival fraction (% of control plating efficiency (PE)) of bystander cells using ^{60}Co source and 20 MeV electrons at 3.0 Gy min^{-1}. The number of flasks used per dose and dose rate is n = 9 for ^{60}Co and n = 6 for electrons. No significant differences seen across all doses.

Figure A-7 shows that at lower dose (0.5 and 5 Gy), there is no difference in bystander cell survival between the low LET radiation sources. However, at a dose of 10 Gy, there was a significant difference in the survival fraction increase with ^{60}Co showing greater recovery ($p = 0.009$). As is shown in Figure A-8, 3.0 Gy min^{-1} γ-radiation created SF results nearly identical to those observed with 20 MeV electrons, and no significant difference was seen across all doses.

Lastly, we examined the effect of increased number of recipients on survival fraction. The goal was to determine if this reporter cell line had a dependence on a "signal-to-cell" ratio between the signal produced in the ICCM and the amount of recipient cells available to take up the signal upon medium transfer. This may explain why the survival fraction of recipient cells appears to saturate after low doses and, as shown here, increases at high doses. The hypothesis was that increases in radiation dose increase the amount of signal present in the ICCM, but that its effects on recipients may be regulated once a saturation point is reached and in fact, the bystander signal may work via some form of negative-feedback mechanism. Therefore, to test the hypothesis, cells were plated as outlined in the Methods section and donor cells were irradiated at dose rates of 5.0 and 10.0 Gy min^{-1} with 20 MeV electrons produced via LINAC. The recipient survival fraction can be seen in Figure A-9.

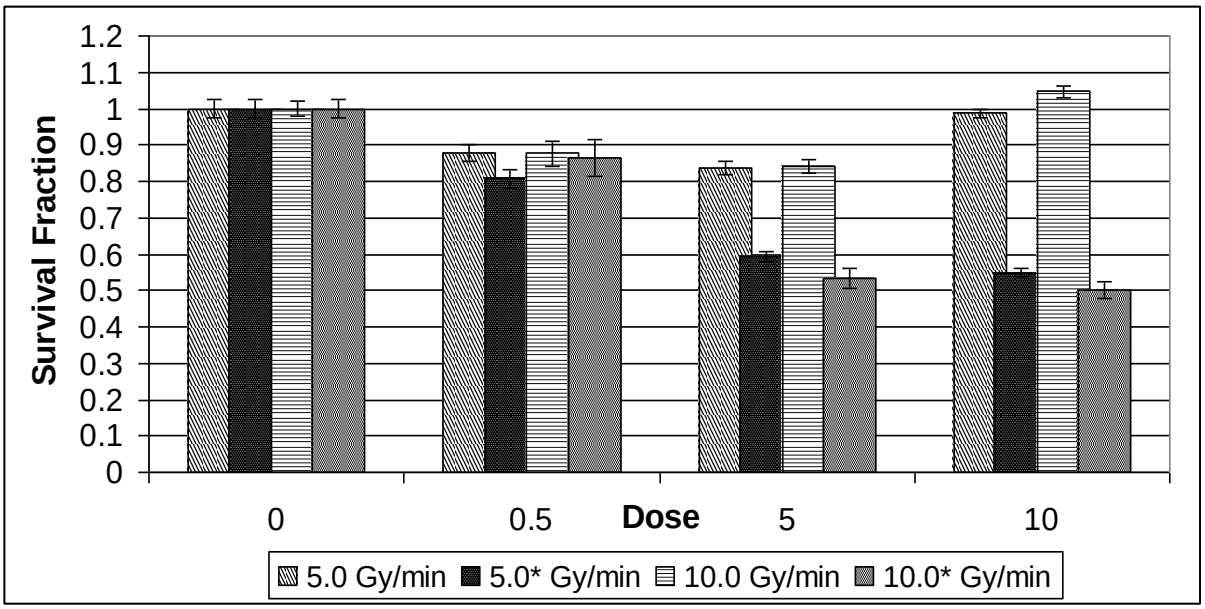

Figure A-9: Variation in the clonogenic survival fraction (% of control plating efficiency (PE)) of bystander recipient cells using 20 MeV electrons at dose rates of 5.0 and 10.0 Gy min^{-1}. The number of flasks used per dose and dose rate is n = 9. For dose rates labelled '5.0 Gy min^{-1}' and '10.0 Gy min^{-1}', recipient flasks were plated with 750 cells at every dose point (PE control: ~10-20%). For flasks labelled '*5.0 Gy min^{-1}' and '*10.0 Gy min^{-1}', recipient flasks were plated with 1000 cells in 0.5 Gy flasks, 2000 cells in 5 Gy flasks, and 3000 cells in 10 Gy flasks (PE control: ~ 10-20%).

Here we see that at doses of 0.5 Gy, small differences in the amount of recipient cells make no significant difference. However, at 5 Gy, differences in recipient numbers caused a dramatic difference in average survival fraction with a difference of 25% for the *5.0 Gy min^{-1} sets and 31% for *10.0 Gy min^{-1}. This effect was enhanced even more at 10 Gy as increased numbers of recipients completely abolished an increase in average survival fraction with a difference of 44% for the *5.0 Gy min^{-1} sets and 55% for *10.0 Gy min^{-1}. Furthermore, increased numbers of recipients caused a continued decrease in survival fraction from 5 Gy to 10 Gy for *5.0 Gy min^{-1} (p = 0.03) while survival fraction for *10.0 Gy min^{-1} sets saturated. Also, an increased number of recipients eliminated any

difference in survival fraction seen earlier between 5.0 and 10.0 Gy min^{-1} at 10 Gy (see Table A-1) and no other differences in dose rate were seen at either 0.5 or 5 Gy.

Discussion

It is clear from the data presented that the dose rate and the source of low – LET radiation produce differential responses in the bystander cell death of the keratinocyte cell line HPV-G. The bystander survival fraction using both ^{60}Co γ-radiation and high energy electrons showed typical decreases associated with doses of 0.5 Gy and 5 Gy and was shown to be independent of the dose rate given by either source. However, upon irradiation with a larger dose of 10 Gy, the bystander cell death associated with lower dose was essentially abolished and in fact a proliferative response was observed. This response was independent of dose rate for ^{60}Co irradiation, while very high doses of high energy electrons received via LINAC exaggerated these responses relative to other dose rates used to give the same dose provided the dose rate difference was large enough. By examination of this higher dose response, this may aid in determining what possible mechanism(s) underlies bystander signalling.

It is well-known that the primary source of cell stress/damage associated with both ^{60}Co γ-radiation and electron irradiation is primarily through the production of free radicals and reactive oxygen species (ROS). Electrons achieve this through direct ionization of target atoms (primarily water molecules) while γ rays emitted from ^{60}Co first produce Compton or photoelectrons and then these secondary electrons produce radicals in the same way with primary electrons (the so-called 'indirect action'). In either

case, the production of free radicals and ROS increases as the dose increases. ROS have been implicated as a possible source of bystander response (Azzam *et al* 2002, Lyng *et al* 2000, 2002, Shao *et al* 2005); however, due to its short half-life (10^{-9} – 10^{-10} seconds) it appears unlikely as the direct 'factor' that mitigates bystander effects via medium transfer. Therefore, a factor(s) that is capable of activation or cleavage from donor cells via ROS is a more likely candidate. It may be that transforming growth factor (TGF) beta1 (TGF-beta1) is just such a secreted factor (for review, see Blobe *et al* (2000), Miyazono (2000), Miyazono *et al* (2000), Wenner and Yan (2003)). TGF-beta1 is a multifunctional cytokine found in nearly all human cells. In particular, for keratinocytes, it increases production of extracellular matrix, increases synthesis of plasminogen activator and its inhibitor (PAI-1) and, most prominently, it causes growth inhibition (Hashimoto 2000). This cytokine has been found to be responsible for bystander effects mediated in both normal human fibroblasts (Iyer *et al* 2000) and glioma cell lines (Burdak-Rothkamm *et al* 2007), and has also been shown to mediate cellular responses to DNA damage *in situ* (Ewan *et al* 2002). Although primarily found as latent complex through association with latency-associated peptide (LAP), Barcellos-Hoff and group have shown that ROS are a potent mediator of activation of TGF-beta1 from its latent complex (Barcellos-Hoff and Dix 1996) and that ^{60}Co γ-irradiation increases the amount of active TGF-beta1 with increases in dose (Barcellos-Hoff *et al* 1994, Ehrhart *et al* 1997). This increase in active TGF-beta1 was seen within 1 hour post-irradiation (the time used here for medium transfer) and shown to persist for days (Barcellos-Hoff *et al* 1994). Also, with keratinocytes, excessive amounts of active TGF-beta1 have been

shown to abolish its growth inhibitory effects thus showing that regulation is controlled via a negative-feedback mechanism (Hashimoto 2000).

This may help explain the bystander response seen for both the γ and higher energy electron irradiation here. As dose increases, this increases the production of free radicals and ROS as well as DNA damage in our donor cells. With these increases, more TGF-beta1 is activated from its latent complex and at the time of medium transfer; active TGF-beta1 is present within the conditioned medium. Upon an application of the ICCM to recipient cells, the survival fraction is decreased in a dose-dependent manner until saturation is reached and a subsequent recovery at high doses. This precisely correlates with the behaviour of TGF-beta1. Small amounts of active TGF-beta1 (produced at low doses) lead to a relatively small amount of active TGF-beta1 able to bind to each recipient. As the amount of active TGF-beta1 in the ICCM increases (caused by increases in dose) more TGF-beta1 is able to bind to each cell and negative feedback starts to prevent its growth inhibitive effects, causing an apparent saturation in the survival fraction. Finally, when relatively large amounts of TGF-beta1 are present in the ICCM (produced by a large dose), each recipient receives large amounts of TGF-beta1. At this point, the negative-feedback mechanism prevents subsequent growth inhibition leading to the apparent 'recovery' in the survival fraction seen at high doses for both γ and high energy electron radiations. With this in mind, this could explain the elimination of the recovery effect and decrease in survival fraction seen when larger numbers of recipients were plated (see Figure A-9). With more recipients present to receive the same amount of signal (donor cell numbers remained constant at 300 000), there would be less

TGF-beta1 binding per recipient cell. With less signal to each cell, activation of a negative-feedback mechanism may be minimized and therefore result in a larger decrease survival fraction. It is important to note that this situation could still play out as outlined above even if TGF-beta1 were not 'the transferred signal' in the medium but rather was a down-stream recipient of the signalling mechanism (i.e. the TGF-beta1 is activated in the recipient cells in a manner that correlates with the amount of signal produced by the donors).

When examining the apparent difference in high dose/dose rate survival fractions seen with 20 MeV electrons, the short lifetime of free radicals and ROS is most likely the dominant contributing factor. At a dose rate of 10.0 Gy min^{-1}, there will be more free radicals and ROS present within the targeted cell per unit time. Thus, with more ROS present at any given time, there is a larger chance of it activating the bystander mechanism (possibly TGF-beta1) prior to reconstituting with other elements and stabilizing. With a larger probability of activating the bystander mechanism, there would be more signal produced at 10.0 Gy min^{-1} and 10 Gy and thus possibly explaining the differing bystander behaviour. If the bystander mechanism (or at least part of it) works via a negative-feedback response at high concentrations, then this could aid in explaining the observed behaviour. With lower doses, the difference in the amount of ROS available per unit time would be negligible (again, due to its short lifetime); thus why no dose rate effect was seen at 0.5 Gy and 5 Gy for 20 MeV electrons. Similarly, with ^{60}Co irradiation, the highest achievable dose rate was 4.7 Gy min^{-1}, and again differences in the amount of available ROS in each cell at any given time may be negligible.

There was also difference in the survival fraction seen at a low dose rate when comparing similar survival fraction data between sources (Figure A-7). This may point to a possibility that simply classifying bystander results in terms of high or low LET may be insufficient. Both 20 MeV electrons and ^{60}Co γ rays are classified as low LET radiation. However, as mentioned above, they differ in the method they produce free radicals and ROS, electrons via direct ionization and γ rays through indirect ionization. Due to Compton scattering causing indirect ionization, γ rays do not have a strict definition for LET but rather a small spectrum of values, approximately 0.2-2 keV μm^{-1}, producing fast recoil electrons of varying energies (Johns and Cunningham 1983, p 672). On the other hand, 20 MeV electrons have a fairly constant LET over energies of 20 MeV down to 500 keV where it subsequently reaches its Bragg peak (Johns and Cunningham 1983, p 213). With an initial energy of 20 MeV, if we assume the electron loses energy by the continuous slowing down approximation (CSDA), then with the irradiation set-up as outlined in Methods, the electrons will have an energy of approximately 15.5 MeV at the irradiation site (i.e. the cells) which is well within the range noted above. Differences in biological radiation responses have been known for quite some time. In particular, experiments with human lymphocytes have shown differences in the ability of different low LET radiation to produce radiation damage. For instance, comparison of work by Purrot *et al* (1977) and Lloyd *et al* (1975) is a clear demonstration of the effects of different dose rates on dicentric chromosome aberrations. Purrot *et al* showed that irradiating healthy, male donor blood with 15 MeV electrons receiving a dose of 7.4 Gy at 1 Gy min^{-1} yielded approximately 2.8 dicentric aberrations

per lymphocyte cell (Purrott *et al* 1977). Work by Lloyd *et al* showed that irradiating healthy male donor blood to 8 Gy at a dose rate of 0.5 Gy min^{-1} with ^{60}Co source yielded approximately 3.4 dicentric chromosome aberrations per cell (Lloyd *et al* 1975). Therefore, it is possible that ^{60}Co ellicits a slightly stronger stress response (i.e. bystander response) than our 20 MeV electrons at these high doses (i.e. 10 Gy) and low dose rates. Thus, there appears to be some LET dependence (at least at high doses) which diminishes with increases in dose rate.

Not only does the data presented here give possible insight into potential mechanism(s) underlying radiation-induced bystander effects, but is also of clinical relevance as well. In particular the data presented here shows not a saturating signal as dose increase but instead a proliferative response at high doses that is dependent of dose rate for high energy electrons. This could be of specific relevancy in radiotherapy where large dose fractions are administered such as with cranial radiosurgery, stereotactic body radiation therapy, and intraoperative radiation therapy (IORT). For example, with IORT, a surgically exposed tumour is bombarded with a single high dose administered via a mobile LINAC system (Beddar *et al* 2006). From the evidence presented here, it is possible that even if positive bystander effects (i.e. one that increases cell death) appear to saturate for a particular cell line, these may in fact not be the case when single large doses are used. Therefore, if bystander responses are confirmed *in vivo* and wish to be taken into effect to amplify treatment effects, 'slightly' lower dose might be more beneficial in treatment planning to ensure that no proliferation response is mediated. Also, extra attention may be needed when delivering high doses depending on the cell

type mediating the bystander responses. For cell types that produce a proliferative bystander response, ensuring that all appropriate tissue is irradiated is of even more importance as any cells left indirectly irradiated may be stimulated to increase proliferation and thus decrease the efficiency of treatment. Even in conventional radiation therapy where dose fractionazation is utilized to spare normal tissue, such bystander effects observed here may be important factors in treatment planning if determined *in vivo*. Specifically, it has been shown that fractionating the dose in medium transfer experiments does not reduce the ability of the ICCM to produce bystander effects (Mothersill and Seymour 2002). Thus if bystander effects are to be utilized *in vivo*, careful consideration of the total dose (and not just the individual fractionated doses) must be taken into account. As can be seen from the data presented here, larger total doses might be in fact beneficial in non-targeted, normal tissue as bystander cell death may be abolished and proliferation of healthy tissue stimulated. Finally, the choice of source used in treatment may be important if two different radiotherapy sources are used to treat similar cell types. As shown here, different low LET radiotherapy sources produced different bystander effects at high doses and low dose rates. Therefore, if bystander responses are to be incorporated into external radiotherapy treatment planning, such differences may need to be taken into account in order to maximize treatment efficiency and minimize negative effects such as signal saturation or induction of proliferation responses.

Lastly, significant variability in SF for different dose rates is evident in Figure A-3. From the radiobiological standpoint these differences are not expected in this range of

dose rates. It is possible that the limited sensitivity of the clonogenic assay is responsible for the ‘noise’ in the direct irradiation data. This also limits our ability to characterize dose rate effects accurately in the ICCM – exposed cells. Further experiments using more sensitive endpoints such as calcium flux may help quantify this effect.

Conclusion

The effect of dose rate on the radiation-induced bystander cell survival was studied. Cells were irradiated using a ^{60}Co radiotherapy unit as well as with 20 MeV electrons produced via a LINAC. The medium from the irradiated donor cells (ICCM) was filtered and applied to recipient cells, whereby a clonogenic assay was undertaken ~12 days after medium transfer. It was found for both γ and electron irradiation that the survival fraction of recipients decreased for doses of 0.5 Gy and 5 Gy. A subsequent recovery of the survival fraction to near or above control levels was observed for the ICCM from 10 Gy irradiation for both irradiation sets. There was no dose dependence for ^{60}Co irradiation, but a significant difference in the survival fraction was observed for electron irradiation at high doses and dose rates. Furthermore, a comparison of survival fractions was demonstrated between ^{60}Co and 20 MeV electron irradiations with closely matched dose rates. This showed a significant increase in survival fraction 'recovery' at 10 Gy with a low dose rate for ^{60}Co compared to 20 MeV electrons. Lastly, the apparent increase in the survival fraction at 10 Gy could be abolished by the plating of increased numbers of recipient cells, leading to a greater decrease in the survival fraction at doses of 5 Gy and 10 Gy. Such evidence may lead to possible insight into the mechanism(s) and nature of bystander signal production, how these phenomena are tested and eventually their use in optimization in external radiotherapy.

References

Azzam E I, de Toledo S M, Spitz D R and Little J B 2002 Oxidative metabolism modulates signal transduction and micronucleus formation in bystander cells from alpha-particle-irradiated normal human fibroblast cultures *Cancer Res.* **62** 5436-5442

Barcellos-Hoff M H, Derynck R, Tsang M L and Weatherbee J A 1994 Transforming growth factor-beta activation in irradiated murine mammary gland *J.Clin.Invest* **93** 892-899

Barcellos-Hoff M H and Dix T A 1996 Redox-mediated activation of latent transforming growth factor-beta 1 *Mol.Endocrinol.* **10** 1077-1083

Beddar A S, Briere T M and Ouzidane M 2006 Intraoperative radiation therapy using a mobile electron linear accelerator: field matching for large-field electron irradiation *Phys.Med.Biol.* **51** N331-N337

Belyakov O V, Mitchell S A, Parikh D, Randers-Pehrson G, Marino S A, Amundson S A, Geard C R and Brenner D J 2005 Biological effects in unirradiated human tissue induced by radiation damage up to 1 mm away *Proc.Natl.Acad.Sci.U.S.A* **102** 14203-14208

Bishayee A, Hill H Z, Stein D, Rao D V and Howell R W 2001 Free radical-initiated and gap junction-mediated bystander effect due to nonuniform distribution of incorporated radioactivity in a three-dimensional tissue culture model *Radiat.Res.* **155** 335-344

Blobe G C, Schiemann W P and Lodish H F 2000 Role of transforming growth factor beta in human disease *N.Engl.J.Med.* **342** 1350-1358

Burdak-Rothkamm S, Short S C, Folkard M, Rothkamm K and Prise K M 2007 ATR-dependent radiation-induced gammaH2AX foci in bystander primary human astrocytes and glioma cells *Oncogene* **26** 993-1002

Cooper B, Schneider S, Bohl J, Jiang Y, Beaudet A and Vande P S 2003 Requirement of E6AP and the features of human papillomavirus E6 necessary to support degradation of p53 *Virology* **306** 87-99

Ehrhart E J, Segarini P, Tsang M L, Carroll A G and Barcellos-Hoff M H 1997 Latent transforming growth factor beta1 activation in situ: quantitative and functional evidence after low-dose gamma-irradiation *FASEB J.* **11** 991-1002

Ewan K B, Henshall-Powell R L, Ravani S A, Pajares M J, Arteaga C, Warters R, Akhurst R J and Barcellos-Hoff M H 2002 Transforming growth factor-beta1 mediates cellular response to DNA damage in situ *Cancer Res.* **62** 5627-5631

Hall E J 2003 The bystander effect *Health Phys.* **85** 31-35

Hashimoto K 2000 Regulation of keratinocyte function by growth factors *J.Dermatol.Sci.* **24 Suppl 1** S46-S50

Hei T K 2006 Cyclooxygenase-2 as a signaling molecule in radiation-induced bystander effect *Mol.Carcinog.* **45** 455-460

Iyer R and Lehnert B E 2002a Alpha-particle-induced increases in the radioresistance of normal human bystander cells *Radiat.Res.* **157** 3-7

Iyer R and Lehnert B E 2002b Low dose, low-LET ionizing radiation-induced radioadaptation and associated early responses in unirradiated cells *Mutat.Res.* **503** 1-9

Iyer R, Lehnert B E and Svensson R 2000 Factors underlying the cell growth-related bystander responses to alpha particles *Cancer Res.* **60** 1290-1298

Johns H E and Cunningham J R 1983 *The Physics of Radiology* ed 4 (Springfield, IL: Charles C. Thomas) 213, 672

Little J B 2006 Cellular radiation effects and the bystander response *Mutat.Res.* **597** 113-118

Liu Z, Mothersill C E, McNeill F E, Lyng F M, Byun S H, Seymour C B and Prestwich W V 2006 A dose threshold for a medium transfer bystander effect for a human skin cell line *Radiat.Res.* **166** 19-23

Lorimore S A, Coates P J and Wright E G 2003 Radiation-induced genomic instability and bystander effects: inter-related nontargeted effects of exposure to ionizing radiation *Oncogene* **22** 7058-7069

Lyng F M, Maguire P, Kilmurray N, Mothersill C, Shao C, Folkard M and Prise K M 2006a Apoptosis is initiated in human keratinocytes exposed to signalling factors from microbeam irradiated cells *Int.J.Radiat.Biol.* **82** 393-399

Lyng F M, Maguire P, McClean B, Seymour C and Mothersill C 2006b The involvement of calcium and MAP kinase signaling pathways in the production of radiation-induced bystander effects *Radiat.Res.* **165** 400-409

Lyng F M, Seymour C B and Mothersill C 2000 Production of a signal by irradiated cells which leads to a response in unirradiated cells characteristic of initiation of apoptosis *Br.J.Cancer* **83** 1223-1230

Lyng F M, Seymour C B and Mothersill C 2002 Initiation of apoptosis in cells exposed to medium from the progeny of irradiated cells: a possible mechanism for bystander-induced genomic instability? *Radiat.Res.* **157** 365-370

Maguire P, Mothersill C, Seymour C and Lyng F M 2005 Medium from irradiated cells induces dose-dependent mitochondrial changes and BCL2 responses in unirradiated human keratinocytes *Radiat.Res.* **163** 384-390

Matsumoto H, Hayashi S, Hatashita M, Ohnishi K, Shioura H, Ohtsubo T, Kitai R, Ohnishi T and Kano E 2001 Induction of radioresistance by a nitric oxide-mediated bystander effect *Radiat.Res.* **155** 387-396

McIlrath J, Lorimore S A, Coates P J and Wright E G 2003 Radiation-induced genomic instability in immortalized haemopoietic stem cells *Int.J.Radiat.Biol.* **79** 27-34

Mitchell S A, Marino S A, Brenner D J and Hall E J 2004 Bystander effect and adaptive response in C3H 10T(1/2) cells *Int.J.Radiat.Biol.* **80** 465-472

Miyazono K 2000 Positive and negative regulation of TGF-beta signaling *J.Cell Sci.* **113 (Pt 7)** 1101-1109

Miyazono K, ten Dijke P and Heldin C H 2000 TGF-beta signaling by Smad proteins *Adv.Immunol.* **75** 115-157

Mothersill C, Lyng F, Seymour C, Maguire P, Lorimore S and Wright E 2005 Genetic factors influencing bystander signaling in murine bladder epithelium after low-dose irradiation in vivo *Radiat.Res.* **163** 391-399

Mothersill C, Rea D, Wright E G, Lorimore S A, Murphy D, Seymour C B and O'Malley K 2001 Individual variation in the production of a 'bystander signal' following irradiation of primary cultures of normal human urothelium *Carcinogenesis* **22** 1465-1471

Mothersill C and Seymour C 1997 Medium from irradiated human epithelial cells but not human fibroblasts reduces the clonogenic survival of unirradiated cells *Int.J.Radiat.Biol.* **71** 421-427

Mothersill C and Seymour C 2001 Radiation-induced bystander effects: past history and future directions *Radiat.Res.* **155** 759-767

Mothersill C and Seymour C 2005 Radiation-induced bystander effects: are they good, bad or both? *Med.Confl.Surviv.* **21** 101-110

Mothersill C and Seymour C B 1998 Cell-cell contact during gamma irradiation is not required to induce a bystander effect in normal human keratinocytes: evidence for release during irradiation of a signal controlling survival into the medium *Radiat.Res.* **149** 256-262

Mothersill C and Seymour C B 2002 Bystander and delayed effects after fractionated radiation exposure *Radiat.Res.* **158** 626-633

Mothersill C, Seymour C B and Joiner M C 2002 Relationship between radiation-induced low-dose hypersensitivity and the bystander effect *Radiat.Res.* **157** 526-532

Mothersill C, Seymour R J and Seymour C B 2004 Bystander effects in repair-deficient cell lines *Radiat.Res.* **161** 256-263

Nagasawa H and Little J B 1992 Induction of sister chromatid exchanges by extremely low doses of alpha-particles *Cancer Res.* **52** 6394-6396

Nagasawa H and Little J B 1999 Unexpected sensitivity to the induction of mutations by very low doses of alpha-particle radiation: evidence for a bystander effect *Radiat.Res.* **152** 552-557

Pirisi L, Creek K E, Doniger J and DiPaolo J A 1988 Continuous cell lines with altered growth and differentiation properties originate after transfection of human keratinocytes with human papillomavirus type 16 DNA *Carcinogenesis* **9** 1573-1579

Poon R C, Agnihotri N, Seymour C and Mothersill C 2007 Bystander effects of ionizing radiation can be modulated by signaling amines *Environ.Res.* **105** 200-211

Prise K M, Belyakov O V, Folkard M and Michael B D 1998 Studies of bystander effects in human fibroblasts using a charged particle microbeam *Int.J.Radiat.Biol.* **74** 793-798

Prise K M, Folkard M and Michael B D 2003 A review of the bystander effect and its implications for low-dose exposure *Radiat.Prot.Dosimetry.* **104** 347-355

Puck T T and Marcus P I 1956 Action of x-rays on mammalian cells *J.Exp.Med.* **103** 653-666

Sawant S G, Randers-Pehrson G, Geard C R, Brenner D J and Hall E J 2001 The bystander effect in radiation oncogenesis: I. Transformation in C3H 10T1/2 cells

in vitro can be initiated in the unirradiated neighbors of irradiated cells *Radiat.Res.* **155** 397-401

Sawant S G, Zheng W, Hopkins K M, Randers-Pehrson G, Lieberman H B and Hall E J 2002 The radiation-induced bystander effect for clonogenic survival *Radiat.Res.* **157** 361-364

Seymour C B and Mothersill C 2000 Relative contribution of bystander and targeted cell killing to the low-dose region of the radiation dose-response curve *Radiat.Res.* **153** 508-511

Shao C, Aoki M and Furusawa Y 2001 Medium-mediated bystander effects on HSG cells co-cultivated with cells irradiated by X-rays or a 290 MeV/u carbon beam *J.Radiat.Res.(Tokyo)* **42** 305-316

Shao C, Aoki M and Furusawa Y 2003a Bystander effect on cell growth stimulation in neoplastic HSGc cells induced by heavy-ion irradiation *Radiat.Environ.Biophys.* **42** 183-187

Shao C, Folkard M, Michael B D and Prise K M 2004 Targeted cytoplasmic irradiation induces bystander responses *Proc.Natl.Acad.Sci.U.S.A* **101** 13495-13500

Shao C, Folkard M, Michael B D and Prise K M 2005 Bystander signaling between glioma cells and fibroblasts targeted with counted particles *Int.J.Cancer* **116** 45-51

Shao C, Furusawa Y, Aoki M and Ando K 2003b Role of gap junctional intercellular communication in radiation-induced bystander effects in human fibroblasts *Radiat.Res.* **160** 318-323

Wenner C E and Yan S 2003 Biphasic role of TGF-beta1 in signal transduction and crosstalk *J.Cell Physiol* **196** 42-50

Zhou H, Randers-Pehrson G, Waldren C A, Vannais D, Hall E J and Hei T K 2000 Induction of a bystander mutagenic effect of alpha particles in mammalian cells *Proc.Natl.Acad.Sci.U.S.A* **97** 2099-2104

Part B

Induction of bystander response in human glioma cell line using high energy electrons: A role for TGF – β1

M. D. Gow, C. B. Seymour, L. A. Ryan and C. E. Mothersill[1]

[1] Medical Physics and Applied Radiation Sciences Department, McMaster University, Hamilton, Ontario, Canada L8S 4K1

Address for correspondence:
Medical Physics and Applied Radiation Sciences Department
McMaster University
1280 Main Street West, Hamilton, Ontario, Canada
L8S 4K1

OBJECTIVE

To determine if through manipulation of dose and dose rate in ICCM irradiation treatment for medium transfer experiments, a bystander cell death can be induced in a cell line where no previous effect has been observed. Any potentially observed effect is to be compared and contrasted against a well - established reporter cell line. Examination of ICCM for the presence of possible cytokines TGF-α and TGF-β1 is also pursued to determine any possible correlation with observed behaviour. This examination seeks to stress the importance of dose rate and dose in ICCM production and resultant observed bystander cell death response as well as identify potentially critical factors to any observed effect.

Note: This work has been published in the academic journal *Radiation Research*:

Gow, M. D., Seymour, C. B., Ryan, L. A. and Mothersill, C. E. Induction of Bystander Response in Human Glioma Cells using High-Energy Electrons: A Role for TGF-β1. Radiat. Res. 173, 769–778 (2010).

Differences from the published version include minor modification to figure numbering and formatting to coincide with the structure of the thesis.

Abstract

We examined bystander cell death produced in T98G cells by exposure to irradiated cell conditioned medium (ICCM) produced by high-energy 20 MeV electrons at a dose rate of 10 Gy min^{-1} and doses up to 20 Gy. ICCM induced a bystander response in T98G glioma cells, reducing recipient cell survival by more than 25% below controls at 5 and 10 Gy. Higher doses increased survival to near control levels. ICCM was analyzed for the presence of transforming growth factor α (TGF-α) and transforming growth factor β1 (TGF-β1). Monoclonal antibodies for TGF-α (TGF-α mAb) and TGF-β1 (TGF-β1 mAb) were added to the ICCM to neutralize any potential effect of the cytokines. The results indicate that TGF-α was not present in the ICCM and addition of TGF-α mAb to the ICCM had no effect on bystander cell survival. No active TGF-β1 was present in the ICCM; however, addition of TGF-β1 mAb completely abolished bystander death of reporter cells at all doses. These results indicate that bystander cell death can be induced in T98G glioma if a large enough radiation stress is applied and that TGF-β1 plays a downstream role in this response.

Introduction

Radiation-induced bystander effects are a well-established phenomenon associated with exposure of biological material to radiation. The effects can be observed through various responses detected in nonirradiated cells that are influenced by irradiated cells *(1–4)*. This effect has been observed in a variety of cell types, and it appears to be independent of TP53 mutation or tumour status, although radioresistant cell lines tend not to show bystander effects *(5–7)*. Exposure to both high- and low-LET radiation have resulted in bystander effects for a variety of end points, including sister chromatid exchange *(8)*, gene mutation *(9,10)*, micronucleus formation *(11–13)*, chromosomal instability *(14)*, transformation *(15)*, decreased clonogenic survival *(6,16–19)*, and apoptosis *(20)*.

A cell's ability to induce or respond to bystander signals is influenced by genetic factors as well as environmental factors *(21,22)*. Targeted microbeam irradiation of cell cytoplasm *(23)* as well as experiments in which medium is transferred from irradiated cells to nonirradiated cells *(6,16,18,24,25)* indicate the release of signalling factors from irradiated cells that influence nonirradiated cells. Although the nature of the bystander signals remains in question, recent research using both targeted microbeam and medium transfer experiments have shown that communication between irradiated and nonirradiated cells can take place via gap junctions *(26,27)* and / or secreted factors *(18,28–30)*, leading to the observed extension of the radiation / stress response beyond targeted cells. In addition, reactive oxygen species (ROS) *(7,31–33)*, nitric oxide (NO)

(7, 23, 34), and Ca^{2+} *(33,35)* have been found to affect bystander signal transmission and / or transduction.

Recently, our group demonstrated that classification of bystander responses as resulting from high- and low-LET radiation may be insufficient *(36)*. It appears from this work that different sources of low-LET radiation can produce slightly different effects. We also showed with human keratinocytes that bystander effects at high doses differ significantly from those seen at low doses (i.e. recovery of surviving fraction of bystander cells back to control levels at 10 Gy) and that high doses and dose rates could exaggerate this effect when high-energy electrons are used.

In light of this, our group undertook an investigation to see whether bystander cell death could be induced in a cell line in which we had not previously seen a bystander effect by irradiating T98G human glioma cells with high-energy electrons at a high dose rate. In previous studies, we found no bystander cell death at 0.5 and 2 Gy using 240 kVp X-rays at 0.2–0.4 Gy min^{-1} *(24)* as well as no cell death for doses up to 5 Gy using ^{60}Co γ-rays at 1.7 Gy min^{-1} *(37)*. T98G cells have shown other bystander effects, such as micronucleus formation and calcium influxes, in previous studies using high-energy microbeam irradiation for both medium transfer and coculture protocols *(38,39)*. In the present study, we used 20 MeV electrons at a dose rate of 10 Gy min^{-1} and cell death was assayed for doses up to 20 Gy.

We also examined the irradiated cell conditioned medium (ICCM) for the presence of two factors possibly associated with the bystander effects observed in T98G cells: transforming growth factor α (TGF-α) and transforming growth factor β1 (TGF-

β1). Irradiation of tumour cells has been shown to increase cleavage of pro-TGF-α and lead to subsequent release of TGF-α into culture medium *(40–42)*. Furthermore, it was shown previously that TGF-α is a primary factor involved in the growth of T98G cells *in vitro (43)* and that it has been a trigger that is responsible for protection of carcinoma cells against radiation-induced cell death *(41)*. We examined the possibility that TGF-α is involved in the lack of bystander cell death observed in T98G cells. TGF-β1 was also examined as a possible bystander signalling factor.

TGF-β1 exists primarily in a latent form (latent TGF-β1 complex) through its association with the latent-associated peptide (LAP). TGF-β1 exerts its effects once LAP has disassociated from the complex and is involved in cell division, differentiation, migration, adhesion, organization and programmed cell death *(44)*. Previous work has shown that ROS are capable of activating TGF-β1 via oxidation of the latency-associated complex *(45)*. TGF-β1 has also been implicated in several bystander end points, including increases in human lung fibroblast growth after α-particle irradiation *(30)* as well as bystander micronucleus formation *(46,47)* and γ-H2AX focus formation indicating DNA double-strand breaks in T98G cells *(28)*. We examined the potential role of TGF-β1 in bystander signalling using a medium transfer protocol and cell death as an end point.

Methods

Cell Culture

T98G human glioma tumor cells [TP53 mutated *(48)*] were grown in DMEM:F12 medium (1:1) supplemented with 10% fetal bovine serum (FBS), 1 µg ml^{-1} hydrocortisone (Sigma, Poole Dorset, UK), 1% penicillin:streptomycin solution and 1% L-glutamine solution. Hepes buffer (12.5 ml of IM solution) was added to help maintain pH.

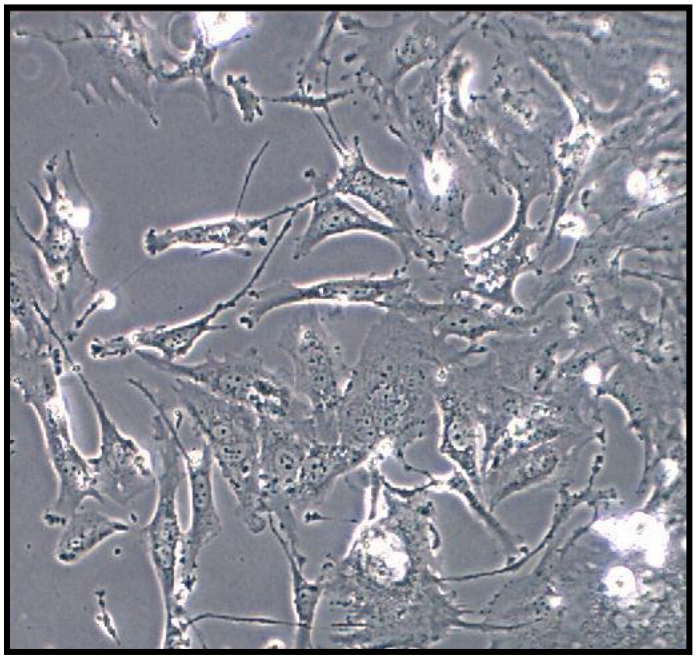

Figure B-1: Morphology of T98G cells.

Except where indicated, all reagents were obtained from Gibco Biocult, supplied by VWR, Burlington Ontario. The cells were maintained in T-75 flasks (NUNC Inc., Uden, Netherlands) and subcultured into T-25 flasks (40 ml volume) for experiments. HPV-G cells were used as a reporter cell line in parallel with autologous T98G reporter cells so

we could compare the response in a well-established line that responds to bystander signals. HPV-G keratinocytes are adherent epithelial cells that were originally derived from a human foreskin primary culture and immortalized by the HPV virus *(49)*. They were obtained as a gift from Prof. J. DiPaolo, NIH, Bethesda, MD, and have been used in our laboratory as a reporter system for bystander signal production in a wide range of experiments *(50,51)*. These cells are non-tumorigenic, have about 30% wild-type p53 expression *(52)*, have a normal epithelial pattern of cobblestone density-inhibited cell growth and demonstrate a stable bystander response when exposed to medium harvested from irradiated cells *(53)*. In a previous study, we used these cells to examine the dependence of the source of the radiation on radiation-induced bystander effects *(36)*.

Bystander Medium Transfer Protocol and Clonogenic Assay

Flasks containing cells that were 85–90% confluent and that had received a medium change the previous day were selected. Cells were removed from the flask using 0.25% w/v trypsin/1 mM EDTA solution (1:1). When the cells had detached, they were resuspended in medium, and an aliquot was counted using a Coulter counter model D_N set at a threshold calibrated for each cell line using a hemocytometer. Appropriate cell numbers were plated for survival using the clonogenic assay technique of Puck and Marcus *(54)*. Flasks destined to donate medium (i.e. donor flasks) were plated with approximately 3×10^5 cells in 5 ml of medium in T-25 flasks (Nucleon, Denmark). Recipient flasks destined to receive irradiated conditioned medium (ICCM) were set up with a plating of approximately 750 cells at the same time that donor flasks were plated.

Medium was harvested 1-h postirradiation, which took place 5 h after plating. Controls for medium only and actual radiation effects (i.e. directly irradiated flasks) were included in each experiment. Controls for transfer of unirradiated medium from densely seeded cultures to cultures seeded at cloning densities were also included in all experiments. Cultures were incubated in 5 ml of culture medium in 25-cm^2, 40-ml flasks (Nunclon) in a humidified 37ºC incubator in an atmosphere of 5% CO_2 in air.

The technique used has been described in detail previously [e.g., see ref. *(6)*]. Briefly, medium was poured off donor flasks, and, as shown previously, contact times after irradiation from 30 min–4 h showed no significant difference in effect on recipient plating efficiency *(6)*. Donor medium was filtered through a 0.22-µm filter used for sterilizing solutions to ensure that no cells could still be present in the transferred medium. ICCM was then either left intact or supplemented with monoclonal anti-TGF-β1 antibody (R&D Systems) at 7 µg ml^{-1} , monoclonal anti-TGF-α antibody (Calbiochem) at 7 µg ml^{-1}, or mouse IgG_1 isotype control at 7 µg ml^{-1}. Culture medium was then removed from the flasks designated to receive irradiated conditioned medium and the filtrate was immediately added to these recipient flasks. A medium change of unirradiated but similarly filtered medium from unirradiated donor flasks containing cells seeded at the donor density of 3 x 10^5 cells/flask was given to controls at the same time. Standard plating efficiency controls were also set up. There was never a significant difference between these two controls. Standard clonogenic survival points after irradiation were also always included and no effect of changing the medium alone was found.

After medium transfer, cultures were left undisturbed in the incubator for 12–13 days to allow for macroscopic colonies to develop. These were then stained with carbol fuchsin.

TGF-α and TGF-β1 Assay

The concentrations of TGF-α and TGF-β1 in the ICCM from irradiated T98G cells was assayed using the human TGF-β1 and TGF-α Quantikine ELISA (R&D Systems) according to the manufacturer's instructions. Small samples were collected from ICCM used in clonogenic assays outlined above and stored in polypropylene tubes at -70ºC. To ensure that freezing TGF-β1 samples did not adversely affect any active TGF-β1 being present in the ICCM, we set up an experiment where ICCM was plated into wells for ELISA immediately after filtering in a time frame very similar to that needed to apply ICCM to recipient cells. Positive controls for the ELISA were those included in the ELISA kit and used to produce the standard calibration curve (0 to 500 pg ml^{-1} for TGF-α and 0 to 2000 pg ml^{-1} for TGF-β1). ''Negative'' controls were the 0 Gy dose and the medium-only samples used to correct for the TGF-β1 present in the serum component. When determining total TGF-β1 content of a sample, acidification by addition of HCl to the samples was performed in accordance with the manufacturer's instructions. This process causes dissociation of the latency-associated peptide (LAP) from the TGF-β1, causing it to be activated and measurable by the ELISA. Total TGF-β1 content was determined for medium-only samples, and this value was subtracted from acidified ICCM samples to determine the TGF-β1 content produced by radiation. In

additional experiments, ICCM was tested by ELISA without acidification to determine whether any active TGF-β1 was present.

Irradiation Procedures

Cultures were irradiated at room temperature with 20 MeV electrons produced by a Varian 21C/D linear accelerator (LINAC) with a linear energy transfer of 0.2 keV μm^{-1} *(55)*. A dose rate of 10 Gy min^{-1} was used, and since 20 MeV electrons have an approximate depth dose maximum of 1.8 cm in water, 1.3 cm of polystyrene was used as build-up material in addition to a medium depth of 0.5 cm. Identical cultures were irradiated at a dose rate of 1.7 Gy min^{-1} to compare the results with previous data for ^{60}Co γ-rays obtained at this dose rate. Control and recipient flasks were sham-irradiated by placing them on the radiotherapy couch without exposing them to the radiation beam *(24)*. This controlled for the effects of temperature, movement and light.

Statistical Analysis

Unless otherwise indicated, results are presented as means ± SE for n = 9 over three independent experiments for determining the bystander effect of 20 MeV electrons. For ELISA sampling, $n \geq 7$ for at least two independent experiments unless otherwise indicated. For antibody treatment, n = 5 for each dose tested. Significance was determined using Student's t test at a confidence level of $p < 0.05$. Potential outliers were determined using a Grubb's Test for outliers.

Results

Induction of Bystander Cell Death in T98G Cells

The first experiments were performed at doses of 0.5, 5 and 10 Gy at a dose rate of 1.7 Gy min^{-1} using 20 MeV electrons to identify any differences between the bystander responses to 20 MeV electrons and ^{60}Co γ-rays at the same dose rate. Table B-1 shows the surviving fractions. Neither ^{60}Co γ-rays nor 20 MeV electrons induced statistically significant bystander cell death relative to controls. Therefore, any bystander cell death that may occur at the higher dose rate of 20 MeV electrons would be the result of the higher dose rate rather than an effect of using high-energy electrons.

Table B-1: Survival Fraction data (mean percentage ± SEM) for T98G Cells Exposed to ^{60}Co γ-rays and 20 MeV electrons at 1.7 Gy min^{-1}[a]

Source, treatment type	0 Gy	0.5 Gy	5 Gy	10 Gy
^{60}Co γ-rays, direct cells	1.00 ± 0.02	0.99 ± 0.02	0.25 ± 0.01	na
^{60}Co γ-rays, recipient cells	1.00 ± 0.06	0.94 ± 0.04	1.08 ± 0.05	na
20 MeV electrons, direct cells	0.99 ± 0.04	0.96 ± 0.02	0.21 ± 0.02	0.015 ± 0.003
20 MeV electrons, recipient cells	0.99 ± 0.04	0.98 ± 0.05	0.93 ± 0.04	0.92 ± 0.06

[a]Number of flasks used is n = 9 for ^{60}Co γ-rays and n = 6 for 20 MeV electrons. For both sets of recipient data presented, no statistically significant results were seen relative to controls. The ^{60}Co experiments were performed by L. A. Ryan, and recipient data for these experiments can be found in ref. *(37)*.

The next set of experiments focused on whether it was possible to induce bystander cell death in T98G glioma cells using 20MeV electrons after a significant increase in the dose rate (in this case 10 Gy min^{-1}, the maximum achieved by the LINAC

we used). This was measured using the clonogenic assay described earlier. In light of previous work by our group that showed different bystander responses after high and low doses [see ref. *(36)*], doses up to 20 Gy were tested for their ability to induce bystander signals in T98G cells. HPV-G keratinocytes were used as a positive control to ensure that clonogenic bystander responses were in accordance with previous work. Figure B-2 shows the recipient surviving fractions for HPV-G and T98G cells:

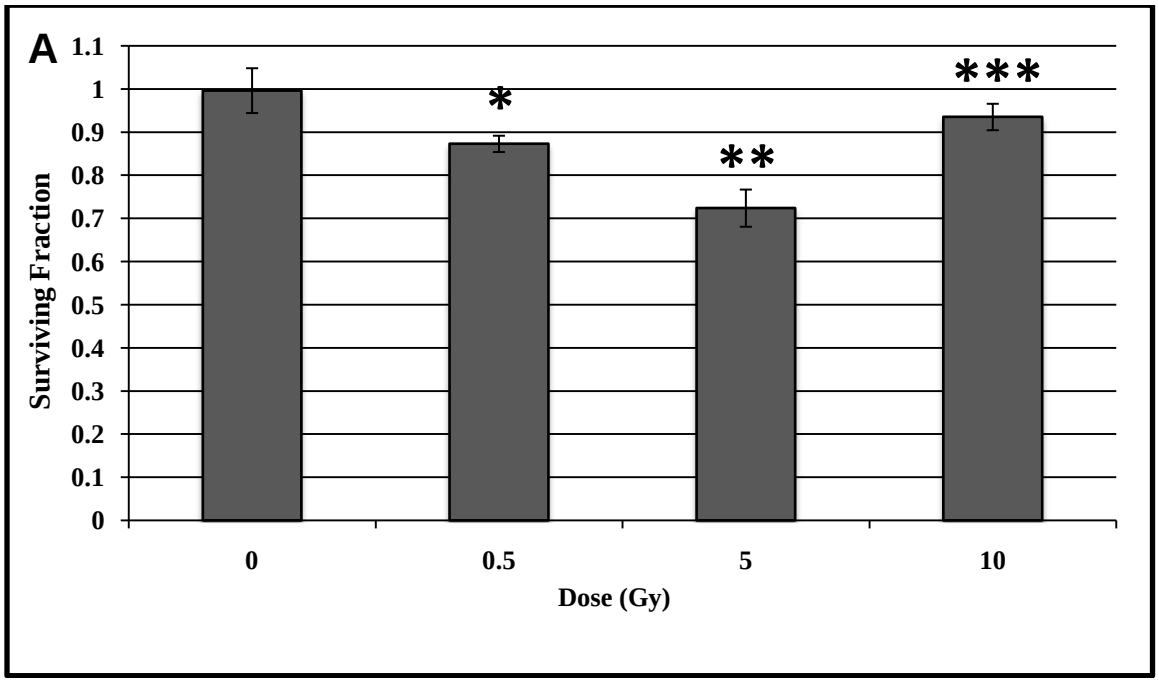

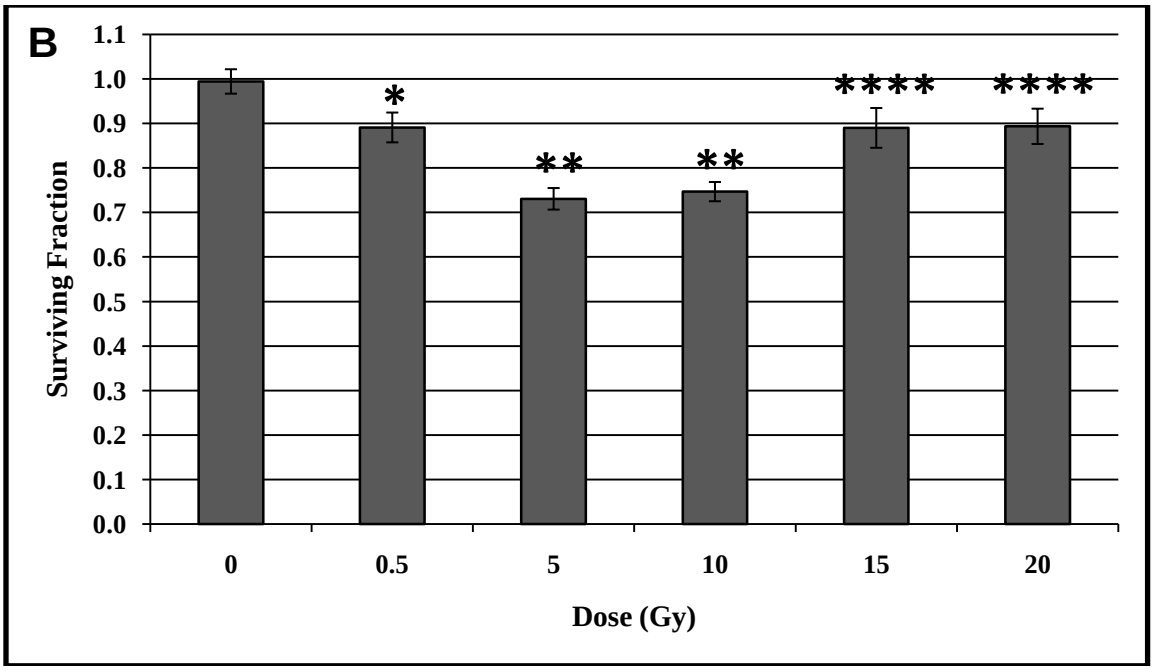

Figure B-2: Bystander survival fraction of HPV-G (panel A) and T98G (panel B) using 20 MeV electrons at 10 Gy min^{-1} dose rate. The number of flasks used for HPV-G is n = 9. For T98G cells, n = 15 for doses up to 10 Gy and n = 6 for 15 and 20 Gy. * $p < 0.03$, ** $p << 0.01$, *** $p > 0.05$, **** surviving fraction data equal to those for 0.5 Gy for T98G cells.

It is clear from Fig. B-2B that bystander cell death is induced in T98G cells after high-dose-rate irradiation with high-energy electrons. Examination of Fig. B-2A and B indicates that HPV-G cells and T98G cells have very similar bystander cell death in that both have a surviving fraction decreased to ~0.70 at 5 Gy and a subsequent recovery. This ‘‘recovery’’ occurs at a lower threshold and more efficiently in HPV-G cells, which return to control levels by 10 Gy ($p > 0.05$ relative to control data). On the other hand, T98G cells recover to survival levels equivalent to 0.5 Gy cells but not until 15 and 20 Gy. These results clearly demonstrate the importance of the dose rate used during irradiation in measuring bystander cell death.

TGF-α and Active TGF-β1 Not Present in Irradiated Cell Conditioned Medium (ICCM)

We examined the ICCM for the presence of either TGF-α or TGF-β1. For TGF-α, after medium from irradiated donor cells was filtered (1-h postirradiation), samples of the medium were divided into aliquots and frozen until they were tested for the presence of TGF-α by ELISA with a sensitivity of approximately 2 pg ml $^{-1}$. Across all our experiments, ELISA yielded null results.

We also tested for the presence of TGF-β1 by determining the total amount of TGF-β1 present (i.e. both latent and active TGF-β1) in the ICCM. Samples were collected and handled in the same way as for TGF-β. Since the TGF-β1 ELISA recognizes only active TGF-β1, samples were activated by acidification with HCl to determine the total TGF-β1. Because we supplemented the tissue culture medium with FBS, which contains high levels of TGF-β1, separate medium-only samples were also activated with HCl to determine the amount of TGF-β1 present in the medium. These tests showed levels of TGF-β1 of 1425 ± 62 pg ml^{-1} present in the medium alone. This value for TGF-β1 was subtracted from results collected from the ICCM at doses up to 10 Gy (where maximal bystander death occurred) to determine the amount of TGF-β1 produced by the cells (Fig. B-3). There was no statistically significant increase in TGF-β1 production 1-h after irradiation. The slight decrease in TGF-β1 production after exposure to 10 Gy was not statistically significant.

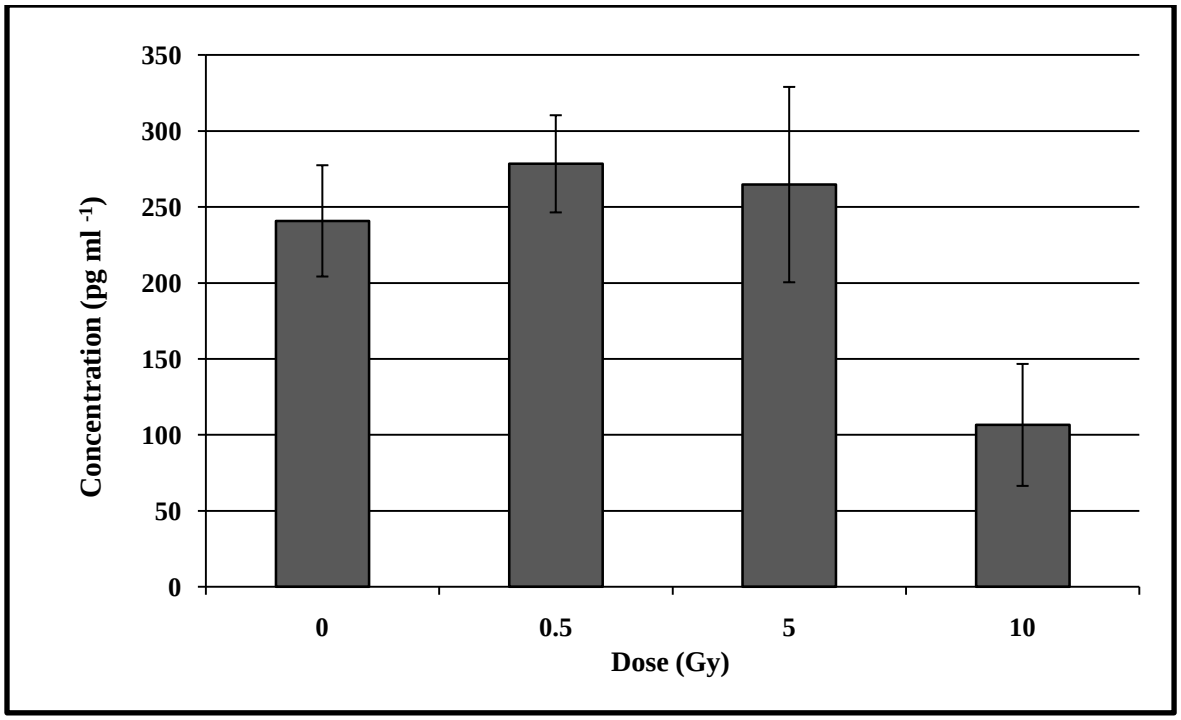

Figure B-3: Total TGF-β1content in ICCM from T98G cells found 1-h postirradiation and collected after filtering of donor medium. These results were corrected for the presence of TGF-β1 found in the medium only. The number of flasks is ≥ 7 except for 10 Gy, where n = 4. No statistically significant differences were seen.

We also determined the portion of total TGF-β1 content (Fig. B-3) that was of the active form to examine the hypothesis that the ratio of active to latent TGF-β1 would change within the 1-h after donor cell irradiation and any dependence on dose present. These tests were carried out on samples taken directly from ICCM after filtering. The ELISA did not detect any active TGF-β1 present in the medium at 1-h postirradiation, which is when treatment of recipient cells takes place.

Application of TGF-β1 mAb to ICCM Abolishes Bystander Cell Death but TGF-α mAb Produces No Effect

In the experiments described above, no TGF-α or active TGF-β1 was in ICCM from T98G cells. To determine whether TGF-α and / or TGF-β1 were possible downstream factors involved in the observed bystander cell death, monoclonal antibodies for TGF-α (TGF-α mAb) and TGF-β1 (TGF-β1 mAb) were added to ICCM after filtering but prior to its application to recipient cells. The appropriate IgG_1 control vector was also tested. Figure B-4 shows the recipient cell surviving fractions for TGF-α mAb and TGF-β1 mAb. Treatment of ICCM with TGF-α mAb had no effect on the observed bystander cell surviving fraction (Fig. B-4A). It appears that TGF-α does not play a role in the bystander response of our T98G cells. On the other hand, treatment of ICCM with TGF-β1 mAb brought recipient cell surviving fractions back to control levels and completely abolished bystander cell death in the T98G cells (Fig. B-4B). This provides strong evidence that TGF-β1 plays a downstream role in the mitigation of death of bystander T98G cells after high-dose, high-dose-rate irradiation of donor cells.

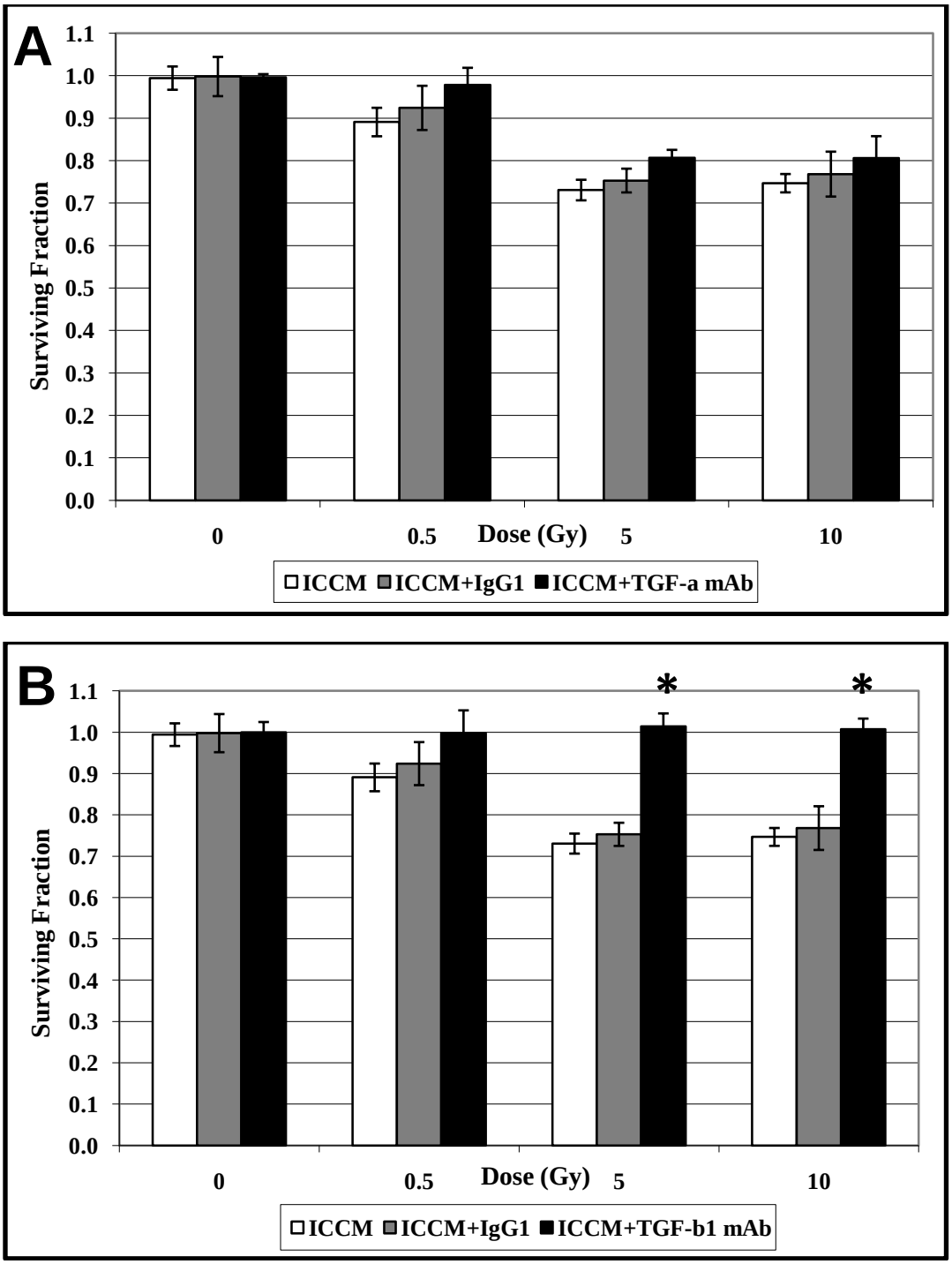

Figure B-4: Treatment of ICCM from T98G cells with monoclonal antibodies for TGF-α (TGF-a mAb) (panel A) and TGF-β1 (TGF-b1 mAb) (panel B). Panel A shows that TGF-α mAb had no effect on recipient cell surviving fraction while panel B shows that TGF-β1 mAb completely eliminated bystander cell death at 5 and 10 Gy (*$p < 0.01$). Five flasks were used.

Discussion

It is clear from the evidence presented here that induction of death in bystander T98G glioma cells is possible after irradiation with high-energy electrons at high dose and high dose rate. Our initial experiments examining bystander cell death after exposure to ^{60}Co γ-rays and 20 MeV electrons at a dose rate of 1.7 Gy min^{-1} produced no statistically significant differences from control levels. However, after irradiation of T98G cells with 20 MeV electrons at a dose rate of 10 Gy min^{-1}, a significant decrease in surviving fraction was observed. This evidence is in line with earlier work by our group that showed a dependence of HPV-G bystander cell response on dose and dose rate *(36)*. Additionally, if the surviving fraction of HPV-G cells is compared with that of T98G cells (see Fig. B-2), nearly identical bystander responses were seen at 0.5 and 5 Gy. A difference occurred at 10 Gy, where the survival of HPV-G cells returned to control levels while that of T98G cells did not. The recovery to control levels that occurred in HPV-G cells occurred in T98G cells only at higher doses and only to levels similar to that of the 0.5 Gy recipient cells rather than the controls. This suggests that the radiation exposure in earlier experiments with T98G cells [both here with ^{60}Co γ-rays and low-dose-rate electron irradiation as well as in ref. *(24)* with 240 kVp X-rays at 0.2–0.4 Gy min^{-1}] did not reach a needed ‘‘bystander activation potential’’ or threshold of radiation stress adequate to induce bystander cell death that could be achieved with high-energy electrons at a high dose rate. Thus classifying a particular cell type as capable of producing bystander effects or not may be premature. Some cells may have a higher bystander

activation potential that may require using a higher dose rate or dose. With a strong enough radiation stress, T98G cells, which are radioresistant, had levels of bystander cell death similar to those of HPV-G keratinocytes, a more radiosensitive cell line with a well-defined bystander cell death response. We suggest that it is possible that bystander cell responses (or more specifically, bystander cell death) may be generally similar across various cell types, including those that have previously been labelled as not exhibiting bystander cell death. Once a given cell type's bystander activation potential is met (which may require a more or less aggressive radiation treatment depending on the cell type), bystander signalling cascades are initiated, and the response (i.e. bystander cell death) may generally be similar. In an attempt to verify this hypothesis, a literature search was undertaken, but while we found a number of studies investigating LET dependence, we found no systematic studies of dose-rate effects using bystander signal production as an end point. Comparing work from different laboratories is difficult because of the widely different conditions used. For example, Chen *et al (56)* used ^{125}I seeds at low dose rate to deliver 2–4 Gy to cells of human tumour cell lines of differing radiosensitivities. They concluded that bystander effects were induced but drew no conclusions about the role of dose rate. Many authors have documented protective effects of low-dose, low-dose-rate exposure, but none have linked the protective responses to bystander mechanisms. Groesser *et al (57)* did a comprehensive study of bystander effects in several cell lines, including some we previously investigated. They did not see bystander effects after high-LET radiation exposures or discuss the role of dose rate but suggested that epigenetic factors may be involved in producing bystander

responses. In studies in our laboratory using neutrons *(16)*, we concluded that neutron doses (γ-ray dose shielded) up to 30 cGy did not result in bystander effects even though they were triggered by 0.2–0.3 cGy of γ-rays. There may be a sensitive window (i.e. dose/dose-rate range) in which bystander effects can be induced that is specific for different radiation qualities, dose rates, tissues or cell lines. Doses / dose rates below the bystander activation potential fail to trigger bystander responses, while at higher dose / dose rates, the stress to the cells is such that responses other than bystander signalling dominate. A similar window is thought to occur for apoptotic cell responses that are dominant in the low-dose region. This idea needs to be tested using different combinations of dose, dose rate and cell lines in a systematic way.

TGF-α and TGF-β1, which are known to contribute to T98G cell behaviour, were examined to determine whether they have any role in mitigating the bystander responses observed in T98G cells. There was no detectable TGF-α in ICCM obtained from donor flasks. Additionally, exogenous application of TGF-α mAb to ICCM prior to recipient cell treatment produced no significant difference in bystander cell death (see Fig. B-4A). These results indicate that TGF-α does not appear to be involved in producing / mitigating bystander cell death in T98G cells either through cleavage from irradiated donor cells into the culture medium during the 1-h postirradiation ICCM generating time or as a downstream factor produced by recipient cells. However, TGF-β1 appears to be essential for bystander cell death in T98G cells but does not appear to be the transmissible factor secreted by donor cells into ICCM. ELISA results using ‘‘real-time’’ sampling detected no presence of active TGF-β1 at 1-h postirradiation within the

conditioned medium. Examination of total TGF-β1 content revealed that TGF-β1 is present (see Fig. B-3), but in light of the lack of active TGF-β1, it appears to exist primarily in its latent form. Furthermore, Fig. B-3 also shows no dependence of TGF-β1 levels on dose, and therefore the levels seen are likely just natural levels produced by the cells during *in vitro* culture. These results agree with those of Shao *et al*., which showed that increasing the irradiated fraction of T98G cells in culture had no significant effect on the amount of TGF-β1 produced *(47)*. However, application of TGF-β1 mAb to ICCM prior to treatment of recipient cells completely abolished bystander cell death in T98G cells at 5 and 10 Gy (see Fig. B-4B). This suggests that TGF-β1 is a downstream factor that is essential for inducing bystander cell death but is not itself a transmissible factor produced by donor cells.

To understand this apparent connection between decreased T98G cell survival and TGF-β1, it is important to examine the TGF-β signalling pathway. Once active, TGF-β1 induces its effects by several different pathways as well as through crosstalk with other signalling cascades *(44,58,59)*. The primary signalling mechanism used by TGF-β1 in mammalian cells involves Smad proteins. Once TGF-β1 is activated (via dissociation of its latency-associated peptide, LAP), it is able to bind to its type II receptor (TGFβRII) on the cell surface, which then recruits and phosphorylates type I receptor (TGFβRI).

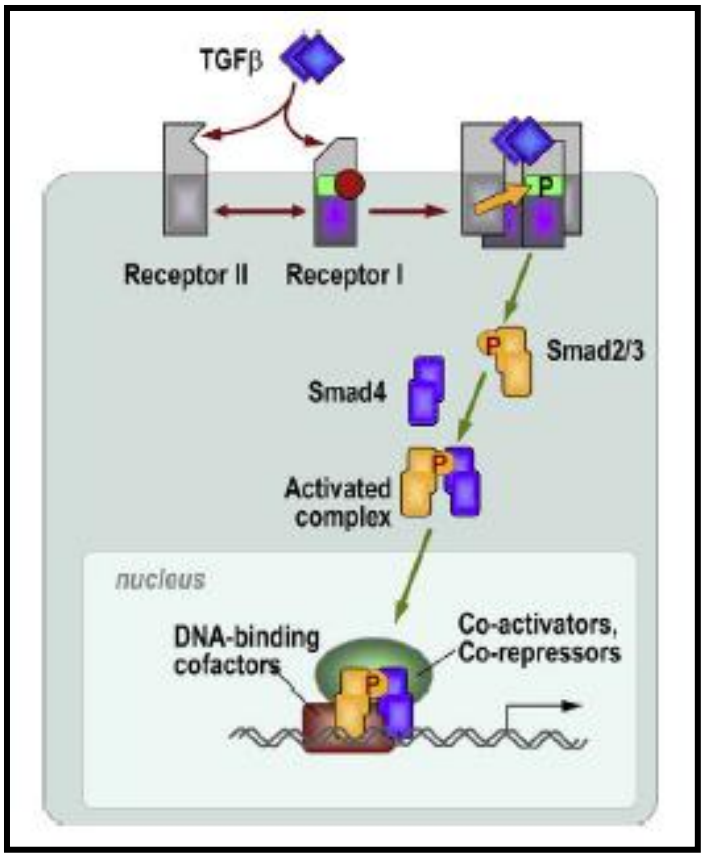

Figure B-5: General representation of TGF-β1 signalling *(44)*.

This complex then allows phosphorylation of Smad2 and Smad3 (R-Smads) proteins, which then form complexes with Smad4 (Co-Smad) and lead to translocation into the nucleus and subsequent gene expression. This entire process is regulated through a negative-feedback mechanism involving Smad6/7 (I-Smads), which actively compete with R-Smads for receptor and Co-Smad interaction as well as degradation of receptors *(58)*. Some of the target genes involved in the regulation of cell growth by TGF-β include C-MYC, CDC25A and the cyclin-dependent kinase inhibitors (CDKIs) $p15^{INK4B}$, $p21^{WAF1/CIP1}$ and $p27^{KIP1}$ *(57)*. Specifically in T98G glioma cells, research has shown that

TGFβRI and TGFβRII receptors are functional and Smad3/4 complex translocates into the nucleus *(60)*. Rich *et al*. showed that T98G cells have approximately 25% growth inhibition after exogenous application of TGF-β1 as well as increases of Smad2/3/4 proteins and induction of CDKI $p15^{INK4B}$, which prevents the progress of cells from G_1 to S phase *(61)*. This appears to indicate that TGF-β1 is capable of causing growth inhibition of T98G cells demonstrated by the decrease in the surviving fraction. By having a negative-feedback mechanism via Smad6/7, this regulation of TGF-β1 activity in the cells may be responsible for the apparent plateau in the surviving fraction at doses of 5 and 10 Gy along with the apparent recovery at 15 and 20 Gy.

Based on the ELISA sampling and monoclonal antibody treatment done here, it appears that TGF-β1 is a downstream factor of some other transmissible factor found in the ICCM. Research by Shao *et al*. has shown using microbeam irradiations of targeted T98G cells that TGF-β1 is essential for the formation of micronuclei in bystander cells and that it is downstream of a nitric oxide (NO)-related pathway *(46,47)*. Furthermore, Shao *et al*. showed that NO can induce the production of TGF-β1 in a time- and dose-dependent manner and can be found in culture medium *(47)*. However, since the diffusion distance of NO is of the order of micrometers, it is unlikely to be a transmissible factor in ICCM when using a medium transfer protocol. Additionally, Shao *et al*. measured TGF-β1 levels in culture medium 4 and 24 h after treatment with DEANO (a NO producer) or irradiation of varying percentages of a cell population *(47)*. This, coupled with the lack of active TGF-β1 in ICCM, again points to some other agent(s) being involved in T98G bystander cell death via the ICCM when a 1-h medium

transfer period is used. However, such ‘‘bystander’’ cell death may also be occurring with the donor cell flasks themselves (i.e. short-distance bystander responses), but these effects would clearly be dominated by cell death produced by the direct irradiation. Since cell culture was performed in the presence of 10% fetal bovine serum, which is rich in latent TGF-β1, the source for TGF-β1 might be the serum and activation would be achieved by the recipient cells. One conceivable scenario would be the release from irradiated cells of a hypothetical factor that induces recipient cells to activate TGF-β1.

One factor that may be involved is tissue plasminogen activator (tPA), which is a secreted serine glycoprotease produced by both normal and malignant cells *(62–65)* and which participates in a multitude of cellular responses. One such response is the formation of active plasmin, which subsequently initiates a number of cascades, including activation of latent TGF-β1 *(66,67)*. Ionizing radiation increases extracellular, intracellular and tPA mRNA in a time-dependent manner in normal and malignant human fibroblasts as well as in malignant melanoma *(68,69)*. More specifically, examination of data by Boothman *et al*. showed peaks in extracellular tPA enzymatic activity after 6 Gy X-ray irradiation of malignant melanoma cells at approximately 20 min and 1-h after irradiation with a slight fluctuation in between *(68)*. Therefore, it is possible that tPA could be a candidate involved in bystander cell death when using 1-h medium transfer protocols. After donor cell irradiation, extracellular tPA levels could increase and collect in the ICCM. Upon transfer of the medium to the recipient cells, tPA could initiate the creation of active plasmin, which could subsequently activate latent TGF-β1 in the recipient cell flasks. Once active, TGF-β1 could induce activation of $p15^{INK4B}$ via the

Smad signalling pathway, which subsequently delays progression of cells from G_1 to S. As the dose to the donor cells increases, the amount of tPA produced increases and eventually leads to the regulation of TGF-β1 activity via Smad6/7 and suppression of bystander cell killing. Addition of TGF-β1 mAb to ICCM would neutralize TGF-β1 produced via tPA, thus preventing $p15^{INK4B}$ induction, and thus no observed decrease in surviving fraction would result. Examination of tPA levels in ICCM produced for different cell lines and irradiation protocols and their correlations with NO concentration is a plausible direction for further research.

In summary, it was found that a decrease in bystander cell survival could be induced in T98G cells previously considered refractive using high-dose and high-dose-rate protocols. These observations may indicate the presence of a bystander activation potential that a radiation stress must reach prior to the secretion/transmission of bystander signalling. Additionally, this study also examined the ICCM produced by T98G donor cells for the presence of TGF-α or TGF-β1. TGF-β1 has previously been shown to be critical for bystander effect induction by microbeam irradiation in this cell line. It appears that TGF-α plays no apparent role in bystander cell survival using a medium transfer protocol. There was no significant amount of active TGF-β1 present in ICCM samples tested directly after filtering. However, addition of TGF-β1 mAb to ICCM prior to medium transfer completely abolished the bystander cell death in recipient cells. This leads to the conclusion that active TGF-β1 does not appear to be a transmissible factor contained in the ICCM provided by irradiated donors. Instead, it appears to be a

downstream cytokine activated by the recipient cells and to be essential for eliciting bystander cell death in T98G glioma cells.

Acknowledgements

We acknowledge funding for this research from the NSERC Industrial Research Chairs and Discovery Grants Programmes as well as the Canada Chairs Programme. We also acknowledge our participation as non-funded third country partners in the European Union Non-Targeted Effects Integrated Project – NOTE.

References

1. E. J. Hall, The bystander effect. *Health Phys.* **85**, 31-35 (2003).

2. T. K. Hei, H. Zhou, V. N. Ivanov, M. Hong, H. B. Lieberman, D. J. Brenner, S. A. Amunson and C. R. Geard, Mechanism of radiation-induced bystander effects: a unifying model. *J. Pharm. Pharmacol.* **60**, 943-950 (2008).

3. J. B. Little, Cellular radiation effects and the bystander response. *Mutat. Res.* **597**, 113-118 (2006).

4. C. Mothersill and C. Seymour, Radiation-induced bystander effects: are they good, bad or both? *Med. Confl. Surviv.* **21**, 101-110 (2005).

5. S. A. Lorimore, M. A. Kadhim, D. A. Pocock, D. Papworth, D. L. Stevens, D. T. Goodhead and E. G. Wright, Chromosomal instability in the descendants of unirradiated surviving cells after α-particle irradiation. *Proc. Natl. Acad. Sci. U.S.A.* **95**, 5730-5733 (1998).

6. C. Mothersill and C. Seymour, Medium from irradiated human epithelial cells but not human fibroblasts reduces the clonogenic survival of unirradiated cells. *Int. J. Radiat. Biol.* **71**, 421-427 (1997).

7. C. Shao, M. Folkard, B. D. Michael and K. M. Prise, Bystander signalling between glioma cells and fibroblasts targeted with counted particles. *Int. J. Cancer.* **116**, 45-51 (2005).

8. H. Nagasawa and J. B. Little, Induction of sister chromatid exchanges by extremely low doses of α-particles. *Cancer Res.* **52**, 6394-6396 (1992).

9. H. Nagasawa and J. B. Little, Unexpected sensitivity to the induction of mutations by very low doses of α-particle radiation: evidence for a bystander effect. *Radiat. Res.* **152**, 552-557 (1999).

10. H. Zhou, G. Randers-Pehrson, C. A. Waldren, D. Vannais, E. J. Hall and T. K. Hei, Induction of a bystander mutagenic effect of α particles in mammalian cells. *Proc. Natl. Acad. Sci. U.S.A.* **97**, 2099-2104 (2000).

11. O. V. Belyakov, S. A. Mitchell, D. Parikh, G. Randers-Pehrson, S. A. Marino, S. A. Amundson, C. R. Geard and D. J. Brenner, Biological effects in unirradiated human tissue induced by radiation damage up to 1 mm away. *Proc. Natl. Acad. Sci. U.S.A.* **102**, 14203-14208 (2005).

12. K. M. Prise, O. V. Belyakov, M. Folkard and B. D. Michael, Studies of bystander effects in human fibroblasts using a charged particle microbeam. *Int. J. Radiat. Biol.* **74**, 793-798 (1998).

13. C. Shao, M. Aoki and Y. Furusawa, Medium-mediated bystander effects on HSG cells co-cultivated with cells irradiated by X-rays or a 290 MeV/u carbon beam. *J. Radiat. Res. (Tokyo).* **42**, 305-316 (2001).

14. S. A. Lorimore, P. J. Coates and E. G. Wright, Radiation-induced genomic instability and bystander effects: inter-related nontargeted effects of exposure to ionizing radiation. *Oncogene.* **22**, 7058-7069 (2003).

15. S. G. Sawant, G. Randers-Pehrson, C. R. Geard, D. J. Brenner and E. J. Hall, The bystander effect in radiation oncogenesis: I. Transformation in C3H 10T1/2 cells in vitro can be initiated in the unirradiated neighbors of irradiated cells. *Radiat. Res.* **155**, 397-401 (2001).

16. Z. Liu, C. E. Mothersill, F. E. McNeill, F. M. Lyng, S. H. Byun, C. B. Seymour and W. V. Prestwich, A dose threshold for a medium transfer bystander effect for a human skin cell line. *Radiat. Res.* **166**, 19-23 (2006).

17. C. Mothersill, R. J. Seymour and C. B. Seymour, Bystander effects in repair-deficient cell lines. *Radiat. Res.* **161**, 256-263 (2004).

18. C. Mothersill and C. B. Seymour, Cell-cell contact during γ irradiation is not required to induce a bystander effect in normal human keratinocytes: evidence for release during irradiation of a signal controlling survival into the medium. *Radiat. Res.* **149**, 256-262 (1998).

19. S. G. Sawant, W. Zheng, K. M. Hopkins, G. Randers-Pehrson, H. B. Lieberman and E. J. Hall, The radiation-induced bystander effect for clonogenic survival. *Radiat. Res.* **157**, 361-364 (2002).

20. F. M. Lyng, P. Maguire, N. Kilmurray, C. Mothersill, C. Shao, M. Folkard and K. M. Prise, Apoptosis is initiated in human keratinocytes exposed to signalling factors from microbeam irradiated cells. *Int. J. Radiat. Biol.* **82**, 393-399 (2006).

21. J. McIlrath, S. A. Lorimore, P. J. Coates and E. G. Wright, Radiation-induced genomic instability in immortalized haemopoietic stem cells. *Int. J. Radiat. Biol.* **79**, 27-34 (2003).

22. C. Mothersill and C. Seymour, Radiation-induced bystander effects: past history and future directions. *Radiat. Res.* **155**, 759-767 (2001).

23. C. Shao, M. Folkard, B. D. Michael and K. M. Prise, Targeted cytoplasmic

irradiation induces bystander responses. *Proc. Natl. Acad. Sci. U.S.A.* **101**, 13495-13500 (2004).

24. C. Mothersill, C. B. Seymour and M. C. Joiner, Relationship between radiation-induced low-dose hypersensitivity and the bystander effect. *Radiat. Res.* **157**, 526-532 (2002).

25. R. C. Poon, N. Agnihotri, C. Seymour and C. Mothersill, Bystander effects of ionizing radiation can be modulated by signaling amines. *Environ. Res.* **105**, 200-211 (2007).

26. A. Bishayee, H. Z. Hill, D. Stein, D. V. Rao and R. W. Howell, Free radical-initiated and gap junction-mediated bystander effect due to nonuniform distribution of incorporated radioactivity in a three-dimensional tissue culture model. *Radiat. Res.* **155**, 335-344 (2001).

27. C. Shao, Y. Furusawa, M. Aoki and K. Ando, Role of gap junctional intercellular communication in radiation-induced bystander effects in human fibroblasts. *Radiat. Res.* **160**, 318-323 (2003).

28. S. Burdak-Rothkamm, S. C. Short, M. Folkard, K. Rothkamm and K. M. Prise, ATR-dependent radiation-induced γH2AX foci in bystander primary human astrocytes and glioma cells. *Oncogene.* **26**, 993-1002 (2007).

29. T. K. Hei, Cyclooxygenase-2 as a signaling molecule in radiation-induced bystander effect. *Mol. Carcinog.* **45**, 455-460 (2006).

30. R. Iyer, B. E. Lehnert and R. Svensson, Factors underlying the cell growth-related bystander responses to α particles. *Cancer Res.* **60**, 1290-1298 (2000).

31. E. I. Azzam, S. M. de Toledo, D. R. Spitz and J. B. Little, Oxidative metabolism modulates signal transduction and micronucleus formation in bystander cells from α-particle-irradiated normal human fibroblast cultures. *Cancer Res.* **62**, 5436-5442 (2002).

32. F. M. Lyng, C. B. Seymour and C. Mothersill, Production of a signal by irradiated cells which leads to a response in unirradiated cells characteristic of initiation of apoptosis *Br. J. Cancer.* **83**, 1223-1230 (2000).

33. F. M. Lyng, C. B. Seymour and C. Mothersill, Initiation of apoptosis in cells exposed to medium from the progeny of irradiated cells: a possible mechanism for bystander-induced genomic instability? *Radiat. Res.* **157**, 365-370 (2002).

34. H. Matsumoto, S. Hayashi, M. Hatashita, K. Ohnishi, H. Shioura, T. Ohtsubo, R. Kitai, T. Ohnishi and E. Kano, Induction of radioresistance by a nitric oxide-

mediated bystander effect *Radiat. Res.* **155**, 387-396 (2001).

35. F. M. Lyng, P. Maguire, B. McClean, C. Seymour and C. Mothersill, The involvement of calcium and MAP kinase signaling pathways in the production of radiation-induced bystander effects. *Radiat. Res.* **165**, 400-409 (2006).

36. M. D. Gow, C. B. Seymour, S. H. Byun and C. E. Mothersill, Effect of dose rate on the radiation-induced bystander response. *Phys. Med. Biol.* **53**, 119-132 (2008).

37. L. A. Ryan, R. W. Smith, C. B. Seymour and C. E. Mothersill, Dilution of irradiated cell conditioned medium and the bystander effect. *Radiat. Res.* **169**, 188-196 (2008).

38. C. Shao, V. Stewart, M. Folkard, B. D. Michael and K. M. Prise, Nitric oxide-mediated signaling in the bystander response of individually targeted glioma cells. *Cancer Res.* **63**, 8437-8442 (2003).

39. C. Shao, F. M. Lyng, M. Folkard and K. M. Prise, Calcium fluxes modulate the radiation-induced bystander responses in targeted glioma and fibroblast cells. *Radiat. Res.* **166**, 479-487 (2006).

40. J. Baselga, J. Mendelsohn, Y. M. Kim and A. Pandiella, Autocrine regulation of membrane transforming growth factor-α cleavage. *J. Biol. Chem.* **271**, 3279-3284 (1996).

41. P. Dent, D. B. Reardon, J. S. Park, G. Bowers, C. Logsdon, K. Valerie and R. Schmidt-Ullrich, Radiation-induced release of transforming growth factor α activates the epidermal growth factor receptor and mitogen-activated protein kinase pathway in carcinoma cells, leading to increased proliferation and protection from radiation-induced cell death. *Mol. Biol. Cell.* **10**, 2493-2506 (1999).

42. R. K. Schmidt-Ullrich, K. Valerie, W. Chan, D. E. Wazer and P. S. Lin, Expression of oestrogen receptor and transforming growth factor-α in MCF-7 cells after exposure to fractionated irradiation. *Int. J. Radiat. Biol.* **61**, 405-415 (1992).

43. M. Rubenstein, R. Glick, T. Lichtor, Y. Mirochnik, P. Chou and P. Guinan, Treatment of the T98G glioblastoma cell line with antisense oligonucleotides directed toward mRNA encoding transforming growth factor-α and the epidermal growth factor receptor. *Med. Oncol.* **18**, 121-130 (2001).

44. J. Massague and R. R. Gomis, The logic of TGFβ signalling. *FEBS Lett.* **580**, 2811-2820 (2006).

45. M. H. Barcellos-Hoff and T. A. Dix, Redox-mediated activation of latent transforming growth factor-β 1. *Mol. Endocrinol.* **10**, 1077-1083 (1996).

46. C. Shao, M. Folkard and K. M. Prise, Role of TGF-β1 and nitric oxide in the bystander response of irradiated glioma cells. *Oncogene.* **27**, 434-440 (2008).

47. C. Shao, K. M. Prise and M. Folkard, Signaling factors for irradiated glioma cells induced bystander responses in fibroblasts. *Mutat. Res.* **638**, 139-145 (2008).

48. P. Lambin, B. Fertil, E. P. Malaise and M. C. Joiner, Multiphasic survival curves for cells of human tumor cell lines: induced repair or hypersensitive subpopulation? *Radiat. Res.* **138**, S32-S36 (1994).

49. L. Pirisi, K. E. Creek, J. Doniger and J. A. DiPaolo, Continuous cell lines with altered growth and differentiation properties originate after transfection of human keratinocytes with human papillomavirus type 16 DNA. *Carcinogenesis.* **9**, 1573-1579 (1998).

50. C. Mothersill, D. Rea, E. G. Wright, S. A. Lorimore, D. Murphy, C. B. Seymour and K. O'Malley, Individual variation in the production of a 'bystander signal' following irradiation of primary cultures of normal human urothelium. *Carcinogenesis.* **22**, 1465-1471 (2001).

51. C. Mothersill, F. Lyng, C. Seymour, P. Maguire, S. Lorimore and E. Wright, Genetic factors influencing bystander signaling in murine bladder epithelium after low-dose irradiation in vivo. *Radiat. Res.* **163**, 391-399 (2005).

52. B. Cooper, S. Schneider, J. Bohl, Y. Jiang, A. Beaudet and P. S. Vande, Requirement of E6AP and the features of human papillomavirus E6 necessary to support degradation of p53. *Virology.* **306**, 87-99 (2003).

53. C. B. Seymour and C. Mothersill, Relative contribution of bystander and targeted cell killing to the low-dose region of the radiation dose-response curve. *Radiat. Res.* **153**, 508-511 (2000).

54. T. T. Puck and P. I. Marcus, Action of x-rays on mammalian cells. *J. Exp. Med.* **103**, 653-666 (1956).

55. H. E. Johns and J. R. Cunningham, *The Physics of Radiology Ed 4*. Charles C. Thomas, Springfield, 1983.

56. H. H. Chen, R. F. Jia, L. Yu, C. L. Shao, and W. Y. Cheng, Bystander effects induced by continuous low-dose-rate 125I seeds potentiate the killing action of irradiation on human lung cancer cells in vitro. *Int. J. Radiat. Oncol. Biol. Phy.* **72**, 1560-1566, (2008)

57. T. Groesser, B. Cooper, B. Rydberg, Lack of bystander effects from high-LET radiation for early cytogenetic endpoints. *Radiat. Res*. **170**, 794-802 (2008).

58. Y. Shi and J. Massague, Mechanisms of TGF-β signalling from cell membrane to the nucleus. *Cell.* **113**, 685-700 (2003).

59. K. E. Bachman and B. H. Park, Duel nature of TGF-β signaling: tumor suppressor vs. tumor promoter. *Curr. Opln. Oncol.* **17**, 49-54 (2004).

60. M. Dziembowska, M. Danilkiewicz, A. Wesolowska, A. Zupanska, S. Chouaib and B. Kaminska, Cross-talk between Smad and p38 MAPK signalling in transforming growth factor β signal transduction in human glioblastoma cells. *Biochem. and Biophys. Res. Comm.* **354**, 1101-1106 (2007).

61. J. N. Rich, M. Zhang, M. B. Datto, D. D. Bigner and X. F. Wang, Transforming growth factor-β-mediated p15(INK4B) induction and growth inhibition in astrocytes is SMAD3-dependent and a pathway prominently altered in human glioma cell lines. *J. Biol. Chem.* **274**, 35053-35058 (1999).

62. K. Dano, P. A. Andreasen, J. Grondahl-Hansen, P. Kristensen, L. S. Nielsen and L. Skriver, Plasminogen activators, tissue degradation, and cancer. *Adv. Cancer Res.* **44**, 139-266 (1985).

63. Y. Hasui, J. Suzumiya, K. Marutsuka, A. Sumiyoshi, S. Hashida and E. Ishikawa, Comparative study of plasminogen activators in cancers and normal mucosae of human urinary bladder. *Cancer Res.* **49**, 1067-1070 (1989).

64. M. Laiho and J. Keski-Oja, Growth factors in the regulation of pericellular proteolysis: a review. *Cancer Res.* **49**, 2533-2553 (1989).

65. D. C. Rijken and D. Collen, Purification and characterization of the plasminogen activator secreted by human melanoma cells in culture. *J. Biol.Chem.* **256**, 7035-7041 (1981).

66. R. Flaumenhaft, M. Abe, P. Mignatti and D. B. Rifkin, Basic fibroblast growth factor-induced activation of latent transforming growth factor β in endothelial cells: regulation of plasminogen activator activity. *J. Cell Biol.* **118**, 901-909 (1992).

67. J. Taipale, K. Miyazono, C. H. Heldin and J. Keski-Oja, Latent transforming growth factor-β 1 associates to fibroblast extracellular matrix via latent TGF-β binding protein. *J. Cell Biol.* **124**, 171-181 (1994).

68. D. A. Boothman, M. Wang and S. W. Lee, Induction of tissue-type plasminogen activator by ionizing radiation in human malignant melanoma cells. *Cancer Res.*

51, 5587-5595 (1991).

69. N. Fukunaga, H. L. Burrows, M. Meyers, R. A. Schea and D. A. Boothman, Enhanced induction of tissue-type plasminogen activator in normal human cells compared to cancer-prone cells following ionizing radiation. *Int. J. Radiat. Oncol. Biol. Phys.* **24**, 949-957 (1992).

Part C

Dose calculations for targeted radiopharmaceutical [^{131}I] *meta*-iodobenzylguanidine *in vitro* for examination of radiation-induced biological bystander effects

Michael D. Gow[1], Colin B. Seymour[1], Marie Boyd[2], Robert J. Mairs[2,3], William V. Prestiwch[1], and Carmel E. Mothersill[1]

[1] Medical Physics and Applied Radiation Sciences Department, McMaster University, Hamilton, Ontario, Canada L8S 4K1
[2] Targeted Therapy Group, Division of Cancer Science and Molecular Pathology, Glasgow University, Cancer Research United Kingdom Beatson Laboratories, Glasgow, United Kingdom
[3] Department of Child Health, Yorkhill Hospital, Glasgow, United Kingdom

Address for correspondence:
Medical Physics and Applied Radiation Sciences Department,
McMaster University,
1280 Main Street West,
Hamilton, Ontario, Canada
L8S 4K1

OBJECTIVE

Develop an efficient dosimetry model for dose and dose rate determination following [^{131}I] MIBG radiopharmaceutical treatment leveraged to produce toxic ICCM in medium transfer experiments following protocol by Boyd *et al* in 2006. This model will be subsequently utilized to re-examine surviving fraction data from Boyd *et al* allowing for direct comparison of bystander responses between external-beam and [^{131}I] MIBG treatments in ICCM production. The aim is threefold: a) determine similarities between the two ICCM treatment types and identify potential underlying cause for discrepancies; b) develop a computational model and application to be utilized by non-technical individuals to expand current *in vitro* experimentation of bystander effects from β-emitting radiopharmaceuticals; c) provide a code-base by which to expand through possible addition of other radionuclide pharmaceuticals in bystander examinations.

This work has been prepared for submission to the *Journal of Nuclear Medicine.*

Abstract

The use of plasmids to infect cells with noradrenaline transporter (NAT) leading to subsequent uptake of radioiodinated *meta*-iodobenzylguanidine [^{131}I] MIBG is a promising method of targeted radiotherapy. In 2006, Boyd *et al* examined the potential ability of [^{131}I] MIBG treatment to produce radiation-induced biological bystander effects (RIBBE). They found a large bystander response from this treatment shown through a substantial decrease in recipient survival fraction. However, without accurate estimates of absorbed dose, it is difficult to compare these effects with conventional external radiation treatment or with previous bystander work using such sources. Therefore, we sought to develop a dosimetry model to calculate the absorbed dose to donor cells during ICCM production via the experimental protocol established by Boyd *et al.* **Methods:** Using the Vynckier – Wambersie dose point kernel, a model for dose rate evaluation was created allowing for calculation of absorbed dose values to UVW/NAT and EJ138/NAT transfected donor cell lines. Developed in MATLAB, this model was also compiled into a standalone application allowing for ICCM dose evaluation on a Windows OS without the need for the MATLAB environment. **Results:** Mean doses required to decrease surviving fraction to ~25 - 30% for UVW/NAT and EJ138/NAT recipient cells was found to be ~1.6 and 1.7 Gy respectively. While never reaching a strict plateau, a decrease in the change in bystander cell death was observed as dose approached 2 Gy, the plateau dose for ^{60}Co treatment. Additionally, the maximum mean dose rates achieved during [^{131}I] MIBG treatment were 0.09 - 0.75 Gy/h for UVW/NAT and 0.07 - 0.78 Gy/h for EJ138/NAT. These were all significantly smaller than the ^{60}Co treatment dose rate of

15 Gy/h. For parental cell lines, with no NAT-transfection, mean absorbed doses to donor cells were relatively small, ranging from 0.03 - 0.23 Gy for UVW and 0.03 - 0.32 Gy for EJ138. **Conclusion**: [^{131}I] MIBG treatment for ICCM production elicits a bystander surviving fraction curve similar to ^{60}Co in behaviour but with significantly greater cell death production. This is believed to be possibly rooted in the response to LDR effects as well as differences in similar low – LET bystander production.

Key words: radiation bystander effect, MIBG, gene therapy, targeted radiotherapy, Vynckier - Wambersie

Introduction

The use of radiation therapy as a primary or adjunct procedure is used in approximately 60% of all cancer patients (*1*). The purpose of this treatment is to deliver a lethal dose of radiation to a tumour site while sparing as much healthy tissue as possible (i.e. optimize the treatment's therapeutic index). Unfortunately, there is a very small window over which to optimize therapeutic index for external beam irradiation, often leading to damage of normal tissues (*1*). Therefore, targeted radiotherapy has come to the forefront of research into clinical radiation oncology (*2-6*).

In this light, radio-labelled [^{131}I] *meta*-iodobenzylguanidine (MIBG), a low-LET β-particle emitter, has been a successful agent in the diagnosis and treatment of patients with tumours derived from the neural crest (*7,8*). An analog to adrenergic neuron blockers (*9*), MIBG is actively taken up with high affinity, saturable and ATPase-dependent by cells that actively synthesize the noradrenaline transporter (NAT) (*10,11*). With NAT expression naturally occurring in cell types derived from the neural crest, today, [^{131}I] MIBG treatment is effectively limited to neuroblastomas and pheochromocytomas (*12-15*). To determine the feasibility of MIBG therapy for a wider range of tumour types, Boyd *et al* developed a methodology whereby a plasmid vector is utilized to transfect a target cell with bovine NAT cDNA in a cell line with no inherent expression of the NAT gene (*16*). These results demonstrated the ability of using this technique *in vitro* for effective radiodinated MIBG uptake to produce direct radiation cell killing and has since been demonstrated on additional cell types (*17-20*).

In conjunction with the promise of exploiting this targeted radionuclide therapy, an assessment of radiation-induced biological bystander effects (RIBBE) is of great importance when understanding the potential therapeutic capabilities of this technique. This is particularly important given the potential for heterogeneous uptake through such factors an inefficient gene transfer / expression or other cellular dynamic variables. In fact, the heterogeneity of radiopharmaceutical uptake is a consideration for radionuclide utilization in order to exploit the "physical" bystander effect (i.e. cross-fire) (*16,20*). In 2006, Boyd *et al* examined RIBBE via measurement of surviving fraction of recipient cells following irradiated-cell conditioned medium (ICCM) transfer protocol (*21*) developed by Mothersill and Seymour (*22*). These results indicate substantial bystander cell death for both UVW glioma and EJ138 bladder carcinoma following NAT transfected donor cell exposure to [^{131}I] MIBG treated medium. While a propitious finding, with no dosimetry model or absorbed dose measurement available for such *in vitro* treatment, surviving fraction data is presented as a function of activity concentration rather than absorbed dose. This leads to difficulties in assessing and comparing the actual capability of RIBBE production with previous literature and the potential efficiency of these products in therapy with no accurate estimate of absorbed dose.

As a result, here we have developed a dosimetric model for calculating absorbed dose to donor cells used in the creation of ICCM following treatment with [^{131}I] MIBG. This is accomplished through utilization of the Vynckier-Wambersie point source dose distribution (*23,24*) applied to the appropriate geometry. Two separate models were developed and compared to determine the most computationally efficient method to

perform calculation of absorbed dose over a range of applied activity concentration. For UVW and EJ138 cell lines in used by Boyd *et al*, dose rate and absorbed dose values were calculated for each activity concentration applied. Following this, a re-examination of survival fraction data is undertaken comparing [^{131}I] MIBG and external beam ^{60}Co treatment in eliciting bystander cell death response in recipient cells treated with each ICCM respectively.

Materials and Methods

Experimental procedures utilized for assessment of recipient bystander cell death (i.e. surviving fraction) following treatment with ICCM generated from donor cell exposure to [^{131}I] MIBG is previously described in detail (*21*).

Cell lines

Cell line hosts utilized were the UVW human glioma cell line (*3*) and the EJ138 human bladder carcinoma cell line (*18*) and were maintained in 75-cm^2 flasks containing Eagle's MEM with 25 mmol/L N-(2-hydroxy-ethyl)piperazine-N9-(2-ethanesulfonic acid) buffer and Earle's Salt, supplemented with 10% (v/v) fetal bovine serum, penicillin/streptomycin (100 U/mL), fungizone (2 mg/mL), L –glutamine (2 mmol/L), and nonessential amino acids (0.1 mmol/L). Cells were cultured at 37ºC in a 5% CO_2 atmosphere. As UVW and EJ138 are not naturally expressive for NAT required for active MIBG uptake, both cell lines were transfected with plasmids containing bNAT cDNA under the control of cytomegalovirus (CMV) (UVW/NAT) and hTR (EJ138/NAT) (*18*). Stable transfectant populations were acquired through treatment with geneticin (G418) with every passage yielding a stable population after approximately 4 wk. Cell size was determined by removing them via trypsinization and dilution in PBS and obtained using a Model TT Cell Counter and Analyzer System (Scharfe System, RJM Sales, NJ, USA). More than 10,000 cells were counted per measurement resulting in a mean ± SD diameter of 16.5 ± 0.9 μm and 12.8 ± 0.7 μm for UVW and EJ138

respectively. In addition to this, the doubling time for each cell line is 18 hours for UVW and 17.5 hours for EJ138.

Uptake and Medium Transfer Experiments

For uptake experiments, monolayers were seeded with an initial density of 0.5 x 10^5 cells per well in 6-well plates and cultured for 48 h. Cells were measured for MIBG incorporation by incubating cells for 2 h at 37ºC in complete medium with a range of [^{131}I] MIBG activities. Radioactivity was extracted via 2 aliquots of 10% (w/v) trichloroacetic acid and measured with a γ-counter (Cobra II Auto-γ-Counting System; Packard Instrument Co.). Results of these experiments indicated the cell accumulated activity as a percentage of the activity in the incubation medium was 31.4% ± 3.7% for UVW/NAT cells and 21.4% ± 1.9% for EJ138/ NAT cells with a linear relation between activity accumulated and administered (*21*).

Medium transfer assay technique has been described in detail in (*22*). Cells were initially seeded at 2 x 10^5 cells per 25-cm^2 flask in 10 ml of complete medium and incubated for 24 h at which point resultant flasks were 65 ± 5% confluent. Irradiation occurred after this period of incubation. Cells destined to be irradiated and produce irradiated-cell conditioned medium (ICCM) were labelled "donors" while cells destined to receive ICCM and not be directly irradiated where labelled "recipients". Irradiation of donor cells occurred by one of two methods:

1) Donor cells were irradiated by way of a ^{60}Co γ-ray source at a dose rate of 15 Gy/h through a range of doses from 0 to 9 Gy. Immediately following treatment, donor cells were returned to the incubator and maintained at 37ºC and 5% CO_2 for one hour followed

by removal of the medium (regardless of dose) which was passed through a 0.22-μm to ensure that no cell was present in the transferred medium (*22*). Medium was removed from recipient cells and replaced with the filtered ICCM. These recipient cells were then incubated for a further 24 h at 37ºC and 5% CO_2 followed by their removal with 0.05% trysin-ethylenediamine-tetraacetic acid in PBS (Gibco/Invitrogen Ltd.) and counted via a hemocytometer to be seeded for clonogenic assay. After 10-14 days in incubation, colonies were fixed with a 50:50 solution of methanol/PBS and stained with 10% Gram's crystal violet solution (BDH Laboratories). Colonies containing 50 cells or more were scored as colonies and surviving fraction calculated. This experiment was performed 6 times in triplicate.

2) Donor cell medium was removed on the day of exposure and replaced with 1 ml of fresh medium. Activity concentrations of 0 to 11 MBq/ml of [^{131}I] MIBG were added as per previous experiments (*3,16,18,25*) and cells were incubated for 2 h at 37ºC. We label this portion of the experiment as the "Uptake" phase. After 2 h, the donor medium is removed; cells are washed with PBS to eliminate unincorporated radiopharmaceutical. Five millilitres of fresh medium is then applied and the donor cells are placed back in the incubator for 1 h to allow for bystander factors to accumulate and yield an ICCM. We label this portion of the experiment as the "Accumulation" phase. Egressed activity from the donor cells was ≤ 1% of activity added for all concentrations during this phase and activity controls indicated no significant cell death from such activity levels (*21*). Following 1 h, ICCM was removed, passed through a 0.22-μm filter, and added to

recipient cells for which the medium had been discarded. These cells were then treated identically to those from ^{60}Co irradiation in preparation for clonogenic assay.

An additional set of cultures was used to determine if bystander effects were induced via this protocol with untransfected UVW and EJ138 donor cells. These cells, with no NAT gene expression, were labelled "parental" and ICCM from these donors was obtained and applied to both transfected and untransfected recipients as occurred with UVW/NAT and EJ138/NAT.

Dosimetry Model

When determining the dose to the donor cells used to create the ICCM, dose contributions occurring during both the Uptake and Accumulation phases of [^{131}I] MIBG treatment need be considered. This is necessary as we are unaware of which "dose" initiates the bystander responses leading to cytotoxic factor accumulation when fresh medium is applied. Previous experiments have illustrated a linear accumulation of MIBG for NAT-expressing cell types during the first two hours of exposure (*26*). This coupled with the $\geq 1\%$ egressed activity seen in both UVW/NAT and EJ138/NAT provides us with a dose rate function, $\dot{D}(t)$, as illustrated in Figure C-1:

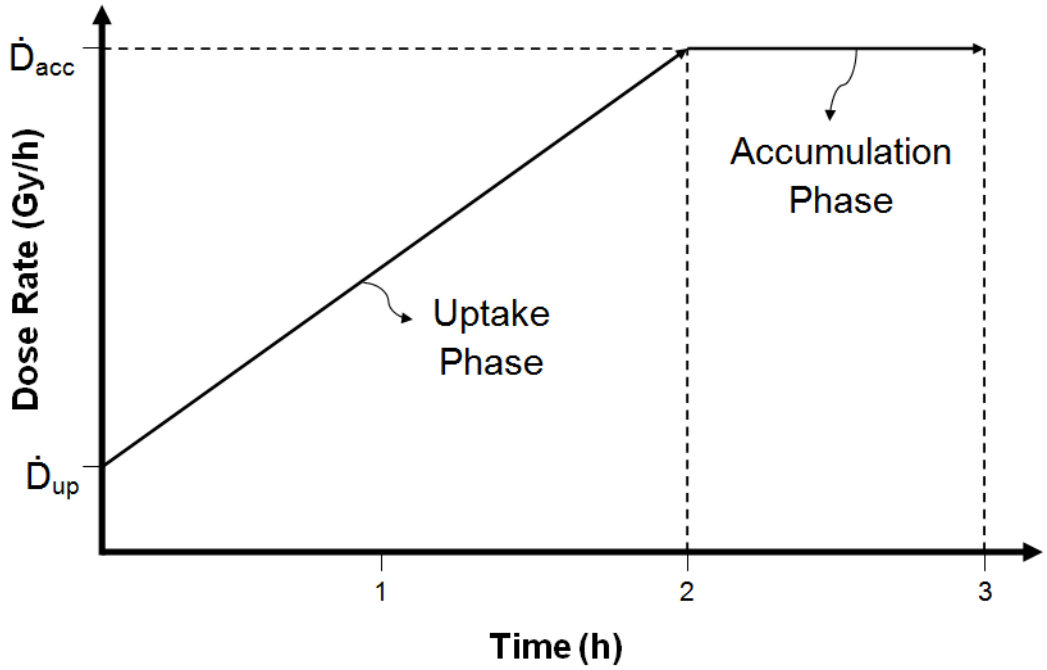

Figure C-1: Irradiation to donor cells used in the production of irradiated-cell conditioned medium (ICCM) occurs in two phases: i) an uptake phase during which [^{131}I] MIBG is taken up by NAT transfected cells and ii) an accumulation phase where fresh medium is applied and bystander factors accrue creating the ICCM. The total dose can be determined through simple integration of the above function.

Upon application of the 1ml of [^{131}I] MIBG-enhanced medium, we assume an instantaneous, homogenous, static mixture uniformly covering all cells with an initial dose rate of $\dot{D}_{up}$ (Gy/h). As donors actively uptake [^{131}I] MIBG over the 2 h allotted, dose rate increases linearly up to a maximum dose rate of $\dot{D}_{acc}$ (Gy/h) when the radioactive medium is removed and cells are washed with PBS. When fresh medium is added to allow for bystander factors to accrue, the dose rate remains effectively constant at $\dot{D}_{acc}$ due to the negligible amount of egress. Therefore, in order to find the total absorbed dose (Gy) to the donor cells used to create the ICCM, we integrate the function presented in Figure C-1:

$$D_{tot} = \frac{\dot{D}_{up} \bullet \dot{D}_{acc}}{2}(2h) + \dot{D}_{acc}(1h) \quad [1]$$

where $\dot{D}_{up}$ and $\dot{D}_{acc}$ are the average initial dose rates upon initiation of the Uptake and Accumulation phases respectively.

To calculate $\dot{D}_{up}$ and $\dot{D}_{acc}$, we utilize the Vynckier-Wambersie point-source dose distribution function (point kernel) (*23*,*24*):

$$J(x) = \frac{B}{(\rho v x)^2}\left\{ c\left[1 - \frac{\rho v x}{c} e^{\left(1 - \frac{\rho v x}{c}\right)}\right] + \rho v x e^{(1-\rho v x)} - \rho v x e^{\left(1 - \frac{\rho v x}{2} - \frac{f}{2}\right)} \right\} \quad [2]$$

with [ ] ≡ 0 for $\rho v x \geq c$ and J(x) ≡ 0 for $\rho v x \geq f$ where:

J(x)	is the absorbed dose rate at a distance x (in cm) from a point source (Gy/MBq·h);
v	is an apparent absorption coefficient (in cm^2/g). Within the maximum β-energy range $0.5\ MeV < E_{\beta_{max}} < 3.5\ MeV$, this value can be expressed as a function of $E_{\beta_{max}}$ (*24*): $$v = 14.5(E_{\beta max})^{-1.17}$$
ρ	is the density of the homogenous medium;
c	is a dimensionless parameter that provides a value for the first term inside the curly brackets to become and remain 0; this parameter was originally defined by Loevinger (*27*) as: $$c = \begin{cases} 1 & 1.5 \leq E_{\beta_{max}} < 3\ MeV \\ 1.5 & 0.5 \leq E_{\beta_{max}} < 1.5\ MeV \\ 2 & 0.17 \leq E_{\beta_{max}} < 0.5\ MeV \end{cases}$$

B	is a normalization constant evaluated for the requirement that the energy emitted by the point source is equal to the energy absorbed by an infinitely large sphere. It is obtained via: $B = (4.6\times10^{2})\rho^{2}v^{3}(E_{\beta avg})\alpha$ in (Gy/MBq·h) where $\alpha^{-1} = 3c^{2} - (c^{2} - 1)e + (3 + f)e^{(1-f)} - 4e^{(1-(f/2))}$ and $E_{\beta avg}$ is the average β-particle energy (in MeV).
f	is a dimensionless parameter where f/ρx represents the distance at which the β dose is required to be zero. Within the energy range $0.5\ \text{MeV} < E_{\beta_{max}} < 3.5\ \text{MeV}$, this value can be described as a function of $E_{\beta_{max}}$ (*24*): $f = 0.269\rho x(E_{\beta max})^{1.31}$

The Vynckier-Wambersie kernel can be integrated over a number of simple geometries to model a variety of source conditions. Here, we apply two versions of the Vynckier-Wambersie kernel; a) during Uptake, a plane of infinite extent and finite thickness and b) during Accumulation, a series of planes of infinite extent that are infinitely thin. The Vynckier-Wambersie kernel can be modelled as infinite in extent, with < 5% correction for radius, provided that the radius of the plane is $\geq 0.5R_{max}$, the continuous slowing-down approximation (CSDA) range of the most energetic β-particle (*28*). For ^{131}I, $E_{\beta max}$ is 0.61 MeV resulting in an approximate CSDA maximum range of 0.227 cm. Under these conditions, the Vynckier-Wambersie plane kernel can be modelled with infinite extent down to a surface area covering 0.04 cm^2. With donor cell treatment occurring in 65% ± 5% confluent 25 cm^2 flasks, we have a true coverage area of 16.25 cm ± 1.25 cm. Thus, under these conditions, we simply apply an identical

transformation to all donor flasks, modelling a typical confluent flask as a singular cylindrical slab of cells as illustrated in Figure C-2.

As the Vynckier-Wambersie kernel is a function of distance from the source, in order to calculate the dose during both the Uptake and Accumulation phase, it is required that the thickness of the cells upon adherence to the flask be determined (i.e. determine the thickness of the slab). To accomplish this, we note that 2 x 10^5 cells were plated 24 h prior to [^{131}I] MIBG treatment at which point donor flasks were 65% ± 5% confluent in 25 cm^2 flasks. With doubling times of 18 h and 17.5 h for UVW and EJ138 respectively, the number of cells present at the time of treatment is given by:

$$C = C_0 e^{\frac{(\text{time})\ln 2}{DT}} \quad [3]$$

where C_0 is the number of cells plated and DT is the doubling time of the cell line used. In addition, volume is conserved upon adhesion to the flask relative to the volume of a cell in suspension. Therefore, with knowledge of the diameter of the UVW and EJ138 cell lines (16.5 ± 0.9 μm and 12.8 ± 0.7 μm respectively), we calculate the total volume for the number of donor cells after 24 h (calculated via Eq. 3) in suspension:

$$V_{tot} = C \bullet \left[\frac{4}{3} \pi \left(0.5 \bullet \text{Cell}_{diam} \right)^3 \right] \quad [4]$$

and determine the thickness of the cellular slab via:

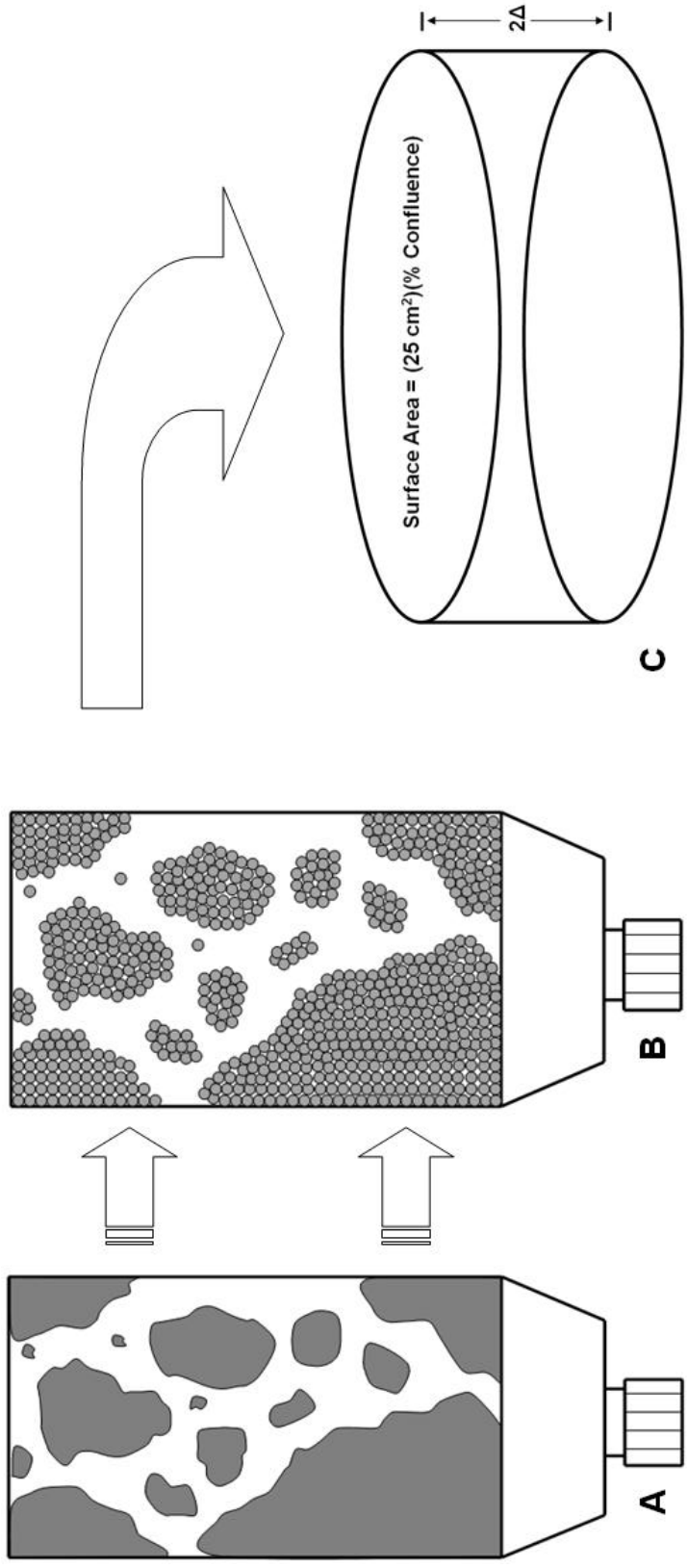

Figure C-2: Schematic representation of cellular distribution in donor flasks used in irradiated-cell conditioned medium (ICCM). **(A)** represents an approximation of the actual distribution and **(B)** represents the same cellular distribution modelled as an aggregation of infinite Vynckier – Wambersie cellular slabs. Since the dose to the entire cellular distribution in **(B)** is the sum of infinite Vynckier – Wambersie cellular slabs, for simplicity, we apply a single transformation to donor cells in **(A)** resulting in a single cylindrical slab of cells **(C)**.

$$\text{thickness} = 2\Delta = \frac{V_{tot}}{(\text{Total Flask Growth Surface Area} \bullet \% \text{ Confluence @ treatment})} \quad [5]$$

where Δ is the half thickness of the cellular slab. Given the experimental conditions in (*21*), the resultant cellular slab thickness was calculated as $(7.3 \pm 0.9) \times 10^{-5}$ cm for UVW and $(3.5 \pm 0.4) \times 10^{-5}$ cm for EJ138.

Dose Rate Calculation: Uptake Phase

As per Figure C-1 and Eq. 1, we aim to calculate the initial dose rate, $\dot{D}_{up}$, upon application of radiopharmaceutical-enhanced medium to donor cells. This scenario is illustrated in Figure C-3:

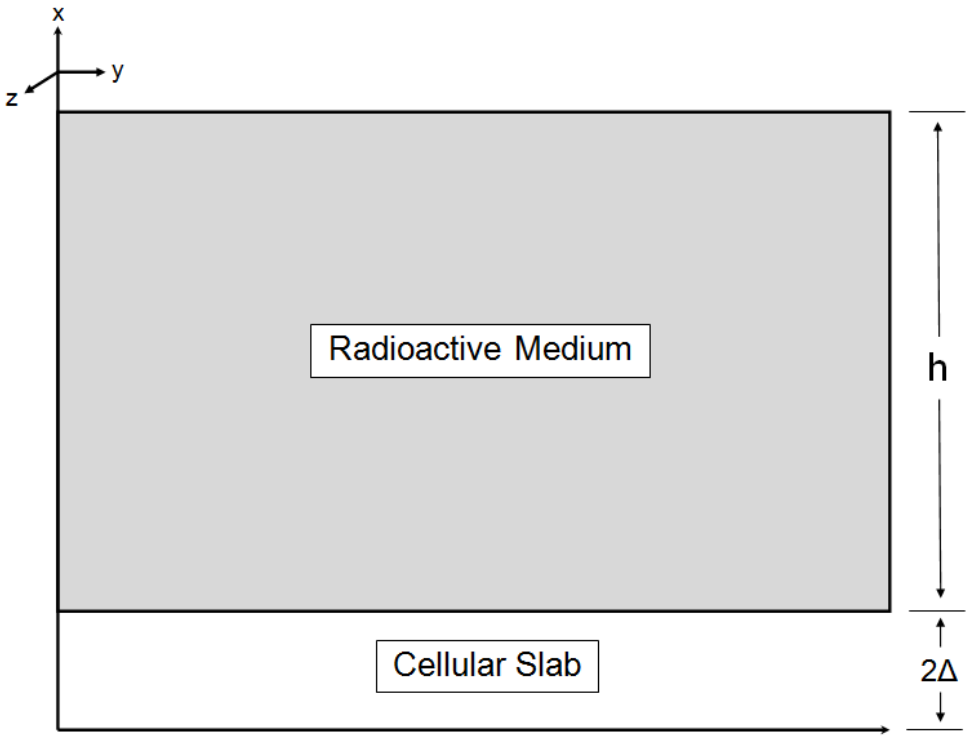

Figure C-3: Illustration of cell and medium distribution at the onset of the uptake phase immediately following application of radiopharmaceutical.

During donor treatment with [^{131}I] MIBG, radiopharmaceutical was added to 1 ml of fresh medium during the 2 h allotted for uptake. First, we observe that the thickness of this 1 ml of radioactive medium at a density equivalent to water (i.e. 1 g/cm^3) covering a 25 cm^2 growth area results is simply 0.04 cm. The density of the radioactive medium and cellular slab is equivalent. The dose rate at a given distance, x, from our source is dependent on the extent (i.e. diameter), d, of the source as well as its thickness, h, resulting in the function $\dot{D}_{up}(x,h,d)$. From (*24*), we have that, for a source of infinite extent and thickness, h, greater than the maximum range of the most energetic β-particle, the dose rate (in Gy/h) is given by:

$$\dot{D}(x,\infty,\infty) = \dot{D}(0,\infty,\infty)\bullet\alpha\bullet \left\{c^2\left[3 - e^{(1-\rho vx)} - \frac{\rho vx}{c}\left(2 + \ln\left(\frac{c}{\rho vx}\right)\right)\right] + e^{(1-\rho vx)} - 4e^{\left(1-\frac{\rho vx}{2}-\frac{f}{2}\right)} + (3 + f - \rho vx)e^{(1-f)}\right\} \quad [6]$$

with [ ] ≡ 0 for ρvx ≥ c and $\dot{D}(x,\infty,\infty) \equiv 0$ for ρvx ≥ f.

Additionally, we note that $\dot{D}(0,\infty,\infty)$ represents the dose rate (in Gy/h) at the edge of an infinite medium. This is equivalent to the dose rate of a semi-infinite medium or half the dose rate of an infinite medium and is expressed by:

$$\dot{D}(0,\infty,\infty) = 0.288 a_m E_{\beta avg} \quad [7]$$

where a_m is the mass activity concentration (MBq/g) and the average β-particle energy in MeV. In our scenario, with our source of unit density, the value for activity is simply the activity concentration (in MBq/ml = MBq/g = MBq/cm^3) administered divided by the number of millilitres of medium (in our case 1 ml). Additionally, since we have assumed

an instant, homogenous, static mixture upon application, radioactive medium covering growth area with no cell present does not contribute dose to the donor cells as this space is effectively located at "infinity". Therefore, we adjust for cellular confluence levels and perform a simple modification to Eq. 7 as follows:

$$\dot{D}(0,\infty,\infty) = 0.288(A_{conc\_up})E_{\beta avg} \quad [8]$$

where $A_{conc\_up} = (A_{admin})(\%\ Confluence)$

With ^{131}I having a maximum CSDA range of 0.226 cm, five times greater than the thickness of the 1 ml of radioactive medium; we cannot neglect the thickness of our source. From simple geometric considerations, we have (*24*):

$$\dot{D}_{up}(x,h,d) = \dot{D}(x,\infty,\infty) - \dot{D}(x+h,\infty,\infty) \quad [9]$$

Utilizing Eq. 6, 8, and 9, $\dot{D}_{up}$ was calculated at x = 0 and 2Δ for h = 0.04 cm. The results were averaged to determine the mean dose rate to the slab upon initial application of the [^{131}I] MIBG-enhanced medium:

$$\dot{D}up = \left\{\left[\dot{D}(0,\infty,\infty) - \dot{D}(0.04,\infty,\infty)\right] + \left[\dot{D}(2\Delta,\infty,\infty) - \dot{D}(2\Delta+0.04,\infty,\infty)\right]\right\} / 2 \quad [10]$$

Due to the small magnitude of the cellular slab thickness, there was < 2% difference in $\dot{D}_{up}(0,0.04,\infty)$ and $\dot{D}_{up}(2\Delta,0.04,\infty)$ resulting in a < 1% difference between the calculated mean $\dot{D}_{up}$ value and the dose rate at any cellular distance from the source.

Dose Rate Calculation: Accumulation Phase

Two separate models were developed for comparison and computational efficiency evaluation. The fundamental difference between the models lies in the manner in which the source is distributed within the slab; homogenously or in discrete planes.

Method #1: "Homogenous-Slab"

During the 1 h Accumulation phase, while bystander factors are allowed to accrue in 5 ml of fresh medium, we assume that the [^{131}I] MIBG taken up by the cells is homogenously distributed within the cellular slab with an activity concentration, A_{conc_acc} (in MBq/cm^3). A_{conc_acc} is dependent on several factors including cellular confluence, (for analogous reasoning as in the Uptake phase), radiopharmaceutical uptake percentage for the cell line, as well as the volume of the cellular slab:

$$A_{conc\_acc} = \frac{(A_{conc\_up})(\%\ \text{Uptake})}{(25\ \text{cm}^2)(\ \%\ \text{Confluence})(2\Delta)} \quad [11]$$

We split the source into a bunch of infinitely thin planes of infinite extent with surface activity, A_s, given by $A_{conc\_acc}\, dx'$ (in MBq/cm^2) (see Figure C-4). The dose rate contribution from a single plane is $d\dot{D} = A_{conc\_acc}\, K(x-x',0,\infty)dx'$ where $K(x-x',0,\infty)$ is the Vynckier –Wambersie dose rate kernel for an infinitely thin, infinite extent plane. This expression is given by (*24*,*28*):

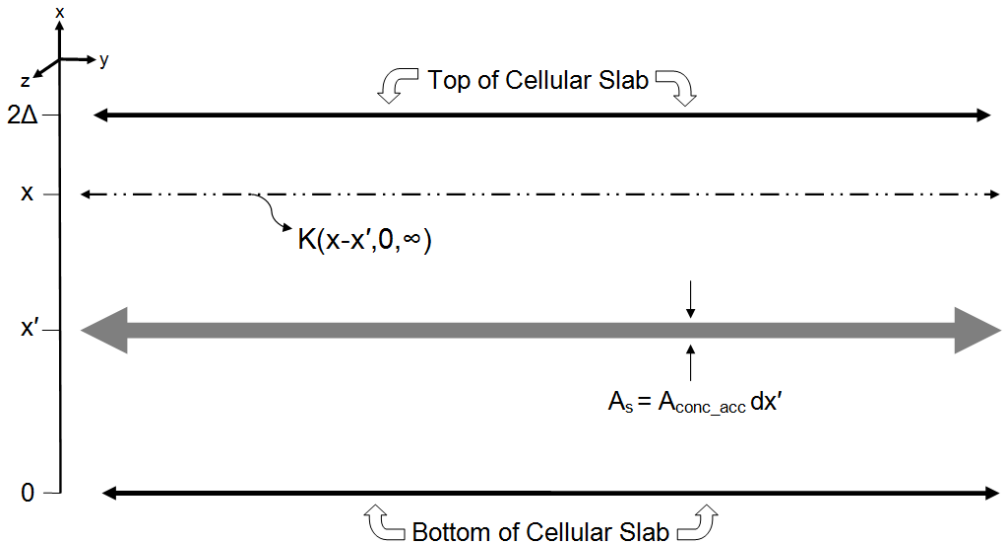

Figure C-4: Illustration of Method #1 radiopharmaceutical modelling during the accumulation phase. We consider the source as split into a bunch of infinite thin disks of surface activity $A_s = A_{conc\_acc}\,dx'$ (MBq/cm^2). For a point x a distance x-x′ from the source, the dose rate contribution is given by $d\dot{D} = A_{conc\_acc}\,K(x\text{-}x',0,\infty)dx'$ where K(x-x′,0,∞) is the Vynckier–Wambersie dose rate kernel for a plane that is infinitely thin and of infinite extent.

$$K(x\text{-}x',0,\infty) = 0.288 \bullet v \bullet \alpha \left\{ c\left[1 + \ln\left(\frac{\rho v(x\text{-}x')}{c} \right) - e^{\left(1 - \frac{\rho v(x\text{-}x')}{c}\right)} \right] + e^{(1 - \rho v(x\text{-}x'))} - 2e^{\left(1 - \frac{\rho v(x\text{-}x')}{c} - \frac{f}{2}\right)} + e^{(1-f)} \right\} \quad [12]$$

To determine the expression for the total dose rate to the cellular slab during the accumulation, we simply integrate over the range x = 0 to 2Δ:

$$\dot{D}(x) = A_{conc\_acc} \int_{x'=0}^{x'=2\Delta} \dot{K}(x\text{-}x',0,\infty)dx' \quad [13]$$

The kernel is actually a function of the distance from the plane to the point of measurement (i.e. |x-x′|). To compensate for this, we make a change of variables to u = x-x′ resulting in:

$$\dot{D}(x)=A_{conc\_acc}\left[\int_{x-2\Delta}^{0}\dot{K}(u,0,\infty)du+\int_{0}^{x}\dot{K}(u,0,\infty)du\right] \quad [14]$$

Then, we let u = |v| providing:

$$\dot{D}(x)=A_{conc\_acc}\left[\int_{0}^{2\Delta-x}\dot{K}(v,0,\infty)dv+\int_{0}^{x}\dot{K}(v,0,\infty)dv\right] \quad [15]$$

Lastly, the average dose rate to the slab, $\dot{D}_{acc}$, is obtained by determining the average dose rate from Eq. 15 over the entire thickness of the slab:

$$\dot{D}_{acc}=\frac{1}{2\Delta}\int_{0}^{2\Delta}\dot{D}(x)dx \quad [16]$$

Method #2: "Multi-isoplane"

Due to the relative thinness of the cells upon adherence to the culture flasks, a second model was created with the aim of improving on the computational efficiency of the model calculations during the Accumulation phase while maintaining the same degree of precision as Method #1. To do this, two paradigms were created in which the activity was evenly distributed into isolated, homogenous planes and dose rates were computed at various positions within the slab (see Figure C-5). Paradigm (A) calculates the dose rate at positions x = 0, Δ, and 2Δ with source planes at x = 0.5Δ and 1.5Δ while paradigm (B) calculates the dose rate at x = 0.5Δ and 1.5Δ with source planes at positions x = 0, Δ, and 2Δ. The surface activity of given plane is provided by:

$$\begin{aligned} A_{tot\_acc} &= \tfrac{1}{2}A_{surf\_acc}+\tfrac{1}{2}A_{surf\_acc} \text{ for Paradigm (A)} \\ &= \tfrac{1}{3}A_{surf\_acc}+\tfrac{1}{3}A_{surf\_acc}+\tfrac{1}{3}A_{surf\_acc} \text{ for Paradigm (B)} \end{aligned} \quad [17]$$

with,

$$A_{surf\_acc} = \frac{(A_{conc\_up})(\%\ Uptake)}{(25\ cm^2)(\%\ Confluence)} \quad [18]$$

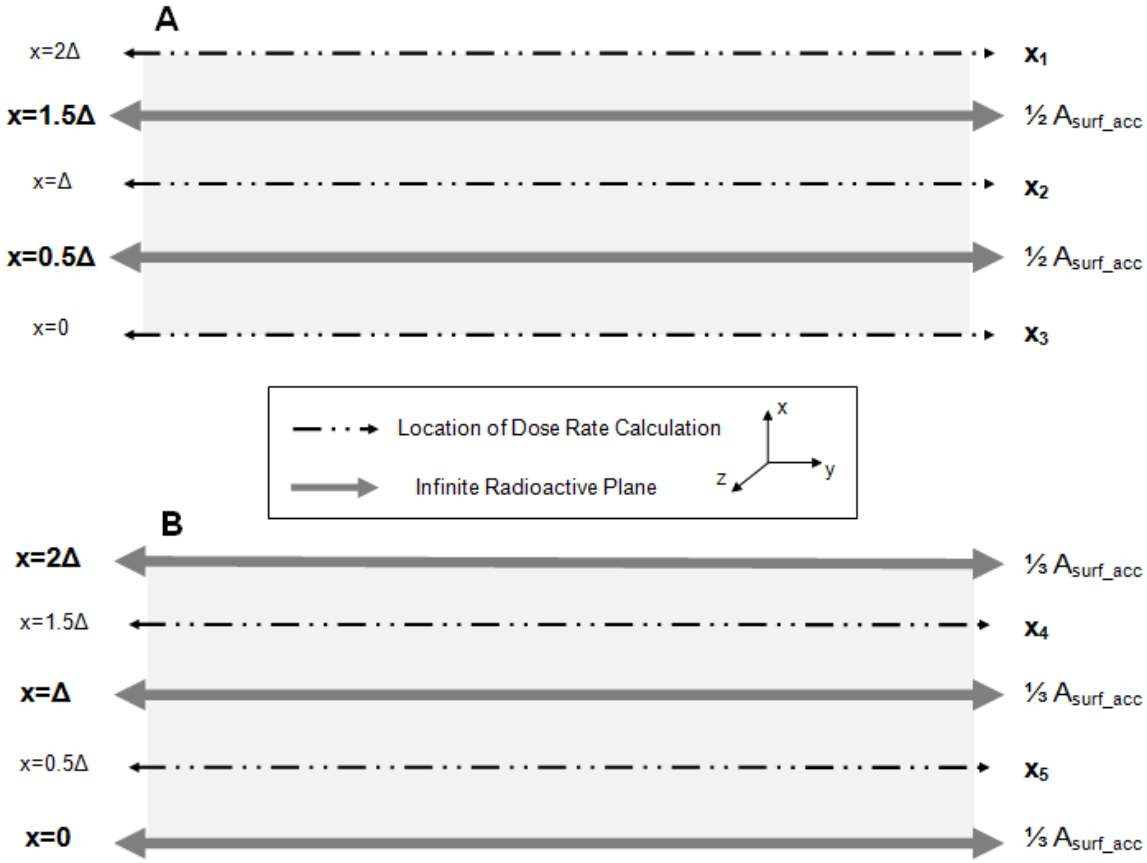

Figure C-5: Illustration of Method #2 radiopharmaceutical modelling during the accumulation phase. The dose rate along five separate planes is calculated via one of two paradigms: **(A)** For equally distributed activity in two infinite planes located at x=0.5Δ and 1.5Δ, calculate $\dot{D}$ at x=0, Δ, and 2Δ. **(B)** For equally distributed activity in three infinite planes located at x=0, Δ, and 2Δ, calculate $\dot{D}$ at x=0.5Δ and 1.5Δ. The average dose rate to the slab, $\dot{D}_{acc}$, is calculated as the average dose rate from these five locations.

The dose rate at a various positions $x_{1\text{-}5}$ are given by:

$$\dot{D}(x_1) = (\tfrac{1}{2} A_{surf\_acc})K(1.5\Delta,0,\infty) + (\tfrac{1}{2} A_{surf\_acc})K(0.5\Delta,0,\infty) = \dot{D}(x_3) \quad [19]$$

$$\dot{D}(x_2) = 2 \bullet (\tfrac{1}{2} A_{surf\_acc})K(0.5\Delta,0,\infty) \quad [20]$$

$$\dot{D}(x_4) = 2\bullet(\tfrac{1}{3}A_{surf\_acc})K(0.5\Delta,0,\infty) + (\tfrac{1}{3}A_{surf\_acc})K(1.5\Delta,0,\infty) = \dot{D}(x_5) \quad [21]$$

The final dose rate during the Accumulation phase using Method #2 is:

$$\dot{D}_{acc} = \frac{1}{5}\sum_{i=1}^{5}\dot{D}(x_i) \quad [22]$$

The results of Eq. 10 and either 16 or 22 were substituted into Eq. 1 in order to obtain the total dose to the donor cells used to create the ICCM for recipient cell treatment.

Software and Statistics

All modelling and calculations were performed using MATLAB 7.9.0 (R2009b; 32-bit; The Mathworks). Analytical integration for the "homogenous-slab" model was performed leveraging either the MATLAB Symbolic Toolbox (ver. 5.3) MuPAD engine or the Maple 13 (Maplesoft) symbolic engine. Two separate MATLAB M-file programs were created: a) comparing the "homogenous-slab" and "multi-isoplane" models during accumulation phase for dose rate results and computation time; and b) the complete dosimetry model allowing automatic calculation of cell slab thickness, dose rates during Uptake and Accumulation phases (using "multi-isoplane" model), and total ICCM dose following user input of the various experimental parameters outlined in Boyd *et al*'s original work (*21*). Both of these programs can be run within the MATLAB environment with output for the dosimetry model being directed to either the terminal or a variety of Microsoft Excel file formats. In addition to this, a standalone Microsoft Windows operating system (OS) application was created for the dosimetry model via utilization of MATLAB's 'deploytool' package and MATLAB compiler (ver. 4.11). This standalone

executable was developed to run on any Windows-based host OS, independent of any MATLAB installation, after a one-time installation of the MATLAB Compiler Runtime libraries (ver. 7.11) delivered with the executable. This application was tested successfully under Windows XP (NT 5.1; SP 3; 32-bit) and Windows 7 (NT 6.1; SP 1; 64-bit) operating systems. All modelling and calculations were performed on the same machine containing an Intel Core 2 Duo T5870 processor at 2.00 GHz (L1 cache = 64 KB; L2 cache = 2 MB) with 3.0 GB of RAM (SODIMM DDR2 at 667 MHz) running a Windows 7 (SP 1) OS.

Particle range data was obtained through the ESTAR program developed by the National Institute of Standards and Technology (NIST) Physical Measurement Laboratory utilizing water as the medium. Recipient cell surviving fractions is presented as the mean ± standard deviation (SD) with significance determined via student's *t* test with confidence value $p = 0.05$. Uncertainty in dose was determined through traditional propagation uncertainty methods (i.e. "square root of the sum of squares") from mean ± minimum/maximum dose rate values obtained from optimization of values for cell slab thickness, donor flask confluence, and [^{131}I] MIBG uptake percentage (e.g. maximum dose rate during the Accumulation phase for Method #1 occurs for maximum uptake percentage for the smallest slab thickness and donor flask confluence).

Results

Comparison of dose rate values and computational performance between "homogenous-slab" and "multi-isoplane" modelling of dose rate during accumulation phase

As an approximated method had been developed ("multi-isoplane" source; Method #2) to model the dose rate to donor cells during ICCM production ("Accumulation Phase"), comparison of the dose rate calculations versus the "homogenous-slab" source (Method #1) was undertaken in order to determine the most optimal methodology to employ. It was anticipated that both methods would yield answers that were in agreement and the method that produced the least amount of computational overhead would be utilized. The results of an activity concentration of 1 MBq/ml for experimental parameters associated with UVW/NAT donor cells can be seen in Table C-1:

Table C-1: Comparison of modelling methodologies used to calculate dose rate during ICCM production.

	Method #1a (MuPAD)	Method #1b (Maple)	Method #2
Avg. Dose Rate during ICCM production (Gy/h)	0.0999 ± (0.033/0.025)	0.0999 ± (0.033/0.025)	0.0937 ± (0.031/0.024)
Avg. Computation Time per Calculation[a] (s)	30.84 ± 0.41	3.98 ± 0.54	0.0215 ± 0.0021

[a] Calculations measured over 9 independent trials (n=9) after computer memory cleared and represented as total time to calculate dose rate and uncertainties ± SD.

As would be expected, both MATLAB's inherent MuPAD symbolic engine and Maple's symbolic engine yielded identical dose rate results via the "homogenous-slab source" model. The Maple symbolic engine greatly outperformed MuPAD in computational efficiency by performing the identical calculation over 7 times faster. By comparison, our "multi-isoplane" model yielded an answer well within agreement of the Method #1 answer, with equivalent relative uncertainty. In addition, this method was over 185 times more efficient than even Maple's symbolic engine. These results directed the use of the "multi-isoplane" method in the further examination of complete survival fraction data from (*21*).

Calculation of dose for [^{131}I] MIBG ICCM and corresponding examination of UVW/NAT and EJ138/NAT recipient cell survival curves

Utilizing the "multi-isoplane" method during the ICCM "accumulation" phase coupled with the associated Vynckier-Wambersie derived expression for a finite-thick, β-emitting slab during the "uptake" phase, dose rates and overall absorbed doses to UVW and EJ138 were calculated. First, the cellular slab thickness was determined for each cell line, resulting in values of 0.73 μm ± 0.09 μm for UVW and 0.35 μm ± 0.04 μm for EJ138. Next, activity concentrations of [^{131}I] MIBG ranging from 1-8 MBq/ml and 1-11 MBq/ml for UVW and EJ138 respectively were utilized to calculate the dose rate during both phases. Mean dose rates for parental lines ranged from 0.015 to 0.116 Gy/h for UVW and 0.014 to 0.161 Gy/h for EJ138 during the "uptake" phase. Corresponding absorbed dose values to parental cell lines (i.e. not transfected with NAT resulting in no active MIBG uptake and no resulting "accumulation" phase) are presented for UVW and

EJ138 in Figure C-6. As clearly seen, the mean dose received by these donor lines is relatively small, obtaining a maximum of only 0.23 Gy for UVW and 0.32 Gy for EJ138 parental lines.

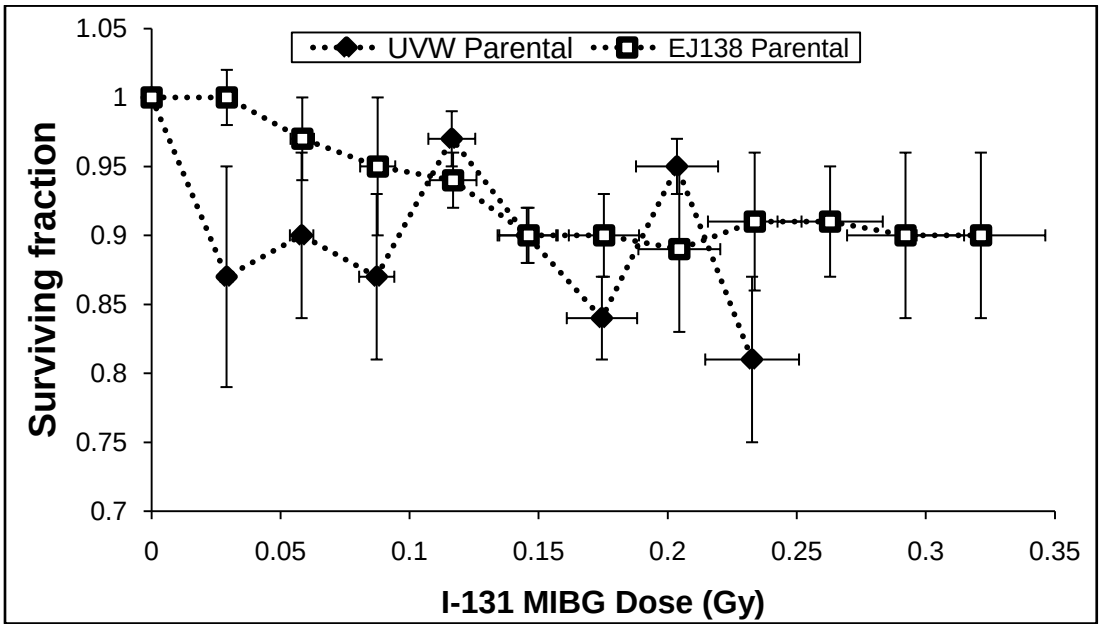

Figure C-6: Plot of recipient surviving fraction (SF) data following ICCM treatment for UVW and EJ138 Parental donor cell types. All SF data was collected across 6 independent experiments performed in triplicate and represented as mean ±SD with no significance observed (*21*).

By contrast, dose rate at the initiation of the "accumulation" phase was significantly great through the entire spread of activity calculations applied for NAT – transfected cells. For UVW/NAT cells, mean dose rates ranged from 0.09 to 0.75 Gy/h while EJ138/NAT mean dose rates ranged from 0.07 to 0.78 Gy/h for the respective range of activity concentrations examined. Total dose to the donor cells producing the ICCM was calculated using Eq. 1 and recipient survival fraction data was plotted for both transfected cell lines (Figure C-7; bottom x-axis). For comparison purposes, ^{60}Co data for these cell lines (*21*) is also shown (Figure C-7; top x-axis).

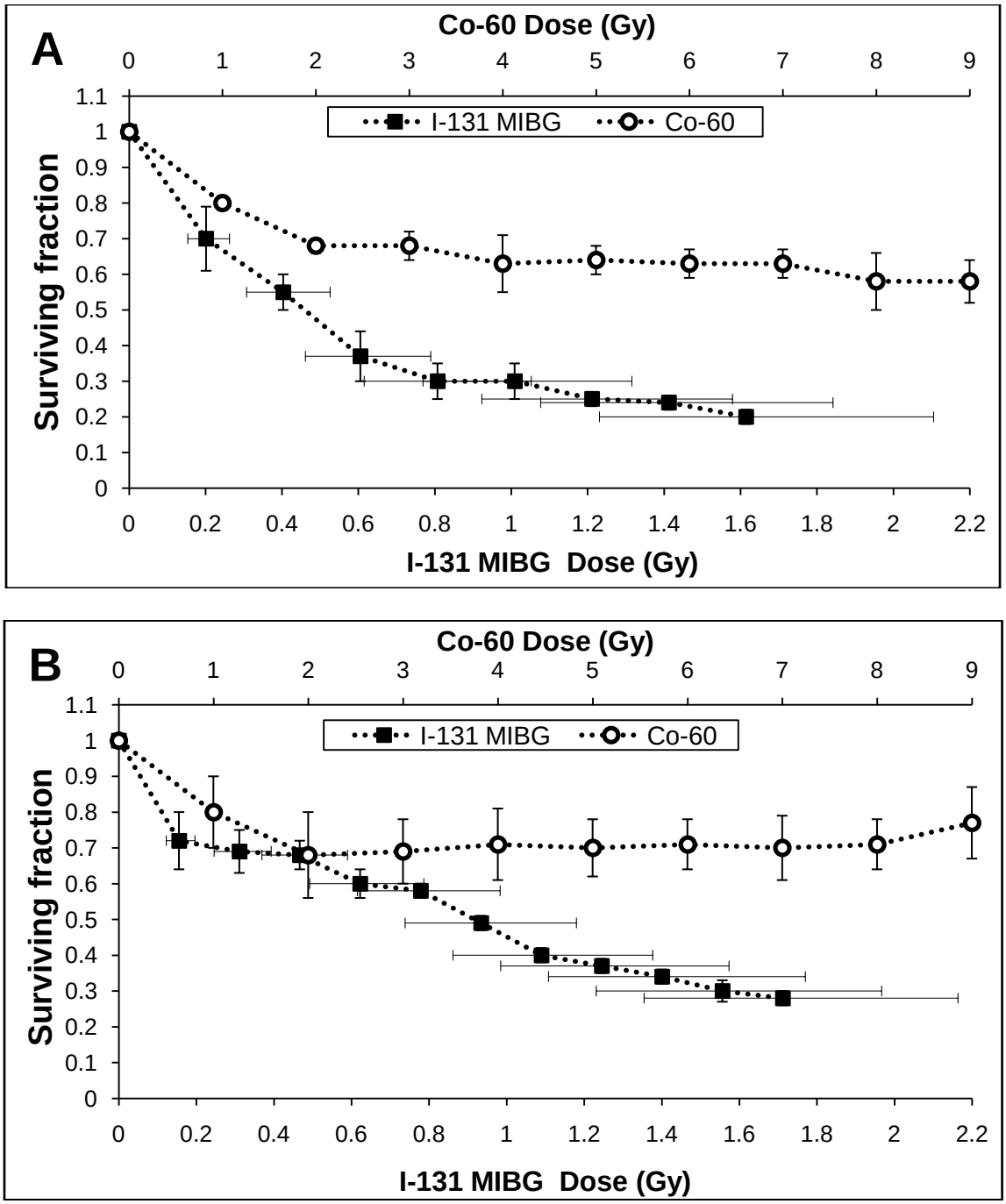

Figure C-7: Plot of surviving fraction (SF) data for **(A)** UVW/NAT and **(B)** EJ138/NAT recipient cells treated irradiated-cell conditioned medium (ICCM) from either [^{131}I] MIBG or ^{60}Co irradiation. All SF data was collected across 6 independent experiments performed in triplicate and represented as mean ±SD (*21*).

Both UVW/NAT and EJ138/NAT require a relatively small ICCM treatment dose to yield a substantial bystander response in recipient cells compared to that used in ^{60}Co treatment. An initial activity concentration of 1 MBq/ml yields mean dose to donor cells of 0.2 and 0.15 Gy for UVW/NAT and EJ138/NAT, increasing linearly with activity concentration and yielding a maximum mean dose 1.6 and 1.7 Gy for each cell line respectively. It is also evident that both cell lines show a decrease in the rate of bystander cell death as dose increases and approaches 2 Gy.

Comparison of survival fractions for similar mean dose ICCM treatments from ^{60}Co and [^{131}I] MIBG

Lastly, surviving fractions of identical or nearly identical mean dose points were examined between ^{60}Co (at a dose rate of 15 Gy/h) and ^{131}I MIBG ICCM treatments. Figure C-8 provides the comparison of these ICCM treatments for UVW/NAT (A) and EJ138/NAT (B). Both cell lines appear to have very similar behaviour compared to their ^{60}Co treated counterpart. For UVW/NAT cells, 5 MBq/ml [^{131}I] MIBG treatment (1 Gy) provided a 50% increase bystander cell death efficiency at a mean maximum dose rate during the accumulation phase of 0.47 Gy/h. On the other hand, EJ138/NAT cells provided a 31% to 40% increase in efficiency at dose points within 10% of 1 Gy ^{60}Co treatment at mean maximum dose rates ranging from 0.42 Gy/h to 0.49 Gy/h.

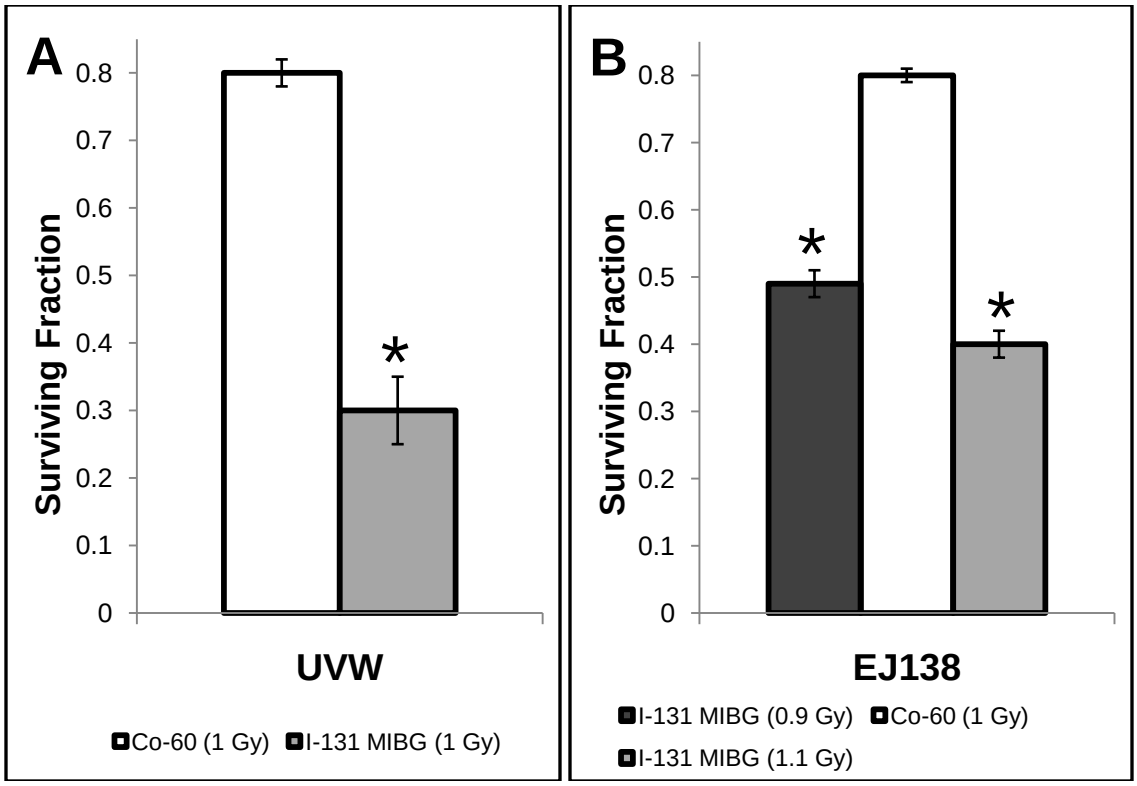

Figure C-8: Comparison of surviving fraction (SF) of **(A)** UVW/NAT and **(B)** EJ138/NAT [^{131}I] MIBG data with similar ^{60}Co dose end points. All SF data was collected across 6 independent experiments performed in triplicate and represented as mean ±SD. ***** indicates $p < 0.05$ for difference in SF at the same dose point.

Discussion

Successful utilization of targeted radionuclide in the treatment of malignancies is vitally dependent on the administration of appropriate levels of absorbed radiation dose to the affected area. Desirable cytotoxic effects to targeted cell types are directly dependent on efficient delivery of the radiopharmaceutical. This is can be confounded by several factors, including heterogeneous uptake and active cellular kinetics resulting from hemodynamic conditions and leading to non-optimal radiopharmaceutical retention. Therefore, in addition to direct physical irradiation, bystander effects will play a prominent role in determining the efficacy of the treatment. For the physical bystander effect, resulting from 'cross-fire' irradiation to neighbouring cells, this consideration has been known for some time and is actively exploited, for example, through the use of long – range β – emitters where heterogeneous uptake is anticipated. In addition to this, research by Boyd *et al* has indicated that RIBBEs can also be elicited resulting in bystander cell death following treatment with radiopharmaceutical to produce cytotoxic ICCM *in vitro* (*20,21*). This effect appears to fall in line with a plethora of research over the better part of the last 20 years indicating the existence of RIBBEs both *in vitro* and *in vivo* (*29*). Such effects are reported following both high – and low – LET irradiations and have been cited as possibly dependent on a number of factors including cytokine release (*30*), nitric oxide (*31*), gap – junction communication (*32*), and reactive oxygen species (ROS) / free radical formation (*33*).

A limitation of radiopharmaceutical RIBBE experiments presented thus far has been the lack of ability to determine appropriate absorbed dose levels to donor cells from radiopharmaceutical treatment utilized to create ICCM. As a consequence, recipient surviving fraction, typically measured against absorbed donor dose, is left to be measured versus administered radiopharmaceutical activity concentration. While able to indeed demonstrate a bystander cell death response, it is difficult to determine and compare the magnitude and efficiency of the effect following radiopharamceutical treatment relative to large amount of literature published to this juncture from external beam ICCM production. Therefore, the current goal of this study was to develop an appropriate model and methodology to calculate absorbed dose to donor cells used in ICCM production following [^{131}I] MIBG treatment enabling a direct comparison of recipient surviving fraction with external ^{60}Co treatment from Boyd *et al*'s study. While additional work has shown bystander cell death for [^{123}I] MIBG and [^{211}At] MABG, we have limited our work here to ^{131}I primarily due to its prevalent use in current clinical applications including widespread utilization of [^{131}I] MIBG in diagnosis and treatment of malignancies derived from the neural crest.

One of the first challenges in this study was an accurate and efficient means to model the source distribution after radiopharmaceutical uptake. This lead to the development of both "homogenous-slab" and "multi-isoplane" source distributions during the accumulation phase. Our hypothesis was that due to the relatively small thickness of the cells upon adherence to the growth surface in culture flasks, the "multi-isoplane" model would provide equivalent calculations for dose rates while being

computational more efficient than the "homogenous-slab" model regardless of symbolic engine. Table C-1 demonstrates these results and confirms our expectation with orders of magnitude computational speed enhancement. Furthermore, the code structure for implementation of the "multi-isoplane" model into the overall absorbed dose calculation model allowed it to be compiled via the MATLAB C-Complier (mcc) something not possible through utilization of the MuPAD or Maple symbolic engine. This allowed for creation of a standalone, Windows – based application that can be utilized for future experiments without the need for acquisition or personal knowledge of the MATLAB environment. This code base can also be shared and modified allowing for additional enhancements and dosimetry modelling within the greater scientific community.

The first surviving fraction behaviour examined was that of the parental cell lines of UVW and EJ138. With no NAT transfection and subsequently no active MIBG uptake, the entire dose to donor cells occurs during the 2 h uptake phase at a dose rate of $\dot{D}_{up}$. With no active uptake of [^{131}I] MIBG, we anticipated a smaller dose and dose rate than during the accumulation phase which would explain the lack of bystander cell death observed. The corresponding calculated dose to the parental cell lines fit this form achieving only maximal mean doses of 0.23 and 0.32 Gy for UVW and EJ138 respectively. Even for well established bystander report cell lines such as HPV-G keratinocytes, typical survival fraction drops are relatively small (10-15%) using medium transfer protocols for doses of 0.5 Gy (*34,35*). Additionally, with no direct cell killing observed in activity control cells (*21*) we would not anticipate any significant bystander

cell death response. Together, these findings aid in instilling confidence in our dosimetry model developed here.

Next, absorbed dose values for [^{131}I] MIBG treatments for transfected UVW/NAT and EJ138/NAT donor cells was undertaken and compared with ^{60}Co external beam ICCM production (Figure C-7). One of the first observations is the decrease in the rate of bystander cell death as dose increases. Although never quite reaching a plateau as occurred with ^{60}Co treatment, absorbed dose calculations for [^{131}I] MIBG treatment indicate that ICCM production never reach the necessary "plateau dose" of 2 Gy for ^{60}Co. However, the [^{131}I] MIBG treatment appears to be rapidly approaching this levelling – off as overall treatment dose moves towards 2 Gy. This behaviour again lends credence to the dosimetry model implemented as we would expect similar overall behaviour of the surviving fraction curve for the same cell lines and similar low – LET irradiation and dose values.

While apparent similarities exist in, significant differences are also obvious in the magnitude of the bystander cell death response following [^{131}I] MIBG versus external beam treatment dose (Figure C-8). With cell line and absorbed dose effectively being (nearly) equal, two essential differences in treatment are: a) radiation type (β – particles versus γ – rays) and b) dose rates (UVW = 0.09 Gy/h – 0.75 Gy/h and EJ138 = 0.07 Gy/h – 0.78 Gy/h for [^{131}I] MIBG versus 15 Gy/h for ^{60}Co). In regards to radiation type, it has long been recognized in experimental biology that similar LET radiations do not all have the same effectiveness at inducing cellular damage. It has been shown via chromosome aberrations in human lymphocytes and mouse oocytes that 200 kV x – rays are two –

three times as effective as γ – rays (*36,37*) while ^{60}Co γ – rays have been shown to be three times more effective then 15 MeV electrons (*37*). Additionally, experiments by Sasaski *et al* (*38*) and Schmid *et al* (*39*) have also pointed to higher chromosome aberrations by lower LET x – rays relative to high energy γ – rays. Furthermore, for bystander responses in particular, our group has indicated a significant difference in bystander cell death between ^{60}Co γ – rays and 20 MeV electrons for low, nearly equivalent, clinical dose rate at high doses (*35*). Therefore, we can not neglect the fact that radiation type may play a role in the observed difference in bystander cell death.

On the other hand, the effects of low – dose – rate (LDR) irradiation (0.1 Gy/h to 1 Gy/h) have been reported to affect multiple biological processes in both normal and tumour cell types (*40*) and have previously been discussed as potentially relevant to radionuclide therapy (*41*). Decreases in dose rate are often associated with sparing effects of direct irradiation (*42*) but have been also shown to invoke a hypersensitivity in some cell lines leading to an increase in cell death relative to higher dose rates (i.e. 'inverse dose-rate effect') (*43*). These inverse dose-rate effects have been seen in a variety of cell types (*44-46*) and have been postulated as possibly reflecting the hyper-radiosensitivity of cell lines in responses to a small, acute dose (*45*). Additionally, animal studies have also illustrated the effectiveness of ^{131}I labelled antibody treatment and low-dose rate versus high-dose rate exposure in significantly decreasing tumour volume (*47*). While the precise mechanism underlying LDR effects are not completely defined, it is likely that these cellular responses have reciprocal, secondary processes working in concert. Furthermore, with any correlation between LDR and bystander

effects currently unclear, we can not preclude the fact that direct LDR effects would not influence subsequent bystander responses measurable through the medium transfer protocol. In fact, with the evidence presented here, we speculate that low – dose rates may be a dominant contributing factor exacerbating the observed biological bystander cell death.

Although not examined here, we make of note of the bystander response seen in ICCM production with [^{123}I] MIBG and [^{211}At] MABG, high – LET radiopharmaceuticals (*21*). These results indicate in both cases that a maximum bystander response is reached followed by a substantial decrease in bystander response resulting in a distinct U – shaped surviving fraction curve. Such a phenomenon has previously been illustrated by our group in other normal HPV-G keratinocytes (*35*) as well as malignant T98G glioma (*30*). In both cases, this novel observation in the reduction of bystander efficiency to or near control levels following significant bystander cell death did not occur until ICCM production occurred with substantially higher doses. In this light, we hypothesize that due to several contributing factors including high – LET, relatively short particle range, and extranuclear cell accumulation of these radiopharmaceuticals, dosimetry models for [^{123}I] MIBG and [^{211}At] MABG could yield high absorbed dose values at top – end activity concentrations tested. This offers a plausible explanation for the observed U – shaped behaviour and is a potential area for further investigation.

Conclusion

In this study, a computationally efficient model for determining absorbed dose values following β – emitting radiopharmaceutical treatment for ICCM production was developed. This model was applied to experimental protocol outlined by Boyd and company (*21*) and used to provide direct comparison with ^{60}Co external beam treatment. This dosimetry provides plausible, quantitative explanation for both the lack of bystander response seen in UVW and EJ138 parental cell lines as well as overall behaviour of surviving fraction curves for NAT transfected recipients. Additionally, the model points to the possibility of LDR effects as an explanation for the observed increase in efficiency of bystander cell death seen with [^{131}I] MIBG treatment. Through development of a standalone application for the dosimetry model, further investigation in bystander responses of additional NAT – expressing or transfected cell lines is a direction of further investigation as well as optimization of biological bystander responses through treatment with various activity concentrations. Identification of RIBBE factors will aid in the development of novel targeted radiopharmaceutical treatment designs, maximizing malignant cell death and sparing normal tissue.

Acknowledgements

The authors would like to mention and give thanks Andrei Hanu (McMaster University) for his MATLAB insights in the early stages of this endeavour.

References

1. Perez CA, Brady LW,editors. *Principles and practice of radiation oncology*. Philadelphia, PA: Lippincott-Raven Publications: 1998:p.957.

2. Boyd M, Spenning HS, Mairs RJ. Radiation and gene therapy: rays of hope for the new millennium? *Curr.Gene Ther.* 2003;3:319-339.

3. Boyd M, Mairs RJ, Keith WN, et al. An efficient targeted radiotherapy/gene therapy strategy utilising human telomerase promoters and radioastatine and harnessing radiation-mediated bystander effects. *J.Gene Med.* 2004;6:937-947.

4. Kufe D, Weichselbaum R. Radiation therapy: activation for gene transcription and the development of genetic radiotherapy-theraputic strategies in oncology. *Cancer Biology Therapy*. 2003;63:326-329.

5. Mitrofanova E, Unfer R, Vahanian N, Link C. Rat sodium iodide symporter allows using lower dose of 131I for cancer therapy. *Gene Ther.* 2006;13:1052-1056.

6. Mairs RJ, Boyd M. Targeting Radiotherapy to Cancer by Gene Transfer. *J.Biomed.Biotechnol.* 2003;2003:102-109.

7. Cunningham S, Boyd M, Brown MM, et al. A gene therapy approach to enhance the targeted radiotherapy of neuroblastoma. *Med.Pediatr.Oncol.* 2000;35:708-711.

8. Mairs RJ. Neuroblastoma therapy using radiolabelled [131I]meta-iodobenzylguanidine ([131I]MIBG) in combination with other agents. *Eur.J.Cancer.* 1999;35:1171-1173.

9. Wieland D.M., Wu J., Brown L.E., Mangner T.J., Swanson D.P., Bierwaltes W.H. Radiolabelled adrenergic neuron-blocking agents: adrenomedullary imaging with [131]iodobenzylguanidine. *J Nucl Med.* 1980;21:349-353.

10. Jacques Jr S., Tobes M.C., Sisson J.C., Baker J.A., Wieland D.M. Comparison of sodium dependence of uptake of meta-iodobenzylguanidine and norepinepherine into cultered bovine adrenomedullarycells. *Mol Pharmacol*. 1984;26:539-546.

11. Mairs RJ, Boyd M. Optimizing MIBG therapy of neuroendocrine tumors: preclinical evidence of dose maximization and synergy. *Nucl.Med.Biol.* 2008;35 Suppl 1:S9-20.

12. Hoefnagel CA, Voute PA, de Kraker J, Marcuse HR. Radionuclide diagnosis and therapy of neural crest tumors using iodine-131 metaiodobenzylguanidine. *J.Nucl.Med.* 1987;28:308-314.

13. Leung A, Shapiro B, Hattner R, et al. Specificity of radioiodinated MIBG for neural crest tumors in childhood. *J.Nucl.Med.* 1997;38:1352-1357.

14. Hoefnagel CA. Nuclear medicine therapy of neuroblastoma. *Q.J.Nucl.Med.* 1999;43:336-343.

15. Rose B, Matthay KK, Price D, et al. High-dose 131I-metaiodobenzylguanidine therapy for 12 patients with malignant pheochromocytoma. *Cancer*. 2003;98:239-248.

16. Boyd M, Cunningham SH, Brown MM, Mairs RJ, Wheldon TE. Noradrenaline transporter gene transfer for radiation cell kill by 131I meta-iodobenzylguanidine. *Gene Ther.* 1999;6:1147-1152.

17. Fullerton NE, Boyd M, Ross SC, et al. Comparison of radiohaloanalogues of meta-iodobenzylguanidine (MIBG) for a combined gene- and targeted radiotherapy approach to bladder carcinoma. *Med.Chem.* 2005;1:611-618.

18. Fullerton NE, Mairs RJ, Kirk D, et al. Application of targeted radiotherapy/gene therapy to bladder cancer cell lines. *Eur.Urol.* 2005;47:250-256.

19. Quigg M, Mairs RJ, Brown SM, et al. Assessment in vitro of a novel therapeutic strategy for glioma, combining herpes simplex virus HSV1716-mediated oncolysis with gene transfer and targeted radiotherapy. *Med.Chem.* 2005;1:423-429.

20. Boyd M, Sorensen A, McCluskey AG, Mairs RJ. Radiation quality-dependent bystander effects elicited by targeted radionuclides. *J.Pharm.Pharmacol.* 2008;60:951-958.

21. Boyd M, Ross SC, Dorrens J, et al. Radiation-induced biologic bystander effect elicited in vitro by targeted radiopharmaceuticals labeled with alpha-, beta-, and auger electron-emitting radionuclides. *J.Nucl.Med.* 2006;47:1007-1015.

22. Mothersill C, Seymour C. Medium from irradiated human epithelial cells but not human fibroblasts reduces the clonogenic survival of unirradiated cells. *Int.J.Radiat.Biol.* 1997;71:421-427.

23. Vynckier S, Wambersie A. Dosimetry of beta sources in radiotherapy I. The beta point source dose function. *Phys.Med.Biol.* 1982;27:1339-1347.

24. Vynckier S, Wambersie A. Dosimetry of beta sources in radiotherapy: Absorbed dose distributions around plane sources. *Radiation Protection Dosimetry*. 1986;14:169-173.

25. Mairs RJ, Russell J, Cunningham S, et al. Enhanced tumour uptake and in vitro radiotoxicity of no-carrier-added [131I]meta-iodobenzylguanidine: implications for the targeted radiotherapy of neuroblastoma. *Eur.J.Cancer*. 1995;31A:576-581.

26. Armour A, Mairs RJ, Gaze MN, Wheldon TE. Modification of meta-iodobenzylguanidine uptake in neuroblastoma cells by elevated temperature. *Br.J.Cancer*. 1994;70:445-448.

27. Loevinger R., Japha E.M.,Brownwell G.L. *Discrete radioisotope sources. I. Beta-radiation*. New York: Academic Press: 1956:p.694.

28. The International Commission on Radiation Units and Measurements. *Appendix C: Calculation of Beta-Ray Dose Distributions By Integration of the Beta-Ray Point-Source Dose Function. In: Dosimetry of Beta Rays and Low-Energy Photons for Brachytherapy with Sealed Sources*. Bethesda, MD: Oxford University Press: 2004:p.155.

29. Brooks AL. Evidence for 'bystander effects' in vivo. *Hum.Exp.Toxicol.* 2004;23:67-70.

30. Gow MD, Seymour CB, Ryan LA, Mothersill CE. Induction of bystander response in human glioma cells using high-energy electrons: a role for TGF-beta1. *Radiat.Res.* 2010;173:769-778.

31. Shao C, Folkard M, Prise KM. Role of TGF-beta1 and nitric oxide in the bystander response of irradiated glioma cells. *Oncogene*. 2008;27:434-440.

32. Shao C, Furusawa Y, Aoki M, Ando K. Role of gap junctional intercellular communication in radiation-induced bystander effects in human fibroblasts. *Radiat.Res.* 2003;160:318-323.

33. Azzam EI, de Toledo SM, Spitz DR, Little JB. Oxidative metabolism modulates signal transduction and micronucleus formation in bystander cells from alpha-particle-irradiated normal human fibroblast cultures. *Cancer Res.* 2002;62:5436-5442.

34. Ryan LA, Smith RW, Seymour CB, Mothersill CE. Dilution of irradiated cell conditioned medium and the bystander effect. *Radiat.Res.* 2008;169:188-196.

35. Gow MD, Seymour CB, Byun SH, Mothersill CE. Effect of dose rate on the radiation-induced bystander response. *Phys.Med.Biol.* 2008;53:119-132.

36. Bond VP, Meinhold CB, Rossi HH. Low-dose RBE and Q for x-ray compared to gamma-ray radiations. *Health Phys.* 1978;34:433-438.

37. Edwards AA, Lloyd RJ, Purott JS,Prosser JS. *The dependence of chromosome aberation yields on dose rate and radiation quality. In: Research and development report 1979 - 1981, RAD 4.* Clinton, UK: National Radiological Protection Board: 1982:p.83.

38. Sasaki MS, Kobayashi K, Hieda K, et al. Induction of chromosome aberrations in human lymphocytes by monochromatic X-rays of quantum energy between 4.8 and 14.6 keV. *Int.J.Radiat.Biol.* 1989;56:975-988.

39. Schmid E, Regulla D, Kramer HM, Harder D. The effect of 29 kV X rays on the dose response of chromosome aberrations in human lymphocytes. *Radiat.Res.* 2002;158:771-777.

40. Gridley DS, Williams JR, Slater JM. Low-dose/low-dose-rate radiation: a feasible strategy for cancer radiotherapy? *Cancer Ther.* 2005;3:105-130.

41. Sgouros G, Knox SJ, Joiner MC, Morgan WF, Kassis AI. MIRD continuing education: Bystander and low dose-rate effects: are these relevant to radionuclide therapy? *J.Nucl.Med.* 2007;48:1683-1691.

42. Hall EJ, Bedford JS. Dose Rate: Its Effect on the Survival of HeLa Cells Irradiated with gamma rays. *Radiat.Res.* 1964;22:305-315.

43. Mitchell JB, Bedford JS, Bailey SM. Dose-rate effects on the cell cycle and survival of S3 HeLa and V79 cells. *Radiat.Res.* 1979;79:520-536.

44. DeWeese TL, Shipman JM, Dillehay LE, Nelson WG. Sensitivity of human prostatic carcinoma cell lines to low dose rate radiation exposure. *J.Urol.* 1998;159:591-598.

45. Mitchell CR, Folkard M, Joiner MC. Effects of exposure to low-dose-rate (60)co gamma rays on human tumor cells in vitro. *Radiat.Res.* 2002;158:311-318.

46. Widel M, Przybyszewski WM. Inverse dose-rate effect for the induction of micronuclei in Lewis lung carcinoma after exposure to cobalt-60 gamma rays. *Radiat.Res.* 1998;149:98-102.

47. Knox SJ, Levy R, Miller RA, et al. Determinants of the antitumor effect of radiolabeled monoclonal antibodies. *Cancer Res.* 1990;50:4935-4940.

CONCLUSION

The effects of dose, dose rate and different radiation types of similar LET have been known for some time on directly irradiated cells. Coupled with the mounting evidence of secondary, bystander responses, investigation into the correlation between these effects and fundamental radiation treatment parameters was, and continues to be, a plausible direction to further research in this arena. In Part A of this work, the objective was simply to test whether changes in dose rate and high dose ICCM production would have a significant impact on bystander cell survival in a well established bystander – responsive cell line. Surviving fraction data indicated that for both ^{60}Co irradiations and high energy electrons, ICCM produced through 10 Gy (a dose largely unexamined due to the apparent observation of a survival plateau for recipient cells) resulted in surviving fractions returning to control levels and greater. While somewhat unexpected, this data suggest that an essential component of the bystander signalling process is possibly mediated by way of a negative – feedback mechanism resulting in the reversal of cellular death and promotion of proliferation. This insight is further strengthened by increase numbers of recipients reversing this proliferative effect again pointing to a signal – to – cell ratio being of importance in mitigating recipient cell death. In regards to dose rate, through utilization of a LINAC – generated electron source, high dose rates showed an exaggeration of this proliferative effect at high doses relative to dose rates 10 times lower. Additionally, a difference between similar LET γ – rays and electrons was observed at high doses and low dose rates. Together, these findings indicate the potential

importance of treatment in ICCM production in recipient cell responses (specifically at high doses and dose rates) and provide telling behaviour in mediation of bystander survival.

With the foundation laid as to the influence of dose and dose rate, this begged the question, "Can a bystander cell death response be instigated in a cell line with no previous observed effect merely through manipulation of ICCM production treatment?" In Part B, a human glioma cell line (T98G) with no previously observed bystander cell death effect was utilized in combination with high dose (up to 20 Gy) and high dose rate (10 Gy min^{-1}) electron irradiation. Irradiation treatment in this manner yielded a medium of equal toxicity to our well – established cell line inducing a significant bystander cell death. Furthermore, while surviving fraction remained lower up to 10 Gy, doses of 15 and 20 Gy returned survival to near control levels resulting in a U – shaped survival curve nearly identical to our well established response. This reemphasized the idea of a essential component of the bystander response that either has a negative feedback response, or is in competition with a proliferative signalling mechanism. Furthermore, while the bystander phenomena has been known to effect both normal and malignant tissues, the near identical nature of the bystander cell death response following mere alteration of ICCM production protocol lends itself to the idea that perhaps important contributing factors are universal. In order to explain the perceived bystander cell death, examination for the presence of TGF-β1, a universal cytokine in vertebrates and previously implicated in bystander responses (Burdak-Rothkamm *et al.*, 2007; Iyer *et al.*, 2000; Shao *et al.*, 2008), was tested for in the ICCM. While no active TGF-β1 was

present in both frozen and "real – time" sampling of ICCM, addition of monoclonal antibodies to recipient medium completely abolished bystander cell death indicating TGF-β1 as an essential downstream factor in mitigating the response. In combination with previous studies, this research continues to lend credence to the prospect of TGF-β1 as an essential factor in the chain of events leading to a variety of bystander responses across varying of cell types.

Lastly, an effort was undertaken to understand the effect of dose and dose rate in ICCM toxicity and recipient response in the "holy – grail" of radiotherapy (Mothersill and Seymour, 2006b), namely targeted radiopharmaceutical treatment. In 2006, work by Boyd *et al* showed the induction of bystander cell death following ICCM treatment produced by the radiopharmaceutical [^{131}I] metaiodobenzylguanidine (MIBG) (Boyd *et al.*, 2006). What's more, this effect appeared to differ to that of traditional ^{60}Co external beam ICCM production in both magnitude and surviving curve shape. A road – block in analysis and comparison between the two treatments types lay in the lack of dosimetry model available to calculate absorbed dose to the donor cells during ICCM production from [^{131}I] MIBG treatment. Thus, the objective of Part C was to develop a robust, accurate model of absorbed dose to donor cells following the protocol utilized by Boyd *et al* allowing for direct comparison of treatment types and potential effects of dose, dose rate, and radiation source on the observed bystander response. Through utilization of the Vynckier – Wambersie point – source distribution function (dose point kernel) coupled with simplified geometry, an estimate of dose rate during radiopharmaceutical uptake and ICCM accumulation phases was established allowing for calculation of absorbed dose to

donor cells. This process was optimized for greatest computational efficiency through comparison of two separate source models during ICCM production and symbolic engines from leading analytical platforms. Coupled with surviving fraction, results point to the dose, dose rate, and possibly radiation type as factors in the observed behaviour. For parental cell lines with no ability for active uptake of [^{131}I] MIBG, dose and dose rates were calculated to be relatively small ($\geq$ 0.3 Gy and 0.16 Gy h^{-1}) providing a plausible explanation for this cell line's lack of bystander response. Contrarily, cells with active MIBG uptake had a surviving curve shape similar to their ^{60}Co counterparts prior to reaching a surviving fraction plateau at 2 Gy. While the behaviour is similar, the magnitude of the response was dramatically more efficient in MIBG treatment. With dose rates an order of magnitude smaller for MIBG treatment as opposed to ^{60}Co treatment, it is believed that is increase in efficiency is possibly a manifestation of Low Dose – Rate (LDR) effects in the donor cells and/or differential behaviours of similar, low - LET irradiation. While further studies are obviously required to confirm a connection between LDR and bystander responses from MIBG treatment, all dosimetry modeling utilized in this investigation was coded and compiled into a standalone, Windows OS application. The hope is that such application will enable further research into the bystander cell death response of β-emitting radiopharmaceuticals. Additionally, through community modification of the source code, additional dosimetry models can be added for alternative radio-labelled drugs with potential in target therapy. It is through a deeper understanding and manipulation of such effects that the scientific community will fully leverage the potential of such novel treatments.

As a whole, the work presented aids in providing further insight into the manipulation and factors involved in the radiation – induced biological bystander response from low – LET radiation. Firstly, it is clear that dose rate is of potential importance in the production of ICCM for the widely utilized medium transfer protocol (Mothersill and Seymour, 1997), especially at high or low dose rates. Additionally, high dose ICCM can yield significantly different bystander responses diverging from a well established plateau and yielding a U – shaped response. Manipulation of dose and dose rate can also be performed to initiate bystander cell death in cell lines previously reported as resistant to this effect. Together, we gain insight into potential critical underlying mechanisms, such as TGF-β1, in mitigating the effect. While adding and advancing the academic knowledge base, more data is required in order to incorporate these findings into a robust, cell – type agnostic model of bystander cell death. Further studies manipulating various combinations of cell types, donor / recipient cell levels, dose and dose rates are needed before a more detailed, prediction-driven model can be developed to augment the classic target – theory of radiation response beyond DNA and even the cell itself.

It is unknown if current bystander experimental methodology lacks a certain necessary rigour to develop a comprehensive and robust model of activation of a variety of bystander phenomena across a plethora of experimental environments. The classical, reductionist approach while capable of identifying key components of the interaction(s) taking place (which could be subsequently exploited / manipulated for benefit) could lack the horizontal breadth necessary of connecting seemingly disparate "dots". In a sense,

reductionist methodologies act as "flash-lights" in illuminating our knowledge. However, the simple fact that the cell itself is not a reductionist system by nature of the massive degree of interoperability between communication signalling and function make holistic, "spot-light" understanding of bystander phenomenon an arduous task to say the least. There has been relatively recent publications pointing to the necessity of leveraging system biology techniques in developing a true understanding of the dynamic mechanisms at play in complex biological process underlying radiation response (Barcellos-Hoff and Costes, 2006; Munro, 2009). At its heart, it has been speculated that it is in fact the "system" that responds, not merely the cell itself, from radiation insult as a means to stabilize a cellular community and remain in a homeostatic state (Barcellos-Hoff and Brooks, 2001). While such response is common in biological systems, it remains to be seen if in fact this is the case radiation exposure and if bystander factors are a component in this response. But regardless of whether a systems approach is required or merely a larger amount of reductionist results, the community undertaking the endeavour to solve bystander radiation responses would be well – off pursuing a closer collaboration and exchange of standardized, structured experimental data. This dives a level deeper than mere repetition of identical experimental methods. The pooling of collected data in an identical structured and standardized method accessible to relevant laboratories would provide a data – layer force multiplier providing research groups with more information to effectively target potential exploitable properties and model these phenomena using a variety of techniques. This is not to say that all groups undertake identical experiments. On the contrary, diversity would be encouraged within a data

acquisition framework, potentially leading to not only closer collaboration but also novel directions in autonomous research in understanding the true nature of biological radiation response.

REFERENCES

Baehrecke E.H., How death shapes life during development. Nature Reviews. *Mol.Cell Biol.* **3**, 779-787 (2002).

Barcellos-Hoff M. H. and Brooks A. L., Extracellular signaling through the microenvironment: a hypothesis relating carcinogenesis, bystander effects, and genomic instability. *Radiat.Res.* **156**, 618-627 (2001).

Barcellos-Hoff M. H. and Costes S. V., A systems biology approach to multicellular and multi-generational radiation responses. *Mutat.Res.* **597**, 32-38 (2006).

Baskar R., Emerging role of radiation induced bystander effects: Cell communications and carcinogenesis. *Genome Integr.* **1**, 13 (2010).

Baskar R., Balajee A. S. and Geard C. R., Effects of low and high LET radiations on bystander human lung fibroblast cell survival. *Int.J.Radiat.Biol.* **83**, 551-559 (2007).

Boyd M., Ross S. C., Dorrens J., Fullerton N. E., Tan K. W., Zalutsky M. R. and Mairs R. J., Radiation-induced biologic bystander effect elicited in vitro by targeted radiopharmaceuticals labeled with alpha-, beta-, and auger electron-emitting radionuclides. *J.Nucl.Med.* **47**, 1007-1015 (2006).

Brenner D. J., Hlatky L. R., Hahnfeldt P. J., Huang Y. and Sachs R. K., The linear-quadratic model and most other common radiobiological models result in similar predictions of time-dose relationships. *Radiat.Res.* **150**, 83-91 (1998).

Brooks A. L., Paradigm shifts in radiation biology: their impact on intervention for radiation-induced disease. *Radiat.Res.* **164**, 454-461 (2005).

Burdak-Rothkamm S., Short S. C., Folkard M., Rothkamm K. and Prise K. M., ATR-dependent radiation-induced gamma H2AX foci in bystander primary human astrocytes and glioma cells. *Oncogene* **26**, 993-1002 (2007).

Burr K. L., Robinson J. I., Rastogi S., Boylan M. T., Coates P. J., Lorimore S. A. and Wright E. G., Radiation-induced delayed bystander-type effects mediated by hemopoietic cells. *Radiat.Res.* **173**, 760-768 (2010).

Charles M. W., LNT-an apparent rather than real controversy? *J.Radiol.Prot.* **26**, 325-329 (2006).

Chen S. et al, Mitochondria-dependent signalling pathway are involved in the early process of radiation-induced bystander effects. *Br.J.Cancer* **98**, 1839-1844 (2008).

Chen S., Zhao Y., Zhao G., Han W., Bao L., Yu K. N. and Wu L., Up-regulation of ROS by mitochondria-dependent bystander signaling contributes to genotoxicity of bystander effects. *Mutat.Res.* **666**, 68-73 (2009).

Cornforth M. N. and Bedford J. S., A quantitative comparison of potentially lethal damage repair and the rejoining of interphase chromosome breaks in low passage normal human fibroblasts. *Radiat.Res.* **111**, 385-405 (1987).

Cuddihy A. R. and Bristow R. G., The p53 protein family and radiation sensitivity: Yes or no? *Cancer Metastasis Rev.* **23**, 237-257 (2004).

Day T. K., Zeng G., Hooker A. M., Bhat M., Scott B. R., Turner D. R. and Sykes P. J., Adaptive response for chromosomal inversions in pKZ1 mouse prostate induced by low doses of X radiation delivered after a high dose. *Radiat.Res.* **167**, 682-692 (2007a).

Day T. K., Zeng G., Hooker A. M., Bhat M., Turner D. R. and Sykes P. J., Extremely low doses of X-radiation can induce adaptive responses in mouse prostate. *Dose.Response* **5**, 315-322 (2007b).

de Toledo S. M. and Azzam E. I., Adaptive and bystander responses in human and rodent cell cultures exposed to low level ionizing radiation: the impact of linear energy transfer. *Dose.Response* **4**, 291-301 (2006).

del Regato J. A., The unfolding of American radiotherapy. *Int.J.Radiat.Oncol.Biol.Phys.* **35**, 5-14 (1996).

Dewey W. C., Ling C. C. and Meyn R. E., Radiation-induced apoptosis: relevance to radiotherapy. *Int.J.Radiat.Oncol.Biol.Phys.* **33**, 781-796 (1995).

Dey S., Spring P. M., Arnold S., Valentino J., Chendil D., Regine W. F., Mohiuddin M. and Ahmed M. M., Low-dose fractionated radiation potentiates the effects of Paclitaxel in wild-type and mutant p53 head and neck tumor cell lines. *Clin.Cancer Res.* **9**, 1557-1565 (2003).

Doll R., Hazards of ionising radiation: 100 years of observations on man. *Br.J.Cancer* **72**, 1339-1349 (1995).

Douglas B. G. and Fowler J. F., The effect of multiple small doses of x rays on skin reactions in the mouse and a basic interpretation. *Radiat.Res.* **66**, 401-426 (1976).

Elkind M.M. and Sutton H., Radiation response of mammalian cells grown in culture. I. Repair of x-ray damage in surviving Chinese hamster cells. *Radiat.Res.* **13**, 556-593 (1960).

Erenpreisa J., Kalejs M. and Cragg M. S., Mitotic catastrophe and endomitosis in tumour cells: an evolutionary key to a molecular solution. *Cell Biol.Int.* **29**, 1012-1018 (2005a).

Erenpreisa J., Kalejs M., Ianzini F., Kosmacek E. A., Mackey M. A., Emzinsh D., Cragg M. S., Ivanov A. and Illidge T. M., Segregation of genomes in polyploid tumour cells following mitotic catastrophe. *Cell Biol.Int.* **29**, 1005-1011 (2005b).

Eriksson D., Blomberg J., Lindgren T., Lofroth P. O., Johansson L., Riklund K. and Stigbrand T., Iodine-131 induces mitotic catastrophes and activates apoptotic pathways in HeLa Hep2 cells. *Cancer Biother.Radiopharm.* **23**, 541-549 (2008a).

Eriksson D., Lofroth P. O., Johansson L., Riklund K. A. and Stigbrand T., Cell cycle disturbances and mitotic catastrophes in HeLa Hep2 cells following 2.5 to 10 Gy of ionizing radiation. *Clin.Cancer Res.* **13**, 5501s-5508s (2007).

Eriksson D., Riklund K., Johansson L., and Stigbrand T., Radiation Induced Cell Deaths. *In: Targeted Radionuclide Tumor Therapy*. NA: Springer Science + Business Media B.V. (2008b).

Eriksson D. and Stigbrand T., Radiation-induced cell death mechanisms. *Tumour.Biol.* **31**, 363-372 (2010).

Ewing J., Early experiences in radiation therapy. *Am.J.Roentgenol.* **31**, 153-163 (1934).

Faguet G. B., Reichard S. M. and Welter D. A., Radiation-induced clastogenic factors. *Cancer Genet.Cytogenet.* **12**, 73-83 (1984).

Fei P. and El Deiry W. S., P53 and radiation responses. *Oncogene* **22**, 5774-5783 (2003).

Furre T., Koritzinsky M., Olsen D. R. and Pettersen E. O., Inverse dose-rate effect due to pre-mitotic accumulation during continuous low dose-rate irradiation of cervix carcinoma cells. *Int.J.Radiat.Biol.* **75**, 699-707 (1999).

Galluzzi L., Maiuri M. C., Vitale I., Zischka H., Castedo M., Zitvogel L. and Kroemer G., Cell death modalities: classification and pathophysiological implications. *Cell Death.Differ.* **14**, 1237-1243 (2007).

Ghiassi-Nejad M., Mortazavi S. M., Cameron J. R., Niroomand-rad A. and Karam P. A., Very high background radiation areas of Ramsar, Iran: preliminary biological studies. *Health Phys.* **82**, 87-93 (2002).

Gow M. D., Seymour C. B., Byun S. H. and Mothersill C. E., Effect of dose rate on the radiation-induced bystander response. *Phys.Med.Biol.* **53**, 119-132 (2008).

Gow M. D., Seymour C. B., Ryan L. A. and Mothersill C. E., Induction of bystander response in human glioma cells using high-energy electrons: a role for TGF-beta1. *Radiat.Res.* **173**, 769-778 (2010).

Gray L. H., Conditions which affect the biologic damage resulting from exposure to radiation. *Acta.Radiol.* **41**, 63-83 (1954).

Hall E. J., Radiobiology for the Radiologist. **5 ed.** Philadelphia, PA.: Lippincott Williams & Williams (2000).

Han W., Chen S., Yu K. N. and Wu L., Nitric oxide mediated DNA double strand breaks induced in proliferating bystander cells after alpha-particle irradiation. *Mutat.Res.* **684**, 81-89 (2010).

Helton E. S. and Chen X., p53 modulation of the DNA damage response. *J.Cell Biochem.* **100**, 883-896 (2007).

Hewitt H. B. and Wilson C. W., A survival curve for mammalian cells irradiated *in vivo*. *Nature* **183**, 1060-1061 (1959).

Hollowell J. G. and Littlefield L. G., Chromosome aberrations induced by plasma from irradiated patients. *J.S.C.Med.Assoc.* **63**, 437-442 (1967).

Hollowell J. G. and Littlefield L. G., Chromsome damage induced by plasma of X-rayed patient: An indirect effect of radiation. *Proc.Soc.Exp.Biol.Med.* **129**, 240-244 (1968).

Ito H., Daido S., Kanzawa T., Kondo S. and Kondo Y., Radiation-induced autophagy is associated with LC3 and its inhibition sensitizes malignant glioma cells. *Int.J.Oncol.* **26**, 1401-1410 (2005).

Iyer R., Lehnert B. E. and Svensson R., Factors underlying the cell growth-related bystander responses to alpha particles. *Cancer Res.* **60**, 1290-1298 (2000).

Joiner M. C., Lambin P. and Marples B., Adaptive response and induced resistance. *C.R.Acad.Sci.III* **322**, 167-175 (1999).

Joiner M. C., Marples B., Lambin P., Short S. C. and Turesson I., Low-dose hypersensitivity: current status and possible mechanisms. *Int.J.Radiat.Oncol.Biol.Phys.* **49**, 379-389 (2001).

Kadhim M. A., Hill M. A. and Moore S. R., Genomic instability and the role of radiation quality. *Radiat.Prot.Dosimetry.* **122**, 221-227 (2006).

Kaplan H. S., Radiobiology's contribution to radiotherapy. *Radiat.Res.* **43**, 460-476 (1970).

Kim K. W., Mutter R. W., Cao C., Albert J. M., Freeman M., Hallahan D. E. and Lu B., Autophagy for cancer therapy through inhibition of pro-apoptotic proteins and mammalian target of rapamycin signaling. *J.Biol.Chem.* **281**, 36883-36890 (2006).

Konopacka M. and Rzeszowska-Wolny J., The bystander effect-induced formation of micronucleated cells is inhibited by antioxidants, but the parallel induction of apoptosis and loss of viability are not affected. *Mutat.Res.* **593**, 32-38 (2006).

Kroemer G., Dallaporta B. and Resche-Rigon M., The mitochondrial death/life regulator in apoptosis and necrosis. *Annu.Rev.Physiol* **60**, 619-642 (1998).

Kroemer G., Petit P., Zamzami N., Vayssiere J. L. and Mignotte B., The biochemistry of programmed cell death. *FASEB J.* **9**, 1277-1287 (1995).

Krueger S. A., Joiner M. C., Weinfeld M., Piasentin E. and Marples B., Role of apoptosis in low-dose hyper-radiosensitivity. *Radiat.Res.* **167**, 260-267 (2007).

Krueger S. A., Wilson G. D., Piasentin E., Joiner M. C. and Marples B., The effects of G2-phase enrichment and checkpoint abrogation on low-dose hyper-radiosensitivity. *Int.J.Radiat.Oncol.Biol.Phys.* **77**, 1509-1517 (2010).

Lambin P., Marples B., Fertil B., Malaise E. P. and Joiner M. C., Hypersensitivity of a human tumour cell line to very low radiation doses. *Int.J.Radiat.Biol.* **63**, 639-650 (1993).

Lea D. E., Actions of Radiations on Living Cells. Cambridge, UK: Cambridge University Press (1946).

Levine B. and Yuan J., Autophagy in cell death: an innocent convict? *J.Clin.Invest* **115**, 2679-2688 (2005).

Little J. B., Genomic instability and bystander effects: a historical perspective. *Oncogene* **22**, 6978-6987 (2003).

Liu Z., Prestwich W. V., Stewart R. D., Byun S. H., Mothersill C. E., McNeill F. E. and Seymour C. B., Effective target size for the induction of bystander effects in medium transfer experiments. *Radiat.Res.* **168**, 627-630 (2007).

Lorimore S. A., Chrystal J. A., Robinson J. I., Coates P. J. and Wright E. G., Chromosomal instability in unirradiated hemaopoietic cells induced by

macrophages exposed in vivo to ionizing radiation. *Cancer Res.* **68**, 8122-8126 (2008).

Lorimore S. A., Coates P. J. and Wright E. G., Radiation-induced genomic instability and bystander effects: inter-related nontargeted effects of exposure to ionizing radiation. *Oncogene* **22**, 7058-7069 (2003).

Lorimore S. A. and Wright E. G., Radiation-induced genomic instability and bystander effects: related inflammatory-type responses to radiation-induced stress and injury? A review. *Int.J.Radiat.Biol.* **79**, 15-25 (2003).

Lyng F. M., Maguire P., Kilmurray N., Mothersill C., Shao C., Folkard M. and Prise K. M., Apoptosis is initiated in human keratinocytes exposed to signalling factors from microbeam irradiated cells. *Int.J.Radiat.Biol.* **82**, 393-399 (2006a).

Lyng F. M., Maguire P., McClean B., Seymour C. and Mothersill C., The involvement of calcium and MAP kinase signaling pathways in the production of radiation-induced bystander effects. *Radiat.Res.* **165**, 400-409 (2006b).

Lyng F. M., Seymour C. B. and Mothersill C., Initiation of apoptosis in cells exposed to medium from the progeny of irradiated cells: a possible mechanism for bystander-induced genomic instability? *Radiat.Res.* **157**, 365-370 (2002).

Marples B. and Joiner M. C., The response of Chinese hamster V79 cells to low radiation doses: evidence of enhanced sensitivity of the whole cell population. *Radiat.Res.* **133**, 41-51 (1993).

Marples B., Wouters B. G., Collis S. J., Chalmers A. J. and Joiner M. C., Low-dose hyper-radiosensitivity: a consequence of ineffective cell cycle arrest of radiation-damaged G2-phase cells. *Radiat.Res.* **161**, 247-255 (2004).

Matsumoto H., Tomita M., Otsuka K. and Hatashita M., A new paradigm in radioadaptive response developing from microbeam research. *J.Radiat.Res.(Tokyo)* **50 Suppl A**, A67-A79 (2009).

Miller R. W., Delayed effects of external radiation exposure: a brief history. *Radiat.Res.* **144**, 160-169 (1995).

Mitchel R. E., The dose window for radiation-induced protective adaptive responses. *Dose.Response* **8**, 192-208 (2010).

Mitchel R. E., Jackson J. S. and Carlisle S. M., Upper dose thresholds for radiation-induced adaptive response against cancer in high-dose-exposed, cancer-prone, radiation-sensitive Trp53 heterozygous mice. *Radiat.Res.* **162**, 20-30 (2004).

Mitchel R. E., Jackson J. S., McCann R. A. and Boreham D. R., The adaptive response modifies latency for radiation-induced myeloid leukemia in CBA/H mice. *Radiat.Res.* **152**, 273-279 (1999).

Mitchel R. E., Jackson J. S., Morrison D. P. and Carlisle S. M., Low doses of radiation increase the latency of spontaneous lymphomas and spinal osteosarcomas in cancer-prone, radiation-sensitive Trp53 heterozygous mice. *Radiat.Res.* **159**, 320-327 (2003).

Monsieurs M. A., Thierens H. M., Vral A. M., Van De W. C., De Ridder L. I. and Dierckx R. A., Adaptive response in patients treated with 131I. *J.Nucl.Med.* **41**, 17-22 (2000).

Moore S. R., Marsden S., Macdonald D., Mitchell S., Folkard M., Michael B., Goodhead D. T., Prise K. M. and Kadhim M. A., Genomic instability in human lymphocytes irradiated with individual charged particles: involvement of tumor necrosis factor alpha in irradiated cells but not bystander cells. *Radiat.Res.* **163**, 183-190 (2005).

Morgan W. F., Day J. P., Kaplan M. I., McGhee E. M. and Limoli C. L., Genomic instability induced by ionizing radiation. *Radiat.Res.* **146**, 247-258 (1996).

Morgan W. F. and Sowa M. B., Non-targeted bystander effects induced by ionizing radiation. *Mutat.Res.* **616**, 159-164 (2007).

Morgan W. F. and Sowa M. B., Non-targeted effects of ionizing radiation: implications for risk assessment and the radiation dose response profile. *Health Phys.* **97**, 426-432 (2009).

Mothersill C., Kadhim M. A., O'Reilly S., Papworth D., Marsden S. J., Seymour C. B. and Wright E. G., Dose- and time-response relationships for lethal mutations and chromosomal instability induced by ionizing radiation in an immortalized human keratinocyte cell line. *Int.J.Radiat.Biol.* **76**, 799-806 (2000).

Mothersill C. and Seymour C., Medium from irradiated human epithelial cells but not human fibroblasts reduces the clonogenic survival of unirradiated cells. *Int.J.Radiat.Biol.* **71**, 421-427 (1997).

Mothersill C. and Seymour C., Radiation-induced bystander effects: past history and future directions. *Radiat.Res.* **155**, 759-767 (2001).

Mothersill C. and Seymour C. B., Cell-cell contact during gamma irradiation is not required to induce a bystander effect in normal human keratinocytes: evidence for release during irradiation of a signal controlling survival into the medium. *Radiat.Res.* **149**, 256-262 (1998).

Mothersill C. and Seymour C. B., Actions of radiation on living cells in the "post-bystander" era. *EXS* , 159-177 (2006a).

Mothersill C. and Seymour C. B., Targeted radiotherapy: is the "Holy Grail" in sight? *J.Nucl.Med.* **47**, 899-900 (2006b).

Mothersill C., Seymour R. J. and Seymour C. B., Bystander effects in repair-deficient cell lines. *Radiat.Res.* **161**, 256-263 (2004).

Munro A. J., Bystander effects and their implications for clinical radiotherapy. *J.Radiol.Prot.* **29**, A133-A142 (2009).

Nagasawa H. and Little J. B., Induction of sister chromatid exchanges by extremely low doses of alpha-particles. *Cancer Res.* **52**, 6394-6396 (1992).

Nagasawa H. and Little J. B., Unexpected sensitivity to the induction of mutations by very low doses of alpha-particle radiation: evidence for a bystander effect. *Radiat.Res.* **152**, 552-557 (1999).

Nagasawa H., Peng Y., Wilson P. F., Lio Y. C., Chen D. J., Bedford J. S. and Little J. B., Role of homologous recombination in the alpha-particle-induced bystander effect for sister chromatid exchanges and chromosomal aberrations. *Radiat.Res.* **164**, 141-147 (2005).

Natarajan M., Gibbons C. F., Mohan S., Moore S. and Kadhim M. A., Oxidative stress signalling: a potential mediator of tumour necrosis factor alpha-induced genomic instability in primary vascular endothelial cells. *Br.J.Radiol.* **80 Spec No 1**, S13-S22 (2007).

Nias A. H., An introduction to radiobiology. **2nd ed.** West Sussex, UK: John Wiley & Sons (1998).

Olivieri G., Bodycote J. and Wolff S., Adaptive response of human lymphocytes to low concentration of radioactive thymidine. *Science* **223**, 594-597 (1984).

Paglin S., Hollister T., Delohery T., Hackett N., McMahill M., Sphicas E., Domingo D. and Yahalom J., A novel response of cancer cells to radiation involves autophagy and formation of acidic vesicles. *Cancer Res.* **61**, 439-444 (2001).

Paglin S. and Yahalom J., Pathways that regulate autophagy and their role in mediating tumor response to treatment. *Autophagy.* **2**, 291-293 (2006).

Parsons W. B., Watkins C. H., Pease G. L. and Childs D. S., Changes in sternal bone marrow following roentgen-ray therapy to the spleen in chronic granulocytic leukaemia. *Cancer* **7**, 179-189 (1954).

Pinto M., Azzam E. I. and Howell R. W., Investigation of adaptive responses in bystander cells in 3D cultures containing tritium-labeled and unlabeled normal human fibroblasts. *Radiat.Res.* **174**, 216-227 (2010).

Plews M. et al, A radiation-induced adaptive response prolongs the survival of prion-infected mice. *Free Radic.Biol.Med.* **49**, 1417-1421 (2010).

Prise K. M., Folkard M. and Michael B. D., A review of the bystander effect and its implications for low-dose exposure. *Radiat.Prot.Dosimetry.* **104**, 347-355 (2003).

Puck T. T. and Marcus P. I., A rapid method for viable cell titration and clone production with HeLa cells in tissue culture: The use of X-irradiatd cells to supply conditioning factors. *Proc.Natl.Acad.Sci.U.S.A* **41**, 432-437 (1955).

Puck T. T. and Marcus P. I., Action of x-rays on mammalian cells. *J.Exp.Med.* **103**, 653-666 (1956).

Reggiori F. and Klionsky D. J., Autophagosomes: biogenesis from scratch? *Curr.Opin.Cell Bio.* **4**, 415-22 (2010).

Rigaud O. and Moustacchi E., Radioadaptation for gene mutation and the possible molecular mechanisms of the adaptive response. *Mutat.Res.* **358**, 127-134 (1996).

Rockwell S., Experimental Radiotherapy: A Brief History. *Radiat.Res.* **150 (Suppl)**, S157-S169 (1998).

Roninson I. B., Broude E. V. and Chang B. D., If not apoptosis, then what? Treatment-induced senescence and mitotic catastrophe in tumor cells. *Drug Resist.Updat.* **4**, 303-313 (2001).

Röntgen W. C., Über Eine Neue Art von Strahlen. Vorläufige (1.) Mitteilung. Würzburg, DE: Sitzungsberichted der Physikalisch-Medizinischen Gesellschoft (1895).

Sachs R. K. and Brenner D. J., The mechanistic basis of the linear-quadratic formalism. *Med.Phys.* **25**, 2071-2073 (1998).

Sachs R. K., Hahnfeld P. and Brenner D. J., The link between low-LET dose-response relations and the underlying kinetics of damage production/repair/misrepair. *Int.J.Radiat.Biol.* **72**, 351-374 (1997).

Sawant S. G., Randers-Pehrson G., Geard C. R., Brenner D. J. and Hall E. J., The bystander effect in radiation oncogenesis: I. Transformation in C3H 10T1/2 cells in vitro can be initiated in the unirradiated neighbors of irradiated cells. *Radiat.Res.* **155**, 397-401 (2001a).

Sawant S. G., Randers-Pehrson G., Metting N. F. and Hall E. J., Adaptive response and the bystander effect induced by radiation in C3H 10T(1/2) cells in culture. *Radiat.Res.* **156**, 177-180 (2001b).

Sawant S. G., Zheng W., Hopkins K. M., Randers-Pehrson G., Lieberman H. B. and Hall E. J., The radiation-induced bystander effect for clonogenic survival. *Radiat.Res.* **157**, 361-364 (2002).

Scott D., The effect of irradiated plasma on normal human chromosomes and its relevance to the long-lived lymphocyte hypothesis. *Cell Tissue Kinet.* **2**, 295-305 (1969).

Shao C., Aoki M. and Furusawa Y., Bystander effect on cell growth stimulation in neoplastic HSGc cells induced by heavy-ion irradiation. *Radiat.Environ.Biophys.* **42**, 183-187 (2003).

Shao C., Folkard M., Michael B. D. and Prise K. M., Targeted cytoplasmic irradiation induces bystander responses. *Proc.Natl.Acad.Sci.U.S.A* **101**, 13495-13500 (2004).

Shao C., Folkard M., Michael B. D. and Prise K. M., Bystander signaling between glioma cells and fibroblasts targeted with counted particles. *Int.J.Cancer* **116**, 45-51 (2005).

Shao C., Folkard M. and Prise K. M., Role of TGF-beta1 and nitric oxide in the bystander response of irradiated glioma cells. *Oncogene* **27**, 434-440 (2008).

Shao C., Lyng F. M., Folkard M. and Prise K. M., Calcium fluxes modulate the radiation-induced bystander responses in targeted glioma and fibroblast cells. *Radiat.Res.* **166**, 479-487 (2006).

Snyder A. R., Review of radiation-induced bystander effects. *Hum.Exp.Toxicol.* **23**, 87-89 (2004).

Sokolov M. V., Dickey J. S., Bonner W. M. and Sedelnikova O. A., gamma-H2AX in bystander cells: not just a radiation-triggered event, a cellular response to stress mediated by intercellular communication. *Cell Cycle* **6**, 2210-2212 (2007).

Sowa Resat M. B. and Morgan W. F., Radiation-induced genomic instability: a role for secreted soluble factors in communicating the radiation response to non-irradiated cells. *J.Cell Biochem.* **92**, 1013-1019 (2004).

Suzuki M., Zhou H., Hei T. K., Tsuruoka C. and Fujitaka K., Effects of irradiated medium on chromatid aberrations in mammalian cells using double mylar dishes. *Biol.Sci.Space* **18**, 110-111 (2004).

Tartier L., Gilchrist S., Burdak-Rothkamm S., Folkard M. and Prise K. M., Cytoplasmic irradiation induces mitochondrial-dependent 53BP1 protein relocalization in irradiated and bystander cells. *Cancer Res.* **67**, 5872-5879 (2007).

Thompson C. B., Apoptosis in the pathogenesis and treatment of disease. *Science* **267**, 1456-1462 (1995).

Timofeeff-Ressovsky N. W. and Zimmer K. G., Das Trefferprinzip in der Biologie. Leipzig, DE: S. Herzel Verlag (1947).

Vousden K. H. and Lu X., Live or let die: the cell's response to p53. *Nat.Rev.Cancer* **2**, 594-604 (2002).

Watson G. E., Lorimore S. A., Macdonald D. A. and Wright E. G., Chromosomal instability in unirradiated cells induced in vivo by a bystander effect of ionizing radiation. *Cancer Res.* **60**, 5608-5611 (2000).

Wouters B. G., Sy A. M. and Skarsgard L. D., Low-dose hypersensitivity and increased radioresistance in a panel of human tumor cell lines with different radiosensitivity. *Radiat.Res.* **146**, 399-413 (1996).

Zhou H., Hong M., Chai Y. and Hei T. K., Consequences of cytoplasmic irradiation: studies from microbeam. *J.Radiat.Res.(Tokyo)* **50 Suppl A**, A59-A65 (2009).

Zhou H., Randers-Pehrson G., Suzuki M., Waldren C. A. and Hei T. K., Genotoxic damage in non-irradiated cells: contribution from the bystander effect. *Radiat.Prot.Dosimetry.* **99**, 227-232 (2002).

Zhou H., Randers-Pehrson G., Waldren C. A. and Hei T. K., Radiation-induced bystander effect and adaptive response in mammalian cells. *Adv.Space Res.* **34**, 1368-1372 (2004).

Appendix A – Part A Data

A.1: Survival Fraction data for HPV-G and ^{60}Co irradiation:

Dose = 0 Gy				
	Dose Rate [cGy/min]			
Direct Cells	110	170	305	465
Survival Fraction	0.966	0.984	0.984	0.966
	0.981	1.020	1.020	0.981
	1.054	0.996	0.996	1.054
	1.021	1.061	1.061	1.021
	0.990	1.000	0.939	0.990
	0.990	0.939	1.000	0.990
	1.026	1.035	1.035	1.026
	1.041	0.970	0.970	1.041
	0.934	0.996	0.996	0.934
Average	1.000	1.000	1.000	1.000
Standard Deviation	0.038	0.036	0.036	0.038
Standard Error	0.013	0.012	0.012	0.013
	Dose Rate [cGy/min]			
Recepient Cells	110	170	305	465
Survival Fraction	1.015	1.014	1.014	1.015
	1.015	1.014	1.014	1.015
	0.971	0.973	0.973	0.971
	1.065	1.022	1.022	1.065
	1.000	1.022	1.022	1.000
	0.935	0.955	0.955	0.935
	1.006	0.954	0.954	1.006
	1.025	0.986	0.986	1.025
	0.968	1.060	1.060	0.968
Average	1.000	1.000	1.000	1.000
Standard Deviation	0.038	0.035	0.035	0.038
Standard Error	0.013	0.012	0.012	0.013

Dose = 0.5 Gy				
	Dose Rate [cGy/min]			
Direct Cells	110	170	305	465
Survival Fraction	0.791	0.797	0.996	0.791
	0.834	0.785	0.926	0.615
	0.732	0.902	0.856	0.410
	0.959	0.758	0.773	1.082
	0.866	0.712	0.773	0.680
	1.082	0.788	0.606	0.711
	0.949	0.653	0.556	0.949
	0.918	0.679	0.640	0.765
	0.827	0.614	0.582	1.041
Average	0.884	0.743	0.745	0.783
Standard Deviation	0.105	0.088	0.159	0.214
Standard Error	0.035	0.029	0.053	0.071
	Dose Rate [cGy/min]			
Recepient Cells	110	170	305	465
Survival Fraction	0.824	0.811	0.892	0.898
	0.942	0.811	0.811	0.824
	1.030	0.838	0.933	0.721
	0.742	0.855	0.955	0.678
	0.678	0.871	0.804	0.710
	0.548	0.888	0.871	0.613
	1.101	1.081	1.007	1.006
	0.892	0.996	0.986	1.025
	0.949	0.933	1.060	0.892
Average	0.856	0.898	0.924	0.818
Standard Deviation	0.176	0.091	0.087	0.147
Standard Error	0.059	0.030	0.029	0.049

Dose = 5 Gy				
	Dose Rate [cGy/min]			
Direct Cells	110	170	305	465
Survival Fraction	0.146	0.270	0.246	0.205
	0.293	0.352	0.258	0.059
	0.278	0.445	0.270	0.117
	0.155	0.106	0.091	0.124
	0.062	0.091	0.106	0.093
	0.062	0.106	0.106	0.093
	0.046	0.446	0.152	0.077
	0.092	0.368	0.165	0.061
	0.046	0.291	0.145	0.046
Average	0.131	0.275	0.171	0.097
Standard Deviation	0.096	0.143	0.070	0.048
Standard Error	0.032	0.048	0.023	0.016
	Dose Rate [cGy/min]			
Recepient Cells	110	170	305	465
Survival Fraction	0.898	0.811	0.824	0.780
	0.912	0.824	0.824	0.898
	0.795	0.933	0.879	0.809
	0.678	0.838	0.838	0.678
	0.742	0.771	0.721	0.548
	0.807	0.721	0.788	0.581
	0.873	0.901	0.763	0.832
	0.835	0.859	0.795	0.851
	0.740	0.859	0.901	0.719
Average	0.809	0.835	0.815	0.744
Standard Deviation	0.079	0.064	0.056	0.122
Standard Error	0.026	0.021	0.019	0.041

Dose = 10 Gy				
	Dose Rate [cGy/min]			
Direct Cells	110	170	305	465
Survival Fraction	0.008	0.056	0.039	0.005
	0.010	0.033	0.043	0.005
	0.017	0.049	0.023	0.003
	0.005	0.031	0.031	0.003
	0.010	0.040	0.028	0.003
	0.012	0.043	0.028	0.003
	0.011	0.032	0.024	N/A
	0.011	0.024	0.032	N/A
	0.007	0.019	0.032	N/A
Average	0.010	0.036	0.031	0.004
Standard Deviation	0.003	0.012	0.007	0.001
Standard Error	0.001	0.004	0.002	0.000
	Dose Rate [cGy/min]			
Recepient Cells	110	170	305	465
Survival Fraction	1.020	0.943	0.831	1.155
	1.035	0.951	0.857	1.080
	1.140	1.003	1.028	1.057
	1.037	1.120	1.048	1.093
	1.093	1.241	1.084	1.053
	0.989	1.060	1.253	1.093
	1.103	1.017	1.049	1.154
	1.169	1.060	1.070	1.167
	1.037	1.081	1.134	1.115
Average	1.069	1.053	1.039	1.108
Standard Deviation	0.060	0.091	0.130	0.043
Standard Error	0.020	0.030	0.043	0.014

A.2: *Survival Fraction data for HPV-G and 20 MeV electron irradiation:*

Dose = 0 Gy				
	Dose Rate [cGy/min]			
Direct Cells	100	300	500	1000
Survival Fraction	1.056	1.056	0.986	0.986
	0.927	0.927	0.986	0.986
	1.017	1.017	1.028	1.028
	1.024	1.024	1.016	1.016
	0.979	0.979	0.992	0.992
	0.997	0.997	0.992	0.992
	1.022	1.022	1.080	1.080
	0.898	0.898	1.027	1.027
	1.080	1.080	0.893	0.893
Average	1.000	1.000	1.000	1.000
Standard Deviation	0.058	0.058	0.050	0.050
Standard Error	0.019	0.019	0.017	0.017
	Dose Rate [cGy/min]			
Recepient Cells	100	300	500	1000
Survival Fraction	0.991	0.991	0.979	0.979
	0.991	0.991	0.985	0.985
	1.019	1.019	1.036	1.036
	0.998	0.998	0.936	0.936
	1.047	1.047	1.018	1.018
	0.956	0.956	1.045	1.045
	1.054	1.054	1.064	1.064
	0.987	0.987	1.014	1.014
	0.959	0.959	0.922	0.922
Average	1.000	1.000	1.000	1.000
Standard Deviation	0.034	0.034	0.049	0.049
Standard Error	0.011	0.011	0.016	0.016

Dose = 0.5 Gy				
	Dose Rate [cGy/min]			
Direct Cells	100	300	500	1000
Survival Fraction	0.721	0.863	0.850	0.696
	0.786	0.773	0.796	0.779
	0.747	0.825	0.767	0.721
	0.587	0.547	0.721	0.489
	0.622	0.512	0.569	0.503
	0.693	0.547	0.595	0.595
	0.460	0.358	0.616	0.601
	0.551	0.428	0.580	0.594
	0.514	0.589	0.630	0.651
Average	0.631	0.605	0.680	0.626
Standard Deviation	0.112	0.177	0.105	0.097
Standard Error	0.037	0.059	0.035	0.032
	Dose Rate [cGy/min]			
Recepient Cells	100	300	500	1000
Survival Fraction	0.892	0.920	0.841	0.789
	0.934	0.920	0.864	0.743
	1.005	0.962	0.818	0.714
	0.864	0.948	0.910	0.937
	0.864	0.913	0.946	0.937
	0.878	0.913	0.955	0.846
	0.826	0.883	0.930	0.964
	0.921	0.949	0.746	0.972
	0.854	0.807	0.897	0.981
Average	0.893	0.913	0.878	0.876
Standard Deviation	0.053	0.047	0.068	0.105
Standard Error	0.018	0.016	0.023	0.035

Dose = 5 Gy				
	Dose Rate [cGy/min]			
Direct Cells	100	300	500	1000
Survival Fraction	0.180	0.103	0.220	0.269
	0.180	0.193	0.271	0.207
	0.219	0.155	0.242	0.228
	0.168	0.141	0.152	0.106
	0.135	0.159	0.152	0.112
	0.163	0.159	0.116	0.129
	0.233	0.241	N/A	N/A
	0.233	0.222	N/A	N/A
	0.300	0.211	N/A	N/A
Average	0.201	0.176	0.192	0.175
Standard Deviation	0.050	0.044	0.061	0.069
Standard Error	0.017	0.015	0.025	0.028
	Dose Rate [cGy/min]			
Recepient Cells	100	300	500	1000
Survival Fraction	0.991	0.849	0.754	0.869
	0.807	0.835	0.818	0.875
	0.750	N/A	0.771	0.835
	0.717	0.815	0.873	0.855
	0.815	0.759	0.864	0.819
	0.731	0.724	0.928	0.855
	0.807	0.731	0.796	0.771
	0.807	0.740	0.855	0.771
	0.769	0.835	0.880	0.930
Average	0.799	0.786	0.838	0.842
Standard Deviation	0.081	0.053	0.057	0.051
Standard Error	0.027	0.019	0.019	0.017

Dose = 10 Gy				
	Dose Rate [cGy/min]			
Direct Cells	100	300	500	1000
Survival Fraction	0.025	0.029	0.046	0.035
	0.032	0.024	0.048	0.035
	0.026	0.032	0.030	0.044
	N/A	N/A	0.045	0.026
	N/A	N/A	0.047	0.029
	N/A	N/A	0.036	0.028
	N/A	N/A	0.025	0.021
	N/A	N/A	0.030	0.027
	N/A	N/A	0.026	0.025
Average	0.028	0.028	0.037	0.030
Standard Deviation	0.004	0.004	0.010	0.007
Standard Error	0.002	0.003	0.003	0.003
	Dose Rate [cGy/min]			
Recepient Cells	100	300	500	1000
Survival Fraction	N/A	N/A	0.950	1.054
	N/A	N/A	0.979	1.077
	N/A	N/A	0.984	1.105
	0.955	1.019	0.955	1.028
	0.998	0.991	0.982	1.055
	0.970	1.054	1.028	1.000
	0.949	0.949	1.006	0.981
	0.902	0.930	1.048	1.006
	0.883	0.921	0.964	1.115
Average	0.943	0.977	0.988	1.047
Standard Deviation	0.043	0.053	0.033	0.047
Standard Error	0.019	0.022	0.011	0.016

A.3: Survival Fraction data for HPV-G and 20 MeV electron irradiation

(Recipient cell numbers = 750, 1000, 2000, and 3000 for Doses f or 0, 0.5, 5, and 10 Gy respectively)

-	**Dose = 0 Gy**			**Dose = 0.5 Gy**	
	Dose Rate [cGy/min]			Dose Rate [cGy/min]	
Direct Cells	500	1000	***Direct Cells***	500	1000
Survival Fraction	1.046	1.046	Survival Fraction	0.693	0.619
	0.968	0.968		0.632	0.576
	0.985	0.985		0.571	0.672
	1.039	1.039		0.779	0.596
	0.946	0.946		0.567	0.538
	1.016	1.016		N/A	0.452
	1.077	1.077		0.636	0.547
	1.019	1.019		0.558	0.469
	0.904	0.904		0.543	0.484
Average	1.000	1.000	Average	0.622	0.550
Standard Deviation	0.054	0.054	Standard Deviation	0.081	0.073
Standard Error	0.018	0.018	Standard Error	0.029	0.024
	Dose Rate [cGy/min]			Dose Rate [cGy/min]	
Recepient Cells	500	1000	***Recepient Cells***	500	1000
Survival Fraction	0.997	0.997	Survival Fraction	0.804	0.754
	0.950	0.950		0.813	0.691
	1.053	1.053		0.779	0.658
	0.955	0.955		0.806	0.964
	1.031	1.031		0.978	0.792
	1.014	1.014		0.848	0.866
	0.892	0.892		0.790	1.023
	1.135	1.135		0.770	0.963
	0.973	0.973		0.679	1.074
Average	1.000	1.000	Average	0.807	0.865
Standard Deviation	0.070	0.070	Standard Deviation	0.079	0.150
Standard Error	0.023	0.023	Standard Error	0.026	0.050

	Dose = 5 Gy			**Dose = 10 Gy**	
	Dose Rate [cGy/min]			Dose Rate [cGy/min]	
Direct Cells	500	1000	***Direct Cells***	500	1000
Survival Fraction	0.179	0.135	Survival Fraction	0.045	0.026
	0.183	0.161		0.047	0.029
	0.164	0.179		0.036	0.028
	N/A	N/A		0.046	0.035
	N/A	N/A		0.048	0.035
	N/A	N/A		0.030	0.044
	0.153	0.171		0.025	0.021
	0.149	0.159		0.030	0.027
	0.188	0.145		0.026	0.025
Average	0.169	0.158	Average	0.037	0.030
Standard Deviation	0.016	0.016	Standard Deviation	0.010	0.007
Standard Error	0.007	0.007	Standard Error	0.004	0.003
	Dose Rate [cGy/min]			Dose Rate [cGy/min]	
Recepient Cells	500	1000	***Recepient Cells***	500	1000
Survival Fraction	0.519	0.438	Survival Fraction	0.515	0.432
	0.580	0.455		0.508	0.443
	0.524	0.475		0.522	0.438
	0.620	0.559		0.516	0.517
	0.622	0.461		0.559	0.453
	0.606	0.510		0.556	0.472
	0.653	0.653		0.588	0.544
	0.628	0.613		0.588	0.594
	0.598	0.643		0.591	0.615
Average	0.594	0.534	Average	0.549	0.501
Standard Deviation	0.046	0.085	Standard Deviation	0.035	0.070
Standard Error	0.015	0.028	Standard Error	0.012	0.023

Appendix B – Part B Data

B.1: Survival Fraction data for T98G and ^{60}Co irradiation (~1.7 Gy/min dose rate):

Recipient Data:

	Dose [Gy]			PE
Recipient Cells	0	0.5	5	
Survival Fraction	1.066	0.95	1.124	0.3
	0.996	0.961	1.019	
	1.066	0.892	1.193	
	1.205	1.043	0.996	0.276
	0.822	0.788	0.927	
	0.846	1.043	1.239	
Average	1.000	0.946	1.083	
Standard Deviation	0.145707	0.09689	0.121752	
Standard Error	0.059485	0.039555	0.049705	

Note: This data was collected by Lorna Ryan PhD, McMaster 2007.

B.2: *Survival Fraction data for T98G and 20 MeV irradiation (~1.7 Gy/min dose rate):*

Direct Data:

	Dose [Gy]				PE
Direct Cells	0	0.5	5	10	
Survival Fraction	1.103	0.948	0.289	0.022	0.116
	0.989	1.069	0.216	0.026	
	0.897	0.905	0.263	0.017	
	1.101	0.967	0.178	0.011	0.092
	0.971	0.924	0.167	0.004	
	0.913	0.967	0.178	0.015	
Average	0.996	0.964	0.215	0.016	
Standard Deviation	0.090	0.057	0.050	0.008	
Standard Error	0.037	0.023	0.021	0.003	

Recipient Data:

	Dose [Gy]				PE
Recipient Cells	0	0.5	5	10	
Survival Fraction	1.130	0.853	1.058	1.130	0.1298
	0.842	0.924	0.966	1.079	
	1.027	1.079	0.801	0.935	
	1.053	0.987	1.013	0.813	0.100
	0.973	1.160	0.813	0.827	
	0.987	0.920	0.947	0.760	
Average	1.002	0.987	0.933	0.924	
Standard Deviation	0.096	0.114	0.105	0.152	
Standard Error	0.039	0.046	0.043	0.062	

B.3: *Survival Fraction data for T98G and 20 MeV irradiation (~10 Gy/min dose rate):*

Direct Data:

	Dose [Gy]				PE
Direct Cells	0	0.5	5	10	
Survival Fraction	1.058	0.720	0.221	0.017	0.121
	1.008	0.771	0.231	0.015	
	0.926	0.683	0.221	0.017	
	0.952	0.733	0.126	0.008	0.105
	0.952	0.743	0.133	0.008	
	1.105	0.714	0.095	0.006	
	1.000	0.739	0.143	0.013	0.092
	1.043	0.859	0.139	0.007	
	0.957	0.783	0.104	0.009	
	1.250	0.458	0.261	0.039	0.072
	0.778	0.653	0.217	0.039	
	0.972	0.472	0.206	0.028	
	1.078	0.801	0.176	0.028	0.141
	1.007	0.702	0.190	0.055	
	0.908	0.610	0.199	0.047	
Average	1.000	0.696	0.178	0.022	
Standard Deviation	0.105	0.111	0.051	0.016	
Standard Error	0.027	0.056	0.013	0.004	

Recipient Data:

	Dose [Gy]				PE
Recipient Cells	0	0.5	5	10	
Survival Fraction	0.924	0.649	0.722	0.750	0.092
	1.068	0.880	0.808	0.750	
	1.010	1.111	0.837	0.866	
	1.066	0.858	0.572	0.806	0.051
	0.832	0.754	0.676	0.676	
	1.014	0.910	0.780	0.754	
	1.083	0.944	0.639	0.833	0.048
	0.889	0.861	0.667	0.722	
	1.028	0.889	0.833	0.778	
	1.217	0.680	0.829	0.603	0.042
	0.783	1.055	0.641	0.603	
	1.000	1.055	0.678	0.641	
	0.991	0.849	0.637	0.793	0.094
	0.991	0.920	0.764	0.778	
	1.019	0.948	0.878	0.849	
Average	0.994	0.891	0.731	0.747	
Standard Deviation	0.106	0.130	0.094	0.084	
Standard Error	0.027	0.033	0.024	0.022	

High Dose Data:

	Dose [Gy]		PE
Recipient Cells	15	20	
Survival Fraction	0.95	0.900	0.08
	0.925	0.925	
	1.025	0.775	
	0.892	0.83	0.151
	0.759	0.821	
	0.954	0.935	
	0.724	1.068	
Average	0.890	0.893	
Standard Deviation	0.109	0.0971	
Standard Error	0.0446	0.0396	

B.4: *Survival Fraction data for HPV-G and 20 MeV irradiation (~10 Gy/min dose rate):*

Direct Data:

	Dose [Gy]				PE
Direct Cells	0	0.5	5	10	
Survival Fraction	1.011	0.588	0.138	0.009	0.270
	1.026	0.536	0.115	0.012	0.274
	0.959	0.569	0.126	0.015	0.256
	1.122	0.476	0.141	0.015	0.276
	0.951	0.549	0.164	0.009	0.234
	0.927	0.447	0.143	0.012	0.228
	1.130	0.833	0.133	0.006	0.218
	0.995	0.774	0.128	0.003	0.192
	0.870	0.801	0.120	0.003	0.168
Average	0.999	0.619	0.134	0.009	0.235
Standard Deviation	0.086	0.145	0.015	0.005	0.038
Standard Error	0.049	0.084	0.008	0.003	0.022

Recipient Data:

	Dose [Gy]				PE
Recipient Cells	0	0.5	5	10	
Survival Fraction	0.969	0.878	0.588	0.928	0.161
	1.060	0.853	0.663	0.845	
	0.961	0.894	0.745	0.886	
	1.067	0.903	0.779	0.974	0.130
	0.944	0.892	0.841	0.974	
	0.974	0.800	0.718	0.985	
	1.133	0.900	0.678	0.933	0.12
	1.033	0.878	0.722	0.889	
	0.822	0.856	0.778	1.000	
Average	0.996	0.873	0.724	0.935	
Standard Deviation	0.090	0.033	0.075	0.053	
Standard Error	0.052	0.019	0.043	0.031	

B.5: *Survival Fraction data of T98G cells following monoclonal antibody application:*

a) mAB-TGF-α (PE = 13.4 & 9.3%)

	Dose [Gy]			
Direct Cells	0	0.5	5	10
Survival Fraction	1.015	0.754	0.179	0.015
	1.030	0.791	0.206	0.021
	0.955	0.918	0.155	N/A
Average	1.000	0.821	0.180	0.018
Standard Deviation	0.039	0.086	0.025	0.004
Standard Error	0.023	0.050	0.015	0.003
Recipient Cells	1.004	1.061	0.774	0.903
	0.989	N/A	N/A	0.817
		1.032	0.860	0.932
		0.860	0.789	0.674
		0.961	0.803	0.703
Average	0.996	0.978	0.806	0.806
Standard Deviation	0.010	0.089	0.038	0.116
Standard Error	0.007168	0.039998	0.018853	0.051772

b) mAB-TGF-β1 (PE = 15.5 and 11.2%)

	Dose [Gy]			
Direct Cells	0	0.5	5	10
Survival Fraction	0.994	0.755	0.245	0.017
	1.019	0.697	0.214	0.017
	0.981	0.665	0.230	0.013
Average	0.998	0.705	0.230	0.015
Standard Deviation	0.020	0.046	0.015	0.002
Standard Error	0.011	0.026	0.009	0.001
Recipient Cells	0.952	0.893	1.024	0.976
	1.036	0.905	1.036	0.952
	1.012	0.952	0.893	1.036
		1.048	1.071	0.976
		1.190	1.048	1.095
Average	1.000	0.998	1.014	1.007
Standard Deviation	0.043	0.124	0.070	0.058
Standard Error	0.02478174	0.05538	0.031361762	0.025973124

c) IgG1 Control Vector (PE=18.9 and 15.9%)

	Dose [Gy]			
Direct Cells	0	0.5	5	10
Survival Fraction	1.143	0.762	0.116	0.016
	0.899	0.698	0.110	0.016
	0.952	0.661	0.138	0.012
Average	0.998	0.707	0.121	0.014
Standard Deviation	0.128	0.051	0.014	0.002
Standard Error	0.074	0.029	0.008	0.001
Recipient Cells	0.914	0.964	0.780	0.646
	1.006	0.805	0.654	0.906
	1.073	1.048	0.730	0.797
		1.006	0.797	0.646
		0.797	0.805	0.847
Average	0.998	0.924	0.753	0.768
Standard Deviation	0.080	0.116	0.063	0.118
Standard Error	0.046185	0.052059197	0.027988795	0.052877

B.6: *ELISA results for T98G sampling:*

a) TGF-α

Standard Curve

Conc.	Opt. Dens.	Opt. Corr.
0	0.05	0
31.25	0.346	0.296
62.5	0.521	0.471
125	0.961	0.911
250	1.105	1.055
500	2.274	2.224

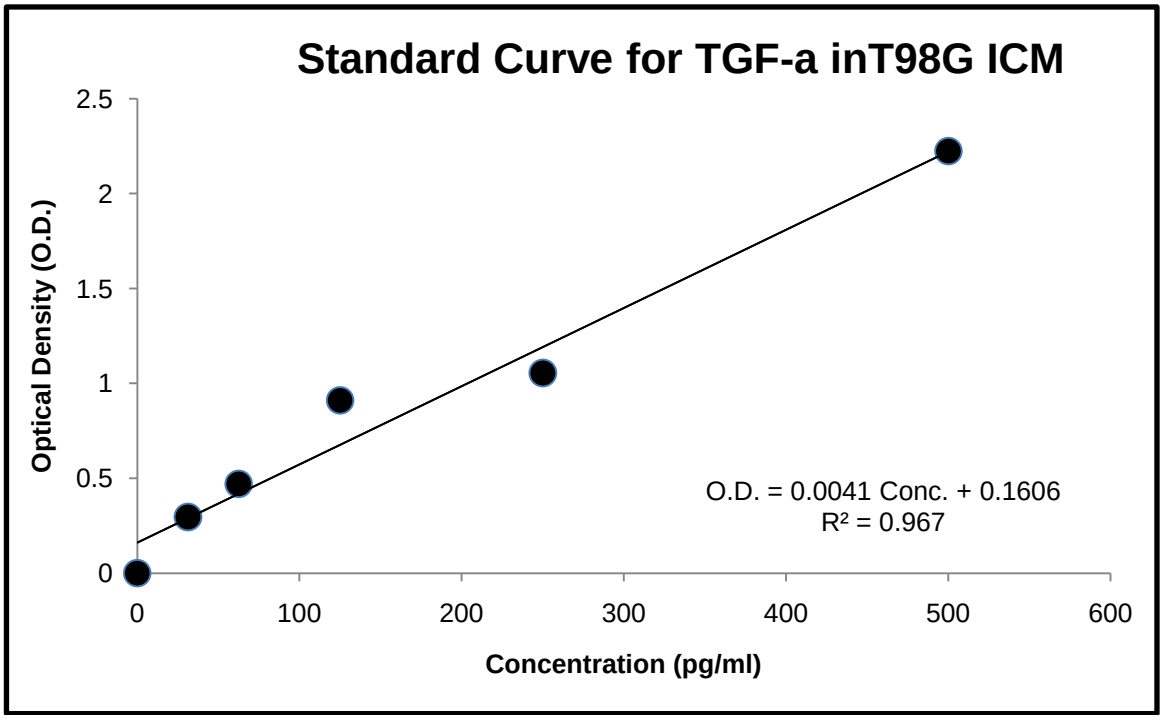

Readings

Experiment #, Dose	Plate Reading	Concentration (pg/ml)
1,0	0.059	-24.780
1,0.5	0.038	-29.902
1,5	0.037	-30.146
1,10	0.038	-29.902
2,0	0.364	49.610
2,0	0.068	-22.585
2,0	0.043	-28.683
2,0	0.045	-28.195
2,0.5	0.038	-29.902
2,0.5	0.039	-29.659
2,0.5	0.04	-29.415
2,0.5	0.043	-28.683
2,5	0.064	-23.561
2,5	0.041	-29.171
2,5	0.042	-28.927
2,5	0.043	-28.683
2,10	0.039	-29.659
2,10	0.037	-30.146
2,10	0.044	-28.439
2,10	0.054	-26.000
3,0	0.069	-22.341
3,0	0.05	-26.976
3,0	0.043	-28.683
3,0	0.049	-27.220
3,0.5	0.048	-27.463
3,0.5	0.051	-26.732
3,0.5	0.053	-26.244
3,0.5	0.064	-23.561
3,5	0.063	-23.805
3,5	0.057	-25.268
3,5	0.048	-27.463
3,5	0.055	-25.756
3,10	0.054	-26.000
3,10	0.057	-25.268
3,10	0.065	-23.317
3,10	0.067	-22.829

Note: Negative values indicate that readings are below sensitivity of 2.27 pg/ml.

b) Total TGF-β1 (activated via HCl to determine total TGF-β1 content)

Standard Curve

Conc.	Opt. Dens.	O.D. Corr.
0	0.08	0
125	0.267	0.187
250	0.442	0.362
500	0.745	0.665
1000	1.309	1.229
2000	2.317	2.237

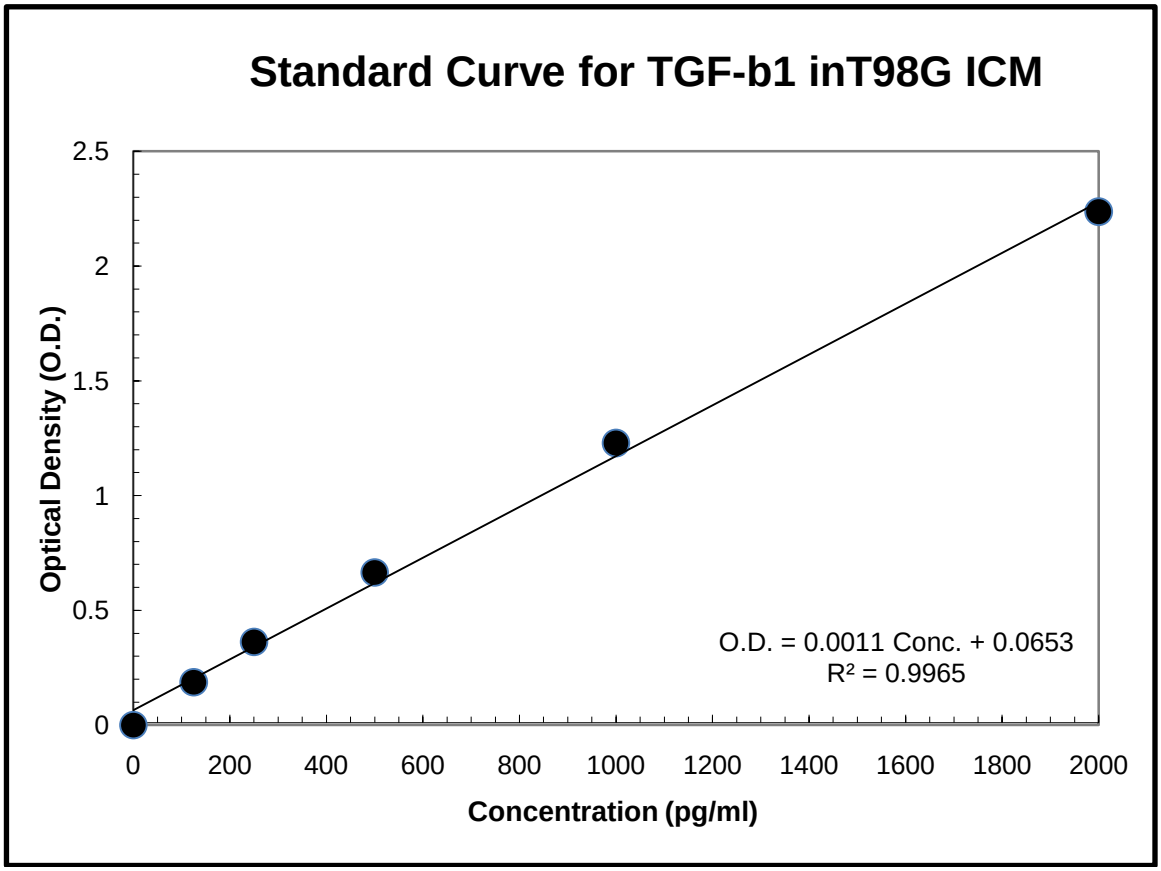

Readings

Experiment #, Dose	Plate Reading	Concentration (pg/ml)	Corrected Concentration (Medium TGF-b1 removed)
Medium	1.209	1410.500	
Medium	1.136	1325.333	1425.667->Average
Medium	1.321	1541.167	62.76551011->SEM
1,0	0.623	1419.600	-6.067
1,0.5	0.57	1284.691	-140.976
1,5	0.59	1335.600	-90.067
1,10	0.58	1310.145	-115.522
2,0	0.792	1849.782	424.115
2,0	0.752	1747.964	322.297
2,0	0.705	1628.327	202.660
2,0	0.687	1582.509	156.842
2,0.5	0.73	1691.964	266.297
2,0.5	0.728	1686.873	261.206
2,0.5	0.737	1709.782	284.115
2,0.5	0.774	1803.964	378.297
2,5	0.823	1928.691	503.024
2,5	0.79	1844.691	419.024
2,5	0.783	1826.873	401.206
2,5	0.775	1806.509	380.842
2,10	0.57	1284.691	-140.976
2,10	0.586	1325.418	-100.249
2,10	0.59	1335.600	-90.067
2,10	0.611	1389.055	-36.612
3,0	0.753	1750.509	324.842
3,0	0.676	1554.509	128.842
3,0	0.701	1618.145	192.478
3,0	0.694	1600.327	174.660
3,0.5	0.671	1541.782	116.115
3,0.5	0.723	1674.145	248.478
3,0.5	0.726	1681.782	256.115
3,0.5	0.789	1842.145	416.478
3,5	0.68	1564.691	139.024
3,5	0.693	1597.782	172.115
3,5	0.63	1437.418	11.751
3,5	0.661	1516.327	90.660
3,10	0.663	1521.418	95.751
3,10	0.606	1376.327	-49.340
3,10	0.695	1602.873	177.206
3,10	0.705	1628.327	202.660

Total TGF-β1 content (seen in Figure B-3)

	0 Gy	0.5 Gy	5 Gy	10 Gy
Concentration(pg/ml)	424.11	266.30	503.02	N/A
Experiment 2	322.30	261.21	419.02	N/A
	202.66	284.11	401.21	N/A
	156.84	378.30	380.84	N/A
Experiment 3	324.84	116.11	139.02	95.75
	128.84	248.48	172.11	-49.34
	192.48	256.11	11.75	177.21
	174.66	416.48	90.66	202.66
Average	240.84	278.39	264.71	106.57
Standard Deviation	103.55	90.43	181.81	113.50
Standard Error	36.61	31.97	64.28	56.76

c) *Active TGF-β1*

(measured via direct ELISA sampling post filtering in a timeline similar to application of ICCM to recipient cells)

Standard Curve

Conc.	Opt. Dens.	Opt Corr
0	0.061	0
31.25	0.106	0.045
125	0.227	0.166
500	0.717	0.656
2000	2.087	2.026

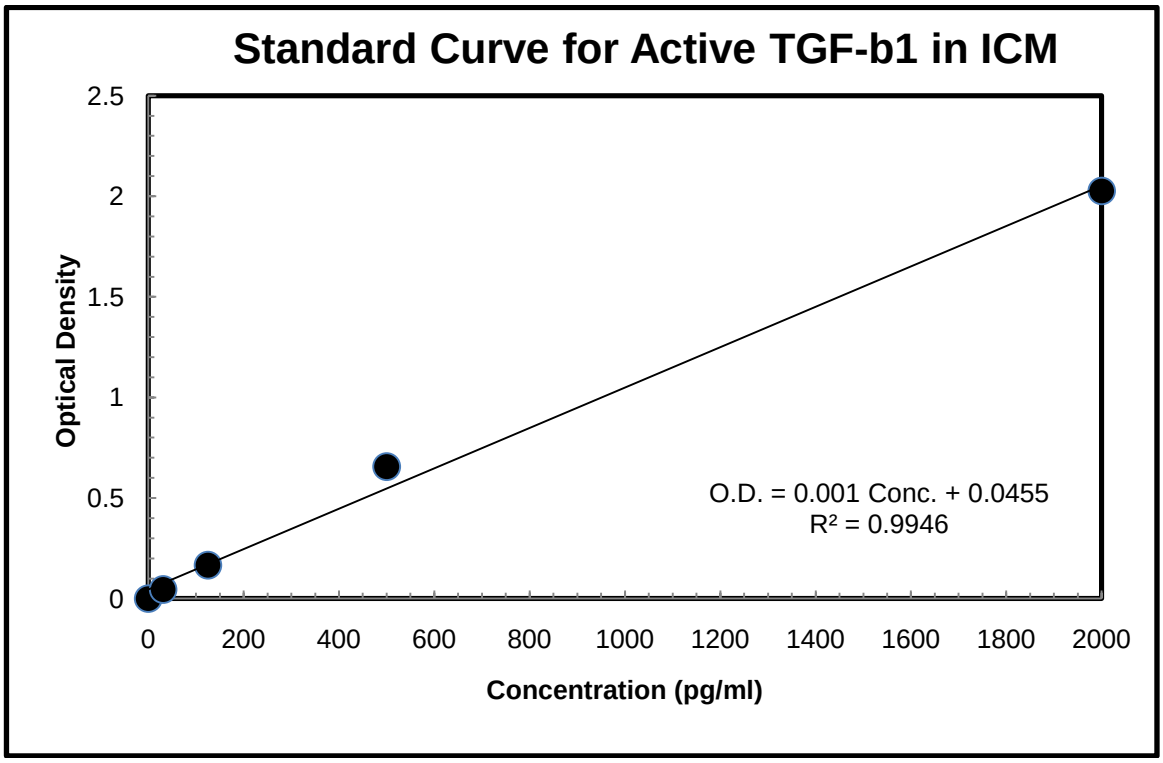

Readings

Sample #, Dose	Plate Reading	Concentration (pg/ml)
Medium	0.05	4.500
Medium	0.062	16.500
Medium	0.062	16.500
1,0	0.039	-6.500
1,0	0.037	-8.500
1,0	0.038	-7.500
2,0	0.034	-11.500
2,0	0.031	-14.500
2,0	0.039	-6.500
3,0	0.041	-4.500
3,0	0.032	-13.500
3,0	0.034	-11.500
4,0	0.03	-15.500
4,0	0.03	-15.500
4,0	0.03	-15.500
4,0	0.03	-15.500
1,0.5	0.031	-14.500
1,0.5	0.026	-19.500
1,0.5	0.035	-10.500
2,0.5	0.033	-12.500
2,0.5	0.044	-1.500
2,0.5	0.036	-9.500
3,0.5	0.032	-13.500
3,0.5	0.025	-20.500
3,0.5	0.028	-17.500
4,0.5	0.019	-26.500
4,0.5	0.029	-16.500
4,0.5	0.031	-14.500

1,5	0.034	-11.500
1,5	0.032	-13.500
1,5	0.035	-10.500
2,5	0.037	-8.500
2,5	0.032	-13.500
2,5	0.032	-13.500
3,5	0.031	-14.500
3,5	0.03	-15.500
3,5	0.028	-17.500
4,5	0.027	-18.500
4,5	0.037	-8.500
4,5	0.036	-9.500
1,10	0.025	-20.500
1,10	0.026	-19.500
1,10	0.028	-17.500
2,10	0.029	-16.500
2,10	0.035	-10.500
2,10	0.034	-11.500
3,10	0.027	-18.500
3,10	0.025	-20.500
3,10	0.025	-20.500
4,10	0.025	-20.500
4,10	0.03	-15.500
4,10	0.028	-17.500

Note: Negative values indicate that readings are below sensitivity of 4.6 pg/ml.

Appendix C: Part C Data

C1:*Cell line Metrics:*

UVW Cell Diameter = 16.5 +/- 0.9 um
UVW Doubling Time = 18 hrs
UVW Uptake % = 31.4 +/- 3.7 %
UVW Slab Thickness is: 7.294 e-5 +/- 9e-6 cm
EJ138 Cell Diameter = 12.8 +/- 0.7 um
EJ138 Doubling Time = 17.5 hrs
EJ138 Uptake % = 21.4 +/- 1.9 %
EJ138 Slab Thickness is: 3.496 e-5 +/-4e-6 cm
^{60}Co Irradiation Dose Rate = 0.25 Gy/min = 15 Gy/h

C2: Survival Fraction Data

Source:	^{60}Co		
	Dose (Gy)	Survival Fraction	Error
UVW/NAT	0	1	0
	1	0.8	0.02
	2	0.68	0.02
	3	0.68	0.04
	4	0.63	0.08
	5	0.64	0.04
	6	0.63	0.04
	7	0.63	0.04
	8	0.58	0.08
	9	0.58	0.06
EJ138/NAT	0	1	0
	1	0.8	0.1
	2	0.68	0.12
	3	0.69	0.09
	4	0.71	0.1
	5	0.7	0.08
	6	0.71	0.07

	7	0.7	0.09
	8	0.71	0.07
	9	0.77	0.1

Source:	^{131}I MIBG		
	Activity Concentration (MBq/ml)	Survival Fraction	Error
UVW/NAT	0	1	0
	1	0.7	0.09
	2	0.55	0.05
	3	0.37	0.07
	4	0.3	0.05
	5	0.3	0.05
	6	0.25	0.02
	7	0.24	0.02
	8	0.2	0.02
EJ138/NAT	0	1	0
	1	0.72	0.08
	2	0.69	0.06
	3	0.68	0.04
	4	0.6	0.04
	5	0.58	0.02
	6	0.49	0.02
	7	0.4	0.02
	8	0.37	0.02
	9	0.34	0.02
	10	0.3	0.03
	11	0.28	0.02

Source:	^{131}I MIBG		
	Activity Concentration (MBq/ml)	Survival Fraction	Error
UVW	0	1	0
Parental	1	0.87	0.08

	2	0.9	0.06
	3	0.87	0.06
	4	0.97	0.02
	5	0.9	0.02
	6	0.84	0.03
	7	0.95	0.02
	8	0.81	0.06
EJ138	0	1	0
Parental	1	1	0.02
	2	0.97	0.03
	3	0.95	0.05
	4	0.94	0.02
	5	0.9	0.02
	6	0.9	0.03
	7	0.89	0.06
	8	0.91	0.05
	9	0.91	0.04
	10	0.9	0.06
	11	0.9	0.06

Source:	Activity Control		
	Activity Concentration (MBq/ml)	Survival Fraction	Error
UVW/NAT	0	1	0
Parental	1	1	0.1
	2	1	0.04
	3	0.94	0.02
	4	0.94	0.02
	5	0.91	0.02
	6	0.89	0.06
	7	0.88	0.04
	8	0.87	0.08
EJ138	0	1	0
Parental	1	1	0.04

	2	0.98	0.04
	3	0.97	0.04
	4	1	0.02
	5	1	0.04
	6	0.97	0.04
	7	0.96	0.04
	8	0.96	0.04
	9	0.96	0.02
	10	0.95	0.04
	11	0.94	0.05

C3: *Dose Rate and Dose Calculations*

UVW/NAT Results: Range is 1 - 8 MBq/ml

Activity	Uptake Dose Rate (Gy/h)	Plus Error Uptake Dose Rate	Minus Error Uptake Dose Rate
0	0	0	0
1	0.014543747	0.001138146	0.001133206
2	0.029087494	0.002276293	0.002266412
3	0.043631241	0.003414439	0.003399617
4	0.058174988	0.004552585	0.004532823
5	0.072718735	0.005690731	0.005666029
6	0.087262482	0.006828878	0.006799235
7	0.101806229	0.007967024	0.007932441
8	0.116349976	0.00910517	0.009065646
Activity	Accum. Dose Rate (Gy/h)	Plus Error Accum. Dose Rate	Minus Error Accum. Dose Rate
0	0	0	0
1	0.093660838	0.030673365	0.023962164
2	0.187321677	0.06134673	0.047924328
3	0.280982515	0.092020095	0.071886492
4	0.374643353	0.122693461	0.095848657
5	0.468304191	0.153366826	0.119810821
6	0.56196503	0.184040191	0.143772985
7	0.655625868	0.214713556	0.167735149

8	0.749286706	0.245386921	0.191697313
Activity	Absorbed Dose (Gy)	Plus Error Absorbed Dose	Minus Error Absorbed Dose
0	0	0	0
1	0.201865424	0.061367839	0.047951109
2	0.403730847	0.122735677	0.095902218
3	0.605596271	0.184103516	0.143853326
4	0.807461694	0.245471355	0.191804435
5	1.009327118	0.306839194	0.239755544
6	1.211192541	0.368207032	0.287706653
7	1.413057965	0.429574871	0.335657762
8	1.614923388	0.49094271	0.38360887

EJ138/NAT Results: Range is 1 - 11 MBq/ml

Activity	Uptake Dose Rate (Gy/h)	Plus Error Uptake Dose Rate	Minus Error Uptake Dose Rate
0	0	0	0
1	0.014608024	0.001134377	0.001131741
2	0.029216048	0.002268754	0.002263482
3	0.043824072	0.003403131	0.003395223
4	0.058432096	0.004537507	0.004526964
5	0.07304012	0.005671884	0.005658705
6	0.087648144	0.006806261	0.006790446
7	0.102256168	0.007940638	0.007922187
8	0.116864191	0.009075015	0.009053928
9	0.131472215	0.010209392	0.010185669
10	0.146080239	0.011343768	0.01131741
11	0.160688263	0.012478145	0.012449151
Activity	Accum. Dose Rate (Gy/h)	Plus Error Accum. Dose Rate	Minus Error Accum. Dose Rate
0	0	0	0
1	0.070535219	0.020516685	0.016235573
2	0.141070437	0.041033369	0.032471146

3	0.211605656	0.061550054	0.048706718
4	0.282140875	0.082066739	0.064942291
5	0.352676094	0.102583423	0.081177864
6	0.423211312	0.123100108	0.097413437
7	0.493746531	0.143616793	0.113649009
8	0.56428175	0.164133477	0.129884582
9	0.634816969	0.184650162	0.146120155
10	0.705352187	0.205166847	0.162355728
11	0.775887406	0.225683531	0.1785913

Activity	Absorbed Dose (Gy)	Plus Error Absorbed Dose	Minus Error Absorbed Dose
0	0	0	0
1	0.155678461	0.041064705	0.032510543
2	0.311356923	0.082129411	0.065021086
3	0.467035384	0.123194116	0.097531629
4	0.622713846	0.164258822	0.130042173
5	0.778392307	0.205323527	0.162552716
6	0.934070769	0.246388233	0.195063259
7	1.08974923	0.287452938	0.227573802
8	1.245427691	0.328517644	0.260084345
9	1.401106153	0.369582349	0.292594888
10	1.556784614	0.410647055	0.325105432
11	1.712463076	0.45171176	0.357615975

C4: *Calculated UVW/NAT Parameters and 1 MBq/ml for Accumulation source modelling comparison. Calculations done one time after RAM cleared.*

Method #2	Time (s)	Method #1a (MuPAD)	Time (s)
	0.02023		30
	0.02351		30.78
	0.02023		30.64
Dose Rate (Gy/h)	0.0202	Dose Rate (Gy/h)	31.25
0.0937 ± (0.031/0.024)	0.02012	0.0999 ± (0.033/0.025)	31.47
	0.02662		30.95
	0.02126		30.74
	0.02094		30.81
	0.02103		30.91
Mean	0.021571111	Mean	30.83888889
Std. Dev	0.002168562	Std. Dev	0.409586512
		Method #1b (Maple)	Time (s)
			4.187
			3.59
		Dose Rate (Gy/h)	4.918
		0.0999 ± (0.033/0.025)	3.624
			3.641
			3.697
			4.827
			3.745
			3.553
		Mean	3.975777778
		Std. Dev	0.542141766

C4: *Comparison of similar dose points for ^{60}Co and [^{131}I] MIBG treatment*

UVW/NAT		
Co-60 Dose (Gy)	Co-60 SF	Co-60 SF Err
1	0.8	0.02
Mean I-131 MIBG Dose	I-131 MIBG SF	I-131 MIBG SF Err
1 (5 MBq/ml)	0.3	0.05

EJ138/NAT		
Co-60 Dose (Gy)	Co-60 SF	Co-60 SF Err
1	0.8	0.01
Mean I-131 MIBG Dose	I-131 MIBG SF	I-131 MIBG SF Err
0.9 (6 MBq/ml)	0.49	0.02
1.1 (7 MBq/ml)	0.4	0.02

UVW/NAT	
Co-60 vs. I-131 MIBG Dose (Gy)	T Values
1 vs. 1	106.0660172
EJ138/NAT	
Co-60 vs. I-131 MIBG Dose (Gy)	T Values
1 vs. 0.9	131.5218613
1 vs. 1.1	169.7056275
DoF = 34 (18+18-2) > Two - tailed t-distribution Critical T for p = 0.05 is 2.03	

C5: *MATLAB Source Code*

For access to the dosimetry modeling material for Part C:

Please download (~170MB) via:

URL1: http://dl.dropbox.com/u/28272358/GOW_Michael_D_201107_PhD_PartC_Model.zip
or
URL2: http://goo.gl/JXB3G

Instructions:
- Unzip.
- Choose package to examine and Unzip that specific package.
- Make sure to read the appropriate documentation as outlined below.
- The standalone modeling application is “ICCM_Dose_Calcs_4_Radio_Beta_Emitters.exe”, contained in “ICCM_Dose_Calcs_4_Radio_Beta_Emitters.zip”.
- If running the standalone executable ICCM_Dose_Calcs_4_Radio_Beta_Emitters.exe, ensure that you first run MCRInstaller.exe as this contains the requisite libraries. This is a one-time installation only. This program was designed for use in Windows only.
- If running the MATLAB M-files, simply change your directory in MATLAB to the location of the particular extracted ZIP file, select .m file, and run.

Three ZIP files are included in this package:

1) "ICCM_Dose_Calcs_4_Radio_Beta_Emitters"

Description:
Contains the standalone executable program
"Dose_rate_ICCM_prod_2_method_comp.exe" and associated material (e.g. MCR Installer, M-file). Make sure to read document "README_Instructions_READ_FIRST.txt"prior to running the executable for the first time.

Direct Download: http://goo.gl/FK2uT

Checksums:

ICCM_Dose_Calcs_4_Radio_Beta_Emitters.exe:
MD5 - f82a1ad864effbfabbcb31c96cc07885
SHA1 - 5f32303fe985e82abc5f9f08fb45666e45bb9ae9

ICCM_Dose_Calcs_4_Radio_Beta_Emitters.m:
MD5 - 7afd9cf37f8b55c1821a813d3b552311
SHA1 - d92c00e0aa9bd9a2a68e4bc88b842636c887201e

2) "Dose_rate_ICCM_prod_2_method_comp"

Description:
Contains M-file for program used to compare different source models during radiopharmaceutical "Accumulation Phase". In order to run properly, the version of MATLAB used to run the program must have the Symbolic Toolbox add-on installed in order to complete the analytical integration for the "homogenous-slab" model (aka. Method #1).

Direct Download: http://goo.gl/TRe5E

Checksum (.m):
Dose_rate_ICCM_prod_2_method_comp.m
MD5 - 2be62adef2b99d9a347084334a6d9c6b
SHA1 - 255bd1074e34b007739d92af7f8fa34b463716fd

3) "Source Code"

Description:
Contains the source code for "Dose_rate_ICCM_prod_2_method_comp" and "Dose_rate_ICCM_prod_2_method_comp.m" in an easy to read HTML format that can be opened and viewed in any web browser. A .docx copy is also included.

Direct Download: http://goo.gl/0Hq9A

What follows is the source code from:

ICCM_Dose_Calcs_4_Radio_Beta_Emitters.m
Dose_rate_ICCM_prod_2_method_comp.m

ICCM_Dose_Calcs_4_Radio_Beta_Emitters.m

```
%%%%%%%%%%%%%%%%%%%%%%%%%%%%%%%%%%%%%%%%%%%%%%%%%%%%%%%%%%%%%%%%%%%%%%%%%%
%************************************************************************%
%                                                                        %
% Calculation of Absorbed Dose in Examination of Bystander Effects via   %
% --------------------------------------------------------------------   %
% Irradiation with Beta Emitting Radiopharmaceutical                     %
% --------------------------------------------------                     %
%                                                                        %
% This program is designed to calculate the absorbed dose to a set of    %
% donor cells used in the creation of Irradiated Cell Conditioned Medium %
% (ICCM)as per radiation bystander protocol utilized by Boyd et al in:   %
%                                                                        %
% Boyd M, Ross SC, et al. Radiation-Induced biological bystander effect  %
% elicited in vitro by targeted radiopharmaceuticals labeled with alpa-, %
% beta-, and auger electron-emitting radionuclides. J.Nucl.Med. Vol. 47. %
% pp. 1007-1015 (2006).                                                  %
%                                                                        %
% The application was designed with the purpose of performing this       %
% calculation of absorbed dose from the beta emitting                    %
% radiopharmaceutical I-131 MIBG.  This is accomplished through modelling%
% of in vitro conditions and procedures coupled with the appropriate     %
% utilization of the Vynckier-Wambersie (VW) point-source dose function  %
% (kernel) integrated over the appropriate geometry.                     %
%                                                                        %
% Having said this, this program is also believed to be suitable for     %
% other beta emitting radiopharmaceuticals potentially used for ICCM     %
% production with maximum energies ranging from 0.5 to 3.0 MeV and       %
% utilization of Boyd et al's methodology outlined in the paper above.   %
%                                                                        %
% Created By: Michael Gow                                                %
%             Dept. of Medical Physics and Applied Radiation Sciences    %
%             McMaster University                                        %
%             Hamilton, ON CA                                            %
%             MMXI                                                       %
%                                                                        %
```

```
% Special thanks to Andrei Hanu (McMaster University) for his MATLAB     %
% insight in the early stages of this endeavour.                         %
%************************************************************************%
%%%%%%%%%%%%%%%%%%%%%%%%%%%%%%%%%%%%%%%%%%%%%%%%%%%%%%%%%%%%%%%%%%%%%%%

%   ********************** BRIEF INTRODUCTION **********************   %
%
% This program will allow the user to input variables required
% to carry out the calculations.  These calculations will be based on the
% Vynckier-Wambersie point source dose function (kernel) integrated for the
% appropriate geometries.  In essence, we will use the dose plane kernel
% derived from VW's function.  The following articles are essential
% reference material:
%
% [1] Vynckier S and Wambersie A. Dosimetry of beta sources in radiotherapy
% I. The beta point source dose function. Phys. Med. Bio. Vol 27(11), pp.
% 1339-1347 (1982).
%
% [2] Vynckier S and Wambersie A. Dosimetry of beta sources in
% radiotherapy: Absorbed dose distributions around plane sources. Rad.
% Prot. Dos. Vol 14(2), pp. 169-173 (1986).
%
% [3] Appendix C: Calculation of beta-ray dose distributions by integration
% of the beta-ray point-source dose function. Oxford University Press. J.
% ICRU. Vol. 4(2), pp. 155-163 (2004).
%
% And of course the primary article outlining the I-131 MIBG treatment
% methodology can be found in:
%
% [4] Boyd M et al. Radiation-Induced Biologic Bystander Effect Elicited In
% Vitro by Targeted Radiopharmaceuticals Labeled with alpha-, beta-, and
% Auger Electron - Emitting Radionuclides. J. Nucl. Med. Vol. 47, pp.
% 1007-1015 (2006).
%
% Lastly, reference material indicating a linear uptake of MIBG
% radiopharmaceutical across various neuroblastoma cell lines (see uptake
% section below) is:
%
```

```
% [5] Armour A, Mairs RJ, Gaze MN, and Wheldon TE. Modification of
% meta-iodobenzylguanidine uptake in neuroblastoma cells by elevated
% temperature. Br. J. Cancer. Vol. 70, pp. 445-8 (1994).
%
% The Vynckier Wambersie Point Source Dose Function (Dose Point Kernel) is
% as follows:
%
% J(x)=
% (B/(pvx)^2)*{c[1-((pvx)/c)*exp(1-(pvx)/c)]+(pvx)*exp(1-pvx)
% -(pvx)*exp(1-((pvx)/2)-f/2)}
%
% with [  ] defined as 0 for pvx >= c
% and J(x) defined as 0 for pvx >= f
%
% J(x) = is the absorbed dose at a distance x (in cm) from the point source
% in unit of Gy/(MBq*h); v = apparent absorption coefficient in cm^2/g; p =
% density of the medium in g/cm^3; c = dimensionless parameter, which gives
% the value of the first term inside the curly brackets {} at x=0 and the
% value of pvx at which this term becomes and remains zero; B =
% normalization constant evaluated by the requirement that the total energy
% absorbed by a very large sphere (infinite) must just be the energy
% emitted. Carrying out the integration of J(x) over all x yields:
%
% B = 0.046*p^2*v^3*Eavg*alpha
%
% where Eavg is the average beta energy of the radionuclide and alpha =
% [3c^2-(c^2-1)e+(3+f)exp(1-f)-4exp(1-(f/2))]^-1
%
% The parameter f/pv is the distance where the point kernel becomes zero.
% This is the supplementary term that was added the Loevinger function in
% order to make the beta point kernel equal to zero at f/pv.  The distance
% f/pv is close but always smaller than the CSDA Rmax for the radionuclide,
% since only a very small fraction of the electrons possess the maximum
% energy and additionally the probability that these electrons reach Rmax
% becomes negligible.
%
% ------------------------------------------------------------------------ %
%
```

```
% The irradiation to the donor cells used in ICCM production occurs in two
% phases  (see figure in associated report):
%
% 1) Dose Rate during Uptake Phase (Gy/hr):  Upon application of the
% radiopharmaceutical, we assume an instant, homogenous, static mixture
% into the medium.  According to Ref. (4), at the time of treatment, 1 ml
% of medium was applied followed by the radiopharmaceutical with the
% appropriate activity.  We will make the assumption that the now
% radioactive medium is a source of infinite extent but finite thickness.
% In fact, the thickness is equal to 0.04 cm.
%
% (Note: This is easily obtained by noting that flask itself is 25cm^2, and
% 1 ml of liquid covering the inside of the flask, we have the volume of
% fluid = surface area x thickness.  With 1ml of fluid equivalent to 1
% cm^3, we get the fluid thickness to be 1cm^3/25cm^2 = 0.04cm.  Hence this
% is the thickness of the source).
%
% There are a couple items to mention at this juncture
%
% 1) We can not approximate the source as infinite in along all extents.
% That is, we need to take thickness into account.  The slab can only be
% considered as infinitely thick if it's thickness is greater the range of
% the most energetic beta particle (Ref. 2).  For I-131, Emax is 0.61 MeV
% and a CSDA range of approximately 0.2 cm (Note: CSDA values for electrons
% / beta particles can be found at the National Institute of Standards and
% Technology website:
% http://physics.nist.gov/PhysRefData/Star/Text/ESTAR.html\). So, we will
% need to take this into account in the uptake phase.
%
% 2)  We can approximate the extent (i.e. length and width) of the source
% as "infinite" provided the radius of the source is >= 0.5*Rmax where Rmax
% is the CSDA range of the most energetic beta particle (Ref. 3).  From
% above, we have that the CSDA range for I-131 is ~ 0.227cm.  Under these
% conditions, the VW plane kernel can be modelled as infinite in extent
% down to a cylindrical slab of cells of approximate surface area ~ 0.04
% cm^2.  With the confluence in Ref [4] being 65% (+/- 5%), this covers an
% area of 16.25 cm^2. Thus, rather than model each donor flask
% independently with an appropriate amount of "infinite VW pixels" of
```

```
% surface area 0.04 cm^2 (for 16.25 cm^2, this results in over 400
% "infinite VW pixels") and summing the resultant dose in each pixel for
% the total dose, we perform a simple transformation, assuming all cells
% make up a single infinite slab. This single slab will provide the same
% dose as addition of the appropriate number of "infinite VW pixels" with
% identical performance but far less complication.
%
% Now the dose rate at the surface of an infinite thick plane source is
% equal to the dose rate of a semi - infinite medium or half of the dose
% rate of an infinite medium. This is due to symmetry reasons as the dose
% rate in the inside of an infinite medium, with a homogeneously
% distributed beta source is equal to the energy dissipated per unit mass
% and time (see Ref. [1]-[3]). The dose rate is a function of the distance
% to the source, x, height of the source, h, and diameter of the source, d,
% we have the dose rate at the surface in contact with the infinite medium
% (i.e. Drate(x=0,h=inf,d=inf) is:
%
% Drate(0,inf,inf) [Gy/s] = 0.5*Am[Bq/g]*Eavg[J]                          (1)
% where Am is the activity per unit mass and Eavg is the average energy per
% beta disintegration.  In more convinent units, we can represent this as:
%
% Drate(0,inf,inf) [Gy/h] = 0.288*Am[MBq/g]*Eavg(MeV)                     (2)
%
% Now, since we will be assuming that the density of the medium is
% equivalent to that of water, this is also equivalent to:
%
% Drate(0,inf,inf) [Gy/h] = 0.288*Ac[MBq/ml]*Eavg(MeV)                    (3)
% where Ac is the activity concentration of the radiopharmaceutical
% applied.  {Remember 1 ml water = 1 cm^3 water, and density of water is 1
% g/cm^3 and accordingly 1 MBq/ml = 1MBq/cm^3 = 1MBq/g}
%
% Now, the dose rate a distance x from an infinite medium is calculated as
% follows (see Ref. [2]):
%
% Drate(x,inf,inf)=Drate(0,inf,inf)*alpha*{c^2[3-exp(1-pvx)-((pvx)/c)*(2+ln
% (c/(pvx))]+exp(1-pvx)-4*exp(1-((pvx)/c)-f/2)+(3+f-pvx)*exp(1-f)}      (4)
%
% with [ ] defined as 0 for pvx >= c and Drate(x,inf,inf) defined as 0 for
```

```
% pvx >= f
%
% So in order to take into account the does rate @ x of a source of
% infinite extent but finite thickness, we have by symmetry (Ref. [2]):
%
% Drate(x,h,inf) = Drate (x,inf,inf) - Drate(x+h,inf,inf)
%
% So, we calculate the dose rate at the onset of radiopharmaceutical
% treatment at two points
%
% a) in contact with the edge of the source and,
% b) at the opposite side of the slab a distance equal to the cell slab
% thickness away.
%
% So for a), we would get:
%
% Drate(0,0.04,inf) = Drate(0,inf,inf) - Drate(0.04,inf,inf)            (5)
%
% and for b), we would get:
%
% Drate(Cell_slab_thick,0.04,inf) = Drate(Cell_slab_thick,inf,inf) -
%                                   Drate(Cell_slab_thick+0.04,inf,inf) (6)
%
% and finally:
%
% Drate_uptake = (Drate(0,0.4,inf)+Drate(Cell_slab_thick,0.04,inf))/2   (7)
%
% Alternatively, you can take the average integral as follows:
%
% Drate_uptake = (1/Cell_slab_thick)*int(Drate(x,h,inf),dx)             (8)
%                 between 0 and Cell_slab_thick
%
% The integration is more computationally expensive with little
% gain in precision within uncertainties due to the thickness of the cells
% upon adhesion to the flask.  Additionally, because the thickness of the
% slab is small, there is effectively a less than 2% difference in dose
% rate between the top and bottom of the slab and therefore a less than 1%
% difference between the arithmetic mean and any point in the slab.  Thus,
```

```
% this program utilizes Eq. (7).
%
% ~~~~~~~~~~~~~~~~~~~
%
% 2) Dose Rate from Internal Source (Gy/hr) (Accumulation Phase):  After
% the Uptake phase, fresh medium replaces the treated medium and the
% radiopharmaceutical source is now inside the slab of cells.  To estimate
% the dose rate inside the cells, there are few different approaches. Here,
% we will break up the activity into infinite thin disks, strategically
% placed within the slab.
%
% From Ref. 2 and 3, we have for an infinite plane source:
%
% Drate(x,0,inf)=0.288*Eavg*Ac*v*alpha*{c[1+ln(c/pvx)-exp(1-(pvx)/c)]+exp(1
% -pvx)-2*exp(1-pvx/c-f/2)+exp(1-f)}                                    (9)
%
% with [  ] defined as 0 for pvx >= c and Drate(x,0,inf) defined as 0 for
% pvx >= f [Note: For definitions of v,c,alpha,and f, see below.]
%
% We will calculate the dose rate at various locations in the slab as
% through two scenarios (Note: the slab is located at x=0 to 2delta):
%
% 1)  Break the activity into 2 infinite thin plane sources of equal
% activity (0.5 Aconc) located at x=(0.5)delta and x=(1.5)delta.  Calculate
% Drate(0,0,inf), Drate(delta,o,inf), and Drate(2delta,0,inf).
%
% 2)  Break the activity into 3 infinite thin plane sources of equal
% activity ((1/3) Aconc) located at x=0,delta, and 2delta.  Calculate
% Drate ((0.5)delta,0,inf) and Drate((1.5)delta,0,inf).
%
% We can will then calculate the average dose rate of the above values in
% order to obtain the average dose rate top the slab.
%
% The another approach is (briefly):
%
% Divide the cell into a bunch of infinitely thin plane sources located
% between x'=0 and 2delta.  For a position, x, the dose rate would be:
%
```

```
% Drate(x)=Aconc*int(K(x-x')) from x'=0 to 2delta
% and then take the average over all x.
% This method is computationally very expensive, requiring symbolic
% integration through either the Maple symbolic engine (best if possible)
% or Matlab's MuPAD symbolic engine.
%
% This method yields results in agreement for average dose rates to
% the slab with a decrease in computational performance and/or
% increases in complexity with no increase in precision or accuracy to the
% method employed here.
%
% ~~~~~~~~~~~~~~~~~~~
%
% 3) Total Absorbed Dose for ICCM production (Gy):
%
% Since we have an approximate linear uptake of radiopharmaceutical over
% the given uptake phase, and we collect bystander factors in the fresh
% medium for a specified period after uptake, we simply need to calculate:
%
% a) The instant dose rate upon application of the radiopharmaceutical to
% the medium (Step 1).
% b) The dose rate from the internal source alone (Step 2).
%
% From here, we can use the trapezoid rule of integration for the specified
% periods of time for uptake and bystander factor collection in order to
% determine the total dose to the donor cells providing the irradiated cell
% conditioned medium (ICCM).  Please refer to the associated report for
% complete details.
%
%   ************************ END INTRODUCTION ************************   %

% Prior to the program starting ...

% Clears Memory
clear all

% Clears Command Window
clc
```

```
% Maintains 15 digits of accuracy unless otherwise flagged
format long

% ========================================================================= %

%~~~~~~~~~~~~~~~~~~~~~~~~~~~~~~~~~~~~~~~~~~~~~~~~%
%~Welcome Dialogue for User of Start-up~%
%~~~~~~~~~~~~~~~~~~~~~~~~~~~~~~~~~~~~~~~~~~~~~~~~%

% The following sets up and displays a welcome dialogue box for the user.
% The user can select to continue to proceed to perform the calculations
% or the user may exit the program.

welcome_text = {'Hello!'
                '                                                        '
                'This program is designed to calculate the absorbed dose to a set of donor
cells used in the creation of Irradiated Cell Conditioned Medium (ICCM) as per radiation
bystander protocol utilized by Boyd et al in:',
                '                                                        '
                'Boyd M, Ross SC, et al. Radiation-Induced biological bystander effect elicited
in vitro by targeted radiopharmaceuticals labeled with alpa-, beta-, and auger electron-
emitting radionuclides. J.Nucl.Med. Vol. 47. pp. 1007-1015 (2006).',
                '                                                        '
                'The application was designed with the purpose of being used for the
calculation of absorbed dose from the beta emitting radiopharmaceutical ^1^3^1I meta-
iodobenzylgaunidine (MIBG).  This is accomplished through modelling of the in vitro conditions
and procedures coupled with the appropriate utilization of the Vynckier-Wambersie (VW) point-
source dose function (kernel) integrated over the appropriate geometry.',
                '                                                        '
                'Having said this, this program is also believed to be suitable for other \beta
emitting radiopharmaceuticals that accumulate at extra-nuclear sites (like MIBG) with maximum
energies ranging from 0.5 to 3.0 MeV and utilization of Boyd et al''s methodology outlined in
the paper above.',
                '                                                        '
                'The following sections will guide the user through data entry necessary to
perform these calculations.  Full details of the modelling utilized in this application can be
found in the associated report.',
```

```
                '                                                       '
                'Created by: Michael Gow'
                '                   Dept. of Medical Physics and Applied Radiation Sciences'
                '                   McMaster University'
                '                   Hamilton, ON CA'
                '                   MMXI'
                '                                                       '
                '                                                       '
                '                                                       '
                '                                                       '
                '                                                       '};
welcome_title = 'Welcome!';
str1 = 'Continue';
str2 = 'Exit';
options.Resize='on';
options.Interpreter='tex';
options.Default=str1;
welcome = questdlg(welcome_text, welcome_title, str1, str2, options);

    % Determine if the user hits the 'Cancel' button
    if strcmp(welcome,'Exit')
        disp('Bye Bye')
        return
    end

% The following is for an exit 'while' loop that will be prompted to the
% user upon completion of the calculations at the end of the program
exit_note='Yes & Continue';
while strcmp(exit_note,'Yes & Continue')

% Now, let's provide the user with the option to save the output of their
% calculations to a Microsoft Excel file.

save_text = {'Do you have Microsoft Excel 97 or greater installed?'
            '                                                    '
            'If so, you can save the calculation output to an Excel file in one of the
following formats:'
            '                                                    '
```

```
            'a) .xls -> Excel 97-2003'
            'b) .xlsx, .xlsm, .xlsb -> Excel 2007, 2010'
            '                                                    '
            'Note: If you have Excel 2003 but wish to save to .xlsx format, please ensure that
you have the Excel 2007 Compatibility Pack installed on your local machine.'
            '                                                    '
            'Select ''Yes'' to enter the file details or ''No'' to proceed without saving to a
file (results will simply print to the command window)'
            '                                                    '
            '                                                    '};
save_title = 'Save to Excel?';
str1 = 'Yes';
str2 = 'No';
str3 = 'Exit';
options.Resize='on';
options.Interpreter='tex';
options.Default=str1;
save = questdlg(save_text, save_title, str1, str2, str3, options);

    % Determine if the user hits the 'Exit' button
    if strcmp (save,'Exit')
        disp('Bye Bye')
        return
    end

    if strcmp (save,'Yes')
        prompt_choices = {'Select an Excel file format:'};
        format_choices = {'.xls','.xlsx','.xlsm','.xlsb'};
        size = [180 60];
        excel_format = listdlg('PromptString',prompt_choices,...
                               'SelectionMode','single',...
                               'ListString',format_choices,...
                               'Name','Excel Format',...
                               'ListSize',size);
        if excel_format == 1 || excel_format == 2 || excel_format == 3 || excel_format == 4
            filename_text = {'Please enter the name of the file.  Do not enter the extension
(e.g only ''Results'' NOT ''Results.xls'').  This file will be saved to your current active
directory (i.e. the directory where you are currently running the .exe or .m file).'};
```

```
            title_filename = 'Filename for Calculation Results';
            num_lines_filename = 1;
            options.Resize='on';
            options.Interpreter='tex';

            % Define the standard parameters
            def_filename = {'results'};
            answer_filename =
inputdlg(filename_text,title_filename,num_lines_filename,def_filename,options);

                % Determine if the user hits the 'Cancel' button
                if isempty(answer_filename) == 1
                    disp('Bye Bye')
                    return
                end

                % We are going to make sure the user does not enter an
                % invalid character for Windows file systems
                check=0;
                wrong_char1 = strfind(answer_filename{1},'.');
                    if isempty(wrong_char1)==0
                        check=1;
                    end
                wrong_char2 = strfind(answer_filename{1},''\'');
                    if isempty(wrong_char2)==0
                        check=1;
                    end
                wrong_char3 = strfind(answer_filename{1},'/');
                    if isempty(wrong_char3)==0
                        check=1;
                    end
                wrong_char4 = strfind(answer_filename{1},':');
                    if isempty(wrong_char4)==0
                        check=1;
                    end
                wrong_char5 = strfind(answer_filename{1},'*');
                    if isempty(wrong_char5)==0
                        check=1;
```

```
                    end
                wrong_char6 = strfind(answer_filename{1},'?');
                    if isempty(wrong_char6)==0
                        check=1;
                    end
                wrong_char7 = strfind(answer_filename{1},'"');
                    if isempty(wrong_char7)==0
                        check=1;
                    end
                wrong_char8 = strfind(answer_filename{1},'<');
                    if isempty(wrong_char8)==0
                        check=1;
                    end
                wrong_char9 = strfind(answer_filename{1},'>');
                    if isempty(wrong_char9)==0
                        check=1;
                    end
                wrong_char10 = strfind(answer_filename{1},'|');
                    if isempty(wrong_char10)==0
                        check=1;
                    end
                wrong_char11 = strfind(answer_filename{1},'%');
                    if isempty(wrong_char11)==0
                        check=1;
                    end

                while isempty(answer_filename{1}) || check == 1
                    err_filename_dlg = errordlg({'You need to enter a valid file name!'
                                                 'It can not be empty or contain a one of the
following characters:'
                                                 '                                          '
                                                 '\  /  :  *  ?  "  <  >  |  .  %'},'Error');
                    uiwait(err_filename_dlg);
                    check = 0;
                    answer_filename =
inputdlg(filename_text,title_filename,num_lines_filename,def_filename,options);
                        if isempty(answer_filename) == 1
                            disp('Bye Bye')
```

```
                            return
                        end
                end
        end
    end

% ========================================================================= %

%~~~~~~~~~~~~~~~~~~~~~~~~~~~~~~~~~~~~~~~~~~~~~~~~~~~~~~~~~~~~~~~~~~~~~~~~%
%~Input Variables to Determine Thickness of Slab of Cells~%
%~~~~~~~~~~~~~~~~~~~~~~~~~~~~~~~~~~~~~~~~~~~~~~~~~~~~~~~~~~~~~~~~~~~~~~~~%

% Now let's have the user start entering values but first, a message to the
% user saying what we are doing...

slab_mess_text = {'The cellular distribution within the treated flasks is approximated by a
symmetrical slab of cells of some surface area A and thickness 2\Delta [e.g. cylindrical slab].
Provided the treatment flask is largely confluent, then the majority of cells are in close
contact and such an approximation holds true.'
                  '                                                                    '
                  'With this approximation, we can determine the thickness of the cells,
2\Delta, when adhered to the flask through knowledge of:'
                  '                                                                    '
                  '1) Size (surface area) of the flask used for culturing of donor cells'
                  '2) Confluence of the cell population at the time of radiopharmaceutical
treatment'
                  '3) Diameter of the cell line utilized in suspension (i.e. free float)'
                  '4) Number of cells plated in the donor flasks'
                  '5) Doubling time of cell line used'
                  '6) Time between cell plating and radiopharmaceutical treatment'
                  '                                                                    '
                  'Additionally, parameters involved in measurement of the radiopharmaceutical
uptake which can be noted include:'
                  '                                                                    '
                  '7) Size (surface area) of the culture well / flask for uptake measurements'
                  '8) Number of cells plated in the culture well / flask for uptake
measurements'
```

```
                  '9) Time between plating and radiopharmaceutical application for uptake
measurements'
                  '                                                                    '
                  'NOTE: If entering a fractional number (i.e. less than 1), make sure to enter
a leading '' 0. '' where applicable.'
                  '                                                                    '
                  '                                                                    '
                  '                                                                    '};
slab_mess_title = 'Determine the thickness of the cells in the treatment flask';
str1_slab = 'Continue';
str2_slab = 'Exit';
options.Resize='on';
options.Interpreter='tex';
options.Default=str1_slab;
cell_slab_note = questdlg(slab_mess_text, slab_mess_title, str1_slab, str2_slab, options);

    % Determine if the user hits the 'Cancel' button
    if strcmp (cell_slab_note,'Exit')
        disp('Bye Bye')
        return
    end

% Now, let's have the user input the necessary variable to calculate the
% cell thickness when adhered to the bottom of the treatment flask

prompt_slab = {'1) s_f_l_a_s_k = Size (surface area) of the flask used in treatment (in cm^2):'
               '2a) %_c_o_n_f = Percentage of cell confluence in treatment flask (between 0 and
1):'
               '2b) Err_%_c_o_n_f = Error / Uncertainty in cell confluence in treatment flask
(between 0 and %_c_o_n_f):'
               '3) Name of cell line used:'
               '4a) Cell_D = Cellular diameter while in suspension (in \mum):'
               '4b) Err_D = Error in cellular diameter while in suspension (in \mum):'
               '5) #_c_e_l_l_s = Number of cells plated. NOTE: No commas, spaces, or
scientific/exponential notation:'
               '6) DB_t_i_m_e = Doubling time of cell line used (in hours):'
               '7) T_2_p_l_a_t_e = Time between cell plating and ^1^3^1I treatment (in hours):'
```

```
                '8) s_w_e_l_l = Size (surface area) of the well / flask used in uptake
measurements (in cm^2).  NOTE:  If a 6 - well plate was utilized, the typical surface area is
9.6 cm^2:'
                '9) #_u_p_t_a_k_e = Number of cells plated in well / flask in uptake
measurements. NOTE: No commas, spaces, or scientific/exponential notation:'
                '10) T_2_u_p_t_a_k_e = Time between plating and application of
radiopharmaceutical in uptake measurements (in hours):'};

title_slab = 'Input Parameters for determining cell thickness';
num_lines_slab = [1 100]; % 1 row per prompt 100 characters wide
options.Resize='on';
options.Interpreter='tex';

% Define the standard parameters
def_slab =
{'25.0','0.65','0.05','UVW/NAT','16.5','0.9','200000','18.0','24.0','9.6','50000','48'};

% 'answer_slab' is a four element vector containing the users input results
answer_slab = inputdlg(prompt_slab,title_slab,num_lines_slab,def_slab,options);

    % Determine if the user hits the 'Cancel' button
    if isempty(answer_slab) == 1
        disp('Bye Bye')
        return
    end

    % Checks to ensure that all input parameters have a value
    while isempty(answer_slab{1}) || isempty(answer_slab{2}) || isempty(answer_slab{3}) ||
isempty(answer_slab{4}) || isempty(answer_slab{5}) || isempty(answer_slab{6}) ||
isempty(answer_slab{7}) || isempty(answer_slab{8}) || isempty(answer_slab{9}) ||
isempty(answer_slab{10}) || isempty(answer_slab{11}) || isempty(answer_slab{12})
        empty_err_slab = errordlg({'You have missed entering information into one of the input
parameters.'
                                   'All parameters require a value.  Please Try
Again.'},'Error');
        uiwait(empty_err_slab)
        answer_slab = inputdlg(prompt_slab,title_slab,num_lines_slab,def_slab,options);
            if isempty(answer_slab) == 1
```

```
                disp('Bye Bye')
                return
            end
    end

% Now, we convert the strings entered by the user in to double precision
% floating point numbers.

% Size of the flask
S_flask = str2double(answer_slab{1});
% Percentage confluence
Per_conf = str2double(answer_slab{2});
% Error in Percentage Confluence
Err_per_conf = str2double(answer_slab{3});
% Cell diameter
Cell_diam = str2double(answer_slab{5});
% Error in cell diameter
Err_cell_diam = str2double(answer_slab{6});
% # of Cells Plated
Num_cells = str2double(answer_slab{7});
% Doubling time of cell line used
Db_time = str2double(answer_slab{8});
% Time between plating and treatment
Pl2treat_time = str2double(answer_slab{9});
% Size of well used for uptake experiment
S_well = str2double(answer_slab{10});
% # of cells plated for uptake measurement
Num_uptake = str2double(answer_slab{11});
% Time between plating and uptake experiments
Pl2treat_up_time = str2double(answer_slab{12});

% Also for convenience, lets assign a variable to the name of the cells
Cell_name = answer_slab{4};

    % Check to ensure that the user has entered valid numbers (e.g. not
    % negative).  ISNAN checks to ensure a number was entered as opposed to
    % a alpha or special character.
```

```
    while (S_flask <= 0) || isnan(S_flask) == 1 || (Per_conf <= 0) || (Per_conf > 1) ||
isnan(Per_conf) == 1 || (Err_per_conf < 0) || (isnan(Err_per_conf) == 1) || (Err_per_conf >
Per_conf) || (Cell_diam <= 0) || (isnan(Cell_diam) == 1) || (Err_cell_diam < 0) ||
(isnan(Err_cell_diam) == 1) || (Err_cell_diam > Cell_diam) || (Num_cells <= 0) ||
(isnan(Num_cells) == 1) || (Db_time <= 0) || (isnan(Db_time) == 1) || (Pl2treat_time <= 0) ||
(isnan(Pl2treat_time) == 1) || (S_well <= 0) || (isnan(S_well) == 1) || (Num_uptake <= 0) ||
(isnan(Num_uptake) == 1) || (Pl2treat_up_time <= 0) || (isnan(Pl2treat_up_time) == 1)
        err_slab_neg = errordlg({'This error has resulted from one of the following:'
                                 '--------------------------------------------------------------
--------------'
                                 '                                                   '
                                 'a) You have entered a negative value or a value of zero for
one of the following parameters:'
                                 '-> size of flask, cell diameter, # of cells, doubling time,
and/or time between plating and radiopharmaceutical application'
                                 '                                                   '
                                 'b) The confluence entered is outside the acceptable range.'
                                 '                                                   '
                                 'c) The error/uncertainty in the confluence is greater than
the confluence value entered.'
                                 '                                                   '
                                 'd) The error/uncertainty in the cell diameter is greater than
the cell diameter value entered.'
                                 '                                                   '
                                 'e) You have not entered valid numeric characters (with the
exception of the cell line name). Not enter a leading '' 0. '' for fractional numbers may cause
this error.'
                                 '                                                   '
                                 '                                                   '
                                 'Please ensure all parameters are positive and have been
entered correctly.'
                                 '                                                   '
                                 '                                                   '
                                 '
'},'Error');
        uiwait(err_slab_neg)
        answer_slab = inputdlg(prompt_slab,title_slab,num_lines_slab,def_slab,options);
```

```
            % If the user enters 'Cancel'...
            if isempty(answer_slab) == 1
                disp('Bye Bye')
                return
            end

        % Convert to double floating point precision
        S_flask = str2double(answer_slab{1});
        Per_conf = str2double(answer_slab{2});
        Err_per_conf = str2double(answer_slab{3});
        Cell_diam = str2double(answer_slab{5});
        Err_cell_diam = str2double(answer_slab{6});
        Num_cells = str2double(answer_slab{7});
        Db_time = str2double(answer_slab{8});
        Pl2treat_time = str2double(answer_slab{9});
        S_well = str2double(answer_slab{10});
        Num_uptake = str2double(answer_slab{11});
        Pl2treat_up_time = str2double(answer_slab{12});
    end

% Now, we calculate the cell thickness upon adhesion to the donor flasks
% as follows:

% *******
% First, calculate the volume of one cell in suspension.
% This volume is conserved upon adhesion to the flask:
% NOTE: We multiply by 1E-4 to convert micrometres to centimetres

Cell_vol = (4/3)*pi*(0.5*Cell_diam*0.0001)^3;

% Now, calculate the uncertainty in the cell volume in suspension.
% Remember, if we have Value +/- Error, the error (standard deviation) is
% calculated via: Error = Value*(Square Root of the Sum of the Squares) of
% all the relative errors (i.e. relative error = Error/Value).  So here, if
% we have a power of 3, we calculate the error as:
% (Value^3)*((3*(Err/Value)^2)^0.5)

Err_Cell_vol = ((4/3)*pi)*((0.5*Cell_diam*0.0001)^3*((3*(Err_cell_diam/Cell_diam)^2)^0.5));
```

```
% *******
% Second, determine surface area of the flask taken up by the cells.  For
% example, if a 25 cm^2 flask is 65% confluent, the total surface area
% taken up by the cells is 25*0.65 = 16.25 cm^2

Cell_surf_area = S_flask*Per_conf;

% Uncertainty in surface area

Err_Cell_surf_area = S_flask*Err_per_conf;

% *******
% Third, we need to determine how many cells make up this population
% covering surface area 'Cell_surf_area' above.  To do this, we need to
% take into account the doubling time of the cell line so that the total
% number cells at given time, t, between plating and treatment is as
% follows: C = Co*exp[(t*ln2)/DB] where DB is the doubling time of the cell
% line and Co is the number of cells originally plated.

Tot_num_cells = Num_cells*exp((Pl2treat_time*log(2))/Db_time);

% *******
% Fourth, so the total volume taken up by the cells at time of treatment
% is:

Tot_cell_vol = Cell_vol*Tot_num_cells;

% Uncertainty in total volume

Err_Tot_cell_vol = Err_Cell_vol*Tot_num_cells;

% *******
% Fifth, and final step is to calculate the thickness of the cells upon
% adhering to the flask.  We know the total volume of the cells (Step 4) as
% well as the surface area these cells covered in the flask (Step 2).
% Since Volume = Surface Area*Thickness, we have simply, Cell Slab
% Thickness = 2Delta = (Tot_cell_vol)/(Cell_surf_area):
```

```
Cell_slab_thick = Tot_cell_vol/Cell_surf_area;
Cell_slab_half_thick = 0.5*Cell_slab_thick;

% Uncertainty in slab thickness

Err_Cell_slab_thick = (Tot_cell_vol/Cell_surf_area)*((Err_Tot_cell_vol/Tot_cell_vol)^2 +
(Err_Cell_surf_area/Cell_surf_area)^2)^0.5;
Err_Cell_slab_half_thick = 0.5*Err_Cell_slab_thick;
% *******

% Now, lets print the result!
fprintf(1,'=====================================================\n')
fprintf(1,'The thickness of the slab of %s cells is:\n--> %d', Cell_name,Cell_slab_thick)
fprintf(1,' +/- %.0d cm\n', Err_Cell_slab_thick)
fprintf(1,'\nTherefore, the half-thickness of the slab of %s\n',Cell_name)
fprintf(1,'cells is:\n--> %d',Cell_slab_half_thick)
fprintf(1,' +/- %.0d cm\n=========================================================\n\n',
Err_Cell_slab_half_thick)

% For usage later, lets also calculate the maximum and minimum slab
% thickness
Cell_slab_thick_max = Cell_slab_thick + Err_Cell_slab_thick;
Cell_slab_thick_min = Cell_slab_thick - Err_Cell_slab_thick;
Cell_slab_half_thick_max = 0.5*Cell_slab_thick_max;
Cell_slab_half_thick_min = 0.5*Cell_slab_thick_min;

% *******
% Using the thickness calculated above, coupled with input variables
% provided for the uptake measurement experiments, we will determine the
% confluence of the wells / flask used for determining our
% radiopharmaceutical uptake percentages (to be entered by the user in the
% next section).  Remember, upon application of the radiopharmaceutical to
% the medium, we are assuming an instant, homogenous, static mix.  Because
% we assume it to be static, areas covered with radiopharmaceutical but no
% cells will not have the pharmaceutical taken up.  Thus, we can make a
% correlation between activity administered, well/flask confluence, and
% uptake percentage from our uptake experiment data which will allow us to
```

```
% more accurately determine the the amount of activity taken up by donor
% cells used for ICCM production. We will call this a confluence adjustment
% factor, Conf_adjust_uptake, obtained for an applied activity
% concentration, Aconc, as:
%
% [(% Uptake from exp.)/(Uptake Conf.)] =
%                              [(X actual uptake % by donors)/(Donor Conf.]
%
% where (X actual uptake by donors) = Conf_adjust_uptake*% Uptake from exp.
%
% Typically, the wells in the uptake experiments are
% seeded and allowed to culture for long enough such that they are fully
% confluent at the time of uptake application and subsequent measurement
% (i.e. Uptake Conf. = 1).  In this case, the confluence adjustment is
% straight forward.  Simply multiple the uptake percentage by the donor
% cell confluence.  Intuitively, assuming a static, homogeneous
% radiopharmaceutical distribution / coverage, this is obvious (i.e. cells
% will only uptake the activity that is covering them).  Otherwise the
% expression above will make the appropriate adjustment.
%
% Conf_adjust_uptake is calculated as follows:

% 1) Determine the number of cells after the time between seeding and start
% of uptake experiment (i.e. radiopharmaceutical application).

Tot_num_cells_uptake = Num_uptake*exp((Pl2treat_up_time*log(2))/Db_time);

% 2) Use the cell volume and donor cell thickness calculated above to
% determine the area covered in the well.

Conf_uptake = (Tot_num_cells_uptake*Cell_vol)/Cell_slab_thick;
Err_conf_uptake = Conf_uptake*(Err_Cell_slab_thick);

% We will identify Conf_adjust_uptake below after we define some additional
% variables....keep your eyes open ;)

% ========================================================================= %
```

```
%~~~~~~~~~~~~~~~~~~~~~~~~~~~~~~~~~~~~~~~~~~~~~~~~~~~~~~~~~~~~~~~~~~~~%
%~Input variables to be used in Vynckier Wambersie Kernel~%
%~~~~~~~~~~~~~~~~~~~~~~~~~~~~~~~~~~~~~~~~~~~~~~~~~~~~~~~~~~~~~~~~~~~~%

% A note to the user about what is left to enter.
addn_param_text = {'In order to perform the necessary calculations, we need to account for the
following additional experimental parameters regarding the radiopharmaceutical and medium
utilized:'
                   '                                                                '
                   '1) The mean energy of \beta particles for the nuclide utilized'
                   '2) The maximum energy of \beta particles for the nuclide utilized'
                   '3) Density of the homogenous medium'
                   '4) The activity concentrations applied'
                   '5) Percentage uptake of the radiopharmaceutical into the cell in vitro'
                   '6) Time for uptake phase'
                   '7) Time for bystander factor accumulation'
                   '                                                                '
                   'NOTE: If entering a fractional number (i.e. less than 1), make sure to
enter a leading '' 0. '' where applicable.'
                   '                                                                '
                   '                                                                '};

addn_param_title = 'Additional Experimental Parameters';
str1_addn_param = 'Continue';
str2_addn_param = 'Exit';
options.Resize='on';
options.Interpreter='tex';
options.Default=str1_addn_param;
addn_param_note =
questdlg(addn_param_text,addn_param_title,str1_addn_param,str2_addn_param,options);

    if strcmp (addn_param_note,'Exit')
        disp('Bye Bye')
        return
    end

% Now, lets have the user input the necessary variables
addn_param_input = {'<E_\beta> = Mean \beta energy per disintegration (in MeV):'
```

```
                    'E_\beta_m_a_x = Maximum \beta energy (in MeV). NOTE: Here, this value is
limited to the range of 0.5 MeV to 3.0 MeV (exclusive).  The reason for this due to
E_\beta_m_a_x''s use in evaluating additional variables in the VW kernel (see Vynckier and
Wambersie, 1982, 1986):'
                    '\rho = Density of the homogeneous medium (in g/cm^3; 1 for standard
medium):'
                    'Smallest A_c_o_n_c = Smallest activity concentration of
radiopharmaceutical applied (in MBq/ml; With medium of unit density, then 1 MBq/ml = 1 MBq/cm^3
= 1 MBq/g). NOTE: If the experiment involved only one A_c_o_n_c, enter it here:'
                    'Largest A_c_o_n_c = Largest activity concentration of radiopharmaceutical
applied (in MBq/ml; With medium of unit density, then 1 MBq/ml = 1 MBq/cm^3 = 1 MBq/g). NOTE:
If the experiment involved only one A_c_o_n_c, enter 0 here:'
                    'A_c_o_n_c Increments = Enter the incremental steps utilized for applying
the range of A_c_o_n_c''s across the experiment (ex. Experiments with 1,2, & 3 Mq/ml
A_c_o_n_c''s have A_c_o_n_c Increments = 1).  If your increments were not equal, then each
A_c_o_n_c value should be entered one at a time into "Smallest A_c_o_n_c" field and "A_c_o_n_c
Increments" should remain 0.  Lastly, if you enter a value for Largest A_c_o_n_c, then the
appropriate step value must be entered:'
                    '%_u_p_t_a_k_e = Percentage uptake of radiopharmaceutical (between 0-1):'
                    'Err_%_u_p_t_a_k_e = Error / Uncertainty in uptake of radiopharmaceutical
(between 0 and %_u_p_t_a_k_e):'
                    'T_u_p = Time allotted for radiopharmaceutical uptake (in hours):'
                    'T_a_c_c_u_m = Time allotted for bystander factors to accumulate after
application of fresh medium (in hours):'};

addn_param_input_title = 'Additional Experimental Parameters';
addn_param_num_lines = [1 120];
options.Resize='on';
options.Interpreter='tex';

% Define the standard parameters
def_addn_param = {'0.19','0.61','1.00','1.00','0.00','0','0.314','0.037','2','1'};

% "answer" is the 10 element column vector that contains the user input
% results.
addn_param_answer =
inputdlg(addn_param_input,addn_param_input_title,addn_param_num_lines,def_addn_param,options);
```

```
    % Determine if the user hits the 'Cancel' button and if so displays
    % an exit prompt
    if isempty(addn_param_answer) == 1
        disp('Bye Bye')
        return
    end

    % Checks to ensure that all input parameters have a value
    while isempty(addn_param_answer{1}) || isempty(addn_param_answer{2}) ||
isempty(addn_param_answer{3}) || isempty(addn_param_answer{4}) || isempty(addn_param_answer{5})
|| isempty(addn_param_answer{6}) || isempty(addn_param_answer{7}) ||
isempty(addn_param_answer{8}) || isempty(addn_param_answer{9}) ||
isempty(addn_param_answer{10})
        addn_param_empty_err = errordlg({'You have missed entering information into one of the
input parameters.'
                                         'All parameters require a value (even 0).  Please Try
Again.'},'Error');
        uiwait(addn_param_empty_err)
        addn_param_answer =
inputdlg(addn_param_input,addn_param_input_title,addn_param_num_lines,def_addn_param,options);
            if isempty(addn_param_answer) == 1
                disp('Bye Bye')
                return
            end
    end

% Now, we convert the strings entered by the user in to double precision
% floating point numbers.

% Mean beta energy per disintegration (in Mev)
Mean_beta_eng = str2double(addn_param_answer{1});
% Maximum beta energy (in MeV)
Max_beta_eng = str2double(addn_param_answer{2});
% Density of medium (g/cm^3)
Dens_med = str2double(addn_param_answer{3});
% Smallest A_conc or only A_conc applied (in MBq/ml)
Small_act_conc = str2double(addn_param_answer{4});
% Largest A_conc(in MBq/ml)
```

```
Large_act_conc = str2double(addn_param_answer{5});
% A_conc increments
Increm_act_conc = str2double(addn_param_answer{6});
% % of radiopharmaceutical uptake
Percent_up = str2double(addn_param_answer{7});
% Error / Uncertainty in % of radiopharmaceutical uptake
Err_percent_up = str2double(addn_param_answer{8});
% Time allocated for radiopharmaceutical uptake
Time_up = str2double(addn_param_answer{9});
% Time allocated for bystander factor accumulation
Time_accum = str2double(addn_param_answer{10});

    % Check to ensure that the user has not entered a negative number or
    % that the confluence level is not below the acceptable value.
    while (Mean_beta_eng <= 0) || (isnan(Mean_beta_eng) == 1) || (isnan(Max_beta_eng) == 1) ||
(Max_beta_eng <= 0.5) || (Max_beta_eng >= 3.0) || (Dens_med <= 0) || (isnan(Dens_med) == 1) ||
(Small_act_conc < 0) || (isnan(Small_act_conc) == 1)|| (Large_act_conc < 0) ||
(isnan(Large_act_conc) == 1) || (Small_act_conc > Large_act_conc && Large_act_conc ~= 0) ||
(Increm_act_conc < 0) || (isnan(Increm_act_conc) ==1) || (Increm_act_conc > Large_act_conc) ||
(Increm_act_conc == 0 && Large_act_conc ~= 0) || (Percent_up <= 0) || (isnan(Percent_up) == 1)
|| (Percent_up > 1) || (Err_percent_up <= 0) || (isnan(Err_percent_up) == 1) || (Err_percent_up
> Percent_up) || (Time_up <= 0) || (isnan(Time_up) == 1) || (Time_accum <= 0) ||
(isnan(Time_accum) == 1)
        err_slab_neg = errordlg({'This error has resulted from one of the following:'
                                 '-------------------------------------------------------------
--------------'
                                 '                                                           '
                                 'a) You have entered a negative value or a value of 0 for one
of the following parameters:'
                                 '-> Average beta energy, density of the medium, percentage
uptake, activity concentration, time allotted for uptake, and/or time allotted for bystander
factor accumulation'
                                 '                                                           '
                                 'b) The maximum beta energy entered is outside the accepted
range of 0.5 to 3.0 MeV (exclusive).'
                                 '                                                           '
                                 'c) The "Smallest" activity concentration entered is bigger
than the "Largest" activity concentration entered.'
```

```
                                    '                                                                    '
                                    'd) The incremental steps entered for application of the
activity concentrations is bigger than the "Largest" activity concentration of a "Large"
activity concentration was entered without an "Increment" value.'
                                    '                                                                    '
                                    'e) The percentage of uptake is greater than 100% (i.e.
greater than 1) or the error in uptake is larger than or equal to the entered uptake value.'
                                    '                                                                    '
                                    'f) You have entered a non-numeric character. Not enter a
leading '' 0. '' for fractional numbers may cause this error.'
                                    '                                                                    '
                                    '                                                                    '
                                    'Please ensure all parameters are positive and have been
entered correctly.'
                                    '                                                                    '
                                    '                                                                    '
                                    '
'},'Error');

        uiwait(err_slab_neg)
        addn_param_answer =
inputdlg(addn_param_input,addn_param_input_title,addn_param_num_lines,def_addn_param,options);

            % If the user enters 'Cancel'...
            if isempty(addn_param_answer) == 1
                disp('Bye Bye')
                return
            end

        % Convert to double floating point precision
        Mean_beta_eng = str2double(addn_param_answer{1});
        Max_beta_eng = str2double(addn_param_answer{2});
        Dens_med = str2double(addn_param_answer{3});
        Small_act_conc = str2double(addn_param_answer{4});
        Large_act_conc = str2double(addn_param_answer{5});
        Increm_act_conc = str2double(addn_param_answer{6});
        Percent_up = str2double(addn_param_answer{7});
        Err_percent_up = str2double(addn_param_answer{8});
```

```
        Time_up = str2double(addn_param_answer{9});
        Time_accum = str2double(addn_param_answer{10});
    end

% Now, we have Conf_adjust_uptake as follows:

if (Conf_uptake-Err_conf_uptake) >= S_well
    Conf_uptake = 1;
    Err_conf_uptake = 0;
    %If the minimum area covered by the cells is greater than or equal to
    %the size of the well then we have 100% confluence at time of uptake
    %experiment and Conf_adjust_uptake is simply the percentage confluence:
end

Conf_adjust_uptake = Per_conf/Conf_uptake;
Err_conf_adjust_uptake = (Per_conf/Conf_uptake)*((Err_per_conf/Per_conf)^2 +
(Err_conf_uptake/Conf_uptake)^2)^0.5;


% *******
% Now, let's calculate some of the necessary variables that form part of
% the VW kernel
% *******

% 1) Apparent absorption coefficient, v [cm^2/g -> density thickness].
% This relation is accurate provided the maximum beta energy of the
% radionuclide is between 0.5 and 3.5 MeV.

v = 14.5*(Max_beta_eng)^(-1.17);

% NOTE: By comparison, the original Loevinger kernel, calculated the
% apparent absorption coefficient, v, via:
% v = 18.6*(Emax - 0.036)^(-1.37) for the range 0.17 to 3 MeV
% *******

% 2) Dimensionless parameter c.  Remember we are only looking in the range
% of 0.5 to 3.0 MeV for the maximum beta energy
```

```
if (Max_beta_eng >= 0.5 && Max_beta_eng < 1.5)
    c = 1.5;
elseif (Max_beta_eng > 1.5 && Max_beta_eng <= 3.0)
    c = 1;
end
% *******

% 3) Dimensionless f parameter. The parameter f/pv is the distance where
% the point kernel becomes zero.  This is the primary correction entered by
% VW into Loevinger's work. This relationship again holds true in the
% energy range between 0.5 and 3.5 MeV.

f = Dens_med*v*0.269*(Max_beta_eng)^1.31;
% *******

% 4) Alpha Coefficient. For explanation see Ref. 1-3 in "Brief
% Introduction".

alpha = ((3*c^2) - (c^2-1)*exp(1) + (3+f)*exp(1-f) - 4*exp(1-(f/2)))^-1;
% *******

% 5) Thickness of radiopharmaceutical medium, h (in cm).  Based the
% protocol utilized by Boyd et al, the radiopharmaceutical was added to 1
% ml of medium during the uptake phase.  Based on the size of the flask
% used, S_flask, we have A*t = Vol (of 1 ml) = 1 cm^3.  Therefore, we have
% 1 cm^3/25cm^2 =:

h = 1/S_flask;
% ========================================================================= %

% Let's start the calculations.  If the user enters a range of activity
% concentrations, we have the following:

if Large_act_conc ~= 0

% Start of 'for' loop to cycle through the activity concentrations entered
% by the user and perform the calculations...
```

```
i = 0; % This a counter for us to use in the 'for' loop as a matrix index

% For performance, we pre-allocate memory space for vectors we will be
% creating throughout the calculations:
Activity = zeros(1,(Large_act_conc/Increm_act_conc));
Drate_uptake_avg = zeros(1,(Large_act_conc/Increm_act_conc));
Drate_uptake_x_2delta_plus_err = zeros(1,(Large_act_conc/Increm_act_conc));
Drate_uptake_x_2delta_minus_err = zeros(1,(Large_act_conc/Increm_act_conc));
Drate_slab_avg = zeros(1,(Large_act_conc/Increm_act_conc));
Drate_slab_avg_max = zeros(1,(Large_act_conc/Increm_act_conc));
Drate_slab_avg_min = zeros(1,(Large_act_conc/Increm_act_conc));
Drate_slab_avg_plus_err = zeros(1,(Large_act_conc/Increm_act_conc));
Drate_slab_avg_minus_err = zeros(1,(Large_act_conc/Increm_act_conc));
Dose = zeros(1,(Large_act_conc/Increm_act_conc));
Dose_err_plus = zeros(1,(Large_act_conc/Increm_act_conc));
Dose_err_minus = zeros(1,(Large_act_conc/Increm_act_conc));

for A = Small_act_conc:Increm_act_conc:Large_act_conc
i = i + 1; % start matrix index counter and add 1 for each run through

fprintf(1,'For an activity concentration of: %4.2f MBq/ml\n',A)
fprintf(1,'~~~~~~~\n\n')

Activity(i) = A;

% ========================================================================= %
%~~~~~~~~~~~~~~~~~~~~~~~~~~~~~~~~~%
%~Calculate Dose Rate for Uptake~%
%~~~~~~~~~~~~~~~~~~~~~~~~~~~~~~~~~%

% We will now calculate the dose rate during the uptake phase as noted in
% the section the "Brief Introduction".  The 'if' statements seen below
% take into consideration the appropriate conditions from Eq. (4):

% First, if the f <= p*v*x ...
if f <= (Dens_med*v*Cell_slab_thick_min)
% Note we have used the minimum cell thickness calculated to be the
% most stringent
```

```
    fprintf(1,'The dose rate is 0 Gy/h. No need to go any further...\n')

else % Second, condition on c to alter value of the square brackets

    % First, as stated in the "Brief Introduction" above, we need to
    % calculate this in two parts, a and b (see Eqs. 4,5,and 6).  Step one
    % is calculate Drate(0,0.04,inf) = Drate(0,inf,inf) -
    % Drate(0.04,inf,inf) where Drate(0,inf,inf) [Gy/h] =
    % 0.288*Ac[MBq/ml]*Eavg(MeV):

    Drate_zero_inf_inf = 0.288*A*Per_conf*Mean_beta_eng;
    % Remember, we take into account the confluence adjustment as activity
    % not covering cells does not contribute to the absorbed dose.  This is
    % simply the percentage confluence during the Uptake phase.  During the
    % Accumulation phase, this is the Conf_adjust_uptake factor calculated
    % previously (which is simply Per_conf if Uptake experiments were
    % confluent.

    Drate_h_inf_inf = (Drate_zero_inf_inf)*alpha*(c^2*(3-exp(1-(Dens_med*v*h))-
((Dens_med*v*h)/c)*(2+log(c/(Dens_med*v*h))))+exp(1-(Dens_med*v*h))-4*exp(1-((Dens_med*v*h)/2)-
(f/2))+(3+f-(Dens_med*v*h))*exp(1-f));

        if c <= (Dens_med*v*h)
            Drate_zero_inf_inf = 0.288*A*Per_conf*Mean_beta_eng;
            Drate_h_inf_inf = (Drate_zero_inf_inf)*alpha*(exp(1-(Dens_med*v*h))-4*exp(1-
((Dens_med*v*h)/2)-(f/2))+(3+f-(Dens_med*v*h))*exp(1-f));
        end

    Drate_zero_h_inf = Drate_zero_inf_inf - Drate_h_inf_inf;

    % Step 2 is to calculate
    % Drate(Cell_slab_thick,0.04,inf) = Drate(Cell_slab_thick,inf,inf) -
    %                                   Drate(Cell_slab_thick+0.04,inf,inf)

    Drate_2delta_inf_inf = (Drate_zero_inf_inf)*alpha*(c^2*(3-exp(1-
(Dens_med*v*Cell_slab_thick))-
((Dens_med*v*Cell_slab_thick)/c)*(2+log(c/(Dens_med*v*Cell_slab_thick))))+exp(1-
```

```
(Dens_med*v*Cell_slab_thick))-4*exp(1-((Dens_med*v*Cell_slab_thick)/2)-(f/2))+(3+f-
(Dens_med*v*Cell_slab_thick))*exp(1-f));
    Drate_2delta_h_inf_inf = (Drate_zero_inf_inf)*alpha*(c^2*(3-exp(1-
(Dens_med*v*(Cell_slab_thick+h)))-
((Dens_med*v*(Cell_slab_thick+h))/c)*(2+log(c/(Dens_med*v*(Cell_slab_thick+h)))))+exp(1-
(Dens_med*v*(Cell_slab_thick+h)))-4*exp(1-((Dens_med*v*(Cell_slab_thick+h))/2)-(f/2))+(3+f-
(Dens_med*v*(Cell_slab_thick+h)))*exp(1-f));

        if c <= (Dens_med*v*Cell_slab_thick)
            Drate_2delta_inf_inf = (Drate_zero_inf_inf)*alpha*(exp(1-
(Dens_med*v*Cell_slab_thick))-4*exp(1-((Dens_med*v*Cell_slab_thick)/2)-(f/2))+(3+f-
(Dens_med*v*Cell_slab_thick))*exp(1-f));
            Drate_2delta_h_inf_inf = (Drate_zero_inf_inf)*alpha*(exp(1-
(Dens_med*v*(Cell_slab_thick+h)))-4*exp(1-((Dens_med*v*(Cell_slab_thick+h))/2)-(f/2))+(3+f-
(Dens_med*v*(Cell_slab_thick+h)))*exp(1-f));
        end

    Drate_2delta_h_inf = Drate_2delta_inf_inf - Drate_2delta_h_inf_inf;

    % Since the thickness of the cells is so small (typically ~2%), we
    % expect that the difference between of dose rate to the cells x = o
    % and x = 2delta to be nearly equal.  As such, for performance, rather
    % than integrate as per Eq. (8) above, we will simply calculate the
    % average Drate by adding Drate_zero_h_inf and Drate_2delta_h_inf and
    % dividing by 2 [Eq. (7)].

    Drate_uptake_avg(i) = (Drate_zero_h_inf + Drate_2delta_h_inf)/2;

    % Now we need to take into account the variability / uncertainty in the
    % slab thickness.  This obviously, only effects the value calculated at
    % 2delta.  So we will set up a couple maximum and minimum variables.
    % This will enable to have the full breadth of possible dose rate
    % calculations by appropriately optimizing the values from the
    % experimental parameters for each scenario.

    % Maximum:

    % Maximize activity for uptake
```

```
    Drate_zero_inf_inf_max = 0.288*A*(Per_conf+Err_per_conf)*Mean_beta_eng;
    % Maximize dose rate by slab being of minimal thickness
    Drate_uptake_x_2delta_max_1=(Drate_zero_inf_inf_max)*alpha*(c^2*(3-exp(1-
(Dens_med*v*Cell_slab_thick_min))-
((Dens_med*v*Cell_slab_thick_min)/c)*(2+log(c/(Dens_med*v*Cell_slab_thick_min))))+exp(1-
(Dens_med*v*Cell_slab_thick_min))-4*exp(1-((Dens_med*v*Cell_slab_thick_min)/2)-(f/2))+(3+f-
(Dens_med*v*Cell_slab_thick_min))*exp(1-f));
    Drate_uptake_x_2delta_max_2=(Drate_zero_inf_inf_max)*alpha*(c^2*(3-exp(1-
(Dens_med*v*(Cell_slab_thick_min+h)))-
((Dens_med*v*(Cell_slab_thick_min+h))/c)*(2+log(c/(Dens_med*v*(Cell_slab_thick_min+h)))))+exp(1
-(Dens_med*v*(Cell_slab_thick_min+h)))-4*exp(1-((Dens_med*v*(Cell_slab_thick_min+h))/2)-
(f/2))+(3+f-(Dens_med*v*(Cell_slab_thick_min+h)))*exp(1-f));
    % Drate_uptake_x_2delta_max_2 is the correction for thickness, h

        if c <= (Dens_med*v*Cell_slab_thick_min)
            Drate_uptake_x_2delta_max_1=(Drate_zero_inf_inf_max)*alpha*(exp(1-
(Dens_med*v*Cell_slab_thick_min))-4*exp(1-((Dens_med*v*Cell_slab_thick_min)/2)-(f/2))+(3+f-
(Dens_med*v*Cell_slab_thick_min))*exp(1-f));
            Drate_uptake_x_2delta_max_2=(Drate_zero_inf_inf_max)*alpha*(exp(1-
(Dens_med*v*(Cell_slab_thick_min+h)))-4*exp(1-((Dens_med*v*(Cell_slab_thick_min+h))/2)-
(f/2))+(3+f-(Dens_med*v*(Cell_slab_thick_min+h)))*exp(1-f));
        end


    Drate_uptake_x_2delta_max = Drate_uptake_x_2delta_max_1 - Drate_uptake_x_2delta_max_2;

    % Minimum:

    % Minimize activity for uptake
    Drate_zero_inf_inf_min = 0.288*A*(Per_conf-Err_per_conf)*Mean_beta_eng;
    % Minimize dose rate by slab being of maximal thickness
    Drate_uptake_x_2delta_min_1=(Drate_zero_inf_inf_min)*alpha*(c^2*(3-exp(1-
(Dens_med*v*Cell_slab_thick_max))-
((Dens_med*v*Cell_slab_thick_max)/c)*(2+log(c/(Dens_med*v*Cell_slab_thick_max))))+exp(1-
(Dens_med*v*Cell_slab_thick_max))-4*exp(1-((Dens_med*v*Cell_slab_thick_max)/2)-(f/2))+(3+f-
(Dens_med*v*Cell_slab_thick_max))*exp(1-f));
    Drate_uptake_x_2delta_min_2=(Drate_zero_inf_inf_min)*alpha*(c^2*(3-exp(1-
(Dens_med*v*(Cell_slab_thick_max+h)))-
```

```
((Dens_med*v*(Cell_slab_thick_max+h))/c)*(2+log(c/(Dens_med*v*(Cell_slab_thick_max+h)))))+exp(1
-(Dens_med*v*(Cell_slab_thick_max+h)))-4*exp(1-((Dens_med*v*(Cell_slab_thick_max+h))/2)-
(f/2))+(3+f-(Dens_med*v*(Cell_slab_thick_max+h)))*exp(1-f));
    % Drate_uptake_x_2delta_min_2 is the correction for thickness, h

        if c <= (Dens_med*v*Cell_slab_thick_max)
            Drate_uptake_x_2delta_min_1=(Drate_zero_inf_inf_min)*alpha*(exp(1-
(Dens_med*v*Cell_slab_thick_max))-4*exp(1-((Dens_med*v*Cell_slab_thick_max)/2)-(f/2))+(3+f-
(Dens_med*v*Cell_slab_thick_max))*exp(1-f));
            Drate_uptake_x_2delta_min_2=(Drate_zero_inf_inf_min)*alpha*(exp(1-
(Dens_med*v*(Cell_slab_thick_max+h)))-4*exp(1-((Dens_med*v*(Cell_slab_thick_max+h))/2)-
(f/2))+(3+f-(Dens_med*v*(Cell_slab_thick_max+h)))*exp(1-f));
        end


    Drate_uptake_x_2delta_min = Drate_uptake_x_2delta_min_1 - Drate_uptake_x_2delta_min_2;

    % Therefore, 2Delta Plus error
    Drate_uptake_x_2delta_plus_err(i) = Drate_uptake_x_2delta_max - Drate_2delta_h_inf;

    % and 2Delta Minus error
    Drate_uptake_x_2delta_minus_err(i) = Drate_2delta_h_inf - Drate_uptake_x_2delta_min;

    % Now, lets see if the plus and minus error are in fact equal to one
    % significant digit.  MATLAB does not have a trivial way to accomplish
    % this, so the following is the work around:

    % First, define a string for the plus error output:
    str_plus=sprintf('%.0d',Drate_uptake_x_2delta_plus_err(i));
    % Second, define a string for the plus error output:
    str_minus=sprintf('%.0d',Drate_uptake_x_2delta_minus_err(i));
    % The '.0d' rounds the values to the nearest whole integer in e -
    % notation. For example, 2.13e-005 becomes 2e-005.

    % Convert strings to double precision numbers:
    str_plus_num = str2double(str_plus);
    str_minus_num = str2double(str_minus);
```

```
    % Now, let's create a variable that will compare the first value in
    % str_plus and str_minus and see if they are the same:

    str_error_test=strncmp(str_plus,str_minus,1);
    % If this test is true, we only need to print one of the uncertainty
    % values (either the plus or the minus) as they are equal to one
    % significant digit.  If this is false, we will print out both values.

    % Now, lets print the result!

    fprintf(1,'The average dose rate to the %s cells at \n',Cell_name)
    fprintf(1,'the initiation of the uptake phase is:\n** %d', Drate_uptake_avg(i))

        if (str_error_test == 1)
            fprintf(1,' +/- %.0d', str_plus_num)
            fprintf(1,' Gy/h ** [1]\n\n')
        elseif (str_error_test == 0)
            fprintf(1,' +/- (%.0d/%.0d)',str_plus_num,str_minus_num)
            fprintf(1,' Gy/h ** [1]\n\n')
        end

    fprintf(1,'~~~~~~~\n\n')
end

% ========================================================================= %

%~~~~~~~~~~~~~~~~~~~~~~~~~~~~~~%
%~Calculate Dose Rate in Slab~%
%~~~~~~~~~~~~~~~~~~~~~~~~~~~~~~%

% For our methodology employed here, see "Brief Introduction" above.
% We will create two different activity distribution models (aka paradigms)
% and calculate the dose rate at 5 different locals within the slab of
% cells.  In general, the slab is located infinite in the y-, z- extents
% and has a thickness of 2delta along the x axis.  The bottom of the slab
% lies along x=0.

% 1)  Take the activity, Aconc, and distribute it equally in two infinite
```

```
% planes (i.e. 0.5*Asurf each) located at positions x=(0.5)delta and
% x=(1.5)delta.  Calculate the  dose rate (Drate) at the edges of the slab
% (x=0 and x=2delta) and in the centre (x=delta)
%
% 2)  Take the activity, Aconc, and distribute it equally in three infinite
% planes (i.e. (1/3)Aconc each) located at positions x=0,delta, and
% 2delta).  Calculate the Drate at x=(0.5)delta and x=(1.5)delta.
%
% The average dose rate to the slab will be derived from the values
% calculated at the various locations in paradigms 1) and 2).

% If all activity were isolated to a single plane, the surface activity of
% the plane source would be:
%
% Asurf = (A*%Uptake*Conf_adjust)/(Size of flask*%Confluence)
%
% Therefore, for paradigm 1, Atot = 0.5Asurf + 0.5Asurf
%        and for paradigm 2, Atot = (1/3)Asurf + (1/3)Asurf + (1/3)Asurf

% The expression for dose rate from an infinite disk at distance x from
% source is given in Eq. (9) and provided in Ref. [2] and [3].  Note that
% we have used scalar .* and ./ here so as to ensure a more object-oriented
% design. Remember that the activity in the infinite plane is only the
% appropriate fraction of the percentage of uptake.

Drate_x=@(x)((A.*Percent_up.*Conf_adjust_uptake)/(S_flask*Per_conf)).*0.288.*Mean_beta_eng.*v.*
alpha.*(c+(c.*log(c./(Dens_med.*v.*x)))-(c.*exp(1-((Dens_med.*v.*x)./c)))+exp(1-
(Dens_med.*v.*x))-2.*exp(1-((Dens_med.*v.*x)./2)-(f./2))+exp(1-f));

% Again, we need the appropriate 'if' statements for the conditions on an
% infinite thin plan VW kernel.  If c>=p*v*x, the quantity in the square
% brackets of Eq. [9] becomes 0 and the DPK changes to:

Drate_x_c_cond=@(x)(A.*Percent_up.*Conf_adjust_uptake/(S_flask*Per_conf)).*0.288.*Mean_beta_eng
.*v.*alpha.*(exp(1-(Dens_med.*v.*x))-2.*exp(1-((Dens_med.*v.*x)./2)-(f./2))+exp(1-f));

% Checks on this condition will be done on each evaluation below.
```

```
% Paradigm 1):

% Bottom of the slab:
Drate_bottom = (0.5*Drate_x((0.5)*Cell_slab_half_thick)) +
(0.5*Drate_x((1.5)*Cell_slab_half_thick));
    if (c<=(Dens_med*v*((0.5)*Cell_slab_half_thick)))
        % the smallest condition
        Drate_bottom = (0.5*Drate_x_c_cond((0.5)*Cell_slab_half_thick)) +
(0.5*Drate_x_c_cond((1.5)*Cell_slab_half_thick));
    else
        if (f<=(Dens_med*v*((0.5)*Cell_slab_half_thick)))
            % the smallest condition
            fprintf(1,'The dose rate is 0 Gy/h. No need to go any further...\n')
        end
    end

% Top of the slab (by symmetry):
Drate_top = Drate_bottom;

% Centre of the slab:
Drate_centre = 2*(0.5*Drate_x((0.5)*Cell_slab_half_thick));
    if (c<=(Dens_med*v*((0.5)*Cell_slab_half_thick)))
        Drate_centre = 2*(0.5*Drate_x_c_cond((0.5)*Cell_slab_half_thick));
    else
        if (f<=(Dens_med*v*((1/3)*Cell_slab_half_thick)))
            fprintf(1,'The dose rate is 0 Gy/h. No need to go any further...\n')
        end
    end

% Couple notes to remember is that delta = Cell_slab_half_thick and we are
% multiplying by 0.5 as each infinite plane of activity contains half the
% overall activity taken up by the cells.

% Paradigm 2):

% Where x=(0.5)delta
Drate_delta_one_half =
2*((1/3)*Drate_x((0.5)*Cell_slab_half_thick))+((1/3)*Drate_x((1.5)*Cell_slab_half_thick));
```

```
    if (c<=(Dens_med*v*((0.5)*Cell_slab_half_thick)))
        % the smallest condition
        Drate_one_third =
2*((1/3)*Drate_x_c_cond((0.5)*Cell_slab_half_thick))+((1/3)*Drate_x_c_cond((1.5)*Cell_slab_half
_thick));
    else
        if (f<=(Dens_med*v*((0.5)*Cell_slab_half_thick)))
            % the smallest condition
            fprintf(1,'The dose rate is 0 Gy/h. No need to go any further...\n')
        end
    end

% Where x=(1.5)delta, by symmetry
Drate_delta_one_and_one_half = Drate_delta_one_half;

% Total dose rate in the slab is:

Drate_slab_avg(i) =
(Drate_bottom+Drate_top+Drate_centre+Drate_delta_one_half+Drate_delta_one_and_one_half)/5;

    % Now, we need to determine the +/- uncertainties.  Maximum Drate (i.e.
    % +) occurs when % Uptake is highest, slab thickness is smallest, and
    % confluence is smallest and vice verse for the minimum dose rate.

    % Maximum Drate:

Drate_x_max=@(x)((A.*(Percent_up+Err_percent_up).*(Conf_adjust_uptake+Err_conf_adjust_uptake))/
(S_flask*(Per_conf-
Err_per_conf))).*0.288.*Mean_beta_eng.*v.*alpha.*(c+(c.*log(c./(Dens_med.*v.*x)))-(c.*exp(1-
((Dens_med.*v.*x)./c)))+exp(1-(Dens_med.*v.*x))-2.*exp(1-((Dens_med.*v.*x)./2)-(f./2))+exp(1-
f));
    %With c condition...

Drate_x_max_c_cond=@(x)((A.*(Percent_up+Err_percent_up).*(Conf_adjust_uptake+Err_conf_adjust_up
take))/(S_flask*(Per_conf-Err_per_conf))).*0.288.*Mean_beta_eng.*v.*alpha.*(exp(1-
(Dens_med.*v.*x))-2.*exp(1-((Dens_med.*v.*x)./2)-(f./2))+exp(1-f));

    % Paradigm 1):
```

```
    % Bottom of the slab:
    Drate_bottom_max = (0.5*Drate_x_max((0.5)*(Cell_slab_half_thick_min))) +
(0.5*Drate_x_max((1.5)*(Cell_slab_half_thick_min)));
        if (c<=(Dens_med*v*((0.5)*Cell_slab_half_thick_min)))
            Drate_bottom_max = (0.5*Drate_x_max_c_cond((0.5)*(Cell_slab_half_thick_min))) +
(0.5*Drate_x_max_c_cond((1.5)*(Cell_slab_half_thick_min)));
        else
            if (f<=(Dens_med*v*((0.5)*Cell_slab_half_thick_min)))
                fprintf(1,'The dose rate is 0 Gy/h. No need to go any further...\n')
            end
        end

    % Top of the slab (by symmetry):
    Drate_top_max = Drate_bottom_max;

    % Centre of the slab:
    Drate_centre_max = 2*(0.5*Drate_x_max((0.5)*(Cell_slab_half_thick_min)));
        if (c<=(Dens_med*v*((0.5)*Cell_slab_half_thick_min)))
            Drate_centre_max = 2*(0.5*Drate_x_max_c_cond((0.5)*(Cell_slab_half_thick_min)));
        else
            if (f<=(Dens_med*v*((0.5)*Cell_slab_half_thick_min)))
                frintf(1,'The dose rate is 0 Gy/h. No need to go any further...\n')
            end
        end

    % Paradigm 2):

    % Where x=(0.5)delta
    Drate_delta_one_half_max =
2*((1/3)*Drate_x_max((0.5)*(Cell_slab_half_thick_min)))+((1/3)*Drate_x_max((1.5)*(Cell_slab_hal
f_thick_min)));
        if (c<=(Dens_med*v*((1/3)*Cell_slab_half_thick)))
            Drate_delta_one_half_max =
2*((1/3)*Drate_x_max_c_cond((0.5)*(Cell_slab_half_thick_min)))+((1/3)*Drate_x_max_c_cond((1.5)*
(Cell_slab_half_thick_min)));
        else
            if (f<=(Dens_med*v*((1/3)*Cell_slab_half_thick)))
```

```
                fprintf(1,'The dose rate is 0 Gy/h. No need to go any further...\n')
            end
        end

    % Where x=(1.5)delta, by symmetry
    Drate_delta_one_and_one_half_max = Drate_delta_one_half_max;

    % Total dose rate in the slab is:

    Drate_slab_avg_max(i) =
(Drate_bottom_max+Drate_top_max+Drate_centre_max+Drate_delta_one_half_max+Drate_delta_one_and_o
ne_half_max)/5;

    % Minimum Drate:

    Drate_x_min=@(x)((A.*(Percent_up-Err_percent_up).*(Conf_adjust_uptake-
Err_conf_adjust_uptake))/(S_flask*(Per_conf+Err_per_conf))).*0.288.*Mean_beta_eng.*v.*alpha.*(c
+(c.*log(c./(Dens_med.*v.*x)))-(c.*exp(1-((Dens_med.*v.*x)./c)))+exp(1-(Dens_med.*v.*x))-
2.*exp(1-((Dens_med.*v.*x)./2)-(f./2))+exp(1-f));
    % With c condition...
    Drate_x_min_c_cond=@(x)(A.*(Percent_up-Err_percent_up).*(Conf_adjust_uptake-
Err_conf_adjust_uptake)/(S_flask*(Per_conf+Err_per_conf))).*0.288.*Mean_beta_eng.*v.*alpha.*(ex
p(1-(Dens_med.*v.*x))-2.*exp(1-((Dens_med.*v.*x)./2)-(f./2))+exp(1-f));

    % Paradigm 1):

    % Bottom of the slab:
    Drate_bottom_min = (0.5*Drate_x_min((0.5)*(Cell_slab_half_thick_max))) +
(0.5*Drate_x_min((1.5)*(Cell_slab_half_thick_max)));
        if (c<=(Dens_med*v*((0.5)*Cell_slab_half_thick_max)))
            Drate_bottom_min = (0.5*Drate_x_min_c_cond((0.5)*(Cell_slab_half_thick_max))) +
(0.5*Drate_x_min_c_cond((1.5)*(Cell_slab_half_thick_max)));
        else
            if (f<=(Dens_med*v*((0.5)*Cell_slab_half_thick_max)))
                fprintf(1,'The dose rate is 0 Gy/h. No need to go any further...\n')
            end
        end
```

```
    % Top of the slab (by symmetry):
    Drate_top_min = Drate_bottom_min;

    % Centre of the slab:
    Drate_centre_min = 2*(0.5*Drate_x_min((0.5)*(Cell_slab_half_thick_max)));
        if (c<=(Dens_med*v*((0.5)*Cell_slab_half_thick_max)))
            Drate_centre_min = 2*(0.5*Drate_x_min_c_cond((0.5)*(Cell_slab_half_thick_max)));
        else
            if (f<=(Dens_med*v*((0.5)*Cell_slab_half_thick_max)))
                fprintf(1,'The dose rate is 0 Gy/h. No need to go any further...\n')
            end
        end

    % Paradigm 2):

    % Where x=(0.5)delta
    Drate_delta_one_half_min =
2*((1/3)*Drate_x_min((0.5)*(Cell_slab_half_thick_max)))+((1/3)*Drate_x_min((1.5)*(Cell_slab_hal
f_thick_max)));
        if (c<=(Dens_med*v*((0.5)*Cell_slab_half_thick_max)))
            Drate_one_third_min =
2*((1/3)*Drate_x_min_c_cond((0.5)*(Cell_slab_half_thick_max)))+((1/3)*Drate_x_min_c_cond((1.5)*
(Cell_slab_half_thick_max)));
        else
            if (f<=(Dens_med*v*((0.5)*Cell_slab_half_thick_max)))
                fprintf(1,'The dose rate is 0 Gy/h. No need to go any further...\n')
            end
        end

    % Where x=(1.5)delta, by symmetry
    Drate_delta_one_and_one_half_min = Drate_delta_one_half_min;

    % Total dose rate in the slab is:

    Drate_slab_avg_min(i) =
(Drate_bottom_min+Drate_top_min+Drate_centre_min+Drate_delta_one_half_min+Drate_delta_one_and_o
ne_half_min)/5;
```

```
% Therefore the +/- errors are:

Drate_slab_avg_plus_err(i) = Drate_slab_avg_max(i) - Drate_slab_avg(i);
Drate_slab_avg_minus_err(i) = Drate_slab_avg(i) - Drate_slab_avg_min(i);

    % Now, lets see if the plus and minus error are in fact equal to one
    % significant digit.  MATLAB does not have a trivial way to accomplish
    % this, so the following is the work around:

    % First, define a string for the plus error output:
    str_plus=sprintf('%.0d',Drate_slab_avg_plus_err(i));
    % Second, define a string for the plus error output:
    str_minus=sprintf('%.0d',Drate_slab_avg_minus_err(i));
    % The '.0d' rounds the values to the nearest whole integer in e -
    % notation. For example, 2.13e-005 becomes 2e-005.

    % Convert strings to double precision numbers:
    str_plus_num = str2double(str_plus);
    str_minus_num = str2double(str_minus);

    % Now, let's create a variable that will compare the first value in
    % str_plus and str_minus and see if they are the same:

    str_error_test=strncmp(str_plus,str_minus,1);
    % If this test is true, we only need to print on of the uncertainty
    % values (either the plus or the minus) as they equal to the number of
    % significant digits allotted for uncertainty values.  If this is
    % false, we will print out both values.

% Now, lets print the result!

fprintf(1,'The average dose rate to the slab of %s cells\n',Cell_name)
fprintf(1,'after uptake of the radiopharmaceutical is:\n** %d', Drate_slab_avg(i))

    if (str_error_test == 1)
        fprintf(1,' +/- %.0d', str_plus_num)
        fprintf(1,' Gy/h ** [2]\n\n')
    elseif (str_error_test == 0)
```

```
        fprintf(1,' +/- (%.0d/%.0d)',str_plus_num,str_minus_num)
        fprintf(1,' Gy/h ** [2]\n\n')
    end

fprintf(1,'~~~~~~~\n\n')

% ========================================================================= %

%~~~~~~~~~~~~~~~~~~~~~~~~~~~~~~~~~~~~~~~~~~~~~%
%~Calculate the Total Dose to the Cells~%
%~~~~~~~~~~~~~~~~~~~~~~~~~~~~~~~~~~~~~~~~~~~~~%

% Because there is believed to be a linear uptake of the pharmaceutical
% over the 2 hour time frame coupled with negligible egress of the activity
% following uptake (<1%), we can use a simple Trapezoid integration rule of
% the dose rate over the 3 hour time window to determine the total dose to
% the cells.  Essentially, we are finding the "area under the curve" of a
% Dose rate vs. time plot to get the total dose.

Dose(i) = ((Drate_uptake_avg(i)+Drate_slab_avg(i))/2)*(2)+(Drate_slab_avg(i))*(1);

    % Now calculate the uncertainties.

    Dose_err_plus(i) =
(sqrt(((Drate_uptake_x_2delta_plus_err(i))^2+(Drate_slab_avg_plus_err(i))^2))/2)*(2)+Drate_slab
_avg_plus_err(i)*(1);
    Dose_err_minus(i) =
(sqrt(((Drate_uptake_x_2delta_minus_err(i))^2+(Drate_slab_avg_minus_err(i))^2))/2)*(2)+Drate_sl
ab_avg_minus_err(i)*(1);

    % Now, lets see if the plus and minus error are in fact equal to one
    % significant digit.  MATLAB does not have a trivial way to accomplish
    % this, so the following is the work around:

    % First, define a string for the plus error output:
    str_plus=sprintf('%.0d',Dose_err_plus(i));
    % Second, define a string for the plus error output:
    str_minus=sprintf('%.0d',Dose_err_minus(i));
```

```
    % See MATLAB Help 'sprintf' for function parameter explanation. The
    % '.0d' rounds the values to the nearest whole integer in e - notation.
    % For example, 2.13e-005 becomes 2e-005.

    % Convert strings to double precision numbers:
    str_plus_num = str2double(str_plus);
    str_minus_num = str2double(str_minus);

    % Now, let's create a variable that will compare the first value in
    % str_plus and str_minus and see if they are the same:

    str_error_test=strncmp(str_plus,str_minus,1);
    % If this test is true, we only need to print on of the uncertainty
    % values (either the plus or the minus) as they equal to the number of
    % significant digits allotted for uncertainty values.  If this is
    % false, we will print out both values.

% Now, lets print the result!

fprintf(1,'Therefore, the dose to the %s cells after\n',Cell_name)
fprintf(1,'treatment with %.1d MBq/ml of radiopharmaceutical with\n',A)
fprintf(1,'%.0d hour(s)for uptake and %.0d hour(s) for accumulation
is:\n\n',Time_up,Time_accum)

    if (str_error_test == 1)
        fprintf(1,'**********************************\n')
        fprintf(1,'*** %d',Dose(i))
        fprintf(1,' +/- %.0d', str_plus_num)
        fprintf(1,' Gy ***\n')
        fprintf(1,'**********************************\n')
    elseif (str_error_test == 0)
        fprintf(1,'******************************************\n')
        fprintf(1,'*** %d',Dose(i))
        fprintf(1,' +/- (%.0d/%.0d)',str_plus_num,str_minus_num)
        fprintf(1,' Gy ***\n')
        fprintf(1,'******************************************\n')
    end
```

```
fprintf(1,'_____________________________________________________\n')
fprintf(1,'=====================================================\n')
end

else if Large_act_conc == 0 % The user only enters a single value
i=1;
Activity(i) = Small_act_conc;
A = Activity(i);
fprintf(1,'For an activity concentration of: %4.2f MBq/ml\n',A)
fprintf(1,'~~~~~~~\n\n')

% ========================================================================= %
%~~~~~~~~~~~~~~~~~~~~~~~~~~~~~~~~~%
%~Calculate Dose Rate for Uptake~%
%~~~~~~~~~~~~~~~~~~~~~~~~~~~~~~~~~%

% First, if the f <= p*v*x ...
if f <= (Dens_med*v*Cell_slab_thick_min)
    fprintf(1,'The dose rate is 0 Gy/h. No need to go any further...\n')
else % Second, condition on c to alter value of the square brackets

    Drate_zero_inf_inf = 0.288*A*Per_conf*Mean_beta_eng;
    % Remember, we take into account the confluence adjustment as activity
    % not covering cells does not contribute to the absorbed dose.  This is
    % simply the percentage confluence during the Uptake phase.  During the
    % Accumulation phase, this is the Conf_adjust_uptake factor calculated
    % previously (which is simply Per_conf if Uptake experiments were
    % confluent.

    Drate_h_inf_inf = (Drate_zero_inf_inf)*alpha*(c^2*(3-exp(1-(Dens_med*v*h))-
((Dens_med*v*h)/c)*(2+log(c/(Dens_med*v*h))))+exp(1-(Dens_med*v*h))-4*exp(1-((Dens_med*v*h)/2)-
(f/2))+(3+f-(Dens_med*v*h))*exp(1-f));

        if c <= (Dens_med*v*h)
            Drate_zero_inf_inf = 0.288*A*Per_conf*Mean_beta_eng;
            Drate_h_inf_inf = (Drate_zero_inf_inf)*alpha*(exp(1-(Dens_med*v*h))-4*exp(1-
((Dens_med*v*h)/2)-(f/2))+(3+f-(Dens_med*v*h))*exp(1-f));
        end
```

```
    Drate_zero_h_inf = Drate_zero_inf_inf - Drate_h_inf_inf;

    % Step 2 is to calculate
    % Drate(Cell_slab_thick,0.04,inf) = Drate(Cell_slab_thick,inf,inf) -
    %                                   Drate(Cell_slab_thick+0.04,inf,inf)

    Drate_2delta_inf_inf = (Drate_zero_inf_inf)*alpha*(c^2*(3-exp(1-
(Dens_med*v*Cell_slab_thick))-
((Dens_med*v*Cell_slab_thick)/c)*(2+log(c/(Dens_med*v*Cell_slab_thick))))+exp(1-
(Dens_med*v*Cell_slab_thick))-4*exp(1-((Dens_med*v*Cell_slab_thick)/2)-(f/2))+(3+f-
(Dens_med*v*Cell_slab_thick))*exp(1-f));
    Drate_2delta_h_inf_inf = (Drate_zero_inf_inf)*alpha*(c^2*(3-exp(1-
(Dens_med*v*(Cell_slab_thick+h)))-
((Dens_med*v*(Cell_slab_thick+h))/c)*(2+log(c/(Dens_med*v*(Cell_slab_thick+h)))))+exp(1-
(Dens_med*v*(Cell_slab_thick+h)))-4*exp(1-((Dens_med*v*(Cell_slab_thick+h))/2)-(f/2))+(3+f-
(Dens_med*v*(Cell_slab_thick+h)))*exp(1-f));

        if c <= (Dens_med*v*Cell_slab_thick)
            Drate_2delta_inf_inf = (Drate_zero_inf_inf)*alpha*(exp(1-
(Dens_med*v*Cell_slab_thick))-4*exp(1-((Dens_med*v*Cell_slab_thick)/2)-(f/2))+(3+f-
(Dens_med*v*Cell_slab_thick))*exp(1-f));
            Drate_2delta_h_inf_inf = (Drate_zero_inf_inf)*alpha*(exp(1-
(Dens_med*v*(Cell_slab_thick+h)))-4*exp(1-((Dens_med*v*(Cell_slab_thick+h))/2)-(f/2))+(3+f-
(Dens_med*v*(Cell_slab_thick+h)))*exp(1-f));
        end

    Drate_2delta_h_inf = Drate_2delta_inf_inf - Drate_2delta_h_inf_inf;

    Drate_uptake_avg(i) = (Drate_zero_h_inf + Drate_2delta_h_inf)/2;

    % Now we need to take into account the variability / uncertainty in the
    % slab thickness.  This obviously, only effects the value calculated at
    % 2delta.  So we will set up a couple maximum and minimum variables.
    % This will enable to have the full breadth of possible dose rate
    % calculations by appropriately optimizing the values from the
    % experimental parameters for each scenario.
```

```
    % Maximize activity for uptake
    Drate_zero_inf_inf_max = 0.288*A*(Per_conf+Err_per_conf)*Mean_beta_eng;

    % Maximize dose rate by slab being of minimal thickness
    Drate_uptake_x_2delta_max_1=(Drate_zero_inf_inf_max)*alpha*(c^2*(3-exp(1-
(Dens_med*v*Cell_slab_thick_min))-
((Dens_med*v*Cell_slab_thick_min)/c)*(2+log(c/(Dens_med*v*Cell_slab_thick_min))))+exp(1-
(Dens_med*v*Cell_slab_thick_min))-4*exp(1-((Dens_med*v*Cell_slab_thick_min)/2)-(f/2))+(3+f-
(Dens_med*v*Cell_slab_thick_min))*exp(1-f));
    Drate_uptake_x_2delta_max_2=(Drate_zero_inf_inf_max)*alpha*(c^2*(3-exp(1-
(Dens_med*v*(Cell_slab_thick_min+h)))-
((Dens_med*v*(Cell_slab_thick_min+h))/c)*(2+log(c/(Dens_med*v*(Cell_slab_thick_min+h)))))+exp(1
-(Dens_med*v*(Cell_slab_thick_min+h)))-4*exp(1-((Dens_med*v*(Cell_slab_thick_min+h))/2)-
(f/2))+(3+f-(Dens_med*v*(Cell_slab_thick_min+h)))*exp(1-f));
    % Drate_uptake_x_2delta_max_2 is the correction for thickness, h

        if c <= (Dens_med*v*Cell_slab_thick_min)
            Drate_uptake_x_2delta_max_1=(Drate_zero_inf_inf_max)*alpha*(exp(1-
(Dens_med*v*Cell_slab_thick_min))-4*exp(1-((Dens_med*v*Cell_slab_thick_min)/2)-(f/2))+(3+f-
(Dens_med*v*Cell_slab_thick_min))*exp(1-f));
            Drate_uptake_x_2delta_max_2=(Drate_zero_inf_inf_max)*alpha*(exp(1-
(Dens_med*v*(Cell_slab_thick_min+h)))-4*exp(1-((Dens_med*v*(Cell_slab_thick_min+h))/2)-
(f/2))+(3+f-(Dens_med*v*(Cell_slab_thick_min+h)))*exp(1-f));
        end


    Drate_uptake_x_2delta_max = Drate_uptake_x_2delta_max_1 - Drate_uptake_x_2delta_max_2;

    % Minimize activity for uptake
    Drate_zero_inf_inf_min = 0.288*A*(Per_conf-Err_per_conf)*Mean_beta_eng;

    % Minimize dose rate by slab being of maximal thickness
    Drate_uptake_x_2delta_min_1=(Drate_zero_inf_inf_min)*alpha*(c^2*(3-exp(1-
(Dens_med*v*Cell_slab_thick_max))-
((Dens_med*v*Cell_slab_thick_max)/c)*(2+log(c/(Dens_med*v*Cell_slab_thick_max))))+exp(1-
(Dens_med*v*Cell_slab_thick_max))-4*exp(1-((Dens_med*v*Cell_slab_thick_max)/2)-(f/2))+(3+f-
(Dens_med*v*Cell_slab_thick_max))*exp(1-f));
```

```
    Drate_uptake_x_2delta_min_2=(Drate_zero_inf_inf_min)*alpha*(c^2*(3-exp(1-
(Dens_med*v*(Cell_slab_thick_max+h)))-
((Dens_med*v*(Cell_slab_thick_max+h))/c)*(2+log(c/(Dens_med*v*(Cell_slab_thick_max+h)))))+exp(1
-(Dens_med*v*(Cell_slab_thick_max+h)))-4*exp(1-((Dens_med*v*(Cell_slab_thick_max+h))/2)-
(f/2))+(3+f-(Dens_med*v*(Cell_slab_thick_max+h)))*exp(1-f));
    % Drate_uptake_x_2delta_min_2 is the correction for thickness, h

        if c <= (Dens_med*v*Cell_slab_thick_max)
            Drate_uptake_x_2delta_min_1=(Drate_zero_inf_inf_min)*alpha*(exp(1-
(Dens_med*v*Cell_slab_thick_max))-4*exp(1-((Dens_med*v*Cell_slab_thick_max)/2)-(f/2))+(3+f-
(Dens_med*v*Cell_slab_thick_max))*exp(1-f));
            Drate_uptake_x_2delta_min_2=(Drate_zero_inf_inf_min)*alpha*(exp(1-
(Dens_med*v*(Cell_slab_thick_max+h)))-4*exp(1-((Dens_med*v*(Cell_slab_thick_max+h))/2)-
(f/2))+(3+f-(Dens_med*v*(Cell_slab_thick_max+h)))*exp(1-f));
        end


    Drate_uptake_x_2delta_min = Drate_uptake_x_2delta_min_1 - Drate_uptake_x_2delta_min_2;

    % Therefore, 2Delta Plus error
    Drate_uptake_x_2delta_plus_err(i) = Drate_uptake_x_2delta_max - Drate_2delta_h_inf;

    % and 2Delta Minus error
    Drate_uptake_x_2delta_minus_err(i) = Drate_2delta_h_inf - Drate_uptake_x_2delta_min;

    % Now, lets see if the plus and minus error are in fact equal to one
    % significant digit.  MATLAB does not have a trivial way to accomplish
    % this, so the following is the work around:

    % First, define a string for the plus error output:
    str_plus=sprintf('%.0d',Drate_uptake_x_2delta_plus_err(i));
    % Second, define a string for the plus error output:
    str_minus=sprintf('%.0d',Drate_uptake_x_2delta_minus_err(i));
    % The '.0d' rounds the values to the nearest whole integer in e -
    % notation. For example, 2.13e-005 becomes 2e-005.

    % Convert strings to double precision numbers:
    str_plus_num = str2double(str_plus);
```

```
    str_minus_num = str2double(str_minus);

    % Now, let's create a variable that will compare the first value in
    % str_plus and str_minus and see if they are the same:

    str_error_test=strncmp(str_plus,str_minus,1);
    % If this test is true, we only need to print one of the uncertainty
    % values (either the plus or the minus) as they are equal to one
    % significant digit.  If this is false, we will print out both values.

    % Now, lets print the result!

    fprintf(1,'The average dose rate to the %s cells at \n',Cell_name)
    fprintf(1,'the initiation of the uptake phase is:\n** %d', Drate_uptake_avg(i))

        if (str_error_test == 1)
            fprintf(1,' +/- %.0d', str_plus_num)
            fprintf(1,' Gy/h ** [1]\n\n')
        elseif (str_error_test == 0)
            fprintf(1,' +/- (%.0d/%.0d)',str_plus_num,str_minus_num)
            fprintf(1,' Gy/h ** [1]\n\n')
        end

    fprintf(1,'~~~~~~~\n\n')
end

% ========================================================================= %

%~~~~~~~~~~~~~~~~~~~~~~~~~~~~~~%
%~Calculate Dose Rate in Slab~%
%~~~~~~~~~~~~~~~~~~~~~~~~~~~~~~%

Drate_x=@(x)((A.*Percent_up.*Conf_adjust_uptake)/(S_flask*Per_conf)).*0.288.*Mean_beta_eng.*v.*
alpha.*(c+(c.*log(c./(Dens_med.*v.*x)))-(c.*exp(1-((Dens_med.*v.*x)./c)))+exp(1-
(Dens_med.*v.*x))-2.*exp(1-((Dens_med.*v.*x)./2)-(f./2))+exp(1-f));

% Again, we need the appropriate 'if' statements for the conditions on an
% infinite thin plan VW kernel.  If c>=p*v*x, the quantity in the square
```

```
% brackets of Eq. [9] becomes 0 and the DPK changes to:

Drate_x_c_cond=@(x)((A.*Percent_up.*Conf_adjust_uptake)/(S_flask*Per_conf)).*0.288.*Mean_beta_e
ng.*v.*alpha.*(exp(1-(Dens_med.*v.*x))-2.*exp(1-((Dens_med.*v.*x)./2)-(f./2))+exp(1-f));

% Checks on this condition will be done on each evaluation below.

% Paradigm 1):

% Bottom of the slab:
Drate_bottom = (0.5*Drate_x((0.5)*Cell_slab_half_thick)) +
(0.5*Drate_x((1.5)*Cell_slab_half_thick));
    if (c<=(Dens_med*v*((0.5)*Cell_slab_half_thick)))
        % the smallest condition
        Drate_bottom = (0.5*Drate_x_c_cond((0.5)*Cell_slab_half_thick)) +
(0.5*Drate_x_c_cond((1.5)*Cell_slab_half_thick));
    else
        if (f<=(Dens_med*v*((0.5)*Cell_slab_half_thick)))
            % the smallest condition
            fprintf(1,'The dose rate is 0 Gy/h. No need to go any further...\n')
        end
    end

% Top of the slab (by symmetry):
Drate_top = Drate_bottom;

% Centre of the slab:
Drate_centre = 2*(0.5*Drate_x((0.5)*Cell_slab_half_thick));
    if (c<=(Dens_med*v*((0.5)*Cell_slab_half_thick)))
        Drate_centre = 2*(0.5*Drate_x_c_cond((0.5)*Cell_slab_half_thick));
    else
        if (f<=(Dens_med*v*((1/3)*Cell_slab_half_thick)))
            fprintf(1,'The dose rate is 0 Gy/h. No need to go any further...\n')
        end
    end

% Paradigm 2):
```

```
% Where x=(0.5)delta
Drate_delta_one_half =
2*((1/3)*Drate_x((0.5)*Cell_slab_half_thick))+((1/3)*Drate_x((1.5)*Cell_slab_half_thick));
    if (c<=(Dens_med*v*((0.5)*Cell_slab_half_thick)))
        % the smallest condition
        Drate_one_third =
2*((1/3)*Drate_x_c_cond((0.5)*Cell_slab_half_thick))+((1/3)*Drate_x_c_cond((1.5)*Cell_slab_half
_thick));
    else
        if (f<=(Dens_med*v*((0.5)*Cell_slab_half_thick)))
            % the smallest condition
            fprintf(1,'The dose rate is 0 Gy/h. No need to go any further...\n')
        end
    end

% Where x=(1.5)delta, by symmetry
Drate_delta_one_and_one_half = Drate_delta_one_half;

% Total dose rate in the slab is:

Drate_slab_avg(i) =
(Drate_bottom+Drate_top+Drate_centre+Drate_delta_one_half+Drate_delta_one_and_one_half)/5;

    % Now, we need to determine the +/- uncertainties.  Maximum Drate (i.e.
    % +) occurs when Aconc is highest and slab thickness is smallest.
    % Conversely, minimum Drate occurs when Aconc is lowest and slab
    % thickness is largest. Therefore...

    % Maximum Drate:

Drate_x_max=@(x)((A.*(Percent_up+Err_percent_up).*(Conf_adjust_uptake+Err_conf_adjust_uptake))/
(S_flask*(Per_conf-
Err_per_conf))).*0.288.*Mean_beta_eng.*v.*alpha.*(c+(c.*log(c./(Dens_med.*v.*x)))-(c.*exp(1-
((Dens_med.*v.*x)./c)))+exp(1-(Dens_med.*v.*x))-2.*exp(1-((Dens_med.*v.*x)./2)-(f./2))+exp(1-
f));
    %With c condition...

Drate_x_max_c_cond=@(x)((A.*(Percent_up+Err_percent_up).*(Conf_adjust_uptake+Err_conf_adjust_up
```

```
take))/(S_flask*(Per_Conf-Err_per_conf))).*0.288.*Mean_beta_eng.*v.*alpha.*(exp(1-
(Dens_med.*v.*x))-2.*exp(1-((Dens_med.*v.*x)./2)-(f./2))+exp(1-f));

    % Paradigm 1):

    % Bottom of the slab:
    Drate_bottom_max = (0.5*Drate_x_max((0.5)*(Cell_slab_half_thick_min))) +
(0.5*Drate_x_max((1.5)*(Cell_slab_half_thick_min)));
        if (c<=(Dens_med*v*((0.5)*Cell_slab_half_thick_min)))
            Drate_bottom_max = (0.5*Drate_x_max_c_cond((0.5)*(Cell_slab_half_thick_min))) +
(0.5*Drate_x_max_c_cond((1.5)*(Cell_slab_half_thick_min)));
        else
            if (f<=(Dens_med*v*((0.5)*Cell_slab_half_thick_min)))
                fprintf(1,'The dose rate is 0 Gy/h. No need to go any further...\n')
            end
        end

    % Top of the slab (by symmetry):
    Drate_top_max = Drate_bottom_max;

    % Centre of the slab:
    Drate_centre_max = 2*(0.5*Drate_x_max((0.5)*(Cell_slab_half_thick_min)));
        if (c<=(Dens_med*v*((0.5)*Cell_slab_half_thick_min)))
            Drate_centre_max = 2*(0.5*Drate_x_max_c_cond((0.5)*(Cell_slab_half_thick_min)));
        else
            if (f<=(Dens_med*v*((0.5)*Cell_slab_half_thick_min)))
                frintf(1,'The dose rate is 0 Gy/h. No need to go any further...\n')
            end
        end

    % Paradigm 2):

    % Where x=(0.5)delta
    Drate_delta_one_half_max =
2*((1/3)*Drate_x_max((0.5)*(Cell_slab_half_thick_min)))+((1/3)*Drate_x_max((1.5)*(Cell_slab_hal
f_thick_min)));
        if (c<=(Dens_med*v*((1/3)*Cell_slab_half_thick)))
```

```
            Drate_delta_one_half_max =
2*((1/3)*Drate_x_max_c_cond((0.5)*(Cell_slab_half_thick_min)))+((1/3)*Drate_x_max_c_cond((1.5)*
(Cell_slab_half_thick_min)));
        else
            if (f<=(Dens_med*v*((1/3)*Cell_slab_half_thick)))
                fprintf(1,'The dose rate is 0 Gy/h. No need to go any further...\n')
            end
        end

    % Where x=(1.5)delta, by symmetry
    Drate_delta_one_and_one_half_max = Drate_delta_one_half_max;

    % Total dose rate in the slab is:

    Drate_slab_avg_max(i) =
(Drate_bottom_max+Drate_top_max+Drate_centre_max+Drate_delta_one_half_max+Drate_delta_one_and_o
ne_half_max)/5;

    % Minimum Drate:

    Drate_x_min=@(x)((A.*(Percent_up-Err_percent_up).*(Conf_adjust_uptake-
Err_conf_adjust_uptake))/(S_flask*(Per_conf+Err_per_conf))).*0.288.*Mean_beta_eng.*v.*alpha.*(c
+(c.*log(c./(Dens_med.*v.*x)))-(c.*exp(1-((Dens_med.*v.*x)./c)))+exp(1-(Dens_med.*v.*x))-
2.*exp(1-((Dens_med.*v.*x)./2)-(f./2))+exp(1-f));
    % With c condition...
    Drate_x_min_c_cond=@(x)((A.*(Percent_up-Err_percent_up).*(Conf_adjust_uptake-
Err_conf_adjust_uptake))/(S_flask*(Per_conf+Err_per_conf))).*0.288.*Mean_beta_eng.*v.*alpha.*(e
xp(1-(Dens_med.*v.*x))-2.*exp(1-((Dens_med.*v.*x)./2)-(f./2))+exp(1-f));

    % Paradigm 1):

    % Bottom of the slab:
    Drate_bottom_min = (0.5*Drate_x_min((0.5)*(Cell_slab_half_thick_max))) +
(0.5*Drate_x_min((1.5)*(Cell_slab_half_thick_max)));
        if (c<=(Dens_med*v*((0.5)*Cell_slab_half_thick_max)))
            Drate_bottom_min = (0.5*Drate_x_min_c_cond((0.5)*(Cell_slab_half_thick_max))) +
(0.5*Drate_x_min_c_cond((1.5)*(Cell_slab_half_thick_max)));
        else
```

```
            if (f<=(Dens_med*v*((0.5)*Cell_slab_half_thick_max)))
                fprintf(1,'The dose rate is 0 Gy/h. No need to go any further...\n')
            end
        end

    % Top of the slab (by symmetry):
    Drate_top_min = Drate_bottom_min;

    % Centre of the slab:
    Drate_centre_min = 2*(0.5*Drate_x_min((0.5)*(Cell_slab_half_thick_max)));
        if (c<=(Dens_med*v*((0.5)*Cell_slab_half_thick_max)))
            Drate_centre_min = 2*(0.5*Drate_x_min_c_cond((0.5)*(Cell_slab_half_thick_max)));
        else
            if (f<=(Dens_med*v*((0.5)*Cell_slab_half_thick_max)))
                fprintf(1,'The dose rate is 0 Gy/h. No need to go any further...\n')
            end
        end

    % Paradigm 2):

    % Where x=(0.5)delta
    Drate_delta_one_half_min =
2*((1/3)*Drate_x_min((0.5)*(Cell_slab_half_thick_max)))+((1/3)*Drate_x_min((1.5)*(Cell_slab_hal
f_thick_max)));
        if (c<=(Dens_med*v*((0.5)*Cell_slab_half_thick_max)))
            Drate_one_third_min =
2*((1/3)*Drate_x_min_c_cond((0.5)*(Cell_slab_half_thick_max)))+((1/3)*Drate_x_min_c_cond((1.5)*
(Cell_slab_half_thick_max)));
        else
            if (f<=(Dens_med*v*((0.5)*Cell_slab_half_thick_max)))
                fprintf(1,'The dose rate is 0 Gy/h. No need to go any further...\n')
            end
        end

    % Where x=(4/3)delta, by symmetry
    Drate_delta_one_and_one_half_min = Drate_delta_one_half_min;

    % Total dose rate in the slab is:
```

```
    Drate_slab_avg_min(i) =
(Drate_bottom_min+Drate_top_min+Drate_centre_min+Drate_delta_one_half_min+Drate_delta_one_and_o
ne_half_min)/5;

% Therefore the +/- errors are:

Drate_slab_avg_plus_err(i) = Drate_slab_avg_max(i) - Drate_slab_avg(i);
Drate_slab_avg_minus_err(i) = Drate_slab_avg(i) - Drate_slab_avg_min(i);

    % First, define a string for the plus error output:
    str_plus=sprintf('%.0d',Drate_slab_avg_plus_err(i));
    % Second, define a string for the plus error output:
    str_minus=sprintf('%.0d',Drate_slab_avg_minus_err(i));
    % The '.0d' rounds the values to the nearest whole integer in e -
    % notation. For example, 2.13e-005 becomes 2e-005.

    % Convert strings to double precision numbers:
    str_plus_num = str2double(str_plus);
    str_minus_num = str2double(str_minus);

    % Now, let's create a variable that will compare the first value in
    % str_plus and str_minus and see if they are the same:

    str_error_test=strncmp(str_plus,str_minus,1);
    % If this test is true, we only need to print on of the uncertainty
    % values (either the plus or the minus) as they equal to the number of
    % significant digits allotted for uncertainty values.  If this is
    % false, we will print out both values.

% Now, lets print the result!

fprintf(1,'The average dose rate to the slab of %s cells\n',Cell_name)
fprintf(1,'after uptake of the radiopharmaceutical is:\n** %d', Drate_slab_avg(i))

    if (str_error_test == 1)
        fprintf(1,' +/- %.0d', str_plus_num)
        fprintf(1,' Gy/h ** [2]\n\n')
```

```
    elseif (str_error_test == 0)
        fprintf(1,' +/- (%.0d/%.0d)',str_plus_num,str_minus_num)
        fprintf(1,' Gy/h ** [2]\n\n')
    end

fprintf(1,'~~~~~~~\n\n')

% ====================================================================== %

%~~~~~~~~~~~~~~~~~~~~~~~~~~~~~~~~~~~~~~~%
%~Calculate the Total Dose to the Cells~%
%~~~~~~~~~~~~~~~~~~~~~~~~~~~~~~~~~~~~~~~%

Dose(i) = ((Drate_uptake_avg(i)+Drate_slab_avg(i))/2)*(2)+(Drate_slab_avg(i))*(1);

    % Now calculate the uncertainties.

    Dose_err_plus(i) =
(sqrt(((Drate_uptake_x_2delta_plus_err(i))^2+(Drate_slab_avg_plus_err(i))^2))/2)*(2)+Drate_slab
_avg_plus_err(i)*(1);
    Dose_err_minus(i) =
(sqrt(((Drate_uptake_x_2delta_minus_err(i))^2+(Drate_slab_avg_minus_err(i))^2))/2)*(2)+Drate_sl
ab_avg_minus_err(i)*(1);

    % First, define a string for the plus error output:
    str_plus=sprintf('%.0d',Dose_err_plus(i));
    % Second, define a string for the plus error output:
    str_minus=sprintf('%.0d',Dose_err_minus(i));
    % See MATLAB Help 'sprintf' for function parameter explanation. The
    % '.0d' rounds the values to the nearest whole integer in e - notation.
    % For example, 2.13e-005 becomes 2e-005.

    % Convert strings to double precision numbers:
    str_plus_num = str2double(str_plus);
    str_minus_num = str2double(str_minus);

    % Now, let's create a variable that will compare the first value in
    % str_plus and str_minus and see if they are the same:
```

```
    str_error_test=strncmp(str_plus,str_minus,1);

% Now, lets print the result!

fprintf(1,'Therefore, the dose to the %s cells after\n',Cell_name)
fprintf(1,'treatment with %.1d MBq/ml of radiopharmaceutical with\n',A)
fprintf(1,'%.0d hour(s) for uptake and %.0d hour(s) for accumulation
is:\n\n',Time_up,Time_accum)

    if (str_error_test == 1)
        fprintf(1,'**********************************\n')
        fprintf(1,'*** %d',Dose(i))
        fprintf(1,' +/- %.0d', str_plus_num)
        fprintf(1,' Gy ***\n')
        fprintf(1,'**********************************\n')
    elseif (str_error_test == 0)
        fprintf(1,'******************************************\n')
        fprintf(1,'*** %d',Dose(i))
        fprintf(1,' +/- (%.0d/%.0d)',str_plus_num,str_minus_num)
        fprintf(1,' Gy ***\n')
        fprintf(1,'******************************************\n')
    end

fprintf(1,'_____________________________________________________\n')
fprintf(1,'=====================================================\n')

    end % End of 'if' statement if the user only enter a single value
end % End of 'if' statement if the user enters a range of values

% Now, if the user entered 'Yes' to whether they wanted to save the results
% to a Microsoft Excel file, the following will create the file.

if strcmp(save,'Yes') == 1
    filename = char(strcat(answer_filename,format_choices(excel_format)));
    headings = {'Activity'
                'Uptake Dose Rate (Gy/h)'
                'Plus Error Uptake Dose Rate'
```

```
                'Minus Error Uptake Dose Rate'
                'Accum. Dose Rate (Gy/h)'
                'Plus Error Accum. Dose Rate'
                'Minus Error Accum. Dose Rate'
                'Absorbed Dose (Gy)'
                'Plus Error Absorbed Dose'
                'Minus Error Absorbed Dose'}';
   results_num = [Activity;
                  Drate_uptake_avg;
                  Drate_uptake_x_2delta_plus_err;
                  Drate_uptake_x_2delta_minus_err;
                  Drate_slab_avg;
                  Drate_slab_avg_plus_err;
                  Drate_slab_avg_minus_err;
                  Dose;
                  Dose_err_plus;
                  Dose_err_minus]';
    results = num2cell(results_num);
    output = [headings; results];
    xlswrite(filename, output, 'Sheet1', 'A1'); % Write the results
%     If you want a title on the Excel output, uncomment the following but
%     it will be a 1 - 1.5 sec performance hit. Remember to change the cell
%     output for the results 'output' above from 'A1' to something else.
%     title_string = sprintf('Cell line = %s',Cell_name);
%     title = {title_string}; Converts previous string to a single element
%     xlswrite(filename, title, 'Sheet1', 'A1');
end

% The following is a completion dialogue box that allows the user to either
% redo the calculations or exit the application.

exit_text = {'Calculations are complete. Would you like to do another series?'
             ' '
             ''' Yes '' -  Restarts program'
             ''' No ''  -  Exits program immediately'
             ' '};
exit_title = 'Again?';
str1_exit = 'Yes & Continue';
```

```
str2_exit = 'No & Exit';
options.Resize='on';
options.Interpreter='tex';
options.Default=str1_exit;
exit_note = questdlg(exit_text, exit_title, str1_exit, str2_exit, options);
end % for 'while' loop initiating the exit test function

% ************************** END OF PROGRAM ************************** %
```

Dose_rate_ICCM_prod_2_method_comp.m

```
% This program is an addition to ICCM_Dose_Calcs_4_Radio_Beta_Emitters.m.
% A brief introduction to this program is provided below:

%%%%%%%%%%%%%%%%%%%%%%%%%%%%%%%%%%%%%%%%%%%%%%%%%%%%%%%%%%%%%%%%%%%%%%%%%%%%
%*************************************************************************%
%                                                                         %
% Calculation of Absorbed Dose in Examination of Bystander Effects via    %
% ------------------------------------------------------------------      %
% Irradiation with Beta Emitting Radiopharmaceutical                      %
% ---------------------------------------------------                     %
%                                                                         %
% This program is designed to calculate the absorbed dose to a set of     %
% donor cells used in the creation of Irradiated Cell Conditioned Medium  %
% (ICCM)as per radiation bystander protocol utilized by Boyd et al in:    %
%                                                                         %
% Boyd M, Ross SC, et al. Radiation-Induced biological bystander effect   %
% elicited in vitro by targeted radiopharmaceuticals labeled with alpa-,  %
% beta-, and auger electron-emitting radionuclides. J.Nucl.Med. Vol. 47.  %
% pp. 1007-1015 (2006).                                                   %
%                                                                         %
% The application was designed with the purpose of performing this        %
% calculation of absorbed dose from the beta emitting                     %
% radiopharmaceutical I-131 MIBG.  This is accomplished through modelling%
% of in vitro conditions and procedures coupled with the appropriate      %
% utilization of the Vynckier-Wambersie (VW) point-source dose function   %
% (kernel) integrated over the appropriate geometry.                      %
%                                                                         %
% Having said this, this program is also believed to be suitable for      %
% other beta emitting radiopharmaceuticals potentially used for ICCM      %
% production with maximum energies ranging from 0.5 to 3.0 MeV and        %
% utilization of Boyd et al' s methodology outlined in the paper above.   %
%                                                                         %
% Created By: Michael Gow                                                 %
%             Dept. of Medical Physics and Applied Radiation Sciences     %
%             McMaster University                                         %
```

```
%              Hamilton, ON CA                                                  %
%              MMXI                                                             %
%                                                                               %
% Special thanks to Andrei Hanu (McMaster University) for his MATLAB     %
% insight in the early stages of this endeavour.                                %
%*******************************************************************************%
%%%%%%%%%%%%%%%%%%%%%%%%%%%%%%%%%%%%%%%%%%%%%%%%%%%%%%%%%%%%%%%%%%%%%%%%%%%%%%%

%   ********************** BRIEF INTRODUCTION **********************   %
% This specific M-file was designed in order to compare 2 methods
% used for calculating the average dose rate to the cells during ICCM
% production (aka 'Accumulation Phase' or 'Dose Rate in Slab').
% Effectively, the program computes the dose rate in the slab using both
% the "homogeneous-slab" model (aka Method #1) or the "multi-isoplane"
% model (aka Method #2).  For Method #1, analytical integration is
% performed via utilization of either the MuPAD (Matlab) or Maple symbolic
% engine.  The goal is to compare both methods to determine if their
% answers agree and which Method provides optimal performance for
% integration into the program ICCM_Dose_Calcs_4_Radio_Beta_emitters(.m or
% .exe).
%   ********************** END INTRODUCTION **********************   %

% Prior to the program starting ...

% Clears Memory
clear all

% Clears Command Window
clc

% Maintains 15 digits of accuracy unless otherwise flagged
format long

% ============================================================================= %
%~~~~~~~~~~~~~~~~~~~~~~~~~~~~~~~~~~~~~~~~~~%
%~Welcome Dialogue for User of Start-up~%
%~~~~~~~~~~~~~~~~~~~~~~~~~~~~~~~~~~~~~~~~~~%
```

```
% The following sets up and displays a welcome dialogue box for the user.
% The user can select to continue to proceed to perform the calculations
% or the user may exit the program.
welcome_text = {'Hello!'
                '                                                    '
                'This program is designed to calculate the dose rate during Accumulation Phase
for both "homogenous-slab" (Method #1) and "multi-isoplane" (Method #2) models.  This stage is
after uptake of \beta emitting radiopharmaceutical used in the creation of Irradiated Cell
Conditioned Medium (ICCM) as per radiation bystander protocol utilized by Boyd et al in:'
                '                                                    '
                'Boyd M, Ross SC, et al. Radiation-Induced biological bystander effect elicited
in vitro by targeted radiopharmaceuticals labeled with alpa-, beta-, and auger electron-
emitting radionuclides. J.Nucl.Med. Vol. 47. pp. 1007-1015 (2006).'
                '                                                    '
                'The following prompts will guide the user through data entry necessary to
perform these calculations leveraging the Vynicker-Wambersie (VW) kernel for an infinite plane.
Full details of the modelling utilized in this application can be found in the associated
report.'
                '                                                    '
                'Created by: Michael Gow'
                '                   Dept. of Medical Physics and Applied Radiation Sciences'
                '                   McMaster University'
                '                   Hamilton, ON CA'
                '                   MMXI'
                '                                                    '
                '                                                    '
                '                                                    '
                '                                                    '
                '                                                    '};

welcome_title = 'Welcome!';
str1 = 'Continue';
str2 = 'Exit';
options.Resize='on';
options.Interpreter='tex';
options.Default=str1;
welcome = questdlg(welcome_text, welcome_title, str1, str2, options);
```

```
    % Determine if the user hits the 'Cancel' button
    if strcmp(welcome,'Exit')
        disp('Bye Bye')
        return
    end

% ========================================================================= %

%~~~~~~~~~~~~~~~~~~~~~~~~~~~~~~~~~~~~~~~~~~~~~~~~~~~~~~~~~~~~~~~~~~~~~~~~~~%
%~Identify Symbolic Engine for MATLAB install and optimize if possible~%
%~~~~~~~~~~~~~~~~~~~~~~~~~~~~~~~~~~~~~~~~~~~~~~~~~~~~~~~~~~~~~~~~~~~~~~~~~~%

% For the "homogenous-slab" model, we will need to utilize the Symbolic
% toolbox to perform the analytical integration required.  This section
% allow the user to choose the symbolic engine they wish to use.

% The program will determine the version of the Symbolic toolbox
% installed on the users version of MATLAB. The Maple Kernel, the only
% symbolic kernel utilized in the symbolic toolbox version less than 4.9,
% provides superior performance to the MuPAD symbolic kernel introduced in
% Symbolic Toolbox 4.9.  Although improvements have been made in recent
% versions (5.4 and 5.5 with Matlab R2010a and R2010b), if given the
% choice, the user should utilize the Maple symbolic engine when available
% (i.e. if Maple is installed on the host operating system).  The ability
% to choose between the MuPAD and Maple kernels was given in Symbolic
% toolbox version 4.9 to 5.3 (inclusive) through initiation of the
% 'symengine' command. The following section looks to determine if the
% version of Symbolic toolbox installed has this ability to change symbolic
% engines thus allowing the user to choose the Maple kernel as the symbolic
% engine if available.

v = ver('symbolic');
%Determine the Symbolic Toolbox Version installed in MATLAB

v_num = str2double(v.Version);
% Convert the verision string in 'v' generated above into a number

    if (v_num <= 5.3) && (v_num >= 4.9)
```

```
        % Change symbolic engine if applicable
        symengine
        % If available, Maple's Symbolic engine is
        % preferred as it has superior computation performance over
        % MATLAB's native MuPAD engine.
    end

% NOTE: If the user hits cancel, the calculations will be automatically
% performed with the default engine for that MATLAB session.
% ========================================================================= %

%~~~~~~~~~~~~~~~~~~~~~~~~~~~~~~~~~~~~~~~~~~~~~~~~~~~~~~~~~~~~~~~~~~~~~~~~%
%~Input Variables to Determine Thickness of Slab of Cells~%
%~~~~~~~~~~~~~~~~~~~~~~~~~~~~~~~~~~~~~~~~~~~~~~~~~~~~~~~~~~~~~~~~~~~~~~~~%

% Now let's have the user start entering values:

slab_mess_text = {'The cellular distribution within the treated flasks is approximated by a
symmetrical slab of cells of some surface area A and thickness 2\Delta [e.g. cylindrical
slab].'
                  '                                                                    '
                  'With this approximation, we can determine the thickness of the cells,
2\Delta, when adhered to the flask through knowledge of:'
                  '                                                                    '
                  '1) Size (surface area) of the flask used for culturing of donor cells'
                  '2) Confluence of the cell population at the time of radiopharmaceutical
treatment'
                  '3) Diameter of the cell line utilized in suspension (i.e. free float)'
                  '4) Number of cells plated in the donor flasks'
                  '5) Doubling time of cell line used'
                  '6) Time between cell plating and radiopharmaceutical treatment'
                  '                                                                    '
                  '                                                                    '
                  'Additionally, parameters involved in measurement of the radiopharmaceutical
uptake which can be noted include:'
                  '                                                                    '
                  '7) Size (surface area) of the culture well / flask for uptake measurements'
```

```
                  '8) Number of cells plated in the culture well / flask for uptake
measurements'
                  '9) Time between plating and radiopharmaceutical application for uptake
measurements'
                  '                                                                  '
                  'Note:  When entering fractional numbers (i.e. less than 1) make sure to
include a leading '' 0. '' to prevent an error message.'
                  '                                                                  '
                  '                                                                  '
                  '                                                                 '};
slab_mess_title = 'Determine the thickness of the cells in the treatment flask:';
str1_slab = 'Continue';
str2_slab = 'Exit';
options.Resize='on';
options.Interpreter='tex';
options.Default=str1_slab;
cell_slab_note = questdlg(slab_mess_text, slab_mess_title, str1_slab, str2_slab, options);

    % Determine if the user hits the 'Cancel' button
    if strcmp (cell_slab_note,'Exit')
        disp('Bye Bye')
        return
    end

% Now, let's have the user input the necessary variables to calculate the
% cell thickness when adhered to the bottom of the treatment flask:

prompt_slab = {'1) s_f_l_a_s_k = Size (growth area) of the flask used in treatment (in cm^2):'
               '2a) %_c_o_n_f = Percentage of cell confluence in treatment flask (between 0 and
1):'
               '2b) Err_%_c_o_n_f = Error / Uncertainty in cell confluence in treatment flask
(between 0 and %_c_o_n_f ):'
               '3) Name of cell line used:'
               '4a) Cell_D = Cellular diameter while in suspension (in \mum):'
               '4b) Err_D = Error in cellular diameter while in suspension (in \mum):'
               '5) #_c_e_l_l_s = Number of cells plated. NOTE: No commas, spaces, or
scientific/exponential notation:'
               '6) DB_t_i_m_e = Doubling time of cell line used (in hours):'
```

```
                '7) T_2_p_l_a_t_e = Time between cell plating and ^1^3^1I treatment (in hours):'
                '8) s_w_e_l_l = Size (growth area) of the well / flask used in uptake
measurements (in cm^2).  NOTE:  If a 6 - well plate was utilized, the typical surface area is
9.6 cm^2:'
                '9) #_u_p_t_a_k_e = Number of cells plated in well / flask in uptake
measurements. NOTE: No commas, spaces, or scientific/exponential notation:'
                '10) T_2_u_p_t_a_k_e = Time between plating and application of
radiopharmaceutical in uptake measurements (in hours):'};

title_slab = 'Input Parameters for determining cell thickness:';
num_lines_slab = [1 90]; % 1 row per prompt 100 characters wide
options.Resize='on';
options.Interpreter='tex';

% Define the standard parameters
def_slab =
{'25.0','0.65','0.05','UVW/NAT','16.5','0.9','200000','18.0','24.0','9.6','50000','48'};

% 'answer_slab' is a four element vector containing the users input results
answer_slab = inputdlg(prompt_slab,title_slab,num_lines_slab,def_slab,options);

    % Determine if the user hits the 'Cancel' button
    if isempty(answer_slab) == 1
        disp('Bye Bye')
        return
    end

    % Checks to ensure that all input parameters have a value
    while isempty(answer_slab{1}) || isempty(answer_slab{2}) || isempty(answer_slab{3}) ||
isempty(answer_slab{4}) || isempty(answer_slab{5}) || isempty(answer_slab{6}) ||
isempty(answer_slab{7}) || isempty(answer_slab{8}) || isempty(answer_slab{9}) ||
isempty(answer_slab{10}) || isempty(answer_slab{11}) || isempty(answer_slab{12})
        empty_err_slab = errordlg({'You have missed entering information into one of the input
parameters.'
                                   'All parameters require a value.  Please Try
Again.'},'Error');
        uiwait(empty_err_slab)
        answer_slab = inputdlg(prompt_slab,title_slab,num_lines_slab,def_slab,options);
```

```
            if isempty(answer_slab) == 1
                disp('Bye Bye')
                return
            end
    end

% Now, we convert the strings entered by the user in to double precision
% floating point numbers.

% Size of the flask
S_flask = str2double(answer_slab{1});
% Percentage confluence
Per_conf = str2double(answer_slab{2});
% Error in Percentage Confluence
Err_per_conf = str2double(answer_slab{3});
% Cell diameter
Cell_diam = str2double(answer_slab{5});
% Error in cell diameter
Err_cell_diam = str2double(answer_slab{6});
% # of Cells Plated
Num_cells = str2double(answer_slab{7});
% Doubling time of cell line used
Db_time = str2double(answer_slab{8});
% Time between plating and treatment
Pl2treat_time = str2double(answer_slab{9});
% Size of well used for uptake experiment
S_well = str2double(answer_slab{10});
% # of cells plated for uptake measurement
Num_uptake = str2double(answer_slab{11});
% Time between plating and uptake experiments
Pl2treat_up_time = str2double(answer_slab{12});

% Also for convenience, lets assign a variable to the name of the cells
Cell_name = answer_slab{4};

    % Check to ensure that the user has entered valid numbers (e.g. not
    % negative).  ISNAN checks to ensure a number was entered as opposed to
    % a alpha or special character.
```

```
    while (S_flask <= 0) || isnan(S_flask) == 1 || (Per_conf <= 0) || (Per_conf > 1) ||
isnan(Per_conf) == 1 || (Err_per_conf < 0) || (isnan(Err_per_conf) == 1) || (Err_per_conf >
Per_conf) || (Cell_diam <= 0) || (isnan(Cell_diam) == 1) || (Err_cell_diam < 0) ||
(isnan(Err_cell_diam) == 1) || (Err_cell_diam > Cell_diam) || (Num_cells <= 0) ||
(isnan(Num_cells) == 1) || (Db_time <= 0) || (isnan(Db_time) == 1) || (Pl2treat_time <= 0) ||
(isnan(Pl2treat_time) == 1) || (S_well <= 0) || (isnan(S_well) == 1) || (Num_uptake <= 0) ||
(isnan(Num_uptake) == 1) || (Pl2treat_up_time <= 0) || (isnan(Pl2treat_up_time) == 1)
        err_slab_neg = errordlg({'This error has resulted from one of the following:'
                                 '-------------------------------------------------------------
--------------'
                                 '                                                           '
                                 'a) You have entered a negative value or a value of zero for
one of the following parameters:'
                                 '-> size of flask, cell diameter, # of cells, doubling time,
and/or time between plating and radiopharmaceutical application'
                                 '                                                           '
                                 'b) The confluence entered is outside the acceptable range.'
                                 '                                                           '
                                 'c) The error/uncertainty in the confluence is greater than
the confluence value entered.'
                                 '                                                           '
                                 'd) The error/uncertainty in the cell diameter is greater than
the cell diameter value entered.'
                                 '                                                           '
                                 'e) You have not entered valid numeric characters (with the
exception of the cell line name).  Not entering a leading '' 0. '' for numbers less than 1 may
cause this error.'
                                 '                                                           '
                                 '                                                           '
                                 'Please ensure all parameters are positive and have been
entered correctly.'
                                 '                                                           '
                                 '                                                           '
                                 '                                    '},'Error');
        uiwait(err_slab_neg)
        answer_slab = inputdlg(prompt_slab,title_slab,num_lines_slab,def_slab,options);

            % If the user enters 'Cancel'...
```

```
            if isempty(answer_slab) == 1
                disp('Bye Bye')
                return
            end

        % Convert to double floating point precision
        S_flask = str2double(answer_slab{1});
       Per_conf = str2double(answer_slab{2});
        Err_per_conf = str2double(answer_slab{3});
        Cell_diam = str2double(answer_slab{5});
        Err_cell_diam = str2double(answer_slab{6});
        Num_cells = str2double(answer_slab{7});
        Db_time = str2double(answer_slab{8});
        Pl2treat_time = str2double(answer_slab{9});
        S_well = str2double(answer_slab{10});
        Num_uptake = str2double(answer_slab{11});
        Pl2treat_up_time = str2double(answer_slab{12});
    end

% Now, we calculate the cell thickness upon adhesion to the donor flasks
% as follows:

% *******
% First, calculate the volume of one cell in suspension.
% This volume is conserved upon adhesion to the flask:
% NOTE: We multiply by 1E-4 to convert micrometres to centimetres

Cell_vol = (4/3)*pi*(0.5*Cell_diam*0.0001)^3;

% Now, calculate the uncertainty in the cell volume in suspension.
% Remember, if we have Value +/- Error, the error (standard deviation) is
% calculated via: Error = Value*(Square Root of the Sum of the Squares) of
% all the relative errors (i.e. relative error = Error/Value).  So here, if
% we have a power of 3, we calculate the error as:
% (Value^3)*((3*(Err/Value)^2)^0.5)

Err_Cell_vol = ((4/3)*pi)*((0.5*Cell_diam*0.0001)^3*((3*(Err_cell_diam/Cell_diam)^2)^0.5));
```

```
% *******
% Second, determine surface area of the flask taken up by the cells.  For
% example, if a 25 cm^2 flask is 65% confluent, the total surface area
% taken up by the cells is 25*0.65 = 16.25 cm^2

Cell_surf_area = S_flask*Per_conf;

% Uncertainty in surface area

Err_Cell_surf_area = S_flask*Err_per_conf;

% *******
% Third, we need to determine how many cells make up this population
% covering surface area 'Cell_surf_area' above.  To do this, we need to
% take into account the doubling time of the cell line so that the total
% number cells at given time, t, between plating and treatment is as
% follows: C = Co*exp[(t*ln2)/DB] where DB is the doubling time of the cell
% line and Co is the number of cells originally plated.

Tot_num_cells = Num_cells*exp((Pl2treat_time*log(2))/Db_time);

% *******
% Fourth, so the total volume taken up by the cells at time of treatment
% is:

Tot_cell_vol = Cell_vol*Tot_num_cells;

% Uncertainty in total volume

Err_Tot_cell_vol = Err_Cell_vol*Tot_num_cells;

% *******
% Fifth, and final step is to calculate the thickness of the cells upon
% adhering to the flask.  We know the total volume of the cells (Step 4) as
% well as the surface area these cells covered in the flask (Step 2).
% Since Volume = Surface Area*Thickness, we have simply, Cell Slab
% Thickness = 2Delta = (Tot_cell_vol)/(Cell_surf_area):
```

```
Cell_slab_thick = Tot_cell_vol/Cell_surf_area;
Cell_slab_half_thick = 0.5*Cell_slab_thick;

% Uncertainty in slab thickness

Err_Cell_slab_thick = (Tot_cell_vol/Cell_surf_area)*((Err_Tot_cell_vol/Tot_cell_vol)^2 +
(Err_Cell_surf_area/Cell_surf_area)^2)^0.5;
Err_Cell_slab_half_thick = 0.5*Err_Cell_slab_thick;
% *******

% For usage later, lets also calculate the maximum and minimum slab
% thickness
Cell_slab_thick_max = Cell_slab_thick + Err_Cell_slab_thick;
Cell_slab_thick_min = Cell_slab_thick - Err_Cell_slab_thick;
Cell_slab_half_thick_max = 0.5*Cell_slab_thick_max;
Cell_slab_half_thick_min = 0.5*Cell_slab_thick_min;

% *******
% Using the thickness calculated above, coupled with input variables
% provided for the uptake measurement experiments, we will determine the
% confluence of the wells / flask used for determining our
% radiopharmaceutical uptake percentages (to be entered by the user in the
% next section.  Remember, upon application of the radiopharmaceutical to
% the medium, we are assuming an instant, homogenous, static mix.  Because
% we assume it to be static, areas covered with radiopharmaceutical but no
% cells will not have the pharmaceutical taken up.  Thus, we can make a
% correlation between activity administered, well/flask confluence, and
% uptake percentage from our uptake experiment data which will allow us to
% more accurately determine the the amount of activity taken up by donor
% cells used for ICCM production. We will call this a confluence adjustment
% factor, Conf_adjust_uptake, obtained for an applied activity
% concentration, Aconc, as:
%
% [(% Uptake from exp.)/(Uptake Conf.)] =
%                                 [(X actual uptake by donors)/(Donor Conf.]
%
% where (X actual uptake by donors) = Conf_adjust_uptake
%
```

```
% Typically, the wells in the uptake experiments are
% seeded and allowed to culture for long enough such that they are fully
% confluent at the time of uptake application and subsequent measurement
% (i.e. Uptake Conf. = 1).  In this case, the confluence adjustment is
% straight forward.  Simply multiple the uptake percentage by the donor
% cell confluence.  Intuitively, assuming a static, homogenous
% radiopharmaceutical distribution / coverage, this is obvious (i.e. cells
% will only uptake the activity that is covering them).  Otherwise the
% expression above will make the appropriate adjustment.
%
% Conf_adjust_uptake is calculated as follows:

% 1) Determine the number of cells after the time between seeding and start
% of uptake experiment (i.e. radiopharmaceutical application).

Tot_num_cells_uptake = Num_uptake*exp((Pl2treat_up_time*log(2))/Db_time);

% 2) Use the cell volume and donor cell thickness calculated above to
% determine the area covered in the well.

Conf_uptake = (Tot_num_cells_uptake*Cell_vol)/Cell_slab_thick;
Err_conf_uptake = Conf_uptake*(Err_Cell_slab_thick);

% We will identify Conf_adjust_uptake below after we define some additional
% variables....keep your eyes open ;)

% ========================================================================= %

%~~~~~~~~~~~~~~~~~~~~~~~~~~~~~~~~~~~~~~~~~~~~~~~~~~~~~~~~~~~~~~~~~~~~~~~~%
%~Input variables to be used in Vynckier Wambersie Kernel~%
%~~~~~~~~~~~~~~~~~~~~~~~~~~~~~~~~~~~~~~~~~~~~~~~~~~~~~~~~~~~~~~~~~~~~~~~~%

% A note to the user about what is left to enter.
addn_param_text = {'Additional experimental parameters regarding the radiopharmaceutical and
medium utilized required for the calculations are:'
                   '                                                                '
                   '1) The mean energy of \beta particles for the nuclide utilized'
                   '2) The maximum energy of \beta particles for the nuclide utilized'
```

```
                    '3) Density of the homogenous medium'
                    '4) The activity concentration applied'
                    '5) Percentage uptake of the radiopharmaceutical into the cell in vitro'
                    '6) Time for uptake phase'
                    '7) Time for bystander factor accumulation'
                    '                                                          '
                    'Note:  When entering fractional numbers (i.e. less than 1) make sure to
include a leading '' 0. '' to prevent an error message.'
                    '                                                          '
                    '                                                         '};

addn_param_title = 'Additional Experimental Parameters';
str1_addn_param = 'Continue';
str2_addn_param = 'Exit';
options.Resize='on';
options.Interpreter='tex';
options.Default=str1_addn_param;
addn_param_note =
questdlg(addn_param_text,addn_param_title,str1_addn_param,str2_addn_param,options);

    if strcmp (addn_param_note,'Exit')
        disp('Bye Bye')
        return
    end

% Now, lets have the user input the necessary variables
addn_param_input = {'<E_\beta> = Mean \beta energy per disintegration (in MeV):'
                    'E_\beta_m_a_x = Maximum \beta energy (in MeV). NOTE: Here, this value is
limited to the range of 0.5 MeV to 3.0 MeV (exclusive).  The reason for this due to
E_\beta_m_a_x''s use in evaluating additional variables in the VW kernel (see Vynckier and
Wambersie, 1982, 1986):'
                    '\rho = Density of the homogeneous medium (in g/cm^3; 1 for standard
medium):'
                    'A_c_o_n_c = Activity concentration of radiopharmaceutical applied (in
MBq/cm^3). NOTE: With medium of unit density, then 1 MBq/ml = 1 MBq/cm^3 = 1 MBq/g:'
                    '%_u_p_t_a_k_e = Percentage uptake of radiopharmaceutical (between 0 and
1):'
```

```
                    'Err_%_u_p_t_a_k_e = Error / Uncertainty in uptake of radiopharmaceutical
(between 0 and %_u_p_t_a_k_e):'};

addn_param_input_title = 'Additional Experimental Parameters';
addn_param_num_lines = [1 90];
options.Resize='on';
options.Interpreter='tex';

% Define the standard parameters
def_addn_param = {'0.19','0.61','1.00','1.00','0.314','0.037'};
addn_param_answer =
inputdlg(addn_param_input,addn_param_input_title,addn_param_num_lines,def_addn_param,options);

    % Determine if the user hits the 'Cancel' button and if so displays
    % an exit prompt
    if isempty(addn_param_answer) == 1
        disp('Bye Bye')
        return
    end

    % Checks to ensure that all input parameters have a value
    while isempty(addn_param_answer{1}) || isempty(addn_param_answer{2}) ||
isempty(addn_param_answer{3}) || isempty(addn_param_answer{4}) || isempty(addn_param_answer{5})
|| isempty(addn_param_answer{6})
        addn_param_empty_err = errordlg({'You have missed entering information into one of the
input parameters.'
                                         'All parameters require a value (even 0).  Please Try
Again.'},'Error');
        uiwait(addn_param_empty_err)
        addn_param_answer =
inputdlg(addn_param_input,addn_param_input_title,addn_param_num_lines,def_addn_param,options);
            if isempty(addn_param_answer) == 1
                disp('Bye Bye')
                return
            end
    end

% Now, we convert the strings entered by the user in to double precision
```

```
% floating point numbers.

% Mean beta energy per disintegration (in Mev)
Mean_beta_eng = str2double(addn_param_answer{1});
% Maximum beta energy (in MeV)
Max_beta_eng = str2double(addn_param_answer{2});
% Density of medium (g/cm^3)
Dens_med = str2double(addn_param_answer{3});
% A_conc applied (in MBq/ml)
Act_conc = str2double(addn_param_answer{4});
% % of radiopharmaceutical uptake
Percent_up = str2double(addn_param_answer{5});
% Error / Uncertainty in % of radiopharmaceutical uptake
Err_percent_up = str2double(addn_param_answer{6});

    % Check to ensure that the user has not entered a negative number or
    % that the confluence level is not below the acceptable value.
    while (Mean_beta_eng <= 0) || (isnan(Mean_beta_eng) == 1) || (isnan(Max_beta_eng) == 1) ||
(Max_beta_eng <= 0.5) || (Max_beta_eng >= 3.0) || (Dens_med <= 0) || (isnan(Dens_med) == 1) ||
(Act_conc <= 0) || (isnan(Act_conc) == 1)|| (Percent_up <= 0) || (isnan(Percent_up) == 1) ||
(Percent_up > 1) || (Err_percent_up <= 0) || (isnan(Err_percent_up) == 1) || (Err_percent_up >
Percent_up)
        err_slab_neg = errordlg({'This error has resulted from one of the following:'
                                 '-------------------------------------------------------------
--------------'
                                 '                                                           '
                                 'a) You have entered a negative value or a value of 0 for one
of the following parameters:'
                                 '-> Average beta energy, density of the medium, percentage
uptake, activity concentration, time allotted for uptake, and/or time allotted for bystander
factor accumulation'
                                 '                                                           '
                                 'b) The maximum beta energy entered is outside the accepted
range of 0.5 to 3.0 MeV (exclusive).'
                                 '                                                           '
                                 'e) The percentage of uptake is greater than 100% (i.e.
greater than 1) or the error in uptake is larger than or equal to the entered uptake value.'
                                 '                                                           '
```

```
                                'f) You have entered a non-numeric character.  Not entering a
leading '' 0. '' for numbers less than 1 may cause this error.'
                                '                                                           '
                                '                                                           '
                                'Please ensure all parameters are positive and have been
entered correctly.'
                                '                                                           '
                                '                                                           '
                                '
'},'Error');

        uiwait(err_slab_neg)
        addn_param_answer =
inputdlg(addn_param_input,addn_param_input_title,addn_param_num_lines,def_addn_param,options);

            % If the user enters 'Cancel'...
            if isempty(addn_param_answer) == 1
                disp('Bye Bye')
                return
            end

        % Convert to double floating point precision
        Mean_beta_eng = str2double(addn_param_answer{1});
        Max_beta_eng = str2double(addn_param_answer{2});
        Dens_med = str2double(addn_param_answer{3});
        Act_conc = str2double(addn_param_answer{4});
        Percent_up = str2double(addn_param_answer{5});
        Err_percent_up = str2double(addn_param_answer{6});

    end

% Now, we have Conf_adjust_uptake as follows:

if (Conf_uptake-Err_conf_uptake) >= S_well
    Conf_uptake = 1;
    %If the minimum area covered by the cells is greater than or equal to
    %the size of the well then we have 100% confluence at time of uptake
    %experiment and Conf_adjust_uptake is simply the percentage confluence:
```

```
    Conf_adjust_uptake = Per_conf;
    Err_conf_adjust_uptake = Err_per_conf;
else
    Conf_adjust_uptake = (Per_conf*Percent_up)/Conf_uptake;
    Err_conf_adjust_uptake = Conf_adjust_uptake*(sqrt((Err_per_conf/Per_conf)^2 +
(Err_percent_up/Percent_up)^2));
end


% *******
% Now, let's calculate some of the necessary variables that form part of
% the VW kernel
% *******

% 1) Apparent absorption coefficient, v [cm^2/g -> density thickness].
% This relation is accurate provided the maximum beta energy of the
% radionuclide is between 0.5 and 3.5 MeV.

v = 14.5*(Max_beta_eng)^(-1.17);

% NOTE: By comparison, the original Loevinger kernel, calculated the
% apparent absorption coefficient, v, via: v = 18.6*(Emax - 0.036)^(-1.37)
% for the range 0.17 to 3 MeV *******

% 2) Dimensionless parameter c.  Remember we are only looking in the range
% of 0.5 to 3.0 MeV for the maximum beta energy

if (Max_beta_eng >= 0.5 && Max_beta_eng < 1.5)
    c = 1.5;
elseif (Max_beta_eng >= 1.5 && Max_beta_eng <= 3.0)
    c = 1;
end
% *******

% 3) Dimensionless f parameter. The parameter f/pv is the distance where
% the point kernel becomes zero.  This is the primary correction entered by
% VW into Loevinger's work. This relationship again holds true in the
% energy range between 0.5 and 3.5 MeV.
```

```
f = Dens_med*v*0.269*(Max_beta_eng)^1.31;
% *******

% 4) Alpha Coefficient. For explanation see Ref. 1-3 in "Brief
% Introduction".

alpha = ((3*c^2) - (c^2-1)*exp(1) + (3+f)*exp(1-f) - 4*exp(1-(f/2)))^-1;
% *******

% ========================================================================= %

fprintf(1,'_____________________________________________________\n')
fprintf(1,'=====================================================\n\n\n')
fprintf(1,'For an activity concentration of: %4.2f MBq/ml\n',Act_conc)
fprintf(1,'---------------------------------\n\n')

% ========================================================================= %
tStart_1=tic; % START OF TIMER FOR METHOD 1

%~~~~~~~~~~~~~~~~~~~~~~~~~~~~~~~%
%~Calculate Dose Rate in Slab~% -> METHOD 1; homogenous slab
%~~~~~~~~~~~~~~~~~~~~~~~~~~~~~~~%

% Briefly, we are dividing the cell into a bunch of infinitely thin plane
% sources located between x'=0 and 2delta.  For a position, x, the dose
% rate would be:
%
% Drate(x)=Aconc*int(K(x-x')) from x'=0 to 2delta and then take the average
% over all x.
%
% where K(x-x') is:
%
% K(x-x') =
% 0.288*Eavg*Ac*v*alpha*{c[1+ln(c/pv(x-x'))-exp(1-(pv(x-x'))/c)]+exp(1
% -pv(x-x'))-2*exp(1-pv(x-x')/c-f/2)+exp(1-f)}
%
% i.e. The dose rate kernel for an infinite, thin plane.
```

```
%
% As the dose rate is really a function of the magnitude of x-x', |x-x'|,
% we make the appropriate substitution of variables and work only the
% positive half of the kernel.  Effectively we get that:
%
% K(x-x') = K_low + K_high where K_low is K for x-x'<0 and K_high is K for
% x-x'>0.
%
% See the associated paper for full details.

syms x z real % IDENTIFY SYMBOLIC VARIABLES

K=(0.288*Mean_beta_eng*v*alpha)*(c+(c*log(c/(Dens_med*v*z)))-c*exp(1-((Dens_med*v*z)/c))+exp(1-
(Dens_med*v*z))-2*exp(1-((Dens_med*v*z)/2)-(f/2))+exp(1-f));

    % Test to adjust K if c<= p*v*x.  We will set x=2*Delta to be
    % stringent.
    if c<=Dens_med*v*Cell_slab_thick
        K=(0.288*Mean_beta_eng*v*alpha)*(exp(1-(Dens_med*v*z))-2*exp(1-((Dens_med*v*z)/2)-
(f/2))+exp(1-f));
    else
        if f<=Dens_med*v*Cell_slab_thick % Test for f to adjust K
            fprintf(1,'Dose rate is 0 Gy/h.')
        end
    end

% x-x' < 0
K_low=int(K,z,0,(Cell_slab_thick-x));
% x-x' > 0
K_high=int(K,z,0,x);

Drate_slab_avg_1_prime =
((Act_conc*Percent_up*Conf_adjust_uptake)/(S_flask*Per_conf*Cell_slab_thick))*(K_low+K_high);
Drate_slab_avg_1 = (1/Cell_slab_thick)*int(Drate_slab_avg_1_prime,x,0,Cell_slab_thick);

% Maximum
K_low=int(K,z,0,((Cell_slab_thick-Err_Cell_slab_thick)-x));
```

```
Drate_slab_avg_1_max_prime =
((Act_conc*(Percent_up+Err_percent_up)*(Conf_adjust_uptake+Err_conf_adjust_uptake))/(S_flask*(P
er_conf-Err_per_conf)*(Cell_slab_thick-Err_Cell_slab_thick)))*(K_low+K_high);
Drate_slab_avg_1_max = (1/(Cell_slab_thick-
Err_Cell_slab_thick))*int(Drate_slab_avg_1_max_prime,x,0,(Cell_slab_thick-
Err_Cell_slab_thick));

% Minimum
K_low=int(K,z,0,((Cell_slab_thick+Err_Cell_slab_thick)-x));
Drate_slab_avg_1_min_prime = ((Act_conc*(Percent_up-Err_percent_up)*(Conf_adjust_uptake-
Err_conf_adjust_uptake))/(S_flask*(Per_conf+Err_per_conf)*(Cell_slab_thick+Err_Cell_slab_thick)
))*(K_low+K_high);
Drate_slab_avg_1_min =
(1/(Cell_slab_thick+Err_Cell_slab_thick))*int(Drate_slab_avg_1_min_prime,x,0,(Cell_slab_thick+E
rr_Cell_slab_thick));

% Uncertainty
Drate_slab_avg_plus_err_1 = Drate_slab_avg_1_max - Drate_slab_avg_1;
Drate_slab_avg_minus_err_1 = Drate_slab_avg_1 - Drate_slab_avg_1_min;

tElapsed_1=toc(tStart_1); % END OF TIMER FOR METHOD 2

fprintf(1,'METHOD #1 ("homogenous slab"):\n\n')
fprintf(1,'The average dose rate to the slab of %s cells\n',Cell_name)
fprintf(1,'after uptake of the radiopharmaceutical is:\n** %d ', double(Drate_slab_avg_1))
fprintf(1,' +/- %d/%d Gy/h**\n\n',
double(Drate_slab_avg_plus_err_1),double(Drate_slab_avg_minus_err_1))
fprintf(1,'Total time taken = %.5f sec\n\n', tElapsed_1)
fprintf(1,'~~~~~~~\n\n')

% ======================================================================== %
tStart_2=tic; % START OF TIMER FOR METHOD 2

%~~~~~~~~~~~~~~~~~~~~~~~~~~~~~~%
%~Calculate Dose Rate in Slab~% -> METHOD 2; multi-isoplane
%~~~~~~~~~~~~~~~~~~~~~~~~~~~~~~%

% We will create two different activity distribution models (aka paradigms)
```

```
% and calculate the dose rate at 5 different locals within the slab of
% cells.  In general, the slab is located infinite in the y-, z- extents
% and has a thickness of 2delta along the x axis.  The bottom of the slab
% lies along x=0.

% 1)  Take the activity, Aconc, and distribute it equally in two infinite
% planes (i.e. 0.5*Aconc each) located at positions x=(0.5)delta and
% x=(1.5)delta.  Calculate the  dose rate (Drate) at the edges of the slab
% (x=0 and x=2delta) and in the centre (x=delta)
%
% 2)  Take the activity, Aconc, and distribute it equally in three infinite
% planes (i.e. (1/3)Aconc each) located at positions x=0,delta, and
% 2delta).  Calculate the Drate at x=(0.5)delta and x=(1.5)delta.
%
% The average dose rate to the slab will be derived from the values
% calculated at the various locations in paradigms 1) and 2).

% The expression for dose rate from an infinite disk at distance x from
% source is given by:
%
% Drate(x,0,inf)=0.288*Eavg*Ac*v*alpha*{c[1+ln(c/pvx)-exp(1-(pvx)/c)]+exp(1
% -pvx)-2*exp(1-pvx/c-f/2)+exp(1-f)}
%
% with [  ] defined as 0 for pvx >= c and Drate(x,0,inf) defined as 0 for
% pvx >= f [Note: For definitions of v,c,alpha,and f, see below.]
%
% References:
% [1] Vynckier S and Wambersie A. Dosimetry of beta sources in
% radiotherapy: Absorbed dose distributions around plane sources. Rad.
% Prot. Dos. Vol 14(2), pp. 169-173 (1986).
%
% [2] Appendix C: Calculation of beta-ray dose distributions by integration
% of the beta-ray point-source dose function. Oxford University Press. J.
% ICRU. Vol. 4(2), pp. 155-163 (2004).

% Note that we have used scalar .* and ./ here so as to ensure a more
% object-oriented design. Remember that the activity in the infinite plane
% is only the appropriate fraction of the percentage of uptake.
```

```
Drate_x=@(x)((Act_conc.*Percent_up.*Conf_adjust_uptake)/(S_flask*Per_conf)).*0.288.*Mean_beta_e
ng.*v.*alpha.*(c+(c.*log(c./(Dens_med.*v.*x)))-(c.*exp(1-((Dens_med.*v.*x)./c)))+exp(1-
(Dens_med.*v.*x))-2.*exp(1-((Dens_med.*v.*x)./2)-(f./2))+exp(1-f));

% We need the appropriate 'if' statements for the conditions on an
% infinite thin plan VW kernel.  If c>=p*v*x, the quantity in the square
% brackets of Eq. [9] becomes 0 and the DPK changes to:

Drate_x_c_cond=@(x)((Act_conc.*Percent_up.*Conf_adjust_uptake)/(S_flask*Per_conf)).*0.288.*Mean
_beta_eng.*v.*alpha.*(exp(1-(Dens_med.*v.*x))-2.*exp(1-((Dens_med.*v.*x)./2)-(f./2))+exp(1-f));

% Checks on this condition will be done on each evaluation below.

% Paradigm 1):

% Bottom of the slab:
Drate_bottom = (0.5*Drate_x((0.5)*Cell_slab_half_thick)) +
(0.5*Drate_x((1.5)*Cell_slab_half_thick));
    if (c<=(Dens_med*v*((0.5)*Cell_slab_half_thick)))
        % the smallest condition
        Drate_bottom = (0.5*Drate_x_c_cond((0.5)*Cell_slab_half_thick)) +
(0.5*Drate_x_c_cond((1.5)*Cell_slab_half_thick));
    else
        if (f<=(Dens_med*v*((0.5)*Cell_slab_half_thick)))
            % the smallest condition
            fprintf(1,'The dose rate is 0 Gy/h. No need to go any further...\n')
        end
    end

% Top of the slab (by symmetry):
Drate_top = Drate_bottom;

% Centre of the slab:
Drate_centre = 2*(0.5*Drate_x((0.5)*Cell_slab_half_thick));
    if (c<=(Dens_med*v*((0.5)*Cell_slab_half_thick)))
        Drate_centre = 2*(0.5*Drate_x_c_cond((0.5)*Cell_slab_half_thick));
    else
```

```
        if (f<=(Dens_med*v*((1/3)*Cell_slab_half_thick)))
            fprintf(1,'The dose rate is 0 Gy/h. No need to go any further...\n')
        end
    end

% Couple notes to remember is that delta = Cell_slab_half_thick and we are
% multiplying by 0.5 as each infinite plane of activity contains half the
% overall activity taken up by the cells.

% Paradigm 2):

% Where x=(0.5)delta
Drate_delta_one_half =
2*((1/3)*Drate_x((0.5)*Cell_slab_half_thick))+((1/3)*Drate_x((1.5)*Cell_slab_half_thick));
    if (c<=(Dens_med*v*((0.5)*Cell_slab_half_thick)))
        % the smallest condition
        Drate_one_third =
2*((1/3)*Drate_x_c_cond((0.5)*Cell_slab_half_thick))+((1/3)*Drate_x_c_cond((1.5)*Cell_slab_half
_thick));
    else
        if (f<=(Dens_med*v*((0.5)*Cell_slab_half_thick)))
            % the smallest condition
            fprintf(1,'The dose rate is 0 Gy/h. No need to go any further...\n')
        end
    end

% Where x=(1.5)delta, by symmetry
Drate_delta_one_and_one_half = Drate_delta_one_half;

% Total dose rate in the slab is:

Drate_slab_avg_2 =
(Drate_bottom+Drate_top+Drate_centre+Drate_delta_one_half+Drate_delta_one_and_one_half)/5;

    % Now, we need to determine the +/- uncertainties.  Maximum Drate (i.e.
    % +) occurs when Aconc is highest, slab thickness is smallest, and
    % confluence is greatest.  Conversely, minimum Drate occurs when Aconc
    % is lowest and slab thickness is largest and confluence is lowest.
```

```
    % Therefore...

    % Maximum Drate:

Drate_x_max=@(x)((Act_conc.*(Percent_up+Err_percent_up).*(Conf_adjust_uptake+Err_conf_adjust_up
take))/(S_flask*(Per_conf-
Err_per_conf))).*0.288.*Mean_beta_eng.*v.*alpha.*(c+(c.*log(c./(Dens_med.*v.*x)))-(c.*exp(1-
((Dens_med.*v.*x)./c)))+exp(1-(Dens_med.*v.*x))-2.*exp(1-((Dens_med.*v.*x)./2)-(f./2))+exp(1-
f));
    %With c condition...

Drate_x_max_c_cond=@(x)((Act_conc.*(Percent_up+Err_percent_up).*(Conf_adjust_uptake+Err_conf_ad
just_uptake))/(S_flask*(Per_conf-Err_per_conf))).*0.288.*Mean_beta_eng.*v.*alpha.*(exp(1-
(Dens_med.*v.*x))-2.*exp(1-((Dens_med.*v.*x)./2)-(f./2))+exp(1-f));

    % Paradigm 1):

    % Bottom of the slab:
    Drate_bottom_max = (0.5*Drate_x_max((0.5)*(Cell_slab_half_thick_min))) +
(0.5*Drate_x_max((1.5)*(Cell_slab_half_thick_min)));
        if (c<=(Dens_med*v*((0.5)*Cell_slab_half_thick_min)))
            Drate_bottom_max = (0.5*Drate_x_max_c_cond((0.5)*(Cell_slab_half_thick_min))) +
(0.5*Drate_x_max_c_cond((1.5)*(Cell_slab_half_thick_min)));
        else
            if (f<=(Dens_med*v*((0.5)*Cell_slab_half_thick_min)))
                fprintf(1,'The dose rate is 0 Gy/h. No need to go any further...\n')
            end
        end

    % Top of the slab (by symmetry):
    Drate_top_max = Drate_bottom_max;

    % Centre of the slab:
    Drate_centre_max = 2*(0.5*Drate_x_max((0.5)*(Cell_slab_half_thick_min)));
        if (c<=(Dens_med*v*((0.5)*Cell_slab_half_thick_min)))
            Drate_centre_max = 2*(0.5*Drate_x_max_c_cond((0.5)*(Cell_slab_half_thick_min)));
        else
            if (f<=(Dens_med*v*((0.5)*Cell_slab_half_thick_min)))
```

```
                frintf(1,'The dose rate is 0 Gy/h. No need to go any further...\n')
            end
        end

    % Paradigm 2):

    % Where x=(0.5)delta
    Drate_delta_one_half_max =
2*((1/3)*Drate_x_max((0.5)*(Cell_slab_half_thick_min)))+((1/3)*Drate_x_max((1.5)*(Cell_slab_hal
f_thick_min)));
        if (c<=(Dens_med*v*((1/3)*Cell_slab_half_thick)))
            Drate_delta_one_half_max =
2*((1/3)*Drate_x_max_c_cond((0.5)*(Cell_slab_half_thick_min)))+((1/3)*Drate_x_max_c_cond((1.5)*
(Cell_slab_half_thick_min)));
        else
            if (f<=(Dens_med*v*((1/3)*Cell_slab_half_thick)))
                fprintf(1,'The dose rate is 0 Gy/h. No need to go any further...\n')
            end
        end

    % Where x=(1.5)delta, by symmetry
    Drate_delta_one_and_one_half_max = Drate_delta_one_half_max;

    % Total dose rate in the slab is:

    Drate_slab_avg_max =
(Drate_bottom_max+Drate_top_max+Drate_centre_max+Drate_delta_one_half_max+Drate_delta_one_and_o
ne_half_max)/5;

    % Minimum Drate:

    Drate_x_min=@(x)((Act_conc.*(Percent_up-Err_percent_up).*(Conf_adjust_uptake-
Err_conf_adjust_uptake))/(S_flask*(Per_conf+Err_per_conf))).*0.288.*Mean_beta_eng.*v.*alpha.*(c
+(c.*log(c./(Dens_med.*v.*x)))-(c.*exp(1-((Dens_med.*v.*x)./c)))+exp(1-(Dens_med.*v.*x))-
2.*exp(1-((Dens_med.*v.*x)./2)-(f./2))+exp(1-f));
    % With c condition...
```

```
    Drate_x_min_c_cond=@(x)((Act_conc.*(Percent_up-Err_percent_up).*(Conf_adjust_uptake-
Err_conf_adjust_uptake))/(S_flask*(Per_conf+Err_per_conf))).*0.288.*Mean_beta_eng.*v.*alpha.*(e
xp(1-(Dens_med.*v.*x))-2.*exp(1-((Dens_med.*v.*x)./2)-(f./2))+exp(1-f));

    % Paradigm 1):

    % Bottom of the slab:
    Drate_bottom_min = (0.5*Drate_x_min((0.5)*(Cell_slab_half_thick_max))) +
(0.5*Drate_x_min((1.5)*(Cell_slab_half_thick_max)));
        if (c<=(Dens_med*v*((0.5)*Cell_slab_half_thick_max)))
            Drate_bottom_min = (0.5*Drate_x_min_c_cond((0.5)*(Cell_slab_half_thick_max))) +
(0.5*Drate_x_min_c_cond((1.5)*(Cell_slab_half_thick_max)));
        else
            if (f<=(Dens_med*v*((0.5)*Cell_slab_half_thick_max)))
                fprintf(1,'The dose rate is 0 Gy/h. No need to go any further...\n')
            end
        end

    % Top of the slab (by symmetry):
    Drate_top_min = Drate_bottom_min;

    % Centre of the slab:
    Drate_centre_min = 2*(0.5*Drate_x_min((0.5)*(Cell_slab_half_thick_max)));
        if (c<=(Dens_med*v*((0.5)*Cell_slab_half_thick_max)))
            Drate_centre_min = 2*(0.5*Drate_x_min_c_cond((0.5)*(Cell_slab_half_thick_max)));
        else
            if (f<=(Dens_med*v*((0.5)*Cell_slab_half_thick_max)))
                fprintf(1,'The dose rate is 0 Gy/h. No need to go any further...\n')
            end
        end

    % Paradigm 2):

    % Where x=(0.5)delta
    Drate_delta_one_half_min =
2*((1/3)*Drate_x_min((0.5)*(Cell_slab_half_thick_max)))+((1/3)*Drate_x_min((1.5)*(Cell_slab_hal
f_thick_max)));
        if (c<=(Dens_med*v*((0.5)*Cell_slab_half_thick_max)))
```

```
            Drate_one_third_min =
2*((1/3)*Drate_x_min_c_cond((0.5)*(Cell_slab_half_thick_max)))+((1/3)*Drate_x_min_c_cond((1.5)*
(Cell_slab_half_thick_max)));
        else
            if (f<=(Dens_med*v*((0.5)*Cell_slab_half_thick_max)))
                fprintf(1,'The dose rate is 0 Gy/h. No need to go any further...\n')
            end
        end

    % Where x=(4/3)delta, by symmetry
    Drate_delta_one_and_one_half_min = Drate_delta_one_half_min;

    % Total dose rate in the slab is:

    Drate_slab_avg_min =
(Drate_bottom_min+Drate_top_min+Drate_centre_min+Drate_delta_one_half_min+Drate_delta_one_and_o
ne_half_min)/5;

% Therefore the +/- errors are:

Drate_slab_avg_plus_err_2 = Drate_slab_avg_max - Drate_slab_avg_2;
Drate_slab_avg_minus_err_2 = Drate_slab_avg_2 - Drate_slab_avg_min;

tElasped_2=toc(tStart_2); % END OF TIMER FOR METHOD 2

fprintf(1,'METHOD #2 ("multi-isoplane"):\n\n')
fprintf(1,'The average dose rate to the slab of %s cells\n',Cell_name)
fprintf(1,'after uptake of the radiopharmaceutical is:\n** %d ', Drate_slab_avg_2)
fprintf(1,' +/- %d/%d Gy/h**\n\n', Drate_slab_avg_plus_err_2,Drate_slab_avg_minus_err_2)
fprintf(1,'Total time taken = %.5f sec\n\n', tElasped_2)
fprintf(1,'~~~~~~~\n\n')
fprintf(1,'_____________________________________________________\n')
fprintf(1,'=====================================================\n\n\n')
% ========================================================================= %
```